



THESIS SUBMITTED FOR THE DEGREE OF
DOCTOR OF PHILOSOPHY

On-shell techniques for Effective Field Theories

MANUEL ACCETTULLI HUBER

Supervisors:

PROF. GABRIELE TRAVAGLINI

PROF. ANDREAS BRANDHUBER

Examiners:

PROF. CLAUDIA DE RHAM

DR RICARDO MONTEIRO

July 25, 2022

CENTRE FOR THEORETICAL PHYSICS

SCHOOL OF PHYSICAL AND CHEMICAL SCIENCES

QUEEN MARY UNIVERSITY OF LONDON

Declaration

I, Manuel Accettulli Huber, confirm that the research included within this thesis is my own work or that where it has been carried out in collaboration with, or supported by others, that this is duly acknowledged below and my contribution indicated. Previously published material is also acknowledged below.

I attest that I have exercised reasonable care to ensure that the work is original, and does not to the best of my knowledge break any UK law, infringe any third party's copyright or other Intellectual Property Right, or contain any confidential material.

I accept that the College has the right to use plagiarism detection software to check the electronic version of the thesis.

I confirm that this thesis has not been previously submitted for the award of a degree by this or any other university.

The copyright of this thesis rests with the author and no quotation from it or information derived from it may be published without the prior written consent of the author.

Signature:

Date: 15/07/2022

This thesis describes work carried out with my supervisors Gabriele Travaglini and Andreas Brandhuber as well as my colleague and fellow PhD Stefano De Angelis which was published in [1–4]. The initial part of the thesis also contains the outcome of further research with Stefano De Angelis published in [5]. I have also co-authored a further paper with Sanjaye Ramgoolam, Mehrnoosh Sadrzadeh and Adriana Correia [6] which will not be discussed in this thesis. Where other sources have been used, they are cited in the bibliography.

Abstract

In this thesis I explore a wide range of applications of the so called on-shell methods to Effective Field Theories of gravity and the Standard Model. I will first focus on the tree-level and restrict my attention to four space-time dimensions where the use of spinor-helicity formalism allows for very compact expressions of gauge-invariant quantities as well as the simple classification of contact interactions from the assumptions of locality, Lorentz-invariance and little-group covariance. I discuss how to use unitarity to combine these contact terms into higher-multiplicity tree amplitudes and non-minimal form factors, providing an algorithm which makes only use of on-shell seeds but at the same time is applicable to any given EFT of massless particles. The tree-level results obtained in this first section provide then the necessary input for the results obtained in the remainder of the thesis, where unitarity and generalised unitarity is used to obtain loop-results from trees. In particular, I first discuss the computation of the one-loop mixing matrix of the full set of mass-dimension eight operators in a Standard Model EFT setting and then move on to applications in the context of gravity. Here, amplitudes techniques are used to extract classical information hiding in the perturbative expansion of gravitational theories beyond leading order. More specifically I will consider higher-derivative interactions involving powers of the Riemann tensor and study their effect on observables such as the bending angle and the time delay in a light particle deflection process. I also consider the interactions of heavy binaries mediated by such operators and study their impact on the power radiated through gravitational waves. Finally I discuss how to use six-dimensional spinor-helicity to bypass intrinsic limitations of the four-dimensional unitarity calculations, generalising known techniques for amplitudes to the case of form factors.

Acknowledgments

I owe a debt of gratitude to a great many people, and despite my efforts I will surely fail to acknowledge all of them here, and for that I apologise.

My first thanks clearly go to my supervisors Gabriele Travaglini and Andreas Brandhuber, I am grateful not only for their guidance but also for their continued support going well beyond the academic sphere. Thanks to them, for the whole duration of my PhD I had the feeling that Queen Mary was the place where I belong, not only as a researcher but also on a personal level. In this regard, I want to extend my thanks to the whole theory group at QMUL, owing to the always helpful and positive attitude of all the academics I had the privilege of spending the past four years in an environment fostering growth and collaboration. In particular I am grateful to Sanjaye Ramgoolam, Chris White, Ricardo Monteiro, Rodolfo Russo, Congkao Wen and Costis Papageorgakis. On a similar footing, I am indebted to all of my fellow research students, for making our fourteen-people office a place for sharing all the pains and joys of doing a PhD, as well as forcefully helping me gain the ability to focus even in the noisiest environment. I am thus deeply grateful to Kymani Armstrong-Williams, Enrico Andriolo, Gergely Kantor, George Barnes, Chinmaya Bhargava, Josh Gowdy, Tancredi Schettini-Gherardini, Lewis Sword, Mitchell Woolley, Joseph Hayling, Rodolfo Panerai, Chris Brown, Zoltan Laczko, Linfeng Li, Ricardo Stark-Muchão, Nadia Bahjat-Abbas, Arnau Koemans Collado, Ray Otsuki and especially to Rashid Alawadhi, Graham Brown, Marcel Hughs, Adrian Keyo Shan Padellaro, David Peinador Veiga, Rajath Radhakrishnan, Sam Wikeley and Shun-Qing Zhang. Among the many colleagues turned into good friends, Stefano De Angelis is due a special mention. Stefano has been my most trusted brother in arms, sharing with me 83% of my publications and thus an estimated 70% of the overall joys and pains of the last years (I leave a bit of a margin because some things I certainly liked/disliked more than he did, and the other way around). We shared our papers, we shared our supervisors, we shared meals and for some time a flat, we even shared a job interview: I am grateful for our friendship and really glad that he was my local SAGEX buddy. Speaking of which, I would like to thank my other fellow SAGEX students Andrea Cristofoli, Gabriele Dian, Riccardo Gonzo, Kays Haddad, Ingrid Holm, Sebastian Pögel, Davide Polvara, Marco Saragnese, Canxin Shi, Anne Spiering for the enjoyable schools and the workshops we shared and in particular Luke Corcoran, Nikolai Fadeev and Lorenzo Quintavalle for the time we shared in the US during the internship at Wolfram. I am also indebted to the other members of the SAGEX network, in particular to Jan Plefka for his kind and helpful attitude as my mentor, and to Jenna Lane and Mary Thomas for their constant organizational support.

In a broader context, I would like to thank Pierpaolo Mastrolia for his continued sup-

port, his mentorship since the days of my master's thesis and the always encouraging and helpful advice, along with Luca Mattiazzi, Davide Billo and Nicola Gorini for making the old days in Padova a never fading memory. Further thanks go to Devendra Kapadia for his supervision at Wolfram, to Adriana Correia, Sanjaye Ramgoolam and Mehrnoosh Sadrzadeh for collaboration on Natural Language Processing related topics, and to Ricardo Monteiro and Claudia De Rham for their feedback on this thesis.

Last but not least, I am most grateful to my wife, whose love and support (and cakes) allowed me to keep my mental health intact throughout the PhD and especially during the challenging COVID times.

Contents

1	Introduction	7
2	An invitation to tree-level techniques	16
2.1	Spinor helicity formalism	16
2.2	Little-group transformations and the three-point amplitudes	23
2.3	An off-shell recursion: Berends-Giele	27
2.4	BCFW-like recursions	30
3	On-shell bootstrapping of tree-level amplitudes	35
3.1	The Standard Model from on-shell techniques	37
3.1.1	Four-point amplitudes from factorisation	38
3.2	The on-shell classification of SMEFT operators	42
3.2.1	Kinematic structures from spinor helicity variables	42
3.2.2	The classification of SMEFT interactions	46
3.3	Bootstrapping the tree-level amplitudes	48
3.3.1	Higher-point amplitudes in the SM	49
3.4	Analytics from numerics through finite fields	58
4	Loop-level unitarity and the SMEFT	66
4.1	One-loop unitarity	68
4.2	Hypercharge constraints from gauge anomalies	75
4.3	Anomalous dimension matrix from on-shell techniques	79
4.3.1	A review of the method	79
4.3.2	The Higgs production in association with a W boson	81
5	Higher-derivative operators and gravitational observables	94
5.1	From amplitudes to the deflection angle and time delay via the eikonal .	97
5.2	The relevant scattering amplitudes	102
5.2.1	Four-point scalar/graviton scattering in EH gravity	104
5.2.2	Four-point scalar/graviton scattering in $\text{EH} + R^3$	104
5.2.3	Four-point scalar/graviton scattering in $\text{EH} + R^4$	105

5.2.4	Scattering with the FFR interaction	108
5.3	Eikonal phase matrix, deflection angle and time delay	112
5.3.1	Graviton deflection angle and time delay in EH gravity	113
5.3.2	Graviton deflection angle and time delay in $EH + R^3$	115
5.3.3	Graviton deflection angle and time delay in $EH + R^4$	120
5.3.4	Graviton deflection angle and time delay in $EH + FFR$	121
5.3.5	Photon deflection angle and time delay in $EH + FFR$	123
6	Gravitational radiation from R^3 operators	127
6.1	The EFT action and more about cubic interactions	129
6.2	Quadrupole moments in EFTs of gravity	131
6.2.1	The amplitude with cubic interactions	132
6.2.2	The amplitude with tidal effects	133
6.2.3	The quadrupole corrections	134
6.3	Power radiated by the gravitational waves	136
6.4	Waveforms in EFT of gravity	138
7	Rational terms from six-dimensional unitarity	141
7.1	Six-dimensional spinor-helicity formalism	143
7.1.1	Helicity Spinors in Six Dimensions	143
7.1.2	From Six-Dimensional to Four-Dimensional Quantities	145
7.2	The Dimensional Reconstruction Technique	147
7.2.1	One-Loop Dimensional Reconstruction	147
7.2.2	An L -loop Generalisation	150
7.3	Tree-Level Form Factors	155
7.3.1	$\text{Tr } F^2$ Form Factors	156
7.3.2	$\text{Tr } F^3$ Form Factors	158
7.3.3	$\text{Tr } F^4$ and Higher Dimensional Form Factors	160
7.4	One-Loop Form Factors	163
7.4.1	The Minimal $\text{Tr } F^2$ Form Factors	163
7.4.2	The Non-Minimal $\text{Tr } F^2$ Form Factor	165
7.4.3	The Minimal $\text{Tr } F^3$ Form Factors	168
7.4.4	The Non-Minimal $\text{Tr } F^3$ Form Factor	170
7.4.5	The Minimal $\text{Tr } F^4$ Form Factors	173
8	Conclusions	178
A	SMEFT auxiliary material	182
A.1	The Standard Model gauge group	182
A.2	Three-point amplitudes in the Standard Model	183
A.3	Infrared collinear anomalous dimensions in the Standard Model	184

B Gravity EFTs auxiliary material	187
B.1 Some relevant integrals	187
B.2 Feynman rules	187
B.3 The tree-level amplitudes	188
B.4 Hamiltonians with momentum-dependent potentials	190
C Some six-dimensional results	191
C.1 Six-Dimensional Scattering Amplitudes	191
C.2 Non-Minimal Form Factors	194
C.3 Integral Expressions	197
Bibliography	200

Chapter 1

Introduction

What is our world made of? This is one of the most enticing questions mankind has faced over the centuries, ever since the evolution of society allowed our species to focus on problems going beyond mere day to day survival. Already almost two thousand years before the establishment of the scientific method in the seventeenth century, a group of greek philosophers led by Democritus, relying solely on logic reasoning, came to a conclusion which is surprisingly close to the nowadays experimentally established truth: atoms, inseparable basic constituents of the known universe, the word itself coming from the greek *atomon* meaning “indivisible”. Indeed, not only can the atom be split into a set of electrons orbiting a conglomerate of protons and neutrons, but the latter can themselves be further split into what we call, in a rather oxymoronic way, sub-atomic particles. Furthermore, while in the ancient Greeks’ view, atoms were thought of as inert solids merely excluding other bodies from their volume, in our modern models particles interact with each other in rather complicated ways through the four fundamental forces of electromagnetism, gravity, the weak and the strong force. The central task of high-energy theoretical physics could be summarised as trying to give a complete, accurate and mathematically consistent description of these interactions which form the barebones of every composite structure in the universe.

In order to test the fine-grained structure of matter, collider experiments have proven to be among the most valuable tools at the experimentalists’ disposal. While in their infancy these sort of experiments were essentially of table-top size, like for example the Geiger-Marsden experiments establishing Rutherford’s model of the atom over Thomson’s, nowadays the required instrumentation is on a totally different level. The Large Hadron Collider (LHC) operating at CERN is the world’s biggest single machine, with a ring 27 kilometers in diameter used to accelerate particles at high-enough energies to expose their internal structure when colliding inside one of the four detector areas at a rate of around 10^9 collisions per second. At the time of writing, the LHC harnesses

among others the power of the largest particle detector ever to be built, in the form of ATLAS with its 46 metres in length and 25 in diameter, as well as the largest scientific collaboration in history, in the form of the Compact Muon Solenoid (CMS) collaboration with about 5500 members. These incredible numbers have led throughout the years to equally impressive scientific results, one of the most striking being the first experimental observation of the Higgs boson back in 2012 [7,8]. The importance of this observation could hardly be overstated as it confirmed the existence of a key piece of the Standard Model (SM) of particle physics, which is accepted as the most accurate description to date of all the fundamental forces excluding gravity.

The SM is set within the theoretical framework of Quantum Field Theory (QFT), which encompasses both the quantum nature of the particles and the relativistic description needed for fast moving objects. In this setting, in order to compare the experimental observations with theoretical predictions, a key ingredient are scattering amplitudes, which encode information about the interaction probabilities of particles, and are thus needed to predict the scattering outcomes. These probabilities are typically computed within perturbation theory: the couplings regulating the strengths of the interactions are considered to be small, and scattering amplitudes are computed as a series expansion around these. The more terms in the expansion one considers, the better the accuracy of the final result, but also the greater the complexity of the computation. Each order in the expansion can be computed as a sum of terms whose precise mathematical formulation can be visually represented through Feynman diagrams. These provide an intuitive interpretation of the process in terms of (virtual or off-shell) particles created from an initial state, propagating in spacetime and then annihilating again, giving so rise to the final state of the scattering process.

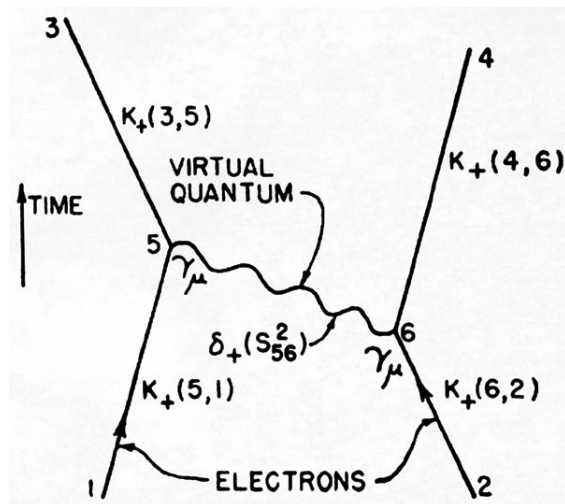


Figure 1.1: One of the first examples of Feynman diagrams to appear in a published paper, representing the photon exchange between two electrons [9].

These diagrams come with associated theory-dependent rules, which establish a bijective relation between sums of diagrams and the terms in the perturbative expansion, the lowest order being represented by tree-level diagrams like the one in Figure 1.1, while higher orders are made up of diagrams with an increasing number of closed loops. While Feynman diagrams have certainly changed the way people thought about QFT, and have provided a powerful computational tool for scattering processes, they have the intrinsic flaw that the number of diagrams is subject to a factorial growth with the number of external particles considered in the process or the number of loops to be considered. In other words the combinatorics of this diagrammatic approach scales badly with the complexity of the process or the increase in the perturbative order one considers. As a consequence, over the past thirty years the focus started to shift towards a set of techniques loosely denoted as on-shell methods [10–13] which bypass the limitations of Feynman diagrams and also provide continuously new theoretical insights in the deeper structure and properties of scattering amplitudes. The main idea is to replace some of the internal virtual off-shell states with on-shell particles. As we will discuss, this leads to enormous simplifications because these states are far more constrained than their off-shell counterparts. For example scattering amplitudes are gauge-invariant objects, while individual Feynman diagrams are not, only sums of diagrams are. Thus what typically happens in the diagrammatic approach is that a proliferation of intermediate expressions may collapse into simple final results due to cancellations among the terms.

The prototypical example is a $2 \rightarrow n$ pure gluon amplitude at tree level. Already for $n = 4$ this process gets contributions from 220 diagrams, and the number quickly growing to around 10^7 for $n = 8$ [14], but for any helicity configuration involving for example two negative- and n positive-helicity gluons all of these contributions can be collapsed into a beautifully simple single term known as the Parke-Taylor formula [15, 16].

Considering the tree-level case, when we put an intermediate state on-shell (which we call performing a unitarity cut) we witness a factorisation of the amplitude into products of lower-point¹ amplitudes, each of which is in itself gauge-invariant and thus bound to be simpler than a sum of diagrams. This idea is exploited for example by the Britto-Cachazo-Feng-Witten (BCFW) recursion relation [12, 13], which is a very effective tool to compute tree-level amplitudes recursively, see Section 2.4. On the other hand, at higher-loop orders one can exploit the branch-cut singularities arising in the amplitude and relate the associated discontinuities to (phase-space integrated) products of lower-order amplitudes, or even better write the amplitude in terms of a basis of integrals and compute the coefficients of the expansion from lower-point amplitudes [17, 18, 12]. All of these methods are based on unitarity of the considered theory, in other words

¹Lower-point amplitudes are those which present a smaller number of external particles.

conservation of probability, as we will discuss in Section 4.1.

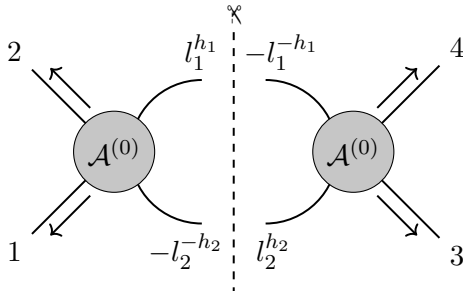


Figure 1.2: Pictorial representation of a so called double-cut of a one-loop amplitude, the dashed line represents the unitarity cut through the propagators (we use an all-outgoing convention for momenta). Every term in the full one-loop amplitude presenting a discontinuity in the $s_{12} = (p_1 + p_2)^2$ kinematic channel contributes to this double-cut, which is expressed in terms of products of tree-amplitudes. Inverting the logic, considering all the possible combinations of cuts allows to reconstruct the one-loop amplitude, see Section 4.1.

On-shell methods have proven to be very powerful in a variety of settings including collider physics [19, 20], the study of the ultraviolet (UV) behaviour of $\mathcal{N} = 8$ supergravity [21, 22], the study of the inspiral phase of binary systems of celestial objects [23–33], the anomalous dimension matrix and non-mixing theorems for Standard Model Effective Field Theories [34–37], the perturbative exploration of supersymmetric gauge theories [38–40] and also the perturbative study of partially off-shell quantities such as form factors [41–50].

In this thesis we focus on applications to effective field theories, in particular to the Standard Model Effective Field Theory (SMEFT) and EFTs of gravity including Einstein-Hilbert (EH) along with some higher-derivative operators. Despite its many successes over the years, the fact that so far LHC measurements are compatible with its predictions, and its undeniable beauty, the Standard Model is still expected to be an incomplete description of nature: many theoretical puzzles are still unsolved, including but not limited to the hierarchy problem, the magnitude of the quartic λ coupling of the Higgs, the origin of CP violation in the quark sector, or the unnatural pattern of the Yukawa couplings. If the SM is incomplete but still reproduces correct results at the energy scales tested by experiment, it means that it can be considered as an Effective Field Theory which requires some sort of UV completion to provide the further answers we seek. To date there are no clear hints at what such a completion should look like, and a very appealing approach to parametrize Beyond Standard Model (BSM) physics is the SMEFT [51, 52]: one considers a Lagrangian of the type

$$\mathcal{L}_{\text{SMEFT}} = \mathcal{L}_{\text{SM}} + \sum_{i,j} \frac{c_i^{(j)}}{\Lambda^{j-4}} \mathcal{O}_i^{(j)}, \quad (1.1)$$

where \mathcal{L}_{SM} is the SM Lagrangian and $\mathcal{O}_i^{(j)}$ are additional non-renormalizable operators

built from Standard Model fields and classified through their mass-dimension, which we labelled by j . Here the couplings $c_i^{(j)}$ are dimensionless and the energy scale Λ , which provides the cut-off scale of the validity of the EFT, compensates for the higher mass-dimension of the operators. The additional operators can be thought as arising from integrating out heavy modes with mass comparable to Λ in the complete theory, leading to an effective description. The power of the method relies within the fact that as long as one considers a complete basis of operators for the given mass dimension, it becomes possible to study in one go the effects of all the theories which would produce any of the effective operators considered, thus no a priori knowledge of the UV completion is required.

One of the problems one has to address in this regard is the identification of a complete basis of operators. The counting of non-redundant operators can be performed via the Hilbert series method, as shown in [53–55], however an explicit construction of the SMEFT operators is rather involved. Traditional techniques require taking care separately of many sources of redundancy, *e.g.* Bianchi identities and Integration By Parts (IBP) identities of operators with derivative insertions, field redefinitions and Fierz identities. More recently, a more direct way of constructing this basis has been proposed, which relies on the classification of the independent effective interactions directly from their S-matrix elements [56–63], and has been used to classify all the SMEFT operators up to mass dimension nine [64, 65]. In other words, one can classify operators by looking at the associated minimal amplitude, which assumes the form of a contact term (no intermediate particles are exchanged). In Chapter 3 we discuss a variation of this method presented in [5], allowing to build a complete operator basis from a graph-based method, and show how to construct the SM from scratch without relying on a Lagrangian but simply considering the amplitudes associated to the minimal interactions of the model.

The operators \mathcal{O}_i in general have a non-vanishing and usually non-diagonal anomalous dimension matrix, meaning that they get renormalised and mix among themselves in non-trivial ways. Consequently the Wilson coefficients of the operators at the scales accessible to collider experiments differ from those at the high-energy matching scale. Furthermore operator mixing implies that experimental constraints on one of them also affects the others. Thus, evaluating the anomalous dimension matrix is a crucial aspect of interpreting SMEFT results.

In this respect, on-shell methods have proven extremely powerful not only in the computation of the anomalous dimension matrix, but even more so in the interpretation of zeroes appearing in the matrix through selection rules implied by helicity [34], operator lengths [35] and angular momentum [36]. Still from an on-shell perspective it has been found that the structure of rational terms influences the zeroes, and that a smart choice

of regularization scheme can lead to further cancellations: this has been studied at two loops in the case of an $SU(N)$ model which presents similarities with the SM but it is far simpler and contains far less operators [37]. While the leading contributions to the SMEFT come from dimension-six operators [66–72], there are interesting processes for which the dominant contribution comes from even higher-dimensional operators. Some examples include the light-by-light scattering [73], the light production via gluon fusion [74] and the neutral bosons production [75] and even, in some scenarios, the $g_\mu - 2$ [76] and Higgs production in association with a W boson [77], which receive the first contribution from dimension-eight operators. Dimension-eight operators can play a relevant role even when appearing as subleading contributions [78], and recently studies of their impact on SMEFT have been performed [79–83]. The first systematic and complete computation of the one-loop anomalous dimension matrix for dimension-six operators has been carried out in [84–86]. On the other hand, the study of the anomalous dimension of SMEFT interactions at dimension eight has produced partial results in [87–93], while the first full calculation (to linear order in the Wilson coefficients) was presented in [5]. We discuss the latter results at the end of Chapter 4.

In Chapters 5 and 6 we move away from SMEFT and discuss applications to EFTs of gravity involving also higher-derivative operators, thus going beyond the Einstein-Hilbert (EH) theory. Very interestingly, in this context it has been shown that through the use of QFT perturbative methods it is possible to compute classical corrections to the gravitational potential, as well as to observables such as the bending angle and the time delay experienced by a particle in gravitational background. These corrections at higher orders in Newton’s constant G are hidden within the loops [94–96] of a theory where heavy galactic objects are described as massive point particles, for example scalars when considering Schwarzschild black holes, which interact through graviton exchange. In this picture one wants to extrapolate the long-range physics, which is the information we have experimental access to, and furthermore one wants to consider those contributions arising from a gravitational interaction, or in other words from virtual gravitons being exchanged among a pair of massive particles. The unitarity and on-shell methods are ideally suited for the task: performing loop-level unitarity cuts in four dimensions will automatically select those pieces of the complete amplitude which present a discontinuity in one or more given kinematic channels. This means that selecting the contributions purely related to a graviton exchange amounts to simply perform the cuts in the correct kinematic channels, and furthermore terms which do not contribute to long-range physics are ignored a priori with the right setup. In fact, if we perform the unitarity cuts in four dimensions we will miss so called rational terms: these are parts of the amplitude which do not present discontinuities in the kinematic channels and thus cannot be detected by the cuts. What would usually be a drawback leading to an incomplete amplitude, is in these specific circumstances

an advantage, since rational terms correspond to local contributions to the potential which can be ignored. Once the relevant terms of the amplitude have been recovered, one can for example extract the corrections to the gravitational potential at a fixed order in G through an EFT matching procedure [97, 98], which was used for example to obtain the state-of-the-art results [29, 99]. On the other hand, it is also possible to extract directly from the amplitude information about physical observables such as the bending angle or the time delay experienced by a particle moving in the gravitational background generated by a heavy object. Particularly well suited for this task is the eikonal approach [100–105], in which one considers the limit where the mass of the object generating the gravitational field is much larger than the energy of the deflected particle and the gravitationally exchanged momentum. We make use of this method in Chapter 5 to study the effect of higher-derivative interactions involving up to four Riemann tensors on the above mentioned observables. The new interactions will feature as modifications to the tree-level amplitudes entering the one-loop unitarity cuts we consider and are thus easily accounted for.

While in this case our study focusses on four-point amplitudes with two external massive scalars, in Chapter 6 we consider instead five-point amplitudes where an external soft graviton is produced by the two interacting scalars. Considering the gravitational binary from far apart, one can approximate its behaviour as that of a single small extended object emitting gravitational radiation through oscillations which can be studied through a multipole expansion. The combination of information coming from the multipole expansion with that of the potential allows to give a description of the gravitational waves emitted by the coalescing binary, computing the wave flux as well as the waveform. We study the impact of purely gravitational operators cubic in the Riemann tensor as well as of some tidal interactions on the quadrupole, comparing then our findings with earlier results which considered operators to quartic power in the Riemann tensor [106].

In the final part of the thesis we take a step back and focus on the very nature of the unitarity methods used so far, and specifically on their limitations. As already mentioned, since unitarity cuts rely on the discontinuities of the loop-level scattering amplitudes in the various kinematic channels, by construction the method is blind to rational terms. This means that four-dimensional unitarity is sufficient to compute complete amplitude results only in the cases where these rational terms are absent such as in supersymmetric theories at one loop [10, 11]. On the other hand, in order to compute results relevant for collider physics in QCD rational terms appear ubiquitously and are required to recover complete results, an example being the all-plus pure gluon interaction at one-loop [107, 108] which are purely rational in the external spinors. There are various methods allowing to compute these rational terms, one being simply to perform the same unitarity calculation in a dimension $D = 4 - 2\epsilon$ [109, 110]: in

order to keep mass-dimensions consistent, the deviation from four dimensions of the coupling needs to be balanced by a kinematic invariant raised to the power -2ϵ , which will produce a discontinuity in the given invariant and thus allow detection through cuts.

The downside of moving to an arbitrary dimension D is that first of all one loses the power of the spinor-helicity formalism, described in Chapter 2, which typically allows for results to be expressed in a very compact form, and furthermore numerical evaluations of the cut amplitudes are not possible. One way to work around this is to perform a “dimensional reconstruction” [111–115], where one investigates the dependence of the loop amplitude on the dimensionality of space-time. Considering for example pure Yang-Mills, this dependence turns out to be polynomial, and the coefficients can be fixed by a simple interpolation evaluating the amplitude in several different integer dimensions. In these integer dimensions one can then again make use of spinor-helicity and numerical methods if needed.

In Chapter 7 we derive the results of [1], where building on the previous amplitudes result an extension of the dimensional reconstruction for form factors is proposed. A form factor $F_{\mathcal{O}}(1, \dots, n; q)$ is defined as the overlap of an n -particle state and the state produced by an operator $\mathcal{O}(x)$ acting on the vacuum:

$$\int d^4x e^{-iq \cdot x} \langle 1, \dots, n | \mathcal{O}(x) | 0 \rangle = (2\pi)^4 \delta^{(4)}\left(q - \sum_{i=1}^n p_i\right) F_{\mathcal{O}}(1, \dots, n; q). \quad (1.2)$$

Notice that at zero momentum transfer, *i.e.* $q = 0$ in (1.2), the form factor of an operator $\mathcal{O}(x)$ represents the correction to the scattering amplitude due to the inclusion of a new local interaction proportional to $\mathcal{O}(x)$. The form factors which will be considered are related to scattering processes of the Higgs boson and many gluons: in the large top-quark mass approximation, these can be described by an effective theory obtained by integrating out the top quark in QCD. This generates an infinite series of higher-dimensional interactions with the gluon field strength and its derivatives, in addition to couplings to light quarks. The leading-order term in the expansion is $H \text{Tr} F^2$ [116–118] where after Wick-contracting the Higgs field, what is left to compute is precisely a form factor of partons in the theory of interest, which we will take to be pure Yang-Mills. In this setting we focus on form factors of operators of the form $\text{Tr} F^n$, for $n = 2, 3, 4$, both in the minimal and non-minimal case up to four external gluons. The key point of the extension of the dimensional reconstruction method we discuss is that it can be applied to generic form factors of operators involving vector fields. Furthermore, it is important to stress that the expectation is that generalizing the procedure to higher loop orders, one needs to perform the same computation in multiple dimensions so to extract the dependence on D through interpolation. However, the method we propose requires evaluations in only one dimension independently of the loop-order one

wants to consider, thus bypassing what was one major drawback of the dimensional reconstruction.

We conclude the thesis with some remarks and discussion of future directions, followed by some auxiliary material required to reproduce the results presented in the main discussion. These appendices include among others all the three-point tree-level amplitudes of the standard model used as seeds for the recursive algorithm presented in Chapter 3, the tree-level amplitudes needed for the unitarity calculations in the EFTs of gravity considered in Chapter 5 and 6 and the six-dimensional amplitudes and non-minimal form factors needed in Chapter 7. Furthermore, we also included the expression of the relevant one-loop integrals used throughout the thesis.

Note: In the field of modern-day amplitudes it is often essential to use dedicated symbolic computational software, such as `Mathematica` [119], in order to carry out the computations of interest. Instead of the implementation of single-use codes, I decided to invest some² time in the development of dedicated `Mathematica` packages which would allow to reproduce results easily and could be shared with the rest of the scientific community, in line with the spirit of the SAGEX collaboration. In particular, the packages I implemented include routines to deal with the four-dimensional and six-dimensional spinor-helicity formalism (symbolically as well as numerically), and the complete implementation of the algorithm for the computation of tree-level amplitudes and non-minimal form factors described in Chapter 3. These packages will be made available shortly at the github repository <https://github.com/acsettullihuber>.

²Often a considerable amount actually...

Chapter 2

An invitation to tree-level techniques

We start by reviewing some well known tree-level techniques, including the powerful spinor-helicity formalism in four dimensions and two different recursion relations for the computation of amplitudes: the Berends-Giele and BCFW recursion. Focusing on the latter, we will discuss advantages and limitations, setting the stage for the algorithm introduced in Section 3.

2.1 Spinor helicity formalism

In this section we review the four-dimensional spinor-helicity formalism, which lies at the core of many applications discussed in this thesis, with the main purpose of setting our notations and conventions. We limit our discussion to Weyl spinors only, which are our building blocks of choice. For a more detailed review of the topic see for example [120–123].

Weyl spinors from fermion fields

Recall first of all that given a spin- $\frac{1}{2}$ particle, it can be described by the fermion field

$$\psi(x) = \int \frac{d^3\vec{p}}{(2\pi)^3} \frac{1}{\sqrt{2E_{\mathbf{p}}}} \sum_{s=1,2} \left(a_s(\vec{p}) u_s(\vec{p}) e^{-ip \cdot x} + b_s^\dagger(\vec{p}) v_s(\vec{p}) e^{ip \cdot x} \right), \quad (2.1)$$

and its conjugate, where u_s and v_s are four-component Dirac spinors, satisfying the momentum-space Dirac equation which for massless particles reduces to

$$i\not{\partial}\psi(x) = 0 \quad \Rightarrow \quad \begin{cases} \not{p}u_s(p) = 0 \\ \not{p}v_s(p) = 0 \end{cases}, \quad (2.2)$$

where $\not{p} = p_\mu \gamma^\mu$ with γ^μ satisfying the Clifford algebra relation $\{\gamma^\mu, \gamma^\nu\} = \eta^{\mu\nu}$. Also, in this thesis we consider a mostly minus convention for the space-time metric.

Clearly, up to normalization conventions, positive and negative energy solutions to (2.2) will be the same. When considering massless particles, helicity is a Lorentz-invariant quantity and it is thus convenient to describe particles in terms of definite helicity solutions to the Dirac equation. Such solutions can be obtained by applying the following projectors¹

$$u_\pm(p) \equiv \frac{\mathbb{1} \pm \gamma_5}{2} u_s(p) \quad \text{and} \quad \bar{u}_\pm(p) = \bar{u}_s(p) \frac{\mathbb{1} \mp \gamma_5}{2}, \quad (2.3)$$

in the fermionic case or equivalently in the anti-fermionic case

$$v_\mp(p) \equiv \frac{\mathbb{1} \pm \gamma_5}{2} v_s(p) \quad \text{and} \quad \bar{v}_\mp(p) = \bar{v}_s(p) \frac{\mathbb{1} \mp \gamma_5}{2}. \quad (2.4)$$

These definite helicity solutions take a particularly simple form when considering the Weyl representation of the gamma matrices

$$\gamma^\mu = \begin{pmatrix} 0 & \sigma^\mu \\ \bar{\sigma}^\mu & 0 \end{pmatrix}, \quad \gamma_5 = \begin{pmatrix} -\mathbb{1}_2 & 0 \\ 0 & \mathbb{1}_2 \end{pmatrix}, \quad (2.5)$$

where $\sigma^\mu = \{\mathbb{1}_2, \vec{\sigma}\}$ and $\bar{\sigma}^\mu = \{\mathbb{1}_2, -\vec{\sigma}\}$ such that the Clifford algebra relation $\{\sigma^\mu, \bar{\sigma}^\nu\} = \eta^{\mu\nu}$ holds. In this representation one can write

$$u_-(p) = v_+(p) = \begin{pmatrix} |p\rangle \\ 0 \end{pmatrix}, \quad u_+(p) = v_-(p) = \begin{pmatrix} 0 \\ |p] \end{pmatrix}, \quad (2.6)$$

and

$$\bar{u}_+(p) = \bar{v}_-(p) = \left(\langle p| \quad 0 \right), \quad \bar{u}_-(p) = \bar{v}_+(p) = \left(0 \quad [p| \right), \quad (2.7)$$

where $|p\rangle$ and $|p]$ is the so called bracket notation for the two-component objects $\lambda_\alpha(p)$ and $\tilde{\lambda}^{\dot{\alpha}}(p)$, with $\alpha, \dot{\alpha} = 1, 2$. These objects are the *Weyl spinors* in terms of which we will write the scattering amplitudes of all the theories considered in this thesis.

While the introduction of Weyl spinors from helicity projections of fermionic fields might provide a good textbook introduction to these objects, it somewhat obscures their deeper and more fundamental nature. Following the guiding philosophy underlying on-shell methods, we would ideally like to avoid using gauge-dependent quantities and focus our attention only on objects with a more direct physical interpretation where redundancies are cut down as much as possible. In this light quantum fields are not the building blocks we want to consider, and instead we use the Weyl spinors in virtue of their intimate relation with the Lorentz-invariance of a given theory, be this a theory

¹The projectors $P^\pm = \frac{1}{2}(\mathbb{1} \pm \gamma_5)$ are actually chirality projectors, but for massless particles helicity and chirality coincide for positive energy solutions and are opposite for negative energy solutions.

including fermions or not.

Weyl spinors and the Lorentz group

The starting point for defining the Weyl spinors λ and $\tilde{\lambda}$ is Lorentz-invariance, a property which we expect from any theory consistent with special relativity. The proper orthochronous Lorentz group $\text{SO}^+(1, 3)$ admits a universal covering given by $\text{SL}(2, \mathbb{C})$, consequently there is a one-to-one correspondence between projective representations of $\text{SO}^+(1, 3)$ on the Hilbert space and the infinite-dimensional unitary representations of $\text{SL}(2, \mathbb{C})$. The states of the theory transform under such unitary representations and induce the fields to transform under finite-dimensional (non-unitary) representation. All the irreducible finite-dimensional representations of $\text{SL}(2, \mathbb{C})$ are labelled by a pair of semi-integers (m_L, m_R) ², and can be obtained from completely symmetrized tensor products of $2m_L$ copies of the fundamental and $2m_R$ copies of the anti-fundamental representations, usually denoted as $(\frac{1}{2}, 0)$ and $(0, \frac{1}{2})$. The fundamental two-dimensional objects transforming in the $(\frac{1}{2}, 0)$ are denoted by λ_α and the associated Lorentz indices are greek undotted letters, whereas $\tilde{\lambda}^{\dot{\alpha}}$ transform in the $(0, \frac{1}{2})$ and the associated indices are dotted greek letters. The spinor indices can be raised and lowered by contraction with a two-dimensional Levi-Civita tensor as

$$\lambda^\alpha = \epsilon^{\alpha\beta} \lambda_\beta, \quad \tilde{\lambda}_{\dot{\alpha}} = \epsilon_{\dot{\alpha}\dot{\beta}} \tilde{\lambda}^{\dot{\beta}}, \quad (2.8)$$

where in our convention

$$\epsilon^{12} = -\epsilon_{12} = \epsilon^{i\dot{2}} = -\epsilon_{i\dot{2}} = 1, \quad (2.9)$$

and

$$\epsilon_{\alpha\beta} \epsilon^{\beta\gamma} = \delta_\alpha^\gamma. \quad (2.10)$$

From here on whenever we will call the two-component Weyl spinors simply spinors, and in order to avoid an often unnecessary cluttering of indices, we introduce the standard shorthand bracket notation (as already used in (2.6) and (2.7)):

$$\lambda_{i\alpha} \equiv |\lambda_i\rangle \equiv |i\rangle, \quad \tilde{\lambda}_i^{\dot{\alpha}} \equiv |\tilde{\lambda}_i\rangle \equiv |i\rangle, \quad \lambda_i^\alpha \equiv \langle \lambda_i| \equiv \langle i|, \quad \tilde{\lambda}_{i\dot{\alpha}} \equiv [\tilde{\lambda}_i| \equiv [i|, \quad (2.11)$$

where we use latin letters, i in this case, as momentum labels.

Lorentz-invariant structures are then simply built by complete contractions of the spinor indices, in the simplest case this amounts to pairing left and right angle/square brackets

²Recall that the algebra $\mathfrak{sl}(2, \mathbb{C})$ is isomorphic to $\mathfrak{su}(2)_L \times \mathfrak{su}(2)_R$, and (m_L, m_R) are related to the eigenvalues of the Casimir operators $\mathbf{J}_{L/R}^2 = (J_{L/R}^1)^2 + (J_{L/R}^2)^2 + (J_{L/R}^3)^2$, with $J_{L/R}^i$ generators of the $\mathfrak{su}(2)_{L/R}$. Elements of the two-dimensional vector space $\mathfrak{su}(2)_L$ will be denoted with λ and elements of $\mathfrak{su}(2)_R$ with $\tilde{\lambda}$.

respectively as follows

$$\begin{aligned}\langle i j \rangle &:= \langle \lambda_i \lambda_j \rangle := \lambda_i^\alpha \lambda_{j\alpha} = -\langle j i \rangle, \\ [i j] &:= [\tilde{\lambda}_i \tilde{\lambda}_j] := \tilde{\lambda}_{i\dot{\alpha}} \tilde{\lambda}_j^{\dot{\alpha}} = -[j i],\end{aligned}\tag{2.12}$$

these contractions will be called *angle* and *square brackets* respectively. Before moving on to the construction of massless momenta from the spinor brackets, we stress the following very useful property of the brackets. Given a triplet of spinors λ_i^α , λ_j^β , λ_k^γ any completely antisymmetrized combination of them gives zero, thus upon contraction with a single Levi-Civita tensor one gets the so called Schouten identity

$$\langle i j \rangle \langle k | + \langle j k \rangle \langle i | + \langle k i \rangle \langle j | = 0,\tag{2.13}$$

and analogously for the $\tilde{\lambda}$ spinors

$$[i j][k] + [j k][i] + [k i][j] = 0.\tag{2.14}$$

An alternative way for deriving the Schouten identity is to make use of the fact that λ (and $\tilde{\lambda}$) is defined on a two-dimensional vector space, thus it is always true that

$$\lambda_i^\alpha = a \lambda_j^\alpha + b \lambda_k^\alpha,\tag{2.15}$$

for some scalar coefficients a and b . The latter can be easily determined by contracting this identity left and right with $\lambda_{j\alpha}$ and $\lambda_{k\alpha}$ which thanks to the antisymmetry of the brackets directly leads to

$$\langle i | = \frac{\langle i k \rangle}{\langle j k \rangle} \langle j | + \frac{\langle i j \rangle}{\langle k j \rangle} \langle k |,\tag{2.16}$$

which is exactly (2.13).

Massless momenta

Given a Lorentz four-vector p^μ , it can be shown that the corresponding finite-dimensional representation of $\text{SL}(2, \mathbb{C})$ is $(\frac{1}{2}, \frac{1}{2})$. The map between the two representations can be explicitly realized through

$$p_{\alpha\dot{\alpha}} := p_\mu \sigma_{\alpha\dot{\alpha}}^\mu = \begin{pmatrix} p_0 - p_3 & -(p_1 - ip_2) \\ -(p_1 + ip_2) & p_0 + p_3 \end{pmatrix},\tag{2.17}$$

and similarly for $p^{\dot{\alpha}\alpha} := \epsilon^{\dot{\alpha}\beta} \epsilon^{\alpha\beta} p_{\beta\dot{\beta}}$. If p^μ is the momentum associated to a particle of mass m , it is easy to see that

$$m^2 = p^2 = \det(p_{\alpha\dot{\alpha}}) = \frac{1}{2} p^{\dot{\alpha}\alpha} p_{\alpha\dot{\alpha}}.\tag{2.18}$$

If we consider now a *massless particle*, the masslessness condition given by the vanishing of the determinant of $p_{\alpha\dot{\alpha}}$ is trivialized by setting

$$p_{\alpha\dot{\alpha}} = \lambda_{\alpha}\tilde{\lambda}_{\dot{\alpha}}, \quad (2.19)$$

due the antisymmetry of the angle and square brackets. Furthermore, notice that in momentum space the massless Dirac equation translates into

$$\begin{cases} p_{\alpha\dot{\alpha}}\lambda_p^{\alpha} = 0 \\ p_{\alpha\dot{\alpha}}\tilde{\lambda}_p^{\dot{\alpha}} = 0 \end{cases} \quad (2.20)$$

which is again automatically satisfied by writing the momentum as in equation (2.19).

We can associate a vector p^{μ} to a momentum given in the spinor representation $p_{\alpha\dot{\alpha}}$ through the inverse map of equation (2.17), given by

$$p^{\mu} = \frac{1}{2}\langle p \sigma^{\mu} p \rangle = \frac{1}{2}[p \bar{\sigma}^{\mu} p]. \quad (2.21)$$

When considering a momentum $k = -p$, it is easy to see from equation (2.19) that we can write the spinors λ_k and $\tilde{\lambda}_k$ in terms of λ_p and $\tilde{\lambda}_p$, simply by defining

$$\lambda_{-p}^{\alpha} \equiv i\lambda_p^{\alpha}, \quad \tilde{\lambda}_{-p}^{\dot{\alpha}} \equiv i\tilde{\lambda}_p^{\dot{\alpha}}. \quad (2.22)$$

Notice that this is a convention, and in general one could set $\lambda_{-p}^{\alpha} \equiv e^{i\phi}\lambda_p^{\alpha}$ and $\tilde{\lambda}_{-p}^{\dot{\alpha}} \equiv e^{i\theta}\tilde{\lambda}_p^{\dot{\alpha}}$ as long as $e^{i(\phi+\theta)} = e^{i\pi} = -1$, the advantage of our choice being the symmetry of the relations. The spinors λ and $\tilde{\lambda}$ are in general complex-valued, and the reality condition on the momentum p^{μ} , see equation (2.21), translates into

$$\lambda = \tilde{\lambda}^* \quad (2.23)$$

up to an arbitrary phase which we set to 1. Usually one is rather lenient towards this condition, since it turns out that, both in some analytic and numeric settings it is very convenient to allow for complex momenta³. Notice that there is no unique way of associating spinors to a given momentum p^{μ} , since the rescaling

$$\lambda \mapsto t\lambda, \quad \tilde{\lambda} \mapsto \frac{1}{t}\tilde{\lambda} \quad (2.24)$$

clearly leaves the momentum invariant. Here $t \in \mathbb{C}$ in general whereas it is just a complex phase if equation (2.23) applies. Equation (2.24) is called little group scaling, and it implements at the level of spinors those Lorentz transformations which preserve the given momentum. One possible explicit parametrization of the spinors in terms of

³Or alternatively to consider a different space-time signature [124], which similarly invalidates equation (2.23).

the momentum is given by

$$|p\rangle = \begin{pmatrix} -\frac{p_1 - ip_2}{\sqrt{p_0 + p_3}} \\ \sqrt{p_0 + p_3} \end{pmatrix}, \quad [p] = \begin{pmatrix} \sqrt{p_0 + p_3} \\ \frac{p_1 + ip_2}{\sqrt{p_0 + p_3}} \end{pmatrix}, \quad (2.25)$$

and

$$\langle p| = \left(\sqrt{p_0 + p_3} \quad \frac{p_1 - ip_2}{\sqrt{p_0 + p_3}} \right), \quad [p| = \left(-\frac{p_1 + ip_2}{\sqrt{p_0 + p_3}} \quad \sqrt{p_0 + p_3} \right), \quad (2.26)$$

which can be checked to satisfy (2.19) and (2.21). We stress here that spinors are not rational functions of the momentum components, which in later sections will be a crucial motivation for us to choose spinors rather than momenta as our fundamental objects. Notice also that considering natural units, the mass-dimension of the momentum is one, thus as can be seen from the explicit parametrization, or equivalently from (2.19), one has that λ and $\tilde{\lambda}$ have mass dimension $\frac{1}{2}$. This fact will be used extensively in subsequent discussions.

When discussing processes involving particles of spin one, polarization vectors are usually required. In our conventions these can be written as

$$\varepsilon_+^{\dot{\alpha}\alpha}(p, r) = \sqrt{2} \frac{\tilde{\lambda}_p^{\dot{\alpha}} \lambda_r^\alpha}{\langle r p \rangle} = \sqrt{2} \frac{|p\rangle \langle r|}{\langle r p \rangle}, \quad \varepsilon_-^{\dot{\alpha}\alpha}(p, r) = \sqrt{2} \frac{\tilde{\lambda}_r^{\dot{\alpha}} \lambda_p^\alpha}{[p r]} = \sqrt{2} \frac{|r\rangle \langle p|}{[p r]}, \quad (2.27)$$

or equivalently as vectors

$$\varepsilon_+^\mu(p, r) = \frac{1}{\sqrt{2}} \frac{\langle r \sigma^\mu p \rangle}{\langle r p \rangle}, \quad \varepsilon_-^\mu(p, r) = \frac{1}{\sqrt{2}} \frac{\langle p \sigma^\mu r \rangle}{[p r]}. \quad (2.28)$$

It can be checked that these satisfy all the properties required for polarization vectors which (in the Lorentz gauge) read:

$$\begin{aligned} \varepsilon_+(p, r)^* &= \varepsilon_-(p, r), & p_\mu \varepsilon_\pm^\mu(p, r) &= 0, \\ |\varepsilon_\pm(p, r)|^2 &= -1, & \varepsilon_+(p, r) \cdot \varepsilon_-(p, r)^* &= 0. \end{aligned} \quad (2.29)$$

The arbitrariness of the reference vector can be seen by taking the difference of two polarizations computed with different reference vectors r and s which leads to:

$$\varepsilon_\pm^\mu(p, r) - \varepsilon_\pm^\mu(p, s) = f_\pm(p, r, s) p^\mu, \quad (2.30)$$

where f_\pm is a rational function of spinor brackets involving p, r, s , and is thus a Lorentz scalar⁴. In other words, the polarizations $\varepsilon_\pm^\mu(p, r)$ and $\varepsilon_\pm^\mu(p, s)$ differ by a quantity proportional to the four-momentum p^μ , which means that once they are dotted into an

⁴For an explicit calculation of f_\pm in the spinor helicity formalism see for example [125].

onshell amplitude the Ward identity ensures their complete physical equivalence.

Given two massless momenta p_i and p_j , the associated Mandelstam invariant is defined as

$$s_{ij} := (p_i + p_j)^2 = 2p_i \cdot p_j = p_i^{\dot{\alpha}\alpha} p_{j\alpha\dot{\alpha}} = \langle i j \rangle [j i], \quad (2.31)$$

where, using $|p\rangle[p] = p$ for massless momenta, we can rewrite

$$\langle i j \rangle [j i] = \langle i j i \rangle. \quad (2.32)$$

We will refer to structures such as this as chains. Other examples of chains include

$$\begin{aligned} \langle q p_1 \dots p_{2n} k \rangle &= -\langle k p_{2n} \dots p_1 q \rangle \\ [q p_1 \dots p_{2n} k] &= -[k p_{2n} \dots p_1 q] \\ [q p_1 \dots p_{2n+1} k] &= \langle k p_{2n+1} \dots p_1 q \rangle \end{aligned} \quad (2.33)$$

where the p_i are not necessarily massless.

Finally we close this subsection by giving another useful identity, known as Fierz rearrangement, for the σ matrices it can be shown that the following holds:

$$\sigma_{\alpha\dot{\alpha}}^\mu \bar{\sigma}_\mu^{\dot{\beta}\beta} = 2\delta_\alpha^\beta \delta_{\dot{\alpha}}^{\dot{\beta}}, \quad (2.34)$$

which leads to the spinorial identity

$$\langle i \sigma^\mu j \rangle [k \bar{\sigma}_\mu l] = 2\langle i l \rangle [k j]. \quad (2.35)$$

Massive momenta

Considering massive particles, while equation (2.17) still applies, equation (2.19) does not hold anymore. It is nonetheless still possible to write the momentum directly in terms of the spinors λ and $\tilde{\lambda}$, by simply considering it as a linear combination of two massless momenta [126]

$$P^\mu := q^\mu + \frac{m^2}{2q \cdot k} k^\mu \quad \rightarrow \quad P_{\alpha\dot{\alpha}} = \lambda_\alpha \tilde{\lambda}_{\dot{\alpha}} + \frac{m^2}{\langle k q \rangle [q k]} \mu_\alpha \tilde{\mu}_{\dot{\alpha}}, \quad (2.36)$$

with $q^2, k^2 = 0$ and $q_{\alpha\dot{\alpha}} = \lambda_\alpha \tilde{\lambda}_{\dot{\alpha}}$ and $k_{\alpha\dot{\alpha}} = \mu_\alpha \tilde{\mu}_{\dot{\alpha}}$. Notice that counting the number of (real) degrees of freedom of the spinors in equation (2.36) one finds three too many. These are spurious degrees of freedom corresponding to the little-group transformations of the massive momentum, which in four dimensions is implemented by an $\text{SO}(3)$ subgroup of the Lorentz group. Just as the massless spinors defined up to the transformation (2.24) are equivalent, one can use these spurious degrees of freedom to set the spinors associated to k to arbitrary values. We will refer to μ and $\tilde{\mu}$ as reference spinors.

From equation (2.36), a possible approach is to define a pair of spinors associated to the massive momentum P through

$$|P\rangle = |q\rangle + \frac{m}{[qk]}|k\rangle, \quad |P] = |q] + \frac{m}{\langle qk\rangle}|k], \quad (2.37)$$

which have very different properties compared to the massless spinors, for example if P and K are massive then in general for these new massive spinors one has $\langle PK\rangle \neq 0$. The advantage of the decomposition of equation (2.36) is that it allows to recycle much of the technology introduced for massless particles. The price to pay however is that certain symmetries of the amplitude are obscured, in particular the covariance of the amplitude under little group transformations of the massive momenta. To make such property manifest it is more convenient to introduce a new set of spinors $\lambda_\alpha^I, \tilde{\lambda}_{\dot{\alpha}}^I$, carrying an additional SU(2) index⁵, accounting explicitly for little group transformations [127]. We then have

$$P_{\alpha\dot{\alpha}} = \lambda_\alpha^I \tilde{\lambda}_{\dot{\alpha}I} = \epsilon_{IJ} \lambda_\alpha^I \tilde{\lambda}_{\dot{\alpha}}^J, \quad (2.38)$$

and the massive equivalent relation of (2.24) reads $\lambda_\alpha^I \rightarrow U_J^I \lambda_\alpha^J$ for $U_J^I \in \text{SU}(2)$. It can be shown that the previously introduced spinors $|P\rangle$ and $|P]$ simply correspond to a specific choice of the λ_α^I and $\tilde{\lambda}_{\dot{\alpha}}^I$, where the little group index has been fixed.

2.2 Little-group transformations and the three-point amplitudes

The little group is defined as the subgroup of the Lorentz group which leaves a given momentum p invariant. In general, in D dimensions, a one-particle state can be defined by a ket $|p^\mu, \sigma\rangle$ in a Hilbert space \mathcal{H} , where p is the particles momentum and σ represents any other label the particle could carry, an example being helicity in the case of massless particles. Under a Lorentz transformation the ket transforms as

$$|p^\mu, h\rangle \mapsto \sum_{h'} G_{hh'} |\Lambda^\mu{}_\nu p^\nu, h'\rangle \quad (2.39)$$

where Λ and G are Lorentz and little group transformations respectively. Considering now a scattering amplitude \mathcal{A}_n involving n particles whose spin is labelled by h_i , equation (2.39) leads to a transformation of the amplitude which can be schematically represented as

$$\mathcal{A}_n \mapsto \varphi(h_1, \dots, h_n) \mathcal{A}_n. \quad (2.40)$$

In general φ is a tensor determined by the little group transformations of all the particles involved in the scattering, or in other words by the spins h_i , and is such that $\varphi^\dagger \varphi = 1$.

⁵While for massless spinors the little group is just an U(1) phase, for massive particles in four dimensions is given by SU(2).

Scattering amplitudes are thus little group *covariant*, whereas the modulus squared of the amplitude is *invariant* under the whole Lorentz group, as it should⁶.

Considering the case of massless particles in four space-time dimensions, ϕ is a simple U(1) phase. More specifically, when considering the amplitude as a rational function of the spinors λ_i , $\tilde{\lambda}_i$ and helicities h_i of the external particles, one has that [124]

$$\left(\lambda_i \frac{\partial}{\partial \lambda_i} - \tilde{\lambda}_i \frac{\partial}{\partial \tilde{\lambda}_i} \right) \mathcal{A}_n(\{\lambda_i, \tilde{\lambda}_i, h_i\}) = -2h_i \mathcal{A}_n(\{\lambda_i, \tilde{\lambda}_i, h_i\}), \quad (2.41)$$

in other words the difference between the number of $|i\rangle$ and $|\bar{i}\rangle$ spinors in the amplitude is proportional to the helicity h_i . Thus, applying the little-group transformation

$$|i\rangle \mapsto t_i |i\rangle, \quad |\bar{i}\rangle \mapsto \frac{1}{t_i} |\bar{i}\rangle, \quad t_i \in \mathbb{C} \quad (2.42)$$

the amplitude transforms as

$$\mathcal{A}_n(\{\lambda_i, \tilde{\lambda}_i, h_i\}) \mapsto t_i^{-2h_i} \mathcal{A}_n(\{\lambda_i, \tilde{\lambda}_i, h_i\}). \quad (2.43)$$

Notice that equation (2.43) is valid at any loop order. Depending on the application at hand, it might be convenient to factor the amplitude into a little-group covariant part which we call Φ_n and depends only on the helicity of the particles, and a little-group invariant part, which can be thought of as a rational function of the Mandelstam invariants (at tree level). The expression for Φ_n can be fixed a priori but except for specific cases it is usually not unique.

The little-group scaling provides a great deal of information, and in some instances especially at low multiplicities it suffices to determine the complete expression of the kinematic part of the amplitude up to a constant. A neat example of this situation is represented by the three-gluon tree-level amplitude in Yang-Mills theory. What one would usually do is start from the Yang-Mills lagrangian

$$\mathcal{L}_{\text{YM}} = -\frac{1}{4} F_{\mu\nu}^a F^{a\mu\nu}, \quad \text{with} \quad F_{\mu\nu}^a = \partial_\mu A_\nu^a - \partial_\nu A_\mu^a + g_{YM} f^{abc} A_\mu^b A_\nu^c, \quad (2.44)$$

where g_{YM} is the coupling and f^{abc} are the SU(3) structure constants, then take appropriate functional derivatives to get the relevant Feynman rules, in particular the three-point vertex rule, and then contract the latter with polarization vectors to get the three-point amplitude. Let us approach the problem from a different angle: we start off from a theory which involves spin one massless particles, the gluons, and which we want to be self interacting and thus admit a three-point vertex. For the time being we disregard the colour part of the amplitude, since we will get back to it in more detail

⁶ $|\mathcal{A}|^2$ enters the cross-section which is a physical observable and must thus be invariant under the Lorentz group.

later in section 3.1, but we will still use the same notation \mathcal{A}_n of the full amplitude when discussing only the kinematic part, since there is usually no risk of confusion.

The theory we consider should of course satisfy locality and Lorentz-invariance, and we want to find the expression for the three-gluon on-shell amplitude if it exists. First, if we were to consider the Mandelstam invariants as building blocks for this amplitude, it would trivially vanish since all the invariants themselves are vanishing. In fact, due to $p_1 + p_2 + p_3 = 0$ and the masslessness of the particles one has

$$s_{12} = \langle 1 2 \rangle [2 1] = 0, \quad s_{23} = \langle 2 3 \rangle [3 2] = 0, \quad s_{13} = \langle 1 3 \rangle [3 1] = 0. \quad (2.45)$$

Indeed $\mathcal{A}_3 = 0$ is the correct answer, provided we limit ourselves to consider only momenta which are real. If we allow momenta to be complex we can do better [128], since releasing this constraint invalidates (2.23), and thus $\langle ij \rangle = 0$ does not imply $[ij] = 0$ anymore and viceversa. This allows us to satisfy equation (2.45) by imposing the vanishing of all the angle or square brackets and then using the set of non-vanishing brackets (which are Lorentz-invariant and little-group covariant structures) to write the amplitude. Considering for example $[ij] = 0$, since there are no other invariants for the amplitude to depend on it must be of the form

$$\mathcal{A}_3(1^{h_1}, 2^{h_2}, 3^{h_3}) = c \langle 1 2 \rangle^{x_3} \langle 2 3 \rangle^{x_1} \langle 1 3 \rangle^{x_2}, \quad (2.46)$$

where the little-group transformation, equation (2.43), fixes $x_1 = h_1 - h_2 - h_3$, $x_2 = h_2 - h_3 - h_1$ and $x_3 = h_3 - h_1 - h_2$. Taking into account that the three-point amplitude must have mass dimension one⁷, only one helicity configuration for the gluons is allowed, namely $(-, -, +)$, leading to the three-point Yang-Mills amplitude

$$\mathcal{A}_3^{\text{MHV}}(1^-, 2^-, 3^+) = g_{YM} \frac{\langle 1 2 \rangle^3}{\langle 1 3 \rangle \langle 2 3 \rangle}, \quad (2.47)$$

where we included the dimensionless Yang-Mills coupling. A similar reasoning applies to the case where $\langle ij \rangle = 0$, from which we obtain⁸

$$\mathcal{A}_3^{\overline{\text{MHV}}}(1^+, 2^+, 3^-) = -g_{YM} \frac{[1 2]^3}{[1 3][2 3]}. \quad (2.48)$$

The reason why the all-plus and all-minus helicity configurations are not allowed, is that they would produce a spinor bracket expression of mass-dimension three, which would require a dimensionfull coupling constant of dimension -2 to compensate. In fact similar amplitudes do appear in non-renormalizable theories including an F^3 interaction,

⁷For now we take this as a given, we will further comment on mass dimension in Section 3.1

⁸The inclusion of the minus sign in the following expression is due to the additional condition we impose that the parity-conjugate of the anti-MHV should be the MHV amplitude.

but are prohibited in pure Yang-Mills which we are considering here

$$\mathcal{A}_3(1^+, 2^+, 3^+) = 0, \quad \mathcal{A}_3(1^-, 2^-, 3^-) = 0. \quad (2.49)$$

There is a simple argument [120] based on the counting of internal three-gluon vertices, which combined with a smart choice of the reference vectors in the external polarizations, allows to show that actually the all-plus and single-minus configurations (as well as their parity conjugates all-minus and single-plus) vanish at tree-level for any number of gluons

$$\mathcal{A}_n^{tree}(1^+, 2^+, \dots, i^\pm, \dots, n^+) = 0. \quad (2.50)$$

Remarkably, there is also a direct generalisation of equation (2.47) and (2.48) to arbitrary n , known as Parke-Taylor tree amplitudes [15, 16]

$$\begin{aligned} \mathcal{A}_n^{\text{MHV}}(1^+, \dots, i^-, \dots, j^-, \dots, n^+) &= i g_{\text{YM}} \frac{\langle i j \rangle^4}{\langle 1 2 \rangle \langle 2 3 \rangle \cdots \langle n-1 n \rangle \langle n 1 \rangle}, \\ \mathcal{A}_n^{\overline{\text{MHV}}}(1^-, \dots, i^+, \dots, j^+, \dots, n^-) &= i g_{\text{YM}} \frac{[i j]^4}{[1 2][2 3] \cdots [n-1 n][n 1]}, \end{aligned} \quad (2.51)$$

which are usually referred to as Maximally Helicity Violating (MHV) amplitudes. For $n > 3$ complexification of momenta is no longer required, also the vanishing of all the angle or square brackets respectively does not hold any more. The proof of equation (2.51) can be achieved inductively using either the Berends-Giele off-shell recursion or the BCFW on-shell recursion, see for example [121, 122]. It is important to stress that (2.51) is not the complete n -gluon amplitude, not even once the appropriate colour factors are restored and multiplied to the kinematic part, it is just one of the many colour-ordered sub-amplitudes constituting the complete result. Colour ordering is an extremely powerful property of Yang-Mills theory which allows to rewrite gluon tree-level amplitudes as a sum of terms each of which is constituted by a kinematic part and a colour part where the order of the gluons is fixed. Each term is gauge invariant on its own, and only a minimal number of colour ordered sub-amplitudes needs to be computed so that the full set can be recovered from symmetry relations and relabelling. We will not discuss colour ordering in further detail here since for the greater part of this thesis we are interested in gravity theories, where colour-ordering is not needed, and Effective Field Theories of the Standard Model, where colour-ordering does not apply. For a review of the topic we refer the reader for example to [120].

The takeaway message of this Section is that once the particle content of a (local and Lorentz-invariant) theory is specified, little-group scaling combined with mass-dimension analysis is sufficient to completely determine the on-shell three-point amplitudes of the theory thanks to (2.46), as first shown in [128]. This fact is immensely powerful since we will see how the combination of these simple seeds with unitarity en-

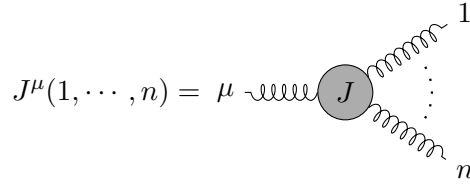


Figure 2.1: Graphical representation of the Berends-Giele current. The leg μ is off-shell, and has been obtained by stripping off a polarization vector from the amplitude and attaching an appropriate propagator to it, while legs from one to n are on-shell.

sure a completely consistent theory without need of a Lagrangian, see Chapter 3, and also how higher multiplicity interactions follow from the three point ones, for example through BCFW as described in Section 2.4 or more generally through the algorithm described in chapter 3.

2.3 An off-shell recursion: Berends-Giele

Before discussing how to compute higher-multiplicity amplitudes from on-shell lower-point seeds, we take a step back and try to understand why it is convenient to do so in the first place.

For the sake of simplicity let us stick with the Yang-Mills theory we already used as an example, and assume we want to get the n -gluon amplitude through a standard Feynman diagram calculation. This computation for $n = 4$ requires only four diagrams, for $n = 6$ it already becomes 220 and for $n = 10$ the number of diagrams is of order 10^7 [14]. The sheer combinatoric scale of the problem makes the Feynman diagrammatic approach more and more unappealing the higher the multiplicity, and clearly also the higher the loop-order which is affected by the same limitations. A very simple approach to this combinatorial problem, which does not bypass its limitations but rather allows to systematically account for all the different diagrams entering the calculation, is the Berends-Giele recursion relation [129] which generates tree-level amplitudes recursively in the number of external legs.

First of all one has to introduce an auxiliary quantity with one leg off-shell, a current which we will denote $J^\mu(1, \dots, n)$, see figure figure 2.1. The current J^μ is the sum of color-ordered $n + 1$ -point tree-level Feynman graphs, where legs $1, \dots, n$ are on-shell gluons and leg μ is off-shell, also an off-shell propagator carrying momentum $P_{1,n}^2 = (p_1 + \dots + p_n)^2$ attached to the uncontracted μ leg is defined to be included in the current. Notice that since J^μ is an off-shell quantity it is gauge-dependent, for example it depends on the reference momenta chosen for the polarization vectors, and consequently it must be kept fixed until an on-shell result has been extracted.

The Berends-Giele current can be shown to satisfy the following identities [120]:

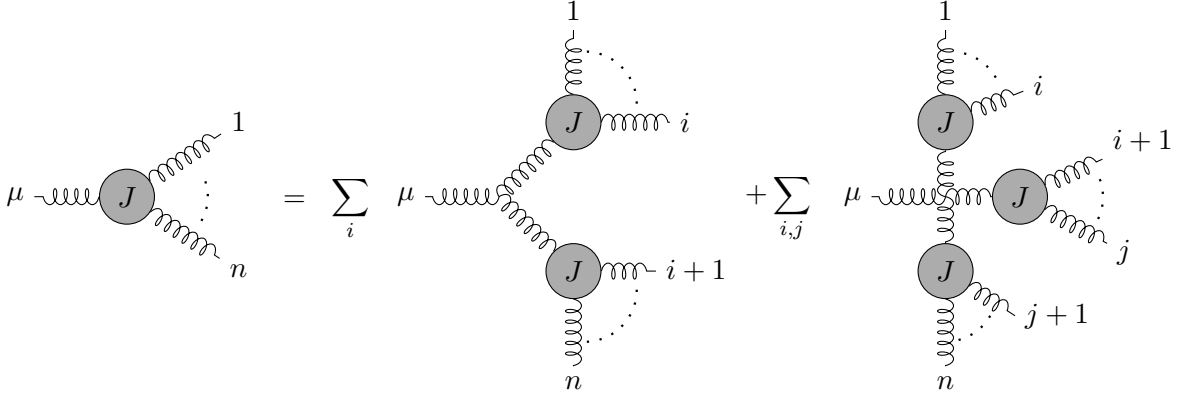


Figure 2.2: Graphical representation of the Berends-Giele recursion in pure Yang-Mills theory.

- photon decoupling relation

$$J^\mu(1, 2, 3, \dots, n) + J^\mu(2, 1, 3, \dots) + \dots + J^\mu(2, 3, \dots, n, 1) = 0, \quad (2.52)$$

- reflection identity

$$J^\mu(1, 2, \dots, n) = (-1)^{n+1} J^\mu(n, \dots, 2, 1), \quad (2.53)$$

- current conservation

$$P_{1,n}^\mu J_\mu(1, \dots, n) = 0. \quad (2.54)$$

At this point the recursion relation is easily established. Since we are considering only gluon interactions at tree-level, if we follow the off-shell line μ back inside the graph there are only two possible scenarios, either we encounter a three-point or a four-point gluon vertex. Attached to these vertices there will be subgraphs with exactly the same form as the initial J^μ we constructed, but with a lower number of on-shell legs, see figure 2.2. Thus the n -point amplitude will be expressible in terms of a sum over all the possible lower-point currents contracted with the three and four-point vertex:

$$J^\mu(1, \dots, n) = \frac{-i}{P_{1,n}^2} \left[\sum_{i=2}^{n-1} V_3^{\mu\nu\rho} J^\nu(1, \dots, i) J^\rho(i+1, \dots, n) + \sum_{i=2}^{n-2} \sum_{j=i+1}^{n-1} V_4^{\mu\nu\rho\sigma} J^\nu(1, \dots, i) J^\rho(i+1, \dots, j) J^\sigma(j+1, \dots, n) \right], \quad (2.55)$$

where $P_{l,m} = \sum_{i=l}^m p_i$ and the V_i are the color-ordered gluon self-interactions equation (2.56) and (2.57):

$$V_3^{\mu\nu\rho}(P, Q) = \frac{i}{\sqrt{2}} (\eta^{\nu\rho}(P-Q)^\mu + 2\eta^{\rho\mu}Q^\nu - 2\eta^{\mu\nu}P^\rho) \quad (2.56)$$

$$V_4^{\mu\nu\rho\sigma} = \frac{i}{2}(2\eta^{\mu\rho}\eta^{\nu\sigma} - \eta^{\mu\nu}\eta^{\rho\sigma} - \eta^{\mu\sigma}\eta^{\nu\rho}) \quad (2.57)$$

The recursion terminates when only currents of the form $J^\mu(i)$, $i \in \{1, \dots, n\}$ are left, which can be easily identified as the polarization vectors

$$J^\mu(i) = \varepsilon^\mu(p_i, q_i). \quad (2.58)$$

Finally in order to get the \mathcal{A}_{n+1} partial amplitude associated to J^μ one first amputates the off-shell propagator, then contracts with the appropriate polarization vector and takes the limit $P_{1,n}^2 = p_{n+1}^2 \rightarrow 0$. If we are not dealing with Yang-Mills theory, Berends-Giele can still be applied by knowing all the particle vertex interactions and then appropriately generalising the summation in (2.55).

From the perspective of finding the analytic expression of an amplitude, Berends-Giele is not the most effective method for two reasons. Assuming the calculation one is tackling goes beyond what can be achieved with pen and paper, computational software like Mathematica could have a hard time dealing with fully analytic input of the size of the one generated by the recursion: it is very likely that both the generation of the amplitude as well as any computation involving it will be very slow due to its size. The second reason is tightly related to the latter problem, the expression of the generated amplitude might present itself in a complicated form which upon use of appropriate identities like momentum conservation reduces to something much simpler. But the simplification process in itself is not trivial at all, so even when Berends-Giele successfully returns an analytic amplitude it might not give any particular insight at all due to its overcomplicated form. On the other hand, this recursion is extremely effective for numeric evaluations of amplitudes. Given a numerical kinematic for the external particles, meaning a set of conserved on-shell momenta and a numeric reference momentum, all the J_1^μ , namely the polarisations, can be easily generated and from there every step of the recursion is just a simple set of four numbers⁹, which translates in a very fast computation. From the perspective of getting an analytic form of the amplitude this might not seem very useful, but on the contrary in recent years many cutting edge (loop-level) results were obtained through reconstructing analytic expressions from numeric evaluations, consider [130–137] just to mention a few. These results rely heavily on the use of so called finite fields to perform fast numeric evaluations but at the same time avoiding precision loss typical of floating point numbers. Finite fields represent a key ingredient also in the algorithm presented in Chapter 3 and will be further discussed in Section 3.4.

⁹In this context the recursion is best performed bottom-up rather than top-down.

2.4 BCFW-like recursions

In this Section we discuss how to compute amplitudes from on-shell lower-point information through the Britto-Cachazo-Feng-Witten (BCFW) [12,13,138] recursion as well as related methods which we call BCFW-like. Once again we focus on Yang-Mills theory for simplicity, but at the end of the section we will dive deeper into generalisations to other theories, since this a critical aspect of the method.

The idea behind the recursion is to exploit the knowledge about the pole structure of tree level scattering amplitudes, in combination with a complex shift of the external kinematics $p_i \mapsto p_i(z)$ for some momenta i and $z \in \mathbb{C}$. This shift associates to the tree amplitude \mathcal{A} an auxiliary holomorphic function $\mathcal{A}(z)$, which is a rational function of z and only presents simple poles coming from intermediate propagators going onshell. As we will now see, the residues at these poles are products of lower-point onshell amplitudes, allowing thus a recursive calculation until the seed of the recursion is reached, *i.e.* until we are left with only three-point amplitudes.

The shift of the external kinematics is most conveniently performed at the level of spinors, in particular we choose the following shift convention:

$$\begin{aligned} |\hat{i}\rangle &\equiv |i\rangle, & |\hat{i}] &\equiv |i] + z|j], \\ |\hat{j}\rangle &\equiv |j\rangle - z|i\rangle, & |\hat{j}] &\equiv |j], \end{aligned} \tag{2.59}$$

which in terms of the momenta reads

$$\hat{p}_i = p_i + \frac{z}{2}\langle i\sigma j], \quad \hat{p}_j = p_j - \frac{z}{2}\langle i\sigma j]. \tag{2.60}$$

Notice that since $\hat{p}_i + \hat{p}_j = p_i + p_j$, momentum conservation is still satisfied, furthermore the property $\langle i\sigma^\mu j]\langle i\sigma_\mu j] = 0$ will be crucial in ensuring that only simple poles appear in the auxiliary function $\mathcal{A}(z)$. Consider then the quantity

$$\frac{1}{2\pi i} \oint_{C_R} \frac{i\mathcal{A}(z)dz}{z} \tag{2.61}$$

where C_R is a circle in the complex z plane centred at the origin and of radius R , see figure 2.3. As we take the limit of $R \rightarrow \infty$ we have that equation (2.61) evaluates to the sum of all the residues of the integrand on the complex plane, including the residue at infinity. For the time being we assume the latter residue to be zero, in other words we assume that the falloff of $\mathcal{A}(z)$ at infinity is at least as fast as $1/z$, condition which will be discussed in more detail towards the end of the section. Obviously, by construction one of the residues at finite values of z is found at $z = 0$, which can be immediately

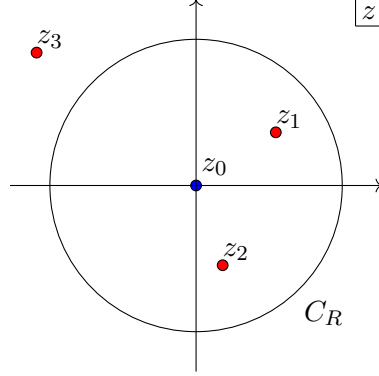


Figure 2.3: The complex z plane on which the function $\frac{\mathcal{A}(z)}{z}$ is defined. The residue associated to the pole in the origin corresponds to the physical tree-level amplitude we want to compute, while red dots represent other poles at finite values of z . Complex analysis ensures that the sum over all the residues in the complex plane vanishes, thus we can re-express the physical amplitude as a sum over all the residues z_α plus the residue at infinity.

recognized as the physical tree-level amplitude we want to compute. Thus, we can write

$$i\mathcal{A}(z=0) = \text{Res}_{z=0} \frac{i\mathcal{A}(z)}{z} = - \sum_{\text{poles } \alpha} \text{Res}_{z=z_\alpha} \frac{i\mathcal{A}(z)}{z}, \quad (2.62)$$

where the values z_α are all finite and are fixed by the poles of $\mathcal{A}(z)$, which can only arise from vanishing propagators, or in other words intermediate states going on-shell. In particular, since only propagators featuring a dependence on z can lead to poles, one has to consider all the possible partitions of the external momenta of the type represented in figure 2.4, where the tree diagram is split into two subdiagrams $\mathcal{A}_L(z)$ and $\mathcal{A}_R(z)$ each containing one of the shifted complex momenta \hat{p}_i, \hat{p}_j . The value of z for which the propagator carrying momentum $\hat{Q}(z) = p_a + \dots + \hat{p}_j + \dots + p_b$ diverges can be computed to be

$$z_{ab} = \frac{Q^2}{\langle i|Q|j \rangle}, \quad (2.63)$$

with $Q = \hat{Q}(0)$, and the associated residue is given by

$$\text{Res}_{z=z_{ab}} \frac{i\mathcal{A}(z)}{z} = i\mathcal{A}_L^\alpha(z_{ab}) \frac{i\eta_{\alpha\beta}}{Q^2} i\mathcal{A}_R^\beta(z_{ab}) \quad (2.64)$$

where we used the fact that

$$\lim_{z \rightarrow z_{ab}} \frac{z - z_{ab}}{z} \frac{1}{\hat{Q}^2(z)} = \frac{1}{Q^2}. \quad (2.65)$$

In equation (2.64), \mathcal{A}_L^α and \mathcal{A}_R^β are on-shell tree-level amplitudes but stripped of a polarization vector. To recover the complete amplitudes recall the completeness relation

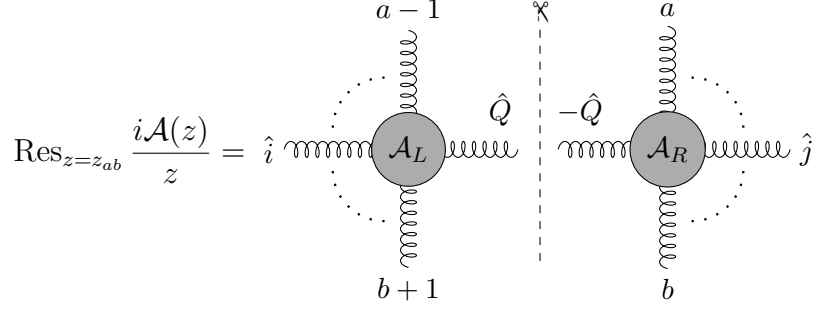


Figure 2.4: Graphic representation of one of the terms in the BCFW recursion. Poles at finite values of z can only come from internal propagators going on-shell, which in turn leads to a factorization into lower point on-shell amplitudes, which can then be recursively computed.

for polarization vectors

$$-\eta^{\mu\rho} = \epsilon_+^\mu(\hat{Q}, q)\epsilon_-^\rho(\hat{Q}, q) + \epsilon_-^\mu(\hat{Q}, q)\epsilon_+^\rho(\hat{Q}, q) - \frac{q^\rho\hat{Q}^\mu + q^\mu\hat{Q}^\rho}{q \cdot \hat{Q}}, \quad (2.66)$$

where q is an arbitrary reference vector and $\hat{Q} = \hat{Q}(z_{ab})$. Notice that due to the Ward identity the last term in equation (2.66) vanishes when dotted into \mathcal{A}_L or \mathcal{A}_R . We get then to the final expression for the physical tree-level amplitude

$$\mathcal{A}(z=0) = \sum_{a,b} \left[\mathcal{A}(b+1, \dots, a-1, \hat{Q}^\pm(z_{a,b})) \frac{1}{Q^2} \mathcal{A}(\hat{Q}^\mp(z_{a,b}), a, \dots, b) \right], \quad (2.67)$$

which is written in terms of lower-point on-shell tree amplitudes. These can be again computed in a similar fashion establishing the recursion and concluding the derivation. Notice how unitarity explicitly enters the derivation through the completeness relation (2.66).

As already mentioned, an important feature in establishing the recursion is the vanishing of the residue at infinity, which requires a sufficiently fast falloff of the holomorphic function $\mathcal{A}(z)$. The behaviour of $\mathcal{A}(z)$ at large z not only depends on the theory one is considering, but it turns out to depend also on the polarizations of the particles whose momenta have been shifted. For a detailed discussion of the topic we refer the interested reader to [139], where BCFW shifts of various theories are studied, and among others Yang-Mills and General Relativity in $D \geq 4$ dimensions. It can be shown that in the pure Yang-Mills case that we are considering, using the shift convention in equation (2.59), the worst possible falloff in relation to the polarizations of the particles i, j is given by

$$\mathcal{A}(z \rightarrow \infty) \sim \begin{array}{ccccc} (i, j) & (+, +) & (-, -) & (-, +) & (+, -) \\ \frac{1}{z} & \frac{1}{z} & \frac{1}{z} & z^3 & \end{array}, \quad (2.68)$$

which implies that for any given helicity configuration of the external particles there is always a suitable shift allowing to construct the amplitude through the BCFW recursion. An interesting example where the residue at infinity is non-vanishing is the $\lambda\phi^4$ theory, nonetheless it can be shown that tree-level amplitudes can still be computed recursively [121]. In fact, the interaction of the theory is so simple that the residue at infinity can be itself computed (also recursively), thus completely determining the n -point amplitude from the four-point interaction which is the seed of the recursion.

The BCFW recursion is certainly powerful and versatile, consider that it can be applied to supersymmetric theories [140–143], string theory [144, 145], theories involving massive particles [146–151] and theories in higher dimensions [152, 115], however it also comes with limitations, an example being its applicability to the Standard Model and Effective Field Theories. In order to make BCFW viable one needs to always make sure the residue at infinity vanishes, which is often not a trivial requirement.

Extensions of the BCFW recursion allow for applicability to a wider range of theories by shifting a larger number of external legs which then results in a better behaviour of $\frac{\mathcal{A}(z)}{z}$ at infinity and thus the vanishing of the residue at $z \rightarrow \infty$. The common foundation of these generalisations are (see for example [121]) that, given a set of conserved on-shell momenta $\{p_i\}_{i=1,\dots,n}$ and defining a set of complex valued vectors $\{q_i\}_{i=1,\dots,n}$, some of which possibly vanishing, which satisfy

- $\sum_i q_i = 0$
- $q_i \cdot q_j = 0$ for all $i, j = 1, \dots, n$
- $p_i \cdot q_i = 0$

One can define a new set of shifted momenta $\hat{p}_i = p_i + zq_i$ with $z \in \mathbb{C}$. It is easy to see that these new momenta still satisfy momentum conservation as well as $\hat{p}_i^2 = 0$, and furthermore propagators involving combinations of these momenta will have denominators which are at most linear in z , which is a crucial property to ensure all poles of the amplitude are simple poles. BCFW is then just a particular case which can be obtained for example by setting $q_1 = \langle 1 \sigma n \rangle$, $q_n = -\langle 1 \sigma n \rangle$ and $q_k = 0$ for $k = 2, \dots, n-1$. The simplest generalisation is to shift three external momenta, this can be done neatly through the so called Risager shift, which takes advantage of the Schouten identity (2.13) by setting

$$q_i = \langle j k \rangle \langle i \sigma \eta \rangle, \quad q_j = \langle k i \rangle \langle j \sigma \eta \rangle, \quad q_k = \langle i j \rangle \langle k \sigma \eta \rangle, \quad (2.69)$$

with η some reference spinor, so that

$$r_i + r_j + r_k = (\langle j k \rangle \langle i | + \langle k i \rangle \langle j | + \langle i j \rangle \langle k |) \sigma \eta = 0. \quad (2.70)$$

This shift allowed to establish a direct proof of the CSW rules [153] previously conjectured in [154]. Another common shifting scheme is the all-line shift where all the external momenta are shifted, in particular it is convenient to do so by acting once again directly at the level of the spinors. We define the anti-holomorphic shift (or equivalently the holomorphic shift where the roles of the angle and square brackets are swapped) to be given by

$$|i] \mapsto |\hat{i}] = |i] + z w_i |\eta], \quad |i\rangle \mapsto |i\rangle, \quad (2.71)$$

with the w_i satisfying $\sum_i w_i |i\rangle = 0$ and $|\eta]$ being once again an arbitrary reference spinor. It can be shown [155] under very general assumptions that with such a shift one has

$$\hat{\mathcal{A}}_n(z) \rightarrow z^s \text{ (or better) as } z \rightarrow \infty, \text{ with } 2s = 4 - n - c - \sum_i h_i, \quad (2.72)$$

where n is the number of external legs, c is the mass-dimension of the coupling and h_i are the helicities of the external states. This condition ensures the vanishing of the residue at infinity for a wide class of theories, which also includes EFTs [156–158]. This wider applicability compared to BCFW comes however at the price of introducing an arbitrary reference spinor $|\eta]$. At the end of the calculation the result will usually depend explicitly on such spinor despite actually being independent from it (independence can easily be verified through the generation of numerical kinematics), which means that ideally one needs to massage the result until the spinor dependence drops out. Clearly this is in general not a trivial task, even more so if it needs to be automated through some computer software. In the next chapter we will discuss an algorithm for the computation of tree-level amplitudes which has at the same time a wide spectrum of applicability but is free of the issues affecting BCFW-like recursions.

Chapter 3

On-shell bootstrapping of tree-level amplitudes

The computation of tree-level scattering amplitudes is a rather ubiquitous task in high-energy physics since it often represents either the starting point or a stepping stone for a variety of different calculations. Considering that state of the art results range from two-loop five parton interactions in QCD (see for example [133–135, 159]) to eight-loop three-point form factors in $\mathcal{N} = 4$ supersymmetric Yang-Mills [160], it would be only natural to consider tree-level a solved problem, which indeed it is. However only in principle: in practice the computation of trees within certain theories or at high multiplicities might still prove challenging. Clearly there are no conceptual obstructions to the computation of tree-amplitudes: given the Lagrangian of the theory one might be content with computing the Feynman rules, feed them into a computer along with an algorithm to do the combinatorics and wait for the result. There are however a few issues with this approach, which make it usually suited at most for numerical evaluations or verification purposes. First, one has to build an algorithm which appropriately takes care of all the possible contractions of the Feynman rules leading to a complete sum of all the diagrams contributing to the process of interest. An example of such an algorithm is the Berends-Giele recursion which we presented in Section 2.3, which thanks to its recursive nature allows to recycle information and lessen the problem of factorial complexity of the calculations. Nevertheless, the combinatorics might be still involved enough for results to require minutes or even hours to be obtained with the final expression being in an unwieldy form due to its sheer size, so much so that further processing can become difficult. A more effective technique is represented by the BCFW-like recursion relations, see Section 2.4, which make use of a complex-parameter shift of the kinematics and use on-shell data at every stage of the calculation. These on-shell expressions are typically more compact and furthermore the involved combinatorics is easier, making on-shell recursions very well suited for the task. On the other hand, these

techniques are not guaranteed to work for any theory, in fact the shifted quantities need to be sufficiently well-behaved at infinity (along particular directions in the complex plane). This is typically the case for most theories once an appropriate complex shift is chosen, however often it comes at the price of introducing some sort of reference spinor/momentum which might be hard to get rid of, and thus appear in the final expression despite being completely arbitrary and physically inconsequential. Another slight disadvantage of these sort of recursions is that often the final expressions depend on spurious poles, which obscure the physics of the process while being removed through the use of spinorial identities and momentum conservation.

In this section we are going to present an algorithm developed in [5] for the on-shell construction of scattering amplitudes in a generic EFT. This algorithm enjoys the advantages of using only on-shell intermediate quantities typical of BCFW-like recursions without suffering from the issues related to large- z behaviour or appearance of reference spinors in the final results. Furthermore, results are directly computed in a compact form which only presents physical poles in the Mandelstam invariants, and are thus well suited for unitarity applications. It is important to stress that, to the best of our knowledge, this procedure for constructing amplitudes is the first to boast all of the above mentioned advantages at the same time. In practical terms, its recursive nature makes it extremely implementation-friendly, with various aspects being also suitable for parallelization. Furthermore, its applicability to essentially any theory combined with the absence of any sort of unphysical reference momentum in the final results, makes it ideal for any application requiring the computation of analytic tree-level amplitudes, be it as intermediate steps for unitarity calculations (as done for example in Chapter 4) or for example as a stepping stone for the study of the analytic properties of a theory itself.

Before diving into the construction of higher-multiplicity amplitudes, we first summarise and discuss a series of results from the literature which allow to build the Standard Model from scratch without the need of ever introducing a Lagrangian or quantum fields¹. Combining these results with our algorithm and the use of generalised unitarity allows in principle for a complete on-shell construction of the theory at any multiplicity and any loop order. The techniques presented in this chapter will provide the tree-level input required for the computation of the SMEFT anomalous dimension matrix at one loop discussed in Chapter 4.

¹It goes without saying that in a wide variety of contexts the Lagrangian perspective provides very simple and clear insights, so for the sake of clarity we will still make use of it when appropriate.

3.1 The Standard Model from on-shell techniques

In this section we present a perturbative on-shell construction of the Standard Model, through the consistency of its S-matrix elements, under the following assumptions:

- The scattering amplitudes are invariant under Poincaré transformations but transform under some representation of the Little Group specified by their particle content. In four dimensions, under Little Group transformations each massless state transforms with a phase $e^{ih_i\phi}$ where h_i is the helicity of the i^{th} -state. These assumptions make the Spinor Helicity variables the most suited for the description of scattering amplitudes.
- In natural units, the *mass dimension* of an n -point scattering amplitude, at any loop order L^2 , is

$$\left[\mathcal{A}_n^{(L)}\right] = 4 - n. \quad (3.1)$$

This can be easily seen by writing the amplitude (in an all-outgoing convention) in terms of the transition matrix T defined by $S = \mathbb{1} + iT$ and the single particle states as $\langle p_1 \cdots p_n | T | 0 \rangle = (2\pi)^4 \delta^4(p_1 + \cdots + p_n) \mathcal{A}_n$, where the single particle state $|p\rangle$ has mass dimension -1 and $[\delta^4] = -4$.

- *Locality*: the non-analytic terms of the scattering amplitudes correspond to intermediate particles going on-shell. In particular, locality manifests itself in the analytic expression of an amplitude through the sole appearance of simple poles in the Mandelstam invariants, corresponding to single-particle exchanges with the intermediate particle going on-shell. Terms in the amplitude which include higher order poles in the invariants must thus be expressible as combinations of simple pole terms in order for locality to hold.
- *Unitarity*: the discontinuities of the amplitudes are given by a proper sum of products of lower-point (and lower-loop) amplitudes. In particular, the residues on the simple poles are given by

$$-i \operatorname{Res}_{s_{1\dots m}} \mathcal{A}_n^{(0)}(p_1^{h_1} \cdots p_n^{h_n}) = f \sum_{s_I, h_I} \mathcal{A}_{m+1}^{(0)}(p_1^{h_1} \cdots p_m^{h_m}, p_I^{h_I}) \mathcal{A}_{n-m+1}^{(0)}(p_I^{h_I} \rightarrow p_{m+1}^{h_{m+1}} \cdots p_n^{h_n}), \quad (3.2)$$

where $f = (-1)^{\Delta s}$ with Δs the respective signature of the fermion ordering between the LHS and the RHS, s_I and h_I are the type and the helicity of the intermediate state propagating³. More concretely, unitarity manifests through conservation of probability encoded by the completeness relation which schemat-

²In the following, when the number of loops is not specified as superscript, we mean tree-level.

³We adopt the following convention: we indicate with $\mathcal{A}_n(p_1^{h_1} \cdots p_n^{h_n})$ an n -point scattering amplitude with all the momenta outgoing and with $\mathcal{A}_n(p_1^{h_1} \cdots p_m^{h_m} \rightarrow p_{m+1}^{h_{m+1}} \cdots p_n^{h_n})$ an n -point amplitude with m incoming and $n - m$ outgoing states.

ically reads $\sum |X\rangle\langle X| = \mathbb{1}$, where the sum is over all the physical states of the theory. It is through insertion of this completeness relation that the right-hand side of (3.2) comes to be, in the limit where an intermediate virtual particle exchange goes on-shell exposing the corresponding simple pole (analyticity) captured by the residue.

Gauge invariance is not assumed a priori. Indeed, it has been proven that the Lie algebra structures are required by consistent factorisation of the four-point tree-level amplitude [128]. We will briefly review and extend this considerations to the Standard Model in Section 3.1.1. Moreover, since we work purely on-shell (in four dimensions) with spinor helicity variable, there is no need for polarisation tensors or Ward identities.

As we already discussed in some detail in Section 2.2, three-point scattering amplitudes in the Standard Model can be fixed by symmetry, helicity weight and mass dimension considerations (up to a constant) [128]. In particular, recall that the kinematic part of any massless three-point amplitude can be written as

$$\mathcal{A}(1^{h_1}, 2^{h_2}, 3^{h_3}) \propto \begin{cases} g \langle 1 2 \rangle^{h_1+h_2-h_3} \langle 2 3 \rangle^{h_2+h_3-h_1} \langle 3 1 \rangle^{h_3+h_1-h_2} & \sum_i h_i = -1 \\ g [1 2]^{h_1+h_2-h_3} [2 3]^{h_2+h_3-h_1} [3 1]^{h_3+h_1-h_2} & \sum_i h_i = 1 \end{cases}, \quad (3.3)$$

where for the time being we take the mass dimension of the coupling constant to be zero $[g] = 0$. This singles out the renormalizable interactions of the Standard Model from the non-renormalizable EFT interactions ($[g] < 0$) as well as the super-renormalizable ones ($[g] > 0$) for example of the ϕ^3 theory. Now, choosing the particle content to match the one of the SM (see Table A.1), building the complete list of all the tree-level three-point amplitudes reduces to a simple classification task. We list all these structures in appendix A.2, including flavour and colour structures. In order to correctly fix the latter we need to make use of unitarity and factorization properties of the four-point amplitudes, as discussed in the following sections.

3.1.1 Four-point amplitudes from factorisation

All the four-point amplitudes in the Standard Model, but $\mathcal{A}(\bar{H}^i, \bar{H}^j, H^k, H^l)$, can be completely fixed by factorisation. This will be proven in Section 3.3.1 but we assume it for the moment. Consistency between different factorisation channels at tree-level for four-point amplitudes then constrains many of the structures in the three-point amplitude. These constraints fix the (gauge-invariant) structures appearing and impose relations between couplings.

The constraints imposed by factorisation are completely equivalent to those found when we construct a consistent gauge-invariant Lagrangian describing a unitary QFT of self-interacting vector bosons [161] and their minimal coupling to fermions and scalars,

i.e. the Lie algebra structures and the universality of Yang-Mills coupling (see, for example, [162]). Moreover, we generalise this argument and find that factorisation also imposes relations between the hypercharges associate to the minimal coupling of matter with (non-self-interacting) $U(1)$ -vectors, which are equivalent from a Lagrangian perspective to the requirement that the Yukawa interactions are $U(1)_Y$ invariant, *i.e.* scattering amplitudes are non zero only for hypercharge-conserving processes.

Jacobi identities from factorisation

In this subsection we review the observations in [128]. We want to bootstrap the four-gluon amplitude through factorisation by considering as seeds the three-gluon amplitudes⁴

$$\mathcal{A}(G_-^A, G_-^B, G_+^C) = g_3 f^{ABC} \frac{\langle 12 \rangle^3}{\langle 23 \rangle \langle 31 \rangle}, \quad \mathcal{A}(G_-^A, G_+^B, G_+^C) = -g_3 f^{BCA} \frac{[23]^3}{[12][31]}, \quad (3.4)$$

where the f^{ABC} have been introduced in order to satisfy Bose-Einstein symmetry: due to the complete antisymmetry of the kinematic part, one needs to have $f^{ABC} = f^{[ABC]}$ for the three-point amplitude to be invariant under particle exchanges. The most generic (slightly redundant) ansatz for the four-point amplitude which is compatible with locality and unitarity is

$$\begin{aligned} \frac{\mathcal{A}(G_-^A, G_-^B, G_+^C, G_+^D)}{\langle 12 \rangle^2 [34]^2} &= \frac{f^{ABE} f^{CDE}}{s_{12}} \left(\frac{c_1}{s_{13}} + \frac{c_2}{s_{14}} \right) + \frac{f^{ACE} f^{BDE}}{s_{13}} \left(\frac{c_3}{s_{12}} + \frac{c_4}{s_{14}} \right) \\ &+ \frac{f^{ADE} f^{BCE}}{s_{14}} \left(\frac{c_5}{s_{12}} + \frac{c_6}{s_{13}} \right). \end{aligned} \quad (3.5)$$

The coefficients c_i can be fixed from factorisation using (3.2) which in the 4-point case reduces to⁵

$$-i \operatorname{Res}_{s_{ij}=0} \mathcal{A}_4 = \mathcal{A}_3 \cdot \mathcal{A}_3. \quad (3.6)$$

Imposing this constraint for all the three distinct channels, we find

$$\begin{cases} f^{ABE} f^{CDE} (c_1 - c_2) + f^{ACE} f^{BDE} c_3 - f^{ADE} f^{BCE} c_5 = -g_3^2 f^{ABE} f^{CDE} \\ f^{ABE} f^{CDE} c_1 + f^{ACE} f^{BDE} (c_3 - c_4) - f^{ADE} f^{BCE} c_6 = -g_3^2 f^{ACE} f^{BDE} \\ f^{ABE} f^{CDE} c_2 - f^{ACE} f^{BDE} c_4 + f^{ADE} f^{BCE} (c_5 - c_6) = -g_3^2 f^{ADE} f^{BCE} \end{cases}. \quad (3.7)$$

This linear system in general has no solutions, unless we impose the following quadratic

⁴The relative minus sign between the so called MHV and $\overline{\text{MHV}}$ amplitudes is fixed by requiring parity invariance of the theory (at the perturbative level).

⁵We remind the reader that when fermions are present in the amplitudes, the RHS of (3.6) might get a minus sign contribution from fermion reordering and a further factor of $-i$ when crossing a fermion from initial to final state. This subtlety will be relevant in the computations of the following sections.

relations among the constants f^{ABC} :

$$f^{ABE} f^{CDE} + f^{BCE} f^{ADE} + f^{CAE} f^{BDE} = 0, \quad (3.8)$$

which can be recognised as the Jacobi identities for the structure constants of a Lie algebra.

Notice that, even ignoring spin-statistics requirements which led us to introduce the tensors f^{ABC} to begin with, one could still not do without them. In fact, repeating the above procedure setting all the f to 1 in (3.5) leads to a system without solutions. In other words, the only consistent way of building a self-interacting theory of spin 1 bosons is by introducing the standard colour factors for the gluons, thus getting Yang-Mills theory. For further discussion on the topic see [127], where on a similar footing it is also shown that the only consistent massless spin 2 particles must reproduce the standard gravity four-point amplitude.

Lie algebras from factorisation

We can apply the same reasoning to scalars and fermions coupled to the non-abelian spin-1 particles and find that also their minimal coupling is tightly constrained by locality and unitarity [127]. We consider as an example the four-point amplitude $\mathcal{A}(G_-^A, G_+^B, \bar{u}^a, u^b)$. The three-point minimal coupling is fixed by little group and in principle can take the general form

$$\mathcal{A}(G_-^A, \bar{u}^a, u^b) = i g_{3,m} \tau^{Aa}_b \frac{\langle 12 \rangle^2}{\langle 23 \rangle}, \quad \mathcal{A}(G_+^A, \bar{u}^a, u^b) = i g_{3,m} \tau^{Aa}_b \frac{[13]^2}{[23]}, \quad (3.9)$$

where, for the moment, τ^{Aa}_b is some generic matrix encoding the interaction properties of the fermions u_a (\bar{u}^a) and the vector bosons, and we factored out an overall numerical coefficient. The most general ansatz for the four-point is then

$$\begin{aligned} \frac{\mathcal{A}(G_-^A, G_+^B, \bar{u}^a, u^b)}{\langle 13 \rangle^2 [23] [24]} &= \frac{f^{ABC} \tau^{Ca}_b}{s_{12}} \left(\frac{c_1}{s_{13}} + \frac{c_2}{s_{14}} \right) + \frac{\tau^{ABa}_b}{s_{13}} \left(\frac{c_3}{s_{12}} + \frac{c_4}{s_{14}} \right) \\ &+ \frac{\tau^{BAa}_b}{s_{14}} \left(\frac{c_5}{s_{12}} + \frac{c_6}{s_{13}} \right) \end{aligned} \quad (3.10)$$

where $\tau^{ABa}_b = \tau^{Aa}_c \tau^{Bc}_b$. Again taking the residues and matching with the factorisation channels as in equation (3.6), we find:

$$\begin{cases} f^{ABC} \tau^{Ca}_b (c_1 - c_2) + \tau^{ABa}_b c_3 - \tau^{BAa}_b c_5 = i g_3 g_{3,m} f^{ABC} \tau^{Ca}_b \\ f^{ABC} \tau^{Ca}_b c_1 + \tau^{ABa}_b (c_3 - c_4) - \tau^{BAa}_b c_6 = g_{3,m}^2 \tau^{ABa}_b \\ f^{ABC} \tau^{Ca}_b c_2 - \tau^{ABa}_b c_4 + \tau^{BAa}_b (c_5 - c_6) = g_{3,m}^2 \tau^{BAa}_b \end{cases}, \quad (3.11)$$

This linear system has solutions if and only if

$$g_{3,m} = g_3 , \quad (3.12)$$

$$\tau^{AB}{}^a{}_b - \tau^{BA}{}^a{}_b = i f^{ABC} \tau^C{}^a{}_b , \quad (3.13)$$

i.e. iff the coupling constant of the interaction is universal and the matrices $\tau^A{}^a{}_b$ are representations of the elements of a Lie algebra, with f^{ABC} the structure constants.

Charge conservation and Yukawa coupling

Next we generalise the procedure of the previous sections to the minimal coupling of the abelian vectors with scalars and fermions interacting via Yukawa coupling. Unitarity and locality will then imply that the hypercharge associated to the minimal coupling of the matter states to the abelian vector is conserved. The relevant three-point amplitudes are

$$\mathcal{A}(B_-, \bar{e}, e) = i g_1 Y_e \frac{\langle 12 \rangle^2}{\langle 23 \rangle} , \quad (3.14)$$

$$\mathcal{A}(B_-, \bar{L}^i, L^j) = i g_1 Y_L \delta_i^j \frac{\langle 12 \rangle^2}{\langle 23 \rangle} , \quad (3.15)$$

$$\mathcal{A}(B_-, \bar{H}^i, H^j) = i g_1 Y_H \delta_i^j \frac{\langle 12 \rangle \langle 31 \rangle}{\langle 23 \rangle} , \quad (3.16)$$

$$\mathcal{A}(L^i, e, \bar{H}^j) = i \bar{\mathcal{Y}}^{(3)} \delta_j^i [12] , \quad (3.17)$$

where Y_i is the hypercharge associated to the i -th state, and $\mathcal{Y}^{(3)}$ is the Yukawa coupling matrix for the electron family, with $\bar{\mathcal{Y}}^{(3)} = \left(\mathcal{Y}^{(3)}\right)^\dagger$. The most generic ansatz consistent with locality and unitarity is

$$\frac{\mathcal{A}(B_-, L^i, e, \bar{H}^j)}{\langle 12 \rangle \langle 13 \rangle [23]^2} = \delta_j^i \left(\frac{c_1}{s_{12}s_{13}} + \frac{c_2}{s_{12}s_{14}} + \frac{c_3}{s_{13}s_{14}} \right) , \quad (3.18)$$

and probing the three different factorisation channels we find the system:

$$\begin{cases} c_1 - c_2 = -g_1 \bar{\mathcal{Y}}^{(3)} Y_L \\ c_1 - c_3 = +g_1 \bar{\mathcal{Y}}^{(3)} Y_e , \\ c_2 - c_3 = +g_1 \bar{\mathcal{Y}}^{(3)} Y_H \end{cases} , \quad (3.19)$$

which has solutions if and only if we impose the hypercharge conserving condition:

$$Y_L = Y_H - Y_e . \quad (3.20)$$

Analogously, one can also find the charge conservation conditions for the processes involving quarks, instead of leptons:

$$Y_Q = Y_H - Y_d , \quad (3.21)$$

$$Y_Q = -Y_H - Y_u . \quad (3.22)$$

It is interesting to stress that there are further relations on the hyper charges in the Standard Model, namely those coming from anomaly cancellation conditions at loop-level. In Section 4.2 we will show how to reproduce these conditions using generalised unitarity in four dimensions.

3.2 The on-shell classification of SMEFT operators

In this section we are going to extend the on-shell methods to the classification of effective interactions [56, 60, 63] in the SMEFT [57–59, 61], corresponding in the Lagrangian formalism to insertions of marginal operators [163–166]. First we are going to classify all the independent kinematic structures in a generic theory in four dimensions introducing an algorithm in terms of graphs [5] and then we will consider the specific case of the Standard Model, combining these with the colour structures⁶.

3.2.1 Kinematic structures from spinor helicity variables

Each effective interaction will be identified by its *minimal* amplitude, this is an amplitude which does not vanish in free theory (if we switch off all the other interactions), crucially it contains no poles because it includes no particle exchanges⁷. In other words, classification of the effective interactions will be achieved by classifying contact terms, namely interactions where there are no intermediate modes propagating, which in practical terms means that we need only to consider those structures involving positive powers of the angle and square spinor brackets.

As a first step in the classification procedure, we fix the mass-dimension $[\mathcal{O}]$ of the operators for which we want to find a complete basis. From the minimal amplitudes we strip off the coupling of the effective interaction, which is related to the dimension of the corresponding marginal operator by

$$[g_{\mathcal{O}}] = 4 - [\mathcal{O}] . \quad (3.23)$$

⁶The approach presented in this section has been coded in `Mathematica` [119], the code and an example notebook are available at the link <https://github.com/StefanoDeAngelis/SMEFT-operators>.

⁷From a Lagrangian perspective, it is simply the amplitude obtained by fully contracting a vertex-interaction Feynman rule with the appropriate external states.

What we are looking for are the kinematic structures which have mass dimension

$$[\mathcal{O}] - n \geq 0, \quad (3.24)$$

where n is the number of external legs in the corresponding minimal amplitude. Equation (3.24) provides a constraint on n which can be further refined by taking into account which types of particles are found in the amplitudes. In fact, in order to get helicity weights right, each vector in the minimal amplitude will contribute at least with two spinor variables and each fermion at least with one. This leads to the stronger constraint⁸

$$[\mathcal{O}] - n \geq 2 \times \frac{1}{2} \times n_g + \frac{1}{2} \times n_f \quad \implies \quad 2n_g + \frac{3}{2}n_f + n_s \leq [\mathcal{O}], \quad (3.25)$$

where n_g , n_f and n_s are respectively the number of vectors, fermions and scalars and clearly $n = n_g + n_f + n_s$. Next, we need to take into account the constraints coming from the condition that our kinematic structures must be $\text{SL}(2, \mathbb{C})$ invariant. This requires to further distinguish between helicities of the different particles, and to find all the $(n_{g-}, n_{g+}, n_{f-}, n_{f+}, n_s)$ ⁹ compatible with the constraint (3.25). Once n_g , n_f and n_s are fixed, we take into account that every state can contribute to the kinematic structures with powers of its momentum, which correspond to derivatives in the operator language. The total number of momenta n_∂ is fixed by saturating the mass dimension constraint to

$$n_\partial = [\mathcal{O}] - 2n_g - \frac{3}{2}n_f - n_s. \quad (3.26)$$

A simple way of finding all the possible structures is to identify them with an oriented multigraph, where each vertex is associated to a particle, and the edges correspond to angle (red) or square (blue) $\text{SL}(2, \mathbb{C})$ invariants. The orientation of the edges then keeps track of the ordering of particles in the brackets and thus provides potential minus signs.

The valence of each vertex is given by two natural numbers $v^i = (v_a^i, v_s^i)$ such that $v_s^i - v_a^i = 2h_i$ is the helicity of the i^{th} particle (see, for example, Figure 3.1). Finally, for reasons which will become clear in the next section, we consider a circular embedding for our graphs, in other words we take all the nodes to be ordered points on a circle. This method has proven to be a computationally efficient way of finding a basis of independent structures up to Schouten and momentum conservation identities. Notice that the former act separately on angle and square invariants, while the latter mixes the two structures. In the following sections we are going to show how to deal with these identities in terms of above mentioned multigraphs.

⁸This condition is not only necessary but also sufficient for having local interactions.

⁹The superscript of the subscript specify the helicity of the particles: $n_g = n_{g-} + n_{g+}$ and $n_f = n_{f-} + n_{f+}$.



Figure 3.1: The graph associate to the kinematic structures $\langle 12 \rangle^2 \langle 14 \rangle \langle 32 \rangle [23] [13]^2 [31]$ and $\langle 13 \rangle \langle 14 \rangle \langle 25 \rangle [23] [34]$ respectively.

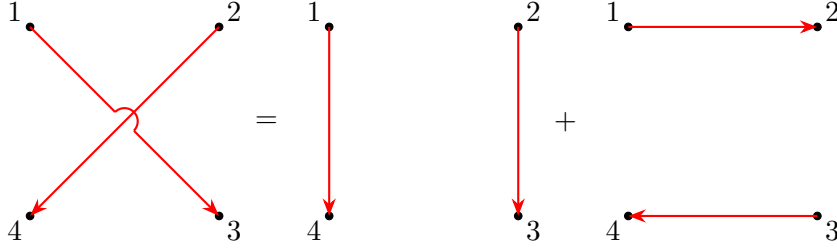


Figure 3.2: Schouten identities are equivalent to untying crossings for both the two graphs in the multigraph: $\langle 13 \rangle \langle 24 \rangle = \langle 14 \rangle \langle 23 \rangle + \langle 12 \rangle \langle 34 \rangle$.

Schouten identities

We recall that the Schouten identities for angle and square brackets for four spinors labelled 1,2,3,4 can be written as

$$\begin{aligned} \langle 12 \rangle \langle 34 \rangle + \langle 23 \rangle \langle 14 \rangle + \langle 31 \rangle \langle 24 \rangle &= 0, \\ [12][34] + [23][14] + [31][24] &= 0. \end{aligned} \tag{3.27}$$

Thinking of the kinematic structures in terms of graphs, specifically using the already mentioned circular embedding, one way of implementing (3.27) is by untying crossing edges as shown in Figure 3.2. In a generic graph, this can be applied recursively until, after a finite number of steps, we end up with graphs which do not have any crossing. It is then clear that a basis of kinematic structures which are independent under Schouten identities can be obtained by building a basis of planar graphs only.

Momentum conservation

In general, it is often the case that the number of momenta in the n -point amplitude (or equivalently derivatives in the interaction) we consider is $n_\partial > 0$. Each momentum in the amplitude can be assigned to any of the n particles, and doing so increases the valence of the corresponding vertex by $(1, 1)$. On the other hand, looking at a given vertex in a graph representing the kinematics of an interaction, the number of momenta associated to the considered vertex is $\min\{v_a^i, v_s^i\}$, where we remind the

reader that the difference in $v_s^i - v_a^i$ gives the helicity of the particle. When building a base, it is then important to take into account how momentum conservation relates different kinematic structures, and once again this can be done at the level of the graphs. First of all, when enumerating all the possible basis elements we simply remove those containing the momentum of the n^{th} -particle, which we choose as the redundant one, the n^{th} -vertex thus having valence of exactly $(\frac{|h_n|+h_n}{2}, \frac{|h_n|-h_n}{2})$. This is not sufficient however to completely remove redundancies coming from momentum conservation, in fact writing $|n\rangle[n] = -\sum_j |j\rangle[j]$ and contracting both sides of the equality with $|n\rangle\langle i|$ and $|i\rangle\langle n|$ respectively we get

$$0 = \begin{cases} \sum_{j=1}^{n-1} \langle i j \rangle [j n] & h_n > 0 \\ \sum_{j=1}^{n-1} \langle n j \rangle [j i] & h_n < 0 \end{cases} \quad (3.28)$$

where we took into account antisymmetry of the spinor brackets¹⁰, and contracting instead with $|i\rangle\langle i|$

$$\sum_{i=1}^{n-2} \sum_{j=i+1}^{n-1} s_{ij} = 0. \quad (3.29)$$

Both the equations in (3.28) are valid identities independently of the helicity of the n -th particle, however only one of them will actually appear in the expressions and needs thus to be accounted for. Some observations are in order:

- The Schouten identities do not change the valences of vertices in the multigraph, so they do not change the number of momenta associated to each vertex.
- Since we want a basis of planar graphs, we solve all but one of the (3.28) for one of the momenta which maximises the number of planar multigraphs, the natural choice being either p_1 or p_{n-1} (a different choice would give an over-counting of the independent structures). The considered identities are then taken into account by simply discarding all the structures involving $\langle i n-1 \rangle [n-1 n]$ or $\langle n n-1 \rangle [n-1 i]$ according to the helicity of the n^{th} -particle (or equivalently $\langle i 1 \rangle [1 n] / \langle n 1 \rangle [1 i]$).
- Among (3.28), there is one relation which does not involve neither p_n nor p_{n-1} . This is taken into account by discarding those structures where $\langle n-1 1 \rangle [1 n] / \langle n 1 \rangle [1 n-1]$ appears (or $\langle 1 n-1 \rangle [n-1 n] / \langle n n-1 \rangle [n-1 1]$).
- Finally, the constraint (3.29) forces us to discard the terms proportional to $s_{1 n-1}$.

This algorithm classifies efficiently all the $\text{SL}(2, \mathbb{C})$ -invariant structures which are polynomial in the spinor variables with fixed mass dimension and helicity configuration, associated to each $(n_{g^-}, n_{g^+}, n_{f^-}, n_{f^+}, n_s)$. It also provides a very simple way of writ-

¹⁰Or equivalently the Dirac equation in its form $p_{n\alpha\dot{\alpha}} \tilde{\lambda}_n^{\dot{\alpha}} = 0 = \lambda_n^\alpha p_{n\alpha\dot{\alpha}}$.

ing the dependent structures as linear combinations of the independent ones. We also notice that this algorithm can be applied beyond gauge theories and in fact we make use of a simplified version of it for the classification of the R^4 interactions in Section 5.2.3.

3.2.2 The classification of SMEFT interactions

The classification of the helicity structures is completely theory-independent and is indeed not limited to gauge theories, but can be applied to effective field theories of gravity, with (massive and spinning) matter as well, see [167]. Information about the Standard Model enters only in the $SU(3) \times SU(2) \times U(1)$ (invariant) structures associated to the chosen set of particles.

The gauge group structures

The classification of the invariant structures of the gauge groups can be worked out using standard group theory techniques. In particular

- $U(1)$: to each $(n_{g^-}, n_{g^+}, n_{f^-}, n_{f^+}, n_s)$ structure we associate all the possible combinations of Standard Model states for which the total hypercharge is zero.
- $SU(2)$: we notice that the algorithm presented in the previous section can be generalised to the case of $SU(2)$ invariants with a single graph associated to the invariants. Each oriented edge from the n^{th} to the m^{th} vertices corresponds to an ϵ^{inim} tensors and the valence of each vertex v_i is fixed by the representation of the i^{th} -particle, labelled by its dimension $\mathbf{v}_i + \mathbf{1}$. The indices associated to the same vertex must be taken as completely symmetric. In the case of the $SU(2)$ group there is no analogous of momentum conservation, so the independent structures can be taken to be in one-to-one correspondence with planar graphs.
- $SU(3)$: the $SU(N)$ invariants have been widely studied both in the mathematics and in the physics literature (see, for example [168–170]), and our related algorithms are just implementations of the standard techniques, in particular we adopt the standard Littlewood-Richardson rule [171, 172] as suggested in [64, 65].

Once the kinematic structures associated to $(n_{g^-}, n_{g^+}, n_{f^-}, n_{f^+}, n_s)$ have been generated and a compatible set of gauge singlets was found, we combine all the invariants in order to find a basis of independent structures enclosing information about both the kinematics and the colour. If no identical fields are present, these structures coincide with the minimal amplitudes, else one needs to impose Bose-Einstein and Dirac-Fermi statistics as explained in the next section.

Repeated fields and Young projectors

In general the minimal amplitudes we consider can involve identical states, for $[g\mathcal{O}] = -2$ two simple examples are the amplitudes for (G^+, G^+, G^+) or (Q, Q, u, d) . The treatment of this subtlety has been systematically taken into account in [64, 173]. Starting from their classification, we take a slightly different approach, since we deal with minimal amplitudes and not with operators. We distinguish between identical bosons and fermions at the level of the minimal amplitude and impose Bose-Einstein statistic on the former and Dirac-Fermi statistic on the latter. In practice, we consider all the previously classified independent structures and we act on them with a proper Young projector over the labels of the identical states:

- in the case of n identical bosons we act on the structures with the symmetriser projector

$$\mathcal{Y}_{\frac{\mathbb{1}}{[n]}} = \frac{1}{n!} \sum_{i=1}^{n!} p_i , \quad (3.30)$$

where p_i are all the permutations of the n labels associated to the identical bosons.

- in the case of n identical fermions we act on the structures with the total anti-symmetriser projector

$$\mathcal{Y}_{\frac{\mathbb{1}}{[n]}} = \frac{1}{n!} \sum_{i=1}^{n!} s_i p_i , \quad (3.31)$$

where s_i is the signature of the permutations p_i .

Once, we apply the Young projectors to the independent minimal amplitudes, we will end up with a sum over terms which will not necessarily belong to the basis of independent structures chosen. In order to find the minimal amplitudes, we need to re-write these symmetrised amplitudes in terms of elements of our structure basis and check if they are linearly independent from each other (which in general will not be the case, some structures will even be automatically zero after projection).

A further subtlety arises in the case of the Standard Model, due to the *flavour* of fermions: to each particle we can associate a further $SU(N_f)$ index, where N_f is the number of flavours. The independent minimal amplitudes can then be classified in terms of inequivalent irreducible representations of $SU(N_f)$, which are in one-to-one correspondence with the irreducible representations of the symmetric group S_n , where n is the number of identical fermions in the same family. For example, for dimension 6 operators we can consider the baryon number violating effective interactions with

(Q, Q, Q, L) ($n = 3$). Then we have a basis of four independent structures:

$$\epsilon^{a_1 a_2 a_3} \epsilon^{i_1 i_4} \epsilon^{i_2 i_3} \langle 12 \rangle \langle 34 \rangle, \quad (3.32)$$

$$\epsilon^{a_1 a_2 a_3} \epsilon^{i_1 i_2} \epsilon^{i_3 i_4} \langle 12 \rangle \langle 34 \rangle, \quad (3.33)$$

$$\epsilon^{a_1 a_2 a_3} \epsilon^{i_1 i_4} \epsilon^{i_2 i_3} \langle 14 \rangle \langle 23 \rangle, \quad (3.34)$$

$$\epsilon^{a_1 a_2 a_3} \epsilon^{i_1 i_2} \epsilon^{i_3 i_4} \langle 14 \rangle \langle 23 \rangle. \quad (3.35)$$

There are three inequivalent representations of S_3 , corresponding to the Young diagrams $\square\square\square$, $\square\square$ and \square . Then we can act on the independent structure with the projectors associated to the standard Young tableaux $\begin{smallmatrix} \square & \square & \square \\ \square & & \end{smallmatrix}$, $\begin{smallmatrix} \square & \square \\ \square & \end{smallmatrix}$, $\begin{smallmatrix} \square \\ \square \\ \square \end{smallmatrix}$ ¹¹. There is a unique linearly independent structure associated to each irreducible representation:

$$C_{m_1 m_2 m_3, m_4}^{\{3\}, \{1\}} \mathcal{Y}_{\begin{smallmatrix} \square \\ \square \\ \square \end{smallmatrix}} \circ \epsilon^{a_1 a_2 a_3} \epsilon^{i_1 i_4} \epsilon^{i_2 i_3} \langle 12 \rangle \langle 34 \rangle, \quad (3.36)$$

$$C_{m_1 m_2 m_3, m_4}^{\{2,1\}, \{1\}} \mathcal{Y}_{\begin{smallmatrix} \square & \square \\ \square & \end{smallmatrix}} \circ \epsilon^{a_1 a_2 a_3} \epsilon^{i_1 i_4} \epsilon^{i_2 i_3} \langle 12 \rangle \langle 34 \rangle, \quad (3.37)$$

$$C_{m_1 m_2 m_3, m_4}^{\{1,1,1\}, \{1\}} \mathcal{Y}_{\begin{smallmatrix} \square & \square & \square \\ \square & & \end{smallmatrix}} \circ \epsilon^{a_1 a_2 a_3} \epsilon^{i_1 i_4} \epsilon^{i_2 i_3} \langle 12 \rangle \langle 34 \rangle, \quad (3.38)$$

where $C_{m_1 m_2 m_3, m_4}^{\pi, \{1\}}$ is a Wilson coefficient tensor associated to each effective minimal amplitude, with π being the integer partition corresponding to the Young diagram for the Q fields. Notice that Dirac-Fermi statistics forces the Wilson coefficient tensor to have the ‘‘opposite’’ symmetry properties with respect to the Young tableau associated to the projector: *e.g.* $C_{m_1 m_2 m_3, m_4}^{\{3\}, \{1\}} = C_{(m_1 m_2 m_3), m_4}^{\{3\}, \{1\}}$, $C_{m_1 m_2 m_3, m_4}^{\{2,1\}, \{1\}} = C_{[m_1 m_2] m_3, m_4}^{\{2,1\}, \{1\}}$, $C_{[m_1 m_2 m_3], m_4}^{\{2,1\}, \{1\}} = 0$ and $C_{m_1 m_2 m_3, m_4}^{\{1,1,1\}, \{1\}} = C_{([m_1 m_2 m_3]), m_4}^{\{1,1,1\}, \{1\}}$. The number of independent operators for this specific case is¹² $\frac{(N_f+2)(N_f+1)N_f}{6}$, $\frac{(N_f+1)N_f(N_f-1)}{3}$ and $\frac{N_f(N_f-1)(N_f-2)}{6}$ for each tensor respectively.

3.3 Bootstrapping the tree-level amplitudes

In the amplitudes literature, the computation of higher-point tree-level amplitudes from on-shell data is usually performed through BCFW recursion relations [12, 13, 174], or its generalisations [153, 155, 157, 175, 176]. These recursion relations are particularly well-suited for the computation of amplitudes involving vector bosons and gravitons, for which the BCFW (2-line) shift gives rather compact results summing over a small subset of the actual factorisation channels. The most general criteria for the shifted amplitude to be well-behaved in the $z \rightarrow \infty$ limit are given in [156]: all renormaliz-

¹¹The fourth standard tableau $\begin{smallmatrix} \square & \square \\ \square & \end{smallmatrix}$ would not give an independent minimal amplitude, because it could be obtained from the second one by relabelling: $\mathcal{Y}_{\begin{smallmatrix} \square & \square \\ \square & \end{smallmatrix}} = (23) \circ \mathcal{Y}_{\begin{smallmatrix} \square & \square \\ \square & \end{smallmatrix}}$, where (23) is the permutation of the labels 2 and 3.

¹²The counting can be performed using the Hook Content Formula.

able theories are shown to be 5-line constructible and, in particular, theories involving fermions and scalars charged under a $U(1)$ are 3-line constructible, as in the case of the Standard Model. Moreover, non-renormalizable amplitudes with no-derivative operator insertions are on-shell constructible, but it is not generally true for operators with derivatives. Finally, n -line shifts with $n \geq 3$ give rather cumbersome results and in no case locality is manifest in the final amplitude.

In this section we present an alternative approach to the above mentioned recursion relations, which is completely general in the type of interactions one can consider and at the same is entirely on-shell. The general strategy has been outlined in the Section 3.1, and in the following section we are going to argue that in our framework any effective field theory is fully on-shell constructible from unitarity and locality. In particular, the singularity structure will be manifest in the final result.

3.3.1 Higher-point amplitudes in the SM

The procedure can be roughly divided into two parts: the construction of an ansatz and a matching procedure on the single-particle cuts to fix the free-parameters, which we perform numerically over finite fields to speed up the computation.

Constructing an ansatz

A generic tree-level amplitude can be schematically written as

$$\mathcal{A}_n(p_1^{a_1, h_1}, \dots, p_n^{a_n, h_n}) = \sum_{i,j,k} \frac{C_{i,j}^{a_1 \dots a_n}}{\mathcal{D}_i} c_{i,j,k} \mathcal{N}_{i,j,k} + \mathcal{P}^{a_1 \dots a_n}, \quad (3.39)$$

where $p_i^{a_i, h_i}$ represents a generic state with helicity h_i and gauge-group index a_i . The tensors $C_{i,j}^{a_1 \dots a_n}$ are the gauge-group invariant structure of the amplitude, whereas \mathcal{D}_j and $\mathcal{N}_{i,j,k}$ are kinematic denominators and numerators respectively, where the latter carry the dependence on the helicity structure. The $c_{i,j,k}$ are rational coefficients associated to the different helicity structures $\mathcal{N}_{i,j,k}$. Finally, the $\mathcal{P}^{a_1 \dots a_n}$ are terms with polynomial dependence in the kinematic variables, in other words contact terms, which vanish whenever we probe any factorisation channel. We will show that in our framework the contact terms are irrelevant and the tree-level amplitudes are fully determined by lower-point amplitudes from factorisation.

First we motivate this assumption for renormalizable theories through a simple dimensional analysis consideration: due to (3.1), for $n > 4$ we have $[\mathcal{A}_n] < 0$. Moreover, all the couplings in the SM are dimensionless, we are considering only massless states (there are no dimension-full parameters in the amplitude), and by construction $[\mathcal{P}^{a_1 \dots a_n}] \geq 0$. These considerations imply necessarily that for renormalizable massless theories for $n > 4$ $\mathcal{P}^{a_1 \dots a_n} = 0$ and every term in the amplitude must possess some

kinematic denominators \mathcal{D}_i . This means that the amplitudes can be fully determined from factorisation, through a recursive procedure described below in this section.

This argument is somehow subtle for $n = 4$, because it is possible to build terms of mass dimension zero which are ratios of spinor variables but vanish on any cut. An example of such a structure for the all-plus four-gluon amplitudes is

$$\frac{[1\ 2]^2[3\ 4]^2}{s_{12}^2} = \frac{[1\ 3]^2[2\ 4]^2}{s_{13}^2} = \frac{[1\ 4]^2[2\ 3]^2}{s_{14}^2}, \quad (3.40)$$

whose residue is zero on any of the three invariants s_{12} , s_{13} and s_{14} . These structures do not introduce any correction to the factorisation channels of four-point amplitudes (*i.e.* they are polynomial in the kinematic variables). We can however discard such contact terms at four points, in fact they are absent at tree-level¹³, and instead appear as one-loop finite rational terms [110, 177–181, 114, 1] and can be computed through d -dimensional generalised unitarity techniques.

The only contact term exception is the four-scalar contact term corresponding in the Lagrangian formalism to the $\lambda\phi^4$ interaction, which in the case of the four-scalar amplitude we will add to the factorisable part as

$$\mathcal{A}_4(\bar{H}^{i_1} \bar{H}^{i_2} H^{i_3} H^{i_4}) = - \left(g_1^2 Y_H^2 \delta_{i_1}^{i_3} \delta_{i_2}^{i_4} + g_2^2 \sigma^{I i_3}_{i_1} \sigma^{I i_4}_{i_2} \right) \frac{s_{12} - s_{14}}{s_{13}} - \lambda \delta_{i_1}^{i_3} \delta_{i_2}^{i_4} + (3 \leftrightarrow 4), \quad (3.41)$$

where one can easily see that the kinematic dependence is trivial and not captured by factorization. We stress that for $n > 4$ non-singular terms such as (3.40) cannot appear: this can be easily seen focusing on real kinematics and by dimensional analysis considerations, which tell us that there must be a singularity for renormalizable amplitudes with more than four external particles.

The argument presented so far for the SM cannot be generalised to the case of scattering amplitudes with insertions of effective interactions. Let us introduce the notation

$$\mathcal{F}_{n,d,i}(p_1^{a_1,h_1}, \dots, p_n^{a_n,h_n}) \quad (3.42)$$

for the effective amplitudes, which encodes the number of external states n , the mass dimension of the operator d , and a label i for the minimal interactions when multiple ones are present, if no confusion can arise we use the operator itself instead of the label i . So consider for example the six-scalar amplitude with an insertion of a $\partial^2\phi^4$ interaction, in the above notation we call it $\mathcal{F}_{6,6,\partial^2\phi^4}$. There is no argument allowing us to discard a ϕ^6 -like contact term contribution arising in the calculation of this amplitude. On the other hand, any physical process involving six external scalars will receive a contribution

¹³For example, we know that such terms can never be generated by any local Lagrangian interaction at tree-level.

from both the $\mathcal{F}_{6,6,\partial^2\phi^4}$ as well as $\mathcal{F}_{6,6,\phi^6}$ (when these are both included in the theory), where the latter is the contact interaction due to the operator ϕ^6 itself. This means that, physically the two contact term contributions cannot be disentangled, any distinction between the terms is only a matter of different descriptions of the same process. As a consequence, if we are already considering an effective field theory with both $\partial^2\phi^4$ and ϕ^6 interactions in our operator basis, neglecting the ϕ^6 -like contact term in $\mathcal{F}_{6,6,\partial^2\phi^4}$ can be compensated by appropriately shifting the Wilson coefficient of the ϕ^6 operator.

This argument can be generalised to more generic theories, like the SMEFT which we are interested in. What we wanted to convey is that, as long as we consider a complete basis of operators up to a given dimension, contact terms can only contribute shifting the Wilson coefficients of a different operator. Then we *choose* our basis of EFT interactions such that it does not generate polynomial terms when computing higher-multiplicity amplitudes and thus we can effectively neglect them in the computations, so $\mathcal{P}^{a_1\cdots a_n} = 0$.

We present now the algorithm to compute higher-point tree-level amplitudes from factorisation.

1. We begin by enumerating all the possible singularity structures of the amplitude consistent with locality, which are provided by all the possible ways the amplitude can consistently factorise into trivalent graphs¹⁴. We enumerate all the possible tree graphs with trivalent and quadrivalent internal vertices, and then a selection criterion is applied to discard channels which are not compatible with Standard Model interactions.
2. To each trivalent graph a unique kinematic denominator \mathcal{D}_i is associated, this is the product of the propagators corresponding to internal edges in the graphs, *i.e.* it is a product of the Mandelstam invariants characterising the channels.
3. Unitarity also fixes the colour structures associated to each graph $\{C_{i,j}^{a_1\cdots a_n}\}_{j=1,\dots,s}$. In particular, different colour structures correspond to different particles propagating in the internal lines. Once the internal particles are determined, the colour structures are obtained from the product of the colour structures in the three-point amplitudes.
4. Finally the kinematic numerators are generated with the algorithm presented in Section 3.2.1¹⁵. The $\{\mathcal{N}_{i,j,k}\}_{k=1,\dots,h}$ are h independent spinor structures in our

¹⁴When talking about trivalent graphs or three-point amplitudes in this section we always mean the building blocks of our theory, which strictly speaking includes not only the three-point amplitudes but also the four-point scalar interaction $-\lambda(\bar{H}H)^2/4$ (with the corresponding quadrivalent vertices in the graphs) and, if we are considering amplitudes with effective operator insertions, also any of the relevant effective interaction classified in Section 3.2.

¹⁵The full algorithm presented in this section can be applied to the case of form factors as well. If this was the case we were interested in, we should consider at this point a simplified version of the

basis, and a set of these numerators is associated to each of the colour structure $C_{i,j}^{a_1 \dots a_n}$ corresponding to the denominator \mathcal{D}_i . The latter fixes the mass dimension of the numerators through $[\mathcal{N}_{i,j,k}] = [\mathcal{A}_n] + [\mathcal{D}_i]$ whereas the helicity weights are given by the external particles. Each of the $\mathcal{N}_{i,j,k}$ is multiplied by arbitrary (rational) coefficients $c_{i,j,k}$ which will be fixed by the matching procedure over the different factorisation channels described in detail in Section 3.3.1. Notice that the basis of numerators does obviously not depend on the colour structures, but only on the mass dimension of the denominator structure: *i.e.* $\mathcal{N}_{i_1,j_1,k} = \mathcal{N}_{i_2,j_2,k}$ if $[\mathcal{D}_{i_1}] = [\mathcal{D}_{i_2}]$ for any colour structure labelled by j_1 and j_2 . This fact has been exploited heavily to speed up the numerical evaluation of the ansatz when solving for the coefficients $\{c_{i,j,k}\}$.

5. Some of the coefficients can be fixed before the matching procedure by demanding that the ansatz is not redundant. In particular, the simplifying observation is that the various coefficients cannot combine in such a way that the sum over the related structures is proportional to any of the Mandelstam invariants appearing in the denominators.
6. Finally we solve for the $\{c_{i,j,k}\}$ by matching over the different factorisation channels as described in 3.3.1.

We consider, as an example, the five-point amplitude $\mathcal{A}_5(Q^{a_1,i_1}, u^{a_2}, \bar{H}^{i_3}, H^{i_4}, H^{i_5})$. There are 21 trivalent graphs compatible with this process, and some of them are shown in Figure 3.3. Most of the graphs do not involve the scalar quadrivalent interaction, except the last one, we then have $[\mathcal{D}_i] = 4$ for $i = 1, \dots, 20$ and $[\mathcal{D}_{21}] = 2$ with:

$$\begin{aligned} \{\mathcal{D}_i\}_{i=1,\dots,21} = \{ & s_{12}s_{35}, s_{14}s_{35}, s_{24}s_{35}, s_{12}s_{34}, s_{15}s_{34}, s_{25}s_{34}, s_{13}s_{25}, s_{14}s_{25}, s_{25}s_{34}, s_{13}s_{24}, \\ & s_{15}s_{24}, s_{24}s_{35}, s_{15}s_{24}, s_{15}s_{34}, s_{14}s_{25}, s_{14}s_{35}, s_{13}s_{24}, s_{13}s_{25}, s_{12}s_{34}, s_{12}s_{35}, s_{12} \} \end{aligned} \quad (3.43)$$

Next we build the kinematic numerators whose structure is fixed by the helicity of the external particles along with the mass dimension of the amplitude and of the denominators as

$$[\mathcal{A}_n] = [\mathcal{N}_{i,j,k}] - [\mathcal{D}_j] \quad \Rightarrow \quad [\mathcal{N}_{i,j,k}] = 4 - n + [\mathcal{D}_j] . \quad (3.44)$$

In our example we have then

$$\{\mathcal{N}_{i,j,k}\}_{k=1,\dots,6} = \{s_{12}[1\ 2], s_{13}[1\ 2], s_{23}[1\ 2], s_{24}[1\ 2], s_{34}[1\ 2], \langle 3\ 4 \rangle [1\ 4][2\ 3]\} , \quad (3.45)$$

$$\{\mathcal{N}_{21,j,k}\}_{k=1} = \{[1\ 2]\} , \quad (3.46)$$

for $i = 1, \dots, 20$. Computing the amplitude then reduces to fixing the rational co-

 algorithm presented in Section 3.2.1, in which we ignore momentum conservation.

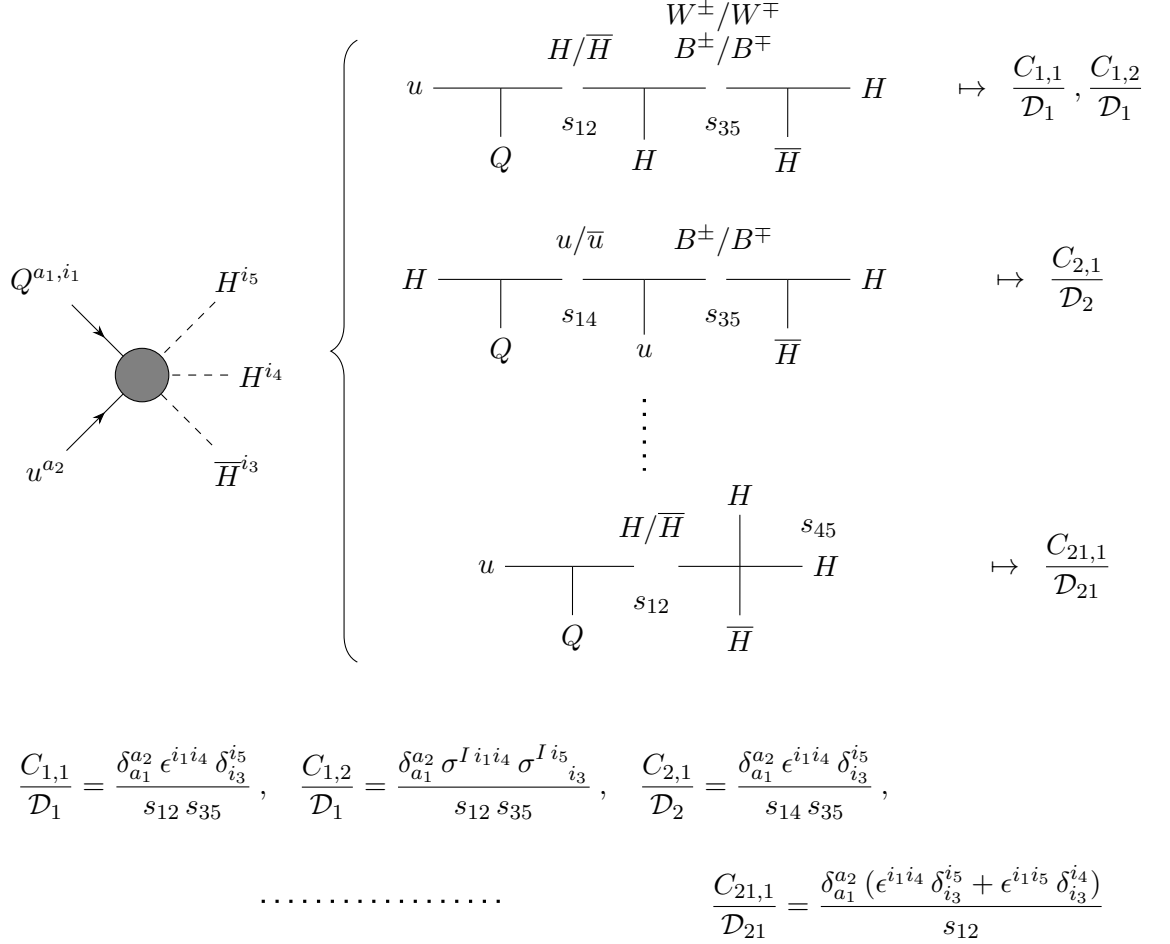


Figure 3.3: The splitting of $\mathcal{A}_5(Q^{a_1, i_1}, u^{a_2}, \bar{H}^{i_3}, H^{i_4}, H^{i_5})$ into trivalent graphs and the associated colour factors and kinematic denominators. There are a total of 21 possible trivalent graphs associated with this amplitude, we showed explicitly the first, the second and the last, as significant examples. The second is a trivial instance of trivalent graphs and there is a unique choice compatible with the Standard Model interactions of internal particle propagating. The same is not true for the first factorisation channel, for which we can have both B s and W s propagating, which give us two different colour structures $C_{1,1}$ and $C_{2,1}$, respectively. The last channel is the only one for this amplitude which involves an insertion of the quadrivalent Higgs interaction.

efficients $c_{i,j,k}$. In fact, before proceeding with the system solution we can fine tune the ansatz in order to remove combinations which would lead to cancellations in the denominators. In particular, since there are two Mandelstam invariants for the first twenty denominators, this would fix a priori two coefficients for each denominator and for each colour structures. We consider, for example, the first two trivalent graphs, shown in Figure 3.3. The general algorithm to fix the coefficient is the following:

- We have a set of independent helicity structures with a specified mass dimension d , *i.e.* $\{\mathcal{N}_{i,j,k}\}_{k=1,\dots,h_1}$, and we assume the existence of a set of structures with the same helicity configuration and mass dimension $d - 2$, *i.e.* $\{\mathcal{M}_{i,j,l}\}_{l=1,\dots,h_2}$. If the latter do not exist, this procedure can be skipped.
- For each Mandelstam invariant $s_{i_1\dots i_n}$ appearing in the denominator \mathcal{D}_i we fix some coefficients $d_{i,j,k}^{(p)}$ through

$$\sum_{k=1}^{h_1} d_{i,j,k}^{(p)} \mathcal{N}_{i,j,k} = s_{i_1\dots i_n} \mathcal{M}_{i,j,l} \quad \forall l. \quad (3.47)$$

These conditions provide us with $p = 1, \dots, \frac{[\mathcal{D}_i]}{2} \cdot h_2$ vectors $d_{i,j,k}^{(p)}$.

- Finally, we impose the orthogonality condition for the c 's with respect to the d 's

$$\sum_{k=1}^{h_1} c_{i,j,k} d_{i,j,k}^{(p)} = 0 \quad \forall p, \quad (3.48)$$

which fixes some of the $c_{i,j,k}$, as anticipated.

In our specific example, for \mathcal{D}_1 we find $c_{1,j,1} = 0$ and $c_{1,j,5} = -c_{1,j,2} - c_{1,j,3}$ with $j = 1, 2$ and for \mathcal{D}_2 we find $c_{2,1,4} = -c_{2,1,1}$ and, again, $c_{2,1,5} = -c_{2,1,2} - c_{2,1,3}$.

The case of external vector bosons

The procedure described so far works very well when we are dealing with amplitudes with scalars and fermions as external particles. But when vector bosons are involved, or more in general massless particles with $|h| \geq 1$, an extension of the method is required. One has to take into account that these particles provide further kinematic denominators which are not due to intermediate particle exchanges. A simple example has already been shown in Section 3.1.1, where we considered the four-gluon amplitude. Indeed, the four-point amplitude has mass-dimension zero, the helicity structure with the smallest mass dimension is $\langle 12 \rangle^2 [34]^2$ which has mass-dimension 4, and consequently a single $\frac{1}{s_{ij}}$ (associated to a trivalent graph) is not enough to get the mass-dimensions right¹⁶. Typically, once a set of denominators has been generated as described in the

¹⁶When we think of the problem in terms of a Feynman diagrammatic approach for $|h| = 1$, this additional kinematic dependence is hidden in the polarisation vectors which in terms of spinor-helicity

previous section, we need to add at least one Mandelstam invariant to each denominator or possibly more in case of higher-point amplitudes. This is done in iterated steps: we first add to every denominator a single Mandelstam invariant s_{ij} in all the possible ways compatible with locality¹⁷, then we build the complete ansatz and try to solve it. If the number of invariants considered for the denominators is insufficient we will find no solution for the c 's, so we add all the possible terms with a further invariant in the denominator and try to solve again. At every step clearly the number of possible denominators grows quite drastically, and so does the number of possible numerators since higher and higher mass-dimensions become available. The latter effect is however counteracted by discarding those numerators which cancel any power of Mandelstam invariants from the denominator, which would indeed reproduce a term of the ansatz already present from previous iterations. This part of the method proves to be the bottleneck when it comes to computing higher-multiplicity amplitudes.

This procedure of adding Mandelstam invariants to the kinematic denominators is clearly responsible for the “mixing” process between different factorisation channels which brought us to the identities between colour structures at the level of the four-point amplitudes in Section 3.1.

Solution of the ansatz

So far we have built an ansatz of the form (3.39), where each of the $\mathcal{N}_{i,j,k}$ has an associated coefficient $c_{i,j,k}$. In order to fix these coefficients we impose the validity of (3.2) in every single kinematic channel, and we do so through repeated numerical evaluations:

$$-i \operatorname{Res}_{s_{i_1 \dots i_m}} \underbrace{\mathcal{A}_n(p_1^{h_1} \dots p_n^{h_n})}_{\text{ansatz}} = f \sum_{s_I, h_I} \underbrace{\mathcal{A}_{m+1}(p_{i_1}^{h_{i_1}} \dots p_{i_m}^{h_{i_m}}, p_I^{h_I}) \mathcal{A}_{n-m+1}(p_I^{h_I} \rightarrow p_{i_{m+1}}^{h_{i_{m+1}}} \dots p_{i_n}^{h_{i_n}})}_{\text{lower point on-shell amplitudes}}. \quad (3.50)$$

The lower point amplitudes in the RHS of (3.50) are known, because our algorithm is recursive. On the LHS we take the residue on the ansatz, which selects a subset of the denominator structures. Next we decompose, through the algorithms described in

variables can be written as

$$\epsilon_{\alpha\dot{\alpha}}^+(p, \xi) = \sqrt{2} \frac{\xi_\alpha \tilde{\lambda}_{\dot{\alpha}}}{\langle \xi \lambda \rangle}, \quad \epsilon_{\alpha\dot{\alpha}}^-(p, \xi) = \sqrt{2} \frac{\lambda_\alpha \tilde{\xi}_{\dot{\alpha}}}{[\tilde{\lambda} \tilde{\xi}]}, \quad (3.49)$$

where $p_{\alpha\dot{\alpha}} = \lambda_\alpha \tilde{\lambda}_{\dot{\alpha}}$ and ξ is an arbitrary reference spinor. In our approach, it is either a simple dimensional analysis as for the four-gluon amplitude which forces us to add more denominators, or for higher-point amplitudes it will be unitarity itself that does so.

¹⁷By this we mean exhausting the combinatorics of possible invariants without however adding those already present in the denominator, which would of course lead to unphysical higher order poles.

Section 3.2.2, the colour structures on both sides of (3.50) in a suitable basis $\{C_l^{a_1 \dots a_n}\}$:

$$C_{i,j}^{a_1 \dots a_n} = \sum_l b_{i,j,l} C_l^{a_1 \dots a_n} . \quad (3.51)$$

Then, we impose the matching of the coefficients of the colour structures in this basis on both sides of the equality (3.50). Here we are taking advantage of the same principle which makes colour-decomposition in Yang-Mills theory so powerful, namely that the kinematic coefficients of the colour structures are by themselves gauge-invariant quantities and can be dealt with independently from each other. So we end up with a set of equations of the type

$$-i \sum_{i',j,k} \frac{b_{i',j,l}}{\widetilde{\mathcal{D}}_{i'}} c_{i',j,k} \mathcal{N}_{i',j,k} = \mathcal{K}_l . \quad (3.52)$$

Here i' runs over the trivalent graph structures for which the specified Mandelstam invariant $s_{i_1 \dots i_m}$ appears, the $\widetilde{\mathcal{D}}_{i'}$ are the $\mathcal{D}_{i'}$ stripped of a factor $s_{i_1 \dots i_m}$ and the $c_{i,j,k}$ are the rational coefficients to be fixed. The \mathcal{K}_l are kinematic coefficients defined by the product of lower point amplitudes as

$$f \sum_{s_1, h_1} \mathcal{A}_{m+1}(p_{i_1}^{h_{i_1}} \dots p_{i_m}^{h_{i_m}}, p_I^{h_I}) \mathcal{A}_{n-m+1}(p_I^{h_I} \rightarrow p_{i_{m+1}}^{h_{i_{m+1}}} \dots p_{i_n}^{h_{i_n}}) := \sum_l C_l^{a_1 \dots a_n} \mathcal{K}_l \quad (3.53)$$

where the colour structures $C_l^{a_1 \dots a_n}$ are elements of the chosen colour basis. The \mathcal{K}_l are known analytic functions of the spinor invariants and Mandelstam invariants, and they also contain the dependence on the couplings g_k , $\mathcal{Y}^{(f)}$ and λ . Each equation (3.52) now only contains kinematic invariants, the $c_{i,j,k}$ for which we want to solve and products of couplings. Thus we repeatedly evaluate the kinematics numerically and so obtain a linear system in the $c_{i',j,k}$ which upon solution yields a subset of the $c_{i',j,k}$ as functions of the couplings and possibly other c 's. Since numerical evaluations are performed on very special kinematic points where intermediate states go on-shell, some of the coefficients $c_{i',j,k}$ might in principle drop out of the system. These coefficients are identified by an a priori numerical evaluation, which then allows to only solve the system in the actually relevant variables.

Repeating this procedure in every kinematic channel might still not completely fix the ansatz, since some of the $c_{i,j,k}$ might be spurious in the sense that using momentum conservation and Schouten identities appropriately they actually drop out altogether from the final result. In particular this happens when we consider amplitudes with external vectors. At the very end of the calculation, we take advantage of the arbitrary nature of these coefficients to set them, for example, either to a value which makes the final result more compact or to zero.

In order to get exact solutions and avoid possible issues tied to precision loss in floating

point arithmetic, we make use of finite fields arithmetic¹⁸ which is made possible by the fact that at tree-level the kinematic dependence of the amplitudes in the spinor variables is rational. More specifically for each subamplitude we generate a set of momentum-twistors [184, 185] with components on \mathbb{Z}_p , where twistors associated to different subamplitudes but to the same internal momentum are by construction taken to be on the same plane¹⁹. From these components then we compute the kinematic invariants and from there the products of the tree-amplitudes, all of which naturally live on the field \mathbb{Z}_p . This approach in general greatly speeds up the calculations, having as single minor drawback the fact that to obtain the solution to the linear system on \mathbb{Q} once it has been computed on \mathbb{Z}_p would generally require repeated sampling for different values of the prime p (see Section 3.4). However, since the coefficients involved in our calculations are typically very small compared to the prime p we consider, the use of a single field is usually enough, further strengthened by checking the solutions a posteriori on rational kinematic points. The system solution itself is done through row reduction: the matrix A to be reduced is obtained from numerically evaluating (3.52) $t + 1$ times, with t being the number of $c_{i',j,k}$ appearing in the latter linear equation²⁰, and can be schematically written as

$$\begin{cases} \sum_{s=1}^S a_{0,s} m_s = 0 \\ \sum_{s=1}^S a_{1,s} m_s = 0 \\ \vdots \\ \sum_{s=1}^S a_{t+1,s} m_s = 0 \end{cases} \mapsto \underbrace{\begin{pmatrix} a_{0,0} & \cdots & a_{0,S} \\ \vdots & & \vdots \\ a_{t+1,0} & \cdots & a_{t+1,S} \end{pmatrix}}_A \underbrace{\begin{pmatrix} m_0 \\ \vdots \\ m_S \end{pmatrix}}_V = 0, \quad (3.54)$$

where the $a_{i,j}$ are numeric constants (from the numerical evaluations of the kinematic parts) and the m_s are the unknowns $c_{i,j,k}$ or monomials in the couplings g , \mathcal{Y} and λ and the imaginary unit i . The explicit mention of the imaginary unit is due to the fact that this needs to be treated with some care when using finite fields. Imaginary units are almost ubiquitous in our construction and we decided to treat them as symbolic objects on the same footing as the coupling constants. Square roots would in principle require a similar treatment, but these are easily removed by choosing appropriate normalisations of the colour factors, and thus are never present in our calculation. Getting back to the system solution, upon row-reducing the numeric matrix A on finite fields one gets to a matrix B in row echelon form, which of course still satisfies $V' \equiv B V = 0$, with V the

¹⁸The use of finite fields in high-energy physics has been introduced in [182] in the context of IBP reductions, and further pioneered in [183] where a much wider range of applications was explored. A brief overview of the topic will be given in Section 3.4.

¹⁹In twistor space, two intersecting lines define a null momentum, and a closed contour with n edges defines n conserved null momenta. When generating kinematics for the two subamplitudes \mathcal{A}_{m+1} and \mathcal{A}_{n-m+1} in (3.53), p_I is defined by the same intersecting lines for both of them.

²⁰Generating and solving a system with an additional redundant equation ensures that when a determined solution is found this is kinematics-independent and thus a true solution. Impossible systems might still admit determined kinematic-dependent solutions which are clearly unacceptable.

vector of constants $c_{i,j,k}$ and couplings. The relation $V' = 0$ can then be trivially solved for the couplings $c_{i,j,k}$ corresponding to the leading (the first non-vanishing) entries in each row of B . These relations provide the solution to the system.

It is worth stressing that, differently from either a Feynman diagrammatic approach or a BCFW-like calculation where the solidity of the code can only be tested a posteriori through cross-checks or other methods, when using factorisation every step of the calculation is in itself a consistency check on the code. The systems of equations we obtain in the end always have a (possibly vanishing) solution, unless there is some physical obstruction. This is indeed the case when vector bosons are present among the external states (or more in general massless particles with helicity $|h| \geq 1$) and not enough invariants have been considered in the denominator construction, see Section 3.3.1. An impossible solution is symptomatic of unitarity breaking telling us that the ansatz was not general enough.

Thanks to many small, but at times significant, expedients²¹ the construction of the numeric system is rather fast despite our use of `Mathematica` rather than dedicated low-level language implementations, for example in C, which are usually better suited for the task. As a consequence, the main bottleneck of the system-solving procedure is the system solution itself. As an aside, we note that our ansatz construction is of course independent of the ansatz solution method. More specifically, if the reader was interested in getting analytic expressions for tree-level amplitudes and already had at her/his disposal a routine for numerically evaluating the amplitude itself, say Berends-Giele [186] recursion for example, then the ansatz solution could be clearly done in one go solving a single large system in all the $c_{i,j,k}$. Despite being viable, we consider our approach far more appealing, not only conceptually because of the use of just on-shell quantities but also practically: solving the ansatz on the different factorisation channels leads to many small systems whose solution is faster than a single large one and furthermore lends itself to effective parallelisation.

3.4 Analytics from numerics through finite fields

In this section we describe in some more detail how it is possible to recover exact analytic results from numerical evaluations over finite fields, and we discuss why the procedure is advantageous compared to direct analytic calculations and more traditional floating point numerical evaluations, as well as the caveats of the method. We feel that it is worthwhile to discuss the topic in some more detail in order to also convince the reader that the algorithm presented in the previous section indeed produces exact analytic

²¹These include, for example, recycling numeric data whenever possible, storing and reusing directly the exact invariant products making up the numerators instead of the single invariants, and generating a minimal parametrization of the kinematic points first, reducing thus the numerical kinematic generation to evaluations of polynomials in one/two variables.

results despite the use of numeric evaluations, which a priori should not be taken for granted.

There is a wide mathematical literature on the topic, we refer the interested reader for example to [187], but we will only deal here with the few key aspects entering our calculations. On a similar footing we will not address the topic of functional reconstruction over finite fields, which is one of the contemporary major applications in high energy physics, for a discussion of that subject and further applications of finite fields we refer to [183, 188].

Why use finite fields

The term finite field refers to the cyclic group of order p , usually denoted \mathbb{Z}_p , which can be represented as the set of integers from one to $p - 1$

$$\mathbb{Z}_p \equiv \{0, 1, \dots, p - 1\}. \quad (3.55)$$

The key aspects of \mathbb{Z}_p are

1. it is a field which can be represented through a finite number of elements
2. for small enough values of p the elements of \mathbb{Z}_p can be represented exactly through machine size integers. Concretely speaking, if we have a 32-bit system and choose for example $p = 2^{31} - 1$ (which is a Mersenne prime number) all the elements of \mathbb{Z}_p can be represented exactly by the machine without incurring in precision loss and without need of any sort of additional software. This means the machine will be extremely fast when processing operations over \mathbb{Z}_p .
3. it is possible to map the field of rational numbers \mathbb{Q} to \mathbb{Z}_p , but more interestingly under appropriate circumstances it is possible to map elements of \mathbb{Z}_p back to \mathbb{Q} . Notice that the simple fact that the field of rationals has infinite elements while \mathbb{Z}_p is finite, is what makes the inverse mapping a non-trivial operation.

Assume now we are interested in obtaining an analytic expression of some sort, where we know that whatever the expression will be, this is a rational function of some variables; an example might be a tree-level amplitude which is a rational function of the spinor components or even better of the momentum-twistor variables. Let us assume that obtaining the result directly through an analytic computation is too challenging, for example because the computational time required could be too large for a result to be successfully obtained. In similar situations it might be a good idea to change the perspective on the problem and try to reformulate it using a numeric approach. In our case this amounts to switching from trying to directly obtain the amplitude from simplifying (3.2) analytically, to building numeric systems to be solved as in 3.3.1.

The advantage of numerical computations is that in principle they are much faster, since potentially large intermediate expressions are replaced with numbers. This is certainly true when dealing for example with floating-point arithmetic. On the other hand, if we want to obtain a final result which is exact we will need to keep intermediate numeric expressions exact as well, meaning that we have to make use of software keeping arbitrary precision of the numbers, so to avoid the possible precision loss which might occur with floating-point numbers. Using arbitrary precision arithmetics however can in general be time consuming, since intermediate and final expressions can be ratios of arbitrary size numbers, and this might lead to a similar issue we started from with the analytics. Here is where finite fields enter the game, since we can map our problem from \mathbb{Q} to \mathbb{Z}_p , which avoids the precision loss of floating point numbers, and then perform the numeric computations on \mathbb{Z}_p , which is extremely fast provided we choose p to be a machine-size prime and thus the whole computation will only involve machine-size natural numbers. The obvious issue is that once the problem at hand has been solved on \mathbb{Z}_p we need to map the solution back to \mathbb{Q} , through a map which cannot by any means be a bijection. Since this can be done, and we will later discuss how, mapping to a finite field complicated problems which allow for numerical evaluations is often a winning strategy.

Mapping the rationals \mathbb{Q} to the finite field \mathbb{Z}_p

First of all, we give a more rigorous definition of \mathbb{Z}_p through equivalence classes of the modulo operation. Given a natural number $p \in \mathbb{N}$, we say that a is equivalent to b modulo p if $a - b = np$ for some $n \in \mathbb{Z}$. The equivalence relation is then usually denoted as $a = b \pmod{p}$, and the equivalence class of which a is a representative is called $[a]_p$. Given the set $S \equiv \{[0]_p, [1]_p, \dots, [p-1]_p\}$, one can show that the group structure under addition in \mathbb{Z} induces a group structure on S as well through the map $a \mapsto [a]_p$. Considering also the multiplication operation induced by \mathbb{Z} , S becomes a ring which we denote \mathbb{Z}_p . Now, the modulo operation provides a natural mapping from \mathbb{Z} to \mathbb{Z}_p , which we would like to extend to

$$F_p : \mathbb{Q} \rightarrow \mathbb{Z}_p$$

$$\frac{a}{b} \mapsto q \tag{3.56}$$

Since

$$\frac{a}{b} \pmod{p} = a(b^{-1} \pmod{p}) \pmod{p}, \tag{3.57}$$

for the modulo operation to be defined on \mathbb{Q} one needs $b^{-1} \pmod{p}$ to be well defined meaning that b must admit a multiplicative inverse such that

$$b^{-1} \in \mathbb{Z}_p \mid bb^{-1} = b^{-1}b = 1 \pmod{p}. \tag{3.58}$$

If such an inverse exists for every non-zero element in \mathbb{Z}_p , then the latter becomes a field. It can be shown that \mathbb{Z}_p is indeed a field when p is a prime number, there are many ways of doing so, but we decided to rely on the following

Proposition 3.4.1. *Given a generic $p \in \mathbb{N}$ defining the ring \mathbb{Z}_p of integers modulo p , and an element $a \in \mathbb{Z}_p$ such that a and p are coprimes, we have that the product \cdot maps a over the entire ring. In other words for any $c \in \mathbb{Z}_p$ there exists $b \in \mathbb{Z}_p$ such that $a \cdot b = c \pmod{p}$, furthermore b is unique.*

Proof. First prove the uniqueness, i.e. given

$$ab = c \pmod{p}, \quad ab' = c' \pmod{p}$$

if $b \neq b'$ then $c \neq c'$. Suppose we had $c = c' \pmod{p}$ then

$$c - c' = 0 \pmod{p} \quad \Rightarrow \quad a(b - b') = 0 \pmod{p}$$

meaning that $a(b - b')$ is a multiple of p . Being a and p coprimes their least common multiple is ap , however clearly $(b - b') < p$, which would lead to a contradiction. Thus $a(b - b')$ can't be a multiple of p so $c \neq c'$.

From uniqueness, it follows that the image of the map $P_a : \mathbb{Z}_p \rightarrow \mathbb{Z}_p$ defined by $P_a(b) = ab$ must be the whole \mathbb{Z}_p in order for no product to yield the same result. \square

Due to proposition 3.4.1 if $a \in \mathbb{Z}_p$ and p are coprimes, there exists a unique $b \in \mathbb{Z}_p$ such that $ab = 1 \pmod{p}$, i.e. a admits a uniquely defined inverse under multiplication. In order for \mathbb{Z}_p to be a field such an inverse must be defined for every element of \mathbb{Z}_p so p must be coprime with $\{0, 1, \dots, p - 1\}$ meaning that p must be a prime.

The different behaviour of multiplication in \mathbb{Z}_p for p generic and p prime can be seen using the Cayley table²² for the product operation, take as an example the ring \mathbb{Z}_8 and the field \mathbb{Z}_7 as shown in Table 3.1. As can be seen $2, 4, 6 \in \mathbb{Z}_8$, which are not coprime with 8, are not mapped over the entire ring, moreover they are mapped several times over 0: each of these zeros is a common multiple of the given element $a \in \mathbb{Z}_8$ and 8 smaller than $a \cdot 8$. On the other hand, every non-zero element in \mathbb{Z}_7 is mapped over the entire field exactly once.

It is important to stress here that the zero element of \mathbb{Z}_p does never admit a multiplicative inverse. This means that given $c = \frac{a}{b}$, if b is a multiple of p then c will not admit an image under mod in \mathbb{Z}_p . In practical terms this does not however represent an issue for the applications we have in mind: since we are always performing some

²²A Cayley table for a given operation is a table reporting the outcome of that operation when applied to any possible pair of elements of the group, ring or field.

·		0	1	2	3	4	5	6	7
0		0	0	0	0	0	0	0	0
1		0	1	2	3	4	5	6	7
2		0	2	4	6	0	2	4	6
3		0	3	6	1	4	7	2	5
4		0	4	0	4	0	4	0	4
5		0	5	2	7	4	1	6	3
6		0	6	4	2	0	6	4	2
7		0	7	6	5	4	3	2	1

(a)

·		0	1	2	3	4	5	6
0		0	0	0	0	0	0	0
1		0	1	2	3	4	5	6
2		0	2	4	6	1	3	5
3		0	3	6	2	5	1	4
4		0	4	1	5	2	6	3
5		0	5	3	1	6	4	2
6		0	6	5	4	3	2	1

(b)

Table 3.1: Cayley tables for the product in \mathbb{Z}_8 and \mathbb{Z}_7 respectively. As can be seen $2, 4, 6 \in \mathbb{Z}_8$, which are not coprime with 8, are not mapped over the entire ring, moreover they are mapped several times over 0.

random sampling over kinematic points, if at any step of the computation we run into a $\frac{a}{0} \pmod p$ case we simply discard that kinematic point and consider a different one.

Mapping from \mathbb{Z}_p to \mathbb{Q} and the Chinese remainder theorem

On the uniqueness of the anti-image

The mapping $F_p : \mathbb{Q} \rightarrow \mathbb{Z}_p$ is clearly not invertible, in the sense that it is not possible to properly define an inverse function F_p^{-1} . This is due to the fact that the map F_p is not injective: starting from an element $c \in \mathbb{Z}_p$ there are infinite possible rationals $z = \frac{a}{b} \in \mathbb{Q}$ that are mapped to that c . Notice however that there are only finitely many such that $a, b < p$ simply because p is finite, and crucially there is only one²³ value of z such that $a^2, b^2 < \frac{p}{2}$:

Proposition 3.4.2. *Given an element $c \in \mathbb{Z}_p$, there is only one $z = \frac{a}{b} \in \mathbb{Q}$ such that $a^2, b^2 < \frac{p}{2}$ and $z = c \pmod p$*

Proof. Suppose that there were another pair of values a', b' such that $\frac{a'}{b'} = c \pmod p$ and $(a')^2, (b')^2 < \frac{p}{2}$, then we would have

$$\frac{a}{b} = \frac{a'}{b'} \pmod p \quad \Rightarrow \quad ab' = ba' \pmod p$$

meaning that there is an integer n such that $ab' - ba' = np$. However $|ab'| < \frac{p}{2}$ and same goes for $|ba'| < \frac{p}{2}$, thus

$$-p < np < p$$

which fixes $n = 0$ and so $ab' = ba'$, then $\frac{a}{b} = \frac{a'}{b'}$ and x is thus uniquely determined. \square

²³See for example [189].

In other words, given a rational $z = \frac{a}{b}$ there is an infinite set of primes $I_z \equiv \{p_1, p_2, \dots\}$ with $p_{i+1} > p_i$, such that $c = F_{p_i}(z)$ and c is not the image of any other rational $z' = \frac{a'}{b'}$ with $(a')^2, (b')^2 < \frac{p_i}{2}$.

For the sake of concreteness, suppose now we want to solve the system (3.54) and we map our problem to the field \mathbb{Z}_p . Upon solving we will be left with a set of coefficients $\{c_1, \dots, c_k\}$ with values in \mathbb{Z}_p , for each of which we need to obtain the corresponding value on \mathbb{Q} , say $\{z_1, \dots, z_n\}$. If the order p of the field is such that $p \in I_{z_1} \cap \dots \cap I_{z_n}$, thus if p is large enough compared to the numerators and denominators of the z_i , the coefficients c_i can be mapped back to \mathbb{Q} without any ambiguity²⁴. Clearly, a priori we cannot know the size of the rationals z_i , thus in general in order to correctly reconstruct them from the c_i one performs the same procedure on multiple different fields $\mathbb{Z}_{p_1}, \dots, \mathbb{Z}_{p_n}$ and then compares the reconstructed coefficients. If the primes p_1, \dots, p_n are large enough the reconstructed values will agree. On the other hand, in order to unambiguously identify the z_i one might need to use a value of p which exceeds machine size, thus bringing us back to the problem of avoiding arbitrary precision arithmetic which was the whole point of introducing finite fields in the first place. This issue can be circumvented through the so called Chinese remainder theorem.

The Chinese remainder theorem

The Chinese remainder theorem allows to recombine the images of z in various fields $F_{p_1}(z) \in \mathbb{Z}_{p_1}, \dots, F_{p_n}(z) \in \mathbb{Z}_{p_n}$ into the single image $X = F_{p_1 p_2 \dots p_n}(z) \in \mathbb{Z}_{p_1 p_2 \dots p_n}$ where $\mathbb{Z}_{p_1 p_2 \dots p_n}$ is a finite ring whose order is the product of all the p_i . Since the product $p_1 \dots p_n$ becomes easily very large even considering a small number n of fields (say two or three), thanks to the proposition 3.4.2 and performing cross-checks on multiple values of the p_i , the anti-image $z = F_{p_1 p_2 \dots p_n}^{-1}(X)$ can be unambiguously recovered. Notice that the proof of the Proposition 3.4.2 works even when p is not a prime, so when \mathbb{Z}_p is simply a ring rather than a field, as long as the inverse element b^{-1} is well defined²⁵. We now state the theorem and give a sketch of the proof.

Theorem 3.4.3 (Chinese remainder). *Let n_1, \dots, n_m be integers greater than 1 and pairwise coprime, let a_1, \dots, a_k be integers such that $0 \leq a_i < n_i$ for every i , then there*

²⁴So far we avoided to discuss how such an inverse map F_p^{-1} is obtained in practice. There are several different routes, the simplest one being probably to use the extended Euclidean algorithm, we will however not go into further detail here.

²⁵In the case of $F_{p_1 p_2 \dots p_n}(z)$ this is essentially true by construction, as long as each of the $F_{p_i}(z)$ is well defined.

exists only one $0 \leq X < N$ with $N = \prod_i n_i$ such that

$$\begin{cases} X = a_1 \pmod{n_1} \\ \vdots \\ X = a_k \pmod{n_k} \end{cases} \quad (3.59)$$

Proof. Uniqueness: In order to prove the uniqueness of the solution suppose that two numbers x and y both solve all the congruences. When divided by n_i they give the same remainder a_i , so their difference $x - y$ is a multiple of each of the n_i . As the n_i are pairwise coprime $x - y$ must also be a multiple of N , say $x - y = cN$. But $x < N$ and $y < N$ so we must have $c = 0$ and $x = y$.

Existence: The existence can be proven by constructing a solution, here we will only provide the final expression for X and show that indeed it satisfies all the requirements. Defining $N = \prod_i p_i$ and $N_i = N/n_i$, and making use of Bezout's identity for the coprimes N and n_i to define two integers m_i and M_i as

$$M_i N_i + m_i n_i = 1, \quad (3.60)$$

we can write the solution X as

$$X = \sum_{i=1}^k a_i M_i N_i \pmod{N}. \quad (3.61)$$

It can be easily seen that this expression solves all the congruences in (3.59). In fact notice that N_j is a multiple of n_i for $i \neq j$ in particular

$$N_j = \frac{N_i}{n_j} n_i$$

then isolating the i -th term and using $M_i N_i = 1 - m_i n_i$

$$\begin{aligned} X &= \sum_{j=1}^m a_j M_j N_j \\ &= a_i (1 - m_i n_i) + \sum_{j \neq i} a_j M_j \frac{N_i}{n_j} n_i \\ &= a_i + \left(\sum_{j \neq i} a_j M_j \frac{N_i}{n_j} - a_i m_i \right) n_i \\ &= a_i \pmod{n_i} \end{aligned}$$

being the term in parenthesis an integer. This is true for every i and completes the proof. \square

Having at disposal the Chinese remainder theorem, what one does in practice is to perform the computation at hand on one prime field \mathbb{Z}_{p_i} at a time and then recursively merge the results into $\mathbb{Z}_{p_1 \dots p_n}$ until the anti-images on successive iterations match. So for example one starts with two fields and gets $a_1 \in \mathbb{Z}_{p_1}, a_2 \in \mathbb{Z}_{p_2}$ which are then merged into some $A_{1,2} \in \mathbb{Z}_{p_1 p_2}$, then the anti-images $F_{p_1}^{-1}(a_1)$ and $F_{p_1 p_2}^{-1}(A_{1,2})$ are compared. If no match is found a new prime p_3 is considered, and a new value $a_3 \in \mathbb{Z}_3$ is computed and merged into $A_{1,2,3} \in \mathbb{Z}_{p_1 p_2 p_3}$. Then one checks for a match between $F_{p_1 p_2}^{-1}(A_{1,2})$ and $F_{p_1 p_2 p_3}^{-1}(A_{1,2,3})$, the procedure is iterated until a positive match is found. In the specific case of the algorithm presented in Section 3.3.1 we never really need to resort to Chinese remainder theorem because of the typically small size of the coefficients which solve the system (3.54) so the use of a single field is sufficient. Furthermore the rational solutions are checked by plugging them back into the original system.

Chapter 4

Loop-level unitarity and the SMEFT

In the first part of this chapter we introduce the one-loop unitarity techniques required for the calculations in the remainder of the thesis. We start by briefly discussing the general structure of loop-level amplitudes and the general strategy to tackle their calculation, but then we immediately focus our attention on the one-loop case which is the one of direct interest to us. This special case is extremely well understood and the deep analytic insights at our disposal make it the perfect playground for unitarity and generalised unitarity methods.

At loop-level, making use of unitarity essentially amounts to¹ perturbatively expanding the transfer matrix T , defined by $S = \mathbb{1} + iT$, and taking advantage of the consistency conditions imposed by $S^\dagger S = \mathbb{1}$ to relate higher-loop orders to products of lower-loop ones integrated over a phase-space: this defines the unitarity cut, more precisely a double-cut which in diagrammatic terms can be thought of as an interaction with two internal propagators going on-shell. The phase space integral is then actually not performed, instead the cut is uplifted [11, 10] and the integral is promoted to a full-fledged Feynman integral which has by construction the correct analytic properties and is a piece of the complete loop-amplitude one wants to compute. Performing an appropriate combination of these cuts then allows to obtain the complete² loop-amplitude piece by piece.

Generalized unitarity [17, 18, 12] is an extension of this method which aims at a more systematic extraction of the various pieces of the answer by putting on-shell a larger number of internal states, *i.e.* increasing the number of cuts one applies. These meth-

¹See for example [122] for a very clear explanation.

²Depending on whether we are in four dimensions or not we might miss rational terms. Later in the thesis, when we refer to a complete loop-level amplitude we mean including these rational terms.

ods allow to completely bypass the construction of the amplitude based on Feynman diagrams, and leave as bottleneck of the modern-day calculations the computation of sets of integrals which are used as a basis in which to express the loop-amplitude itself.

In the second part of this chapter, having now one-loop unitarity at our disposal, we complete the on-shell construction of the Standard Model initiated in Section 3.1. We apply the insights of [190,191] to recover anomaly cancellation conditions from unitarity and locality constraints. The key idea is that building the one-loop amplitudes through cuts will automatically ensure unitarity is respected, but on the other hand locality might be lost: spurious unphysical poles may appear, which in the complete one-loop amplitude must cancel out. These cancellations must be provided by the only part of the amplitude which is not detectable through four-dimensional cuts, namely the rational terms, which can then be fixed precisely so that the desired cancellations happen, at the same time recovering the full one-loop result in the process. There are instances however where, in order for the desired cancellations to happen, one would need to add pieces to the amplitude which are themselves cut-constructible. This leads to a contradiction, which can only be resolved if these terms cancel through other means, in particular thanks to the Standard Model hypercharges satisfying the relations known as anomaly cancellation conditions.

In the final part of the section we discuss an application of the previously mentioned loop-level unitarity techniques: the computation of the operator mixing matrix for mass-dimension eight operators in the Standard Model Effective Field Theory (SMEFT). In recent years EFT approaches have risen to prominence as systematic means to quantify deviations from the Standard Model in a way which does not rely on an understanding of the underlying complete high-energy theory, and because of this it allows to address in one go a variety of models. In the SMEFT, new physics is parametrized by higher-dimensional operators built from Standard Model fields [51,52], whose classification and organization into a complete operator basis we discussed in Section 3.2. These operators in general present a non-vanishing and usually non-diagonal anomalous dimension matrix, meaning that under the running of the coupling constant the operators get renormalised and mix among each other in non-trivial ways.

Consequently the Wilson coefficients of the operators at the scales accessible to collider experiments differ from those at the high-energy matching scale, and furthermore the mixing of the operators implies that experimental constraints on one of them also affects other operators. Hence, evaluating the anomalous dimension matrix is a crucial aspect of interpreting SMEFT results. In this respect, on-shell methods have proven extremely powerful not only in the computation of the anomalous dimension matrix, but even more so in the interpretation of zeroes appearing in the matrix through selection rules implied by helicity [34], operator lengths [35] angular momentum [36].

Still from an on-shell perspective, it has been found that the structure of rational terms influences the zeroes, and that a smart choice of regularization scheme can lead to further cancellations: this has been studied at two loops in the case of an $SU(N)$ model which presents similarities with the SM but it is far simpler and contains far less operators [37]. For the complete SMEFT, the first systematic and complete computation of the one-loop anomalous dimension matrix for dimension-six operators has been carried out in [84–86]. On the other hand, the study of the anomalous dimension of SMEFT interactions at dimension eight has produced partial results in [87–93], the first full calculation (to linear order in the Wilson coefficients) being presented in [5] and being reviewed in this chapter. The recent interest in dimension-eight terms in SMEFT has various reasons, one of them being that for a number of physically relevant observables, the leading dimension six terms actually vanish, as shown for example by means of some helicity selection rules in [192]. Furthermore, the dimension-eight operators are the first subject to positivity constraints on the couplings, namely theoretical bounds on the signs of certain combinations of the Wilson coefficients, which come solely from the requirements of the S-matrix satisfying the principles of unitarity and analyticity [193]. Experimentally finding a violation in any of these bounds would invalidate the EFT itself, for example due to the existence of new light degrees of freedom and thus new physics. In all of these circumstances, the computation of the operator mixing matrix, whose computation we discuss at the end of this chapter, is a key ingredient for the matching procedure to experimental results.

4.1 One-loop unitarity

In this section we give a very brief introduction to the generalized unitarity method, focussing especially on the one-loop case. Our goal is to simply highlight some of the key features which make it so powerful and to somewhat prepare the ground for the calculations featured in the remainder of the thesis. There are several reviews on generalized unitarity and related topics available in the literature to which we refer the interested reader, among others [121–123, 194, 195].

Loop amplitudes

Schematically we can write an L -loop amplitude as

$$\mathcal{A}_m^L(p_1^{h_1}, \dots, p_n^{h_n}) = t \sum_j \int \prod_{i=1}^L \left(\frac{d^D l_i}{(2\pi)^D} \right) \frac{c_j \mathcal{N}_j(\{p_\alpha\}_{\alpha=1, \dots, n}, \{l_\beta\}_{\beta=1, \dots, L})}{S_j \prod_{m_j} D_{m_j}}, \quad (4.1)$$

where the sum in j is over all the contributing L -loop Feynman diagrams, t is a normalisation constant dependent on convention, l_i are the L loop momenta, the c_j contain the colour and coupling information of the diagrams, S_j are possible symmetry factors,

\mathcal{N}_j are the kinematic numerators and m_j label the denominators of the j^{th} term. The denominators take the form $D_a = K_a^2 - m_a^2$ (having omitted the $i\epsilon$ prescription) where K is a linear combination of the external momenta p_i and the loop momenta l_i , and m_a is the mass of the particle associated to the given denominator. While tree amplitudes can be expressed as rational functions of the external kinematics, loop amplitudes have typically a more involved structure since the integration can give rise to various generalized logarithms and special functions. As a consequence, loop amplitudes present not only simple poles but usually also branch cuts: the key feature is that this richer analytic structure can be exploited to reconstruct the amplitude from lower-order on-shell data.

When discussing loop amplitudes one can focus on three distinct aspects of the problem:

- the loop integrand, meaning the rational function under the integration sign.
- the loop integral, as the combination of the integrand and the loop-momentum integration region.
- the full loop amplitude, meaning the integrated result, where one needs to take care of possible Infrared (IR) and Ultraviolet (UV) divergences by means of appropriate regulators.

In general, just as in the tree-level case, when building the loop amplitudes one would like to avoid dealing with the increasingly complex combinatorics of the Feynman diagrams in order to get the integrands, and this is where generalized unitarity is very powerful. But after having computed the integrand, one is still left with a number of non-trivial integrations to carry out. The general strategy is to try and reduce the amplitude into a (possibly minimal) sum of integrals which form a basis for the space of allowed integrals, so that once the integrated form of the basis is known, computing any other process expressible in the same basis does not require further integrations. There are a variety of related techniques, including for example integrand reduction [196–203], Integration-by-Parts identities (IBPs) [204, 205] and differential equations [206, 207] or more recently projection techniques through intersection numbers [208–212]. Computing the integrals is a hard and interesting problem in its own right, and major efforts have been made over the last years to get a better understanding of the integral structures and the algebra they satisfy, see for example [213–217] and references therein.

Restricting our attention to the $L = 1$ case, the structure of the amplitude is extremely well understood. In particular, it can be shown that any tensor integrals (integrals with dependence on the loop momentum in the numerator as well as denominator) can be reduced to a combination of scalar integrals (integrals with dependence on the loop momentum only in the denominator) with appropriate tensor coefficients [218] and

furthermore any scalar integral can be written in terms of a basis [219] of the form

$$\mathcal{A}_n^{(1)} = \sum_i d_i \mathcal{I}_4^i + \sum_i c_i \mathcal{I}_3^i + \sum_i b_i \mathcal{I}_2^i + \mathcal{R}, \quad (4.2)$$

where \mathcal{I}_4 represents so called box integrals, \mathcal{I}_3 triangles and \mathcal{I}_2 bubbles³, more precisely

$$\mathcal{I}_n^i = \int \frac{d^D l}{(2\pi)^D} \frac{1}{l^2(l - K_{i,1})^2 \cdots (l - K_{i,n-1})^2}, \quad (4.3)$$

and $K_{i,j}$ being appropriate subsets of the external momenta. In (4.2) the coefficients d_i, c_i, b_i are rational functions of the external kinematics, the indices i schematically label all the possible inequivalent cyclic orderings of external momenta in the diagrams of Figures 4.1 and 4.2, which show the diagrams associated to the integral basis of (4.2). \mathcal{R} represents the rational terms and does not present discontinuities in any of the kinematic invariants, we will get back to it later, in particular it will be the focus of Chapter 7. The power of the expansion (4.2), is that all the integrals I_2, I_3 and I_4 are known, we report some of them in the Appendix C.3, for a complete list see for example [11]. Once the one-loop amplitude is written in this basis, *i.e.* once the coefficients d_i, c_i, b_i have been computed, there is no need for any integration to be performed. It is also worth noting that the coefficients in the integral expansion are specifically *rational* functions of the external kinematics: this feature holds true also for higher-loop integral expansions and makes these coefficients a perfect target for functional reconstruction over finite fields, see for example [183].

Unitarity and the double-cut

Conservation of probability in a given quantum field theory reflects in the unitarity of the S matrix. The latter can be written as $S = \mathbb{1} + iT$, where the identity accounts for the no-interaction scenario when initial and final states are the same, and the transfer matrix T accounts for the actual interaction processes. From the unitarity of the S matrix one immediately gets that

$$S^\dagger S = \mathbb{1} \quad \Rightarrow \quad T^\dagger T = -i(T - T^\dagger), \quad (4.4)$$

furthermore, one can perturbatively expand T in terms of the coupling constant parametrizing the interaction, say g

$$T = g^2 T^{(0)} + g^4 T^{(1)} + g^6 T^{(2)} + \dots \quad (4.5)$$

³In general one should also consider tadpoles, *i.e.* integrals with only one massive external leg, but in dimensional regularization with massless particles such integrals vanish.

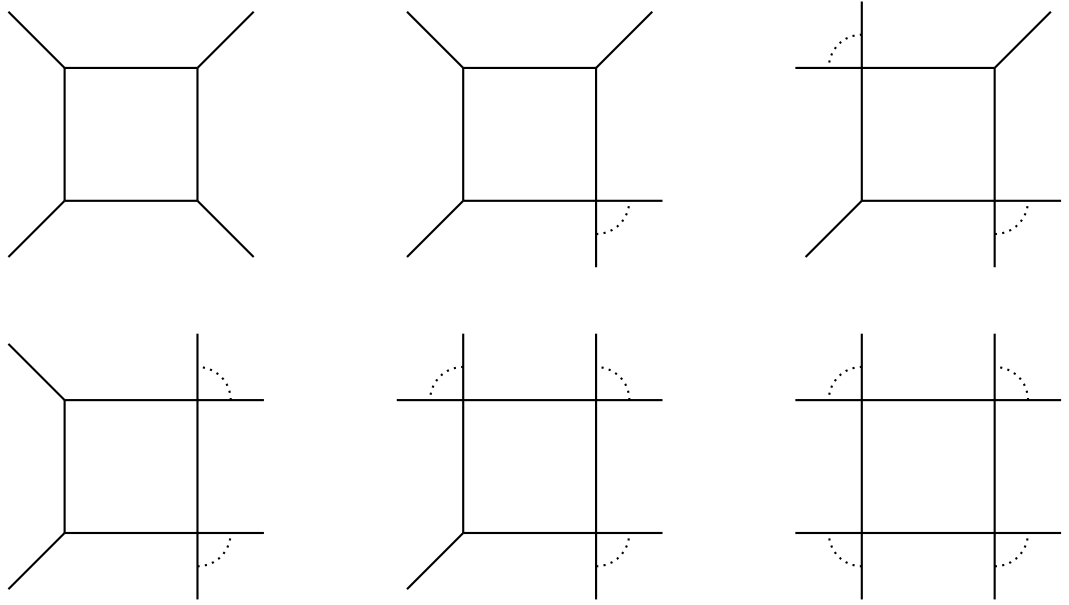


Figure 4.1: Possible box integrals appearing in the Feynman integral decomposition of a one-loop amplitude, simple lines represent massless legs while the dotted corners represent the massive ones.

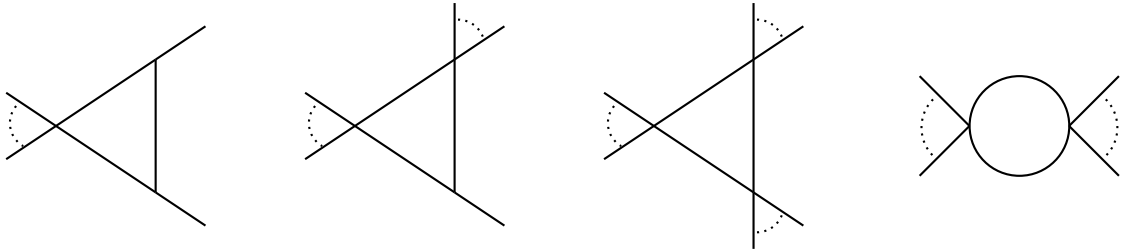


Figure 4.2: Possible triangle and bubble integrals appearing in the Feynman integral decomposition of a one-loop amplitude. Once again simple lines represent massless legs while the dotted corners represent the massive ones.

Combining the above with (4.4) we get relations between contributions to T at different perturbative orders, in particular at the two lowest orders we have

$$T^{(0)} = T^{(0)\dagger}, \quad -i(T^{(1)} - T^{(1)\dagger}) = T^{(0)}T^{(0)} \quad (4.6)$$

Relating the T matrix elements to the amplitude as

$$\langle f|T|i\rangle = (2\pi)^4 \delta^4(p_i - p_f) \mathcal{A}(i \rightarrow f), \quad (4.7)$$

where $|i\rangle, |f\rangle$ are the initial and final states and $\mathcal{A}(i \rightarrow f)$ is the amplitude involving the given states. So if we take relation equation (4.4), sandwich it between an initial

and final state and make use of the completeness relation

$$\mathbb{1} = \sum_X \int d\Pi_X |X\rangle\langle X|, \quad (4.8)$$

where X represents all the states in the theory and the integration is over the appropriate phase space, one gets the following⁴

$$2\text{Im}(\mathcal{A}^{(1)}(i \rightarrow f)) = i \sum_X \int d\Pi_X (2\pi)^4 \delta^4(p_i - p_f) \mathcal{A}^{(0)}(i \rightarrow X) \mathcal{A}^{(0)}(f \rightarrow X). \quad (4.9)$$

In other words, from integrating a product of tree-amplitudes one is in principle able to get the imaginary part of the one-loop amplitude, or equivalently the discontinuity across a branch cut singularity as a function of the kinematic invariants from which such imaginary parts arise.

Next one could in principle perform the dispersive integral $\int ds' \frac{\mathcal{A}(s')}{s-s'}$ for some Mandelstam invariant s to obtain the full amplitude, but this is usually hard and not very practical especially once the number of external legs is greater than four. So what we usually do instead is to make use of the information contained in the expansion (4.2) and compute discontinuities on the left- and right-hand-side. In particular, if we denote the discontinuity in the kinematic channel $s_{i\dots j} = (p_i + \dots + p_j)^2$ as $\text{Disc}(s_{i\dots j})$, we can compute

$$\text{Disc}(s_{i\dots j}) \mathcal{A}_n^{(1)} = \sum_i d_i \text{Disc}(s_{i\dots j}) \mathcal{I}_4^i + \sum_i c_i \text{Disc}(s_{i\dots j}) \mathcal{I}_3^i + \sum_i b_i \text{Disc}(s_{i\dots j}) \mathcal{I}_2^i \quad (4.10)$$

where $\text{Disc}(s_{i\dots j}) \mathcal{R} = 0$ by definition⁵ of \mathcal{R} , and similarly for those integrals \mathcal{I}_n^i which do not have a discontinuity in the considered channel. The discontinuity of the amplitude on the left-hand-side can be easily obtained thanks to (4.9), we call this a two-particle cut or double-cut, where a unitarity cut essentially promotes an off-shell internal line to an on-shell leg through the replacement of the Feynman propagator with

$$\frac{i}{p^2 + i\varepsilon} \rightarrow 2\pi \delta^{(+)}(p^2). \quad (4.11)$$

More explicitly (4.9) can be written as

$$\text{Disc}(s_{i\dots j}) \mathcal{A}_n^{(1)} = \sum_{h_1, h_2} \int \frac{d^D l}{(2\pi)^{D-2}} \delta(l_1^2) \delta(l_2^2) \mathcal{A}^{(0)}(-l_2^{-h_2}, i, \dots, j, l_1^{h_1}) \times \mathcal{A}^{(0)}(-l_1^{-h_1}, j+1, \dots, i-1, l_2^{h_2}), \quad (4.12)$$

where the sum runs over the possible internal helicities. A pictorial representation of

⁴On the left-hand-side we implicitly make use of time-reversal invariance.

⁵In four dimensions.

the previous definition is given in Figure 4.3.

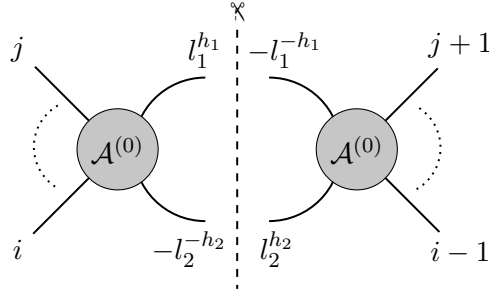


Figure 4.3: Pictorial representation of the double-cut in (4.12), the considered channel is $s_{i\dots j}$ and all the momentum lines are considered as out-going. The dashed line represents the cut, and the two propagators it runs through are considered as being on-shell.

Now one could perform the phase space integral, but following the approach of [10, 11] we instead uplift the cuts to Feynman propagators by the inverse relation (4.11) replacing $\delta(l_i^2) \rightarrow i/l_i^2$ which allows us to obtain a full-fledged Feynman integral that by construction has the correct discontinuity in the considered kinematic channel $s_{i\dots j}$. The so obtained integral can be reduced to the basis (4.2) from which we can then directly read off a subset of the coefficients d_i, c_i, b_i , namely those associated to integrals which present a discontinuity in $s_{i\dots j}$. Reiterating this procedure for all the different invariants $s_{i\dots j}$, which we describe as taking cuts in different invariant channels, one can piece by piece obtain the complete expression for $\mathcal{A}^{(0)}$. Clearly, when iterating over different invariant channels one has to take care not to repeatedly count the same coefficient in the basis (4.2) since the same integral \mathcal{I}_n^i might have multiple discontinuities and thus be identified by multiple different cuts. Also, one needs not to consider all the available invariant channels, but only those giving rise to a set of “spanning cuts”, meaning a set of cuts under which all the integrals \mathcal{I}_n^i can appear at least once.

Notice that as long as we are on the cut, so while we consider the two internal propagators as on-shell, great simplifications in the integrand of (4.12) occur, furthermore while we consider four-dimensional tree amplitudes we can make use of the spinor-helicity formalism to get the easiest possible expressions. On the other hand, by doing so we only get the part of the amplitude which we call cut-constructible namely everything except the rational term \mathcal{R} . There are different available approaches for the reconstruction of rational terms, for example via Feynman diagrammatic reduction techniques [220–223] or using loop-level recursive techniques combined with the previous knowledge of the cut-constructible part of the amplitude [178, 224, 225]. Another approach is to consider intermediate states in D dimensions instead of four, i.e. dimensional regularization, which allows to recover the full amplitude from unitarity cuts with no rational ambiguity [110, 179, 226]. From a cut construction point of view we have that moving from

four to $D = 4 - 2\epsilon$ dimensions⁶ requires every piece of the amplitude to contain a new term with mass dimension -2ϵ , to compensate for the shift in the dimension of the coupling and keep the dimension of the amplitude fixed. Considering only massless internal particles there is no mass available to supply such a term thus the only option left is something like $(-s)^{-2\epsilon}$, with s some kinematic invariant⁷. Expanding in ϵ :

$$(-s)^{-2\epsilon} \simeq 1 - 2\epsilon \ln(-s) + \dots, \quad (4.13)$$

which contains a discontinuity in $s > 0$. Thus also the rational term \mathcal{R} , which in $D = 4 - 2\epsilon$ becomes $\mathcal{R}(-s)^{-2\epsilon}$, is now visible to unitarity cuts. In Section 7 we consider a modification of this approach where instead of taking D arbitrary we consider it to be an integer, specifically $D = 6$ so to be able to still make use of the power of spinor-helicity for simplifications (as well as numeric approaches if required) but being nonetheless able to get the full amplitude including rational terms.

Generalized unitarity

The procedure of cutting propagators in an amplitude selects only those contributions that have those propagators in the first place. When we sew two tree-amplitudes together as in (4.12), out of all the \mathcal{I}_n^i in (4.2) only those that possess both cut propagators can show up in the result. Clearly, assigning a given pair of propagators to be cut uniquely isolates an integral of the bubble-type \mathcal{I}_2^i , but there are in general multiple triangles \mathcal{I}_3^i and boxes \mathcal{I}_4^i featuring those propagators, and so what we find through double cuts are combinations of multiple integrals at once. The idea of generalized unitarity [17, 18, 12] is that the larger the number of cuts one performs, *i.e.* the more propagators one requires to be present in the integrals, the less integrals can contribute until performing a maximum cut (which at one loop in four dimensions amounts to four cuts) one is left with a single integral of the basis. Thus applying a quadrupole-cut will relate directly the coefficient d_i of a single box integral to a product of four tree-amplitudes evaluated on a completely constrained internal kinematics: four cuts means four delta functions which completely constrain the internal loop momentum⁸. In a similar fashion, performing a triple-cut will isolate a single triangle integral from our basis however this time also some box integrals sharing the same propagators will appear and one has to subtract out this ‘‘pollution’’ in order to access the triangle coefficient. This can be done for example as in [229] or [230], or in a systematic way as proposed in [196, 231]: performing the cuts in descending order, *i.e.* starting from the maximum cut and then one by one cutting less propagators until one ends up with double-cuts, allows to use previously extracted information to subtract the redundant

⁶External states can still be kept in four dimensions following the four-dimensional helicity scheme [227, 228].

⁷ s can be different in different terms of the amplitude, it just needs to be an invariant.

⁸Specifically, the four cut conditions allow for two complex valued solutions.

(because already known) information and directly access a single coefficient from each set of cuts. Clearly, the whole method is made extremely powerful by the a priori knowledge of the integral basis expansion (4.2).

The natural question at this point is whether there is a general way to access the single integrals' coefficient without having to perform any sort of subtraction or further manipulations. In $\mathcal{N} = 4$ super-Yang-Mills such a strategy has been devised and is called prescriptive unitarity [232–234], while in non-supersymmetric theories the idea of directly projecting out single integral coefficients is addressed in the already mentioned works on intersection numbers [208–212]. While extremely powerful, these techniques go well beyond what was needed to perform the calculations in the rest of this thesis, for which the presented one-loop unitarity and generalised unitarity methods were sufficient.

4.2 Hypercharge constraints from gauge anomalies

Armed with the previous discussion of unitarity and generalized unitarity, in this section we complete the on-shell construction of the Standard Model initiated in Section 3.1, making use of locality constraints on the on-loop amplitudes to find the anomaly conditions which relate some of the SM hypercharges among each other.

It has long been known that in gauge theories with chiral fermions anomalies arise from fermion loops [235, 236]. These gauge anomalies impose consistency conditions on the theory, which in the case of the SM translate into relations among the hypercharges of the fermions. Interestingly, as first noticed in [190, 191], the same cancellation conditions are required from a purely on-shell point of view by a clash of unitarity and locality in some one-loop amplitudes. In this section we apply this method to recover the SM anomaly cancellation conditions.

The core of the idea is that one-loop amplitudes can be computed and entirely fixed using generalised unitarity methods, up to rational terms which have no branch points. Such amplitudes by construction are unitary, however locality is not guaranteed (spurious poles can appear in the final result) but can be restored by appropriately fixing the rational terms to which the unitarity methods are blind. These rational terms might in turn introduce new corrections to the factorisation of the four-point amplitude, which is inconsistent with the fact that the three-point amplitudes are tree-level exact and fixed by helicity and mass dimension. When this happens additional properties of the theory need to be required for these terms to vanish. In particular, in this section we will show that for the Standard Model this leads to well known anomaly constraints on the fermion hypercharges.

We will specifically consider a fermion loop coupled to four external gauge bosons in

$$c_4^f = -\frac{s_{12}^4 s_{14}^2}{2 s_{13}^4}$$

$$c_4^{\bar{f}} = -\frac{s_{12}^2 s_{14}^4}{2 s_{13}^4}$$

$$c_{3,(12)}^f = \frac{s_{12}^4 s_{14}}{2 s_{13}^4}$$

$$c_{3,(12)}^{\bar{f}} = \frac{s_{12}^2 s_{14}^3}{2 s_{13}^4}$$

$$c_{2,(12)}^f = \frac{s_{14}(2s_{14}^2 + 11s_{12}^2 + 7s_{12}s_{14})}{6s_{13}^3}$$

$$c_{2,(12)}^{\bar{f}} = \frac{s_{14}(2s_{14}^2 - s_{12}^2 - 5s_{12}s_{14})}{6s_{13}^3}$$

Figure 4.4: Kinematic coefficients from generalised unitarity [229], here a kinematic contribution of the type $\frac{(24)^2[13]^2}{s_{12}s_{14}}$ has been factored out.

the MHV configuration. The full one-loop amplitudes in the Standard Model can be schematically written as

$$\mathcal{A}^{(1)} = \mathcal{A}_{\text{vec}}^{(1)} + \mathcal{A}_{\text{ferm}}^{(1)} + \mathcal{A}_{\text{scal}}^{(1)}, \quad (4.14)$$

where the three contributions correspond respectively to vector bosons, fermions or scalars running in the internal loop, the specific type of these particles depending on the external states. We want to focus here on the fermion loop contributions, which are infrared finite and are the only part contributing to the chiral anomaly, since the latter is due to the coupling of vector bosons (which will be chosen as external states) to chiral fermions. The one loop amplitudes we consider have an internal fermion loop coupled to four external gauge bosons in alternating helicity configuration. The kinematic information of these amplitudes is entirely captured by the coefficients of Figure 4.4 with cyclic rotations providing the other orderings. For later convenience we define the following kinematic combinations, which turn out to be ubiquitous in the

one-loop amplitudes

$$K_{\text{even}} := \frac{\langle 24 \rangle^2 [13]^2}{s_{12}s_{14}} \sum_{i,j} (c_{i,j}^f + c_{i,j}^{\bar{f}}) I_i(j), \quad K_{\text{odd}} := \frac{\langle 24 \rangle^2 [13]^2}{s_{12}s_{14}} \sum_{i,j} (c_{i,j}^f - c_{i,j}^{\bar{f}}) I_i(j), \quad (4.15)$$

with $i = 2, 3, 4$ and $j = s_{12}, s_{14}$, and I_2, I_3 and I_4 being the bubble, triangle and box integrals given in Appendix C.3. Notice that in the chosen helicity configuration in the one-loop amplitude there are no discontinuities in the s_{13} channel, because all the tree-amplitudes entering the fermion loop contribution in the generalised unitarity calculation vanish in this channel.

Then we consider as a first example the one-loop amplitude with two W s and two B s as external states, and consequently Q/\bar{Q} and L/\bar{L} as the only possible fermions running through the loop. We find

$$\mathcal{A}_{\text{ferm}}^{1\text{-loop}}(W_+^I, B_-, W_+^J, B_-) \Big|_{\text{cut}} = g_1^2 g_2^2 (Y_L^2 + 3Y_Q^2) \delta^{IJ} K_{\text{even}}. \quad (4.16)$$

The presence of only K_{even} was to be expected due to the interplay of the colour part with the kinematics. The $SU(3)$ colour part is trivial being absent in the case of the L/\bar{L} circulating in the loop and contributing a numeric factor $\delta_a^a = 3$ for the Q/\bar{Q} loop. The $SU(2)$ part on the other hand contributes with a factor of $\text{Tr} \sigma^I \sigma^J = \frac{1}{2} \delta^{IJ}$ in both the s_{12} and s_{14} channels, which then leads to an additive combination of the kinematic parts into K_{even} . Studying the behaviour of K_{even} in the small- s_{13} limit one finds that

$$K_{\text{even}} \xrightarrow{s_{13} \rightarrow 0} \frac{\langle 24 \rangle^2 [13]^2}{s_{12}s_{14}} \left(-\frac{s_{12}^2}{s_{13}^2} - \frac{s_{12}}{s_{13}} + \mathcal{O}(s_{13}^0) \right), \quad (4.17)$$

thus, in order to restore locality, this amplitude requires a rational term whose kinematic part is of the form

$$R_{\text{even}} = -\frac{\langle 24 \rangle^2 [13]^2}{s_{13}^2}, \quad (4.18)$$

which cancels both the spurious poles of (4.17) and does not produces any modification to the residues in the s_{12} and s_{14} channels. Adding together the cut-constructible and rational piece one gets the complete fermion loop contribution

$$\mathcal{A}_{\text{ferm}}^{1\text{-loop}}(W_+^I, B_-, W_+^J, B_-) = g_1^2 g_2^2 (Y_L^2 + 3Y_Q^2) \delta^{IJ} (K_{\text{even}} + R_{\text{even}}). \quad (4.19)$$

On the other hand, considering three external W and a single B , one ends up with

$$\mathcal{A}_{\text{ferm}}^{1\text{-loop}}(W_+^I, W_-^J, W_+^K, B_-) \Big|_{\text{cut}} = \frac{i}{2} g_1 g_2^3 (Y_L + 3Y_Q) \epsilon^{IJK} K_{\text{odd}}, \quad (4.20)$$

where once again the $SU(2)$ colour structure, which is $\text{Tr} \sigma^I \sigma^J \sigma^K = \frac{i}{4} \epsilon^{IJK}$ in the s_{12}

channel and $\text{Tr } \sigma^I \sigma^K \sigma^J = -\frac{i}{4} \epsilon^{IJK}$ in the s_{14} channel, is responsible for the relative sign among the kinematic structures and the combination into K_{odd} .

Now K_{odd} in the small- s_{13} limit goes as

$$K_{\text{odd}} \xrightarrow{s_{13} \rightarrow 0} \frac{\langle 24 \rangle^2 [13]^2}{s_{12} s_{14}} \left(-\frac{s_{12}}{s_{13}} + \mathcal{O}(s_{13}^0) \right), \quad (4.21)$$

requiring a compensating rational term of the form

$$R_{\text{odd}} = \langle 24 \rangle^2 [13]^2 \frac{s_{12} - s_{14}}{2s_{12} s_{13} s_{14}}, \quad (4.22)$$

which would lead to a complete fermion loop contribution of

$$\mathcal{A}_{\text{ferm}}^{1\text{-loop}}(W_+^I, W_-^J, W_+^K, B_-) = \frac{i}{2} g_1 g_2^3 (Y_L + 3Y_Q) \epsilon^{IJK} (K_{\text{odd}} + R_{\text{odd}}). \quad (4.23)$$

However, R_{odd} introduces (unphysical) corrections to the residues in the s_{12} and s_{14} channels, because the one-loop four-point amplitude cannot have any factorisation channel and thus it cannot appear in the one loop amplitude⁹. In order to get an answer which satisfies both unitarity and locality we must then enforce the coefficient of the amplitude to vanish, which means imposing

$$Y_L + 3Y_Q = 0. \quad (4.24)$$

In a similar fashion, when looking at the one-loop interaction of three gluons with a single B we get the condition

$$2Y_Q = Y_u + Y_d, \quad (4.25)$$

which is necessary for the fermion-loop contribution to recombine in the physically meaningful form

$$\mathcal{A}_{\text{ferm}}^{1\text{-loop}}(G_+^A, G_-^B, G_+^C, B_-) \Big|_{\tau^{ABC}} = -2g_1 g_3^3 (Y_u + Y_d) (K_{\text{even}} + R_{\text{even}}). \quad (4.26)$$

This case is somewhat peculiar compared to the previous ones, in the fact that instead of requiring the condition on the hypercharges to cancel a K_{odd} contribution, it is necessary for a correct recombination into K_{even} . The Q (\bar{Q}) part, which gets a factor of 2 from a trace over an $SU(2)$ delta, comes together with the \bar{u} (u) and \bar{d} (d) contributions, and upon requiring (4.25) leads to (4.26). Notice the crucial interplay between the fermions Q and the anti-fermions \bar{u} , \bar{d} (and vice versa) which transform alike under $SU(3)$: if the $SU(3)$ interaction was chiral this could not have happened. Not only that, one would find additional cancellation conditions arising for example

⁹Three-point amplitudes are exact at tree-level and fixed by helicity and mass dimensions consideration. This makes the poles of four-point amplitudes tree-level exact, *i.e.* there are no loop corrections to the residues of these poles.

from the four-gluon one-loop interaction, where this interplay is equally relevant.

Finally, in order to obtain the additional textbook constraint on the hypercharges

$$\left(2Y_L^3 - Y_e^3\right) + 3\left(2Y_Q^3 - Y_u^3 - Y_d^3\right) = 0, \quad (4.27)$$

we need to look at four-point amplitudes involving a fermion loop with three external B and a boson which interacts through the same coupling with all the fermions (leading thus to this coupling dropping out of the constraint), in other words a graviton g . Similarly, considering the fermionic contribution to the one-loop interaction of three gravitons with a single B will lead to the anomaly cancellation condition

$$(2Y_L - Y_e) + 3(2Y_Q - Y_u - Y_d) = 0. \quad (4.28)$$

4.3 Anomalous dimension matrix from on-shell techniques

In this section we discuss how to make use of some of the tools introduced in Section 3 and the unitarity methods of Section 4.1 in order to compute the one-loop operator mixing matrix for mass-dimension eight operators in the SMEFT [5]. In this context two are the major challenges: the complete classification of the independent operators for the given mass-dimension, which we dealt with in Section 3.2, and the computation of the mixing matrix itself. In this thesis we will be only concerned with contributions to the matrix which are leading order in the Wilson coefficients, but we stress that the machinery we utilise, in particular the algorithm allowing for the construction of arbitrary multiplicity amplitudes and non-minimal form factors presented in Section 3.3.1, allows to compute sub-leading contributions as well.

In the first section we briefly review how to compute the anomalous dimension matrix from on-shell methods, for a more complete and general discussion including two-loop applications (for an $SU(N)$ theory) we refer the interested reader to [37]. Since at dimension eight in the SMEFT there are almost a thousand operators, it is not possible for us to display here the complete results computed in [5], instead we present the running of the Wilson coefficients for the dimension six and eight operators relevant for the Higgs production in association with a W boson via photon scattering.

4.3.1 A review of the method

Sticking to the notation introduced in Section 3.3.1, we write the effective amplitudes as $\mathcal{F}_{n,d,i}(p_1^{a_1,h_1}, \dots, p_n^{a_n,h_n})$, where d is the dimension of the operator and i labels the minimal interactions (for example, in the case of $N_f = 1$ and $d = 6$, $i = 1, \dots, 84$), in order to distinguish it from renormalizable amplitudes \mathcal{A} . The central formula for our computations has been presented in [237] and gives the action of the *dilatation operator*

$D = \frac{\partial}{\partial \log \mu}$ on the amplitude in terms of its discontinuity¹⁰:

$$e^{-i\pi D} \mathcal{F}^* = S \otimes \mathcal{F}^* , \quad (4.29)$$

where S is the full S-matrix and on the RHS the product has to be interpreted as a matrix product weighted over a proper Lorentz phase space integral which, via the Optical Theorem, correspond to the discontinuity of the effective amplitude.

The dilatation operator is linked to the UV mixing matrix $\gamma_{i \rightarrow j}^{\text{UV}}$ by the Callan-Symanzik equation [238–240]:

$$D\mathcal{F}_i = \left(\gamma_{j \rightarrow i}^{\text{UV}} - \gamma_i^{\text{IR}} \delta_{ij} + \beta(g_k^2) \frac{\partial}{\partial g_k^2} \delta_{ij} \right) \mathcal{F}_j , \quad (4.30)$$

where $\beta(g_k^2)$ is the beta-function for the coupling g_k and γ_i^{IR} is the IR contribution to the anomalous dimension of the amplitude \mathcal{F}_i which depends only on its external states.

Combining (4.29) and (4.30), expanding to leading order in the coupling and at linear order in the effective interactions, one finds¹¹

$$\begin{aligned} \gamma_{j \rightarrow i}^{\text{UV}} \mathcal{F}_j(p_1^{h_1} \dots p_n^{h_n}) &= -\frac{1}{\pi} \sum_{l=1}^n \sum_{\{l_1, l_2\}} \int \frac{d\Omega_2}{32\pi^2} \left[\mathcal{A}_4(p_{l_1}^{h_{l_1}} p_{l_2}^{h_{l_2}} \rightarrow p_l^{h_l} p_m^{h_m}) - \sum_{k=1}^3 \frac{g_k^2 T_{k,l_1} \cdot T_{k,l_2}}{\cos^2 \theta \sin^2 \theta} \right] \\ &\quad \cdot \mathcal{F}_i(\dots p_{l_1}^{h_{l_1}} \dots p_{l_2}^{h_{l_2}} \dots) \\ &\quad + \mathcal{F}_i(p_1^{h_1} \dots p_n^{h_n}) \cdot \sum_{l=1}^n \frac{\gamma_{\text{coll}}^{(l)}}{16\pi^2} , \end{aligned} \quad (4.31)$$

where

$$\int \frac{d\Omega_2}{4\pi} = \int_0^{2\pi} \frac{d\phi}{2\pi} \int_0^{\frac{\pi}{2}} d\theta \, 2 \cos \theta \sin \theta \quad (4.32)$$

is the Lorentz phase space integral, the sum over $\{l_1, l_2\}$ is over the species and the helicity configurations of the internal particles, $\gamma_{\text{coll}}^{(l)}$ is the IR collinear anomalous dimension associated to the l^{th} -particle and the term with $T_{k,l_1} \cdot T_{k,l_2}$ takes care of the subtraction of the (divergent) IR cusp anomalous dimension (the label k runs over the three factors of the gauge group $U(1) \times SU(2) \times SU(3)$). In particular, the latter is non-zero if the in- and out-states of the four-point amplitude are the same and, if this is the case, it is a proper contraction of the Lie algebra generators (or the product of the

¹⁰This formula has been first presented in [237] for \mathcal{F} being a form factor, but it trivially holds for (effective) amplitudes as well, by setting $g^\mu = 0$ in the form factor.

¹¹In order not to clutter up the notation with factors of 2 and π , the results provided at the end of this section, as well as those for the complete dimension-eight mixing matrix given in the ancillary files of [5] are given in terms of the matrix $\gamma_{ij}^{\text{UV}} \equiv 16\pi^2 \gamma_{j \rightarrow i}^{\text{UV}}$, where we factored out the usual loop factor $\frac{1}{16\pi^2}$.

hypercharges in the case of $U(1)$ associated to the outgoing (or equivalently incoming) particles. For example, if the four-point amplitude is $\mathcal{A}_4(\bar{Q}_{l_1} Q_{l_2} \rightarrow \bar{Q}_l Q_m)$, then

$$\sum_{k=1}^3 g_k^2 T_{k,l} \cdot T_{k,m} = \left(-\frac{1}{6}\right) \cdot \frac{1}{6} g_1^2 + g_2^2 \sigma^I{}^i{}_m \sigma^I{}^j{}_l + g_3^2 \tau^A{}^a{}_m \tau^A{}^b{}_l. \quad (4.33)$$

The helicity variables associated to the internal momenta, on the cut configuration, can be written in terms of the Lorentz phase space angles θ and ϕ and the external momenta p_l and p_m , as first shown in [241]:

$$\begin{pmatrix} \lambda_{l_1} \\ \lambda_{l_2} \end{pmatrix} = \begin{pmatrix} \cos \theta & -\sin \theta e^{i\phi} \\ \sin \theta e^{-i\phi} & \cos \theta \end{pmatrix} \begin{pmatrix} \lambda_l \\ \lambda_m \end{pmatrix}, \quad (4.34)$$

together with the complex conjugate rotation for the spinors $\tilde{\lambda}_{l_1}$ and $\tilde{\lambda}_{l_2}$. The collinear anomalous dimensions for the particles in the Standard Model can be obtained by studying the anomalous dimension of UV protected operators, such as the stress-tensor as emphasised in [237]:

$$\begin{aligned} \langle p_1^{h_1} p_2^{h_2} | T^{\mu\nu} | 0 \rangle \cdot \sum_{l=1}^2 \frac{\gamma_{\text{coll}}^{(l)}}{16\pi^2} &= \frac{1}{\pi} \sum_{\{l_1, l_2\}} \int \frac{d\Omega_2}{32\pi^2} \left[\mathcal{A}_4(p_{l_1}^{h_{l_1}} p_{l_2}^{h_{l_2}} \rightarrow p_1^{h_1} p_2^{h_2}) \right. \\ &\quad \left. - \sum_{k=1}^3 \frac{g_k^2 T_{k,l_1} \cdot T_{k,l_2}}{\cos^2 \theta \sin^2 \theta} \right] \cdot \langle p_{l_1}^{h_{l_1}} p_{l_2}^{h_{l_2}} | T^{\mu\nu} | 0 \rangle, \end{aligned} \quad (4.35)$$

A list of the collinear anomalous dimensions computed from the stress-tensor form factor can be found in Appendix A.3.

4.3.2 The Higgs production in association with a W boson

As an illustrative application of the techniques discussed so far, we consider a subset of dimension-six and dimension-eight operators relevant for the Higgs production in association with a W boson via proton scattering, *i.e.* the operators contributing to the scattering $pp \rightarrow hW$ as considered in [77], with the difference that here we consider a single fermion family so $N_f = 1$. In this section, we will compute the mixing among dimension-six and dimension-eight effective interactions separately. First, we present the relevant minimal amplitudes found using the algorithm presented in Section 3.2, which are in one-to-one correspondence with the independent operators considered in [77]. Then, using the techniques just reviewed we compute the two UV mixing matrices, comparing the mixing matrix for dimension-six operators with known results in the literature [84–86, 242–244]. The full mixing matrix for all the operators in the SMEFT up to dimension eight can be found in the ancillary files of [5].

There are thirteen dimension-six operators (five of which are self-hermitian) contribut-

#	Hilbert series	Minimal amplitude
1	$\bar{H}^3 H^3$	$\mathcal{Y}_{\langle 123 \rangle} \circ \delta_{j_1}^{i_4} \delta_{j_2}^{i_5} \delta_{j_3}^{i_6}$
2	$2D^2 \bar{H}^2 H^2$	$\mathcal{Y}_{\langle 12 \rangle} \circ \mathcal{Y}_{\langle 34 \rangle} \circ \langle 13 \rangle [13] \delta_{j_1}^{i_3} \delta_{j_2}^{i_4}$
3		$\mathcal{Y}_{\langle 12 \rangle} \circ \langle 12 \rangle [12] \delta_{j_1}^{i_3} \delta_{j_2}^{i_4}$
4	$2D\bar{Q}Q\bar{H}H$	$\langle 13 \rangle [23] \delta_{j_1}^{i_2} \delta_{j_3}^{i_4} \delta_{b_1}^{a_2}$
5		$\langle 13 \rangle [23] \delta_{j_3}^{i_2} \delta_{j_1}^{i_4} \delta_{b_1}^{a_2}$
6	$B_- B_- \bar{H}H$	$\langle 12 \rangle^2 \delta_{j_3}^{i_4}$
7	$B_+ B_+ \bar{H}H$	$[12]^2 \delta_{j_3}^{i_4}$
8	$W_- W_- \bar{H}H$	$\langle 12 \rangle^2 \delta^{I_1 I_2} \delta_{j_3}^{i_4}$
9	$W_+ W_+ \bar{H}H$	$[12]^2 \delta^{I_1 I_2} \delta_{j_3}^{i_4}$
10	$G_- G_- \bar{H}H$	$\langle 12 \rangle^2 \delta^{A_1 A_2} \delta_{j_3}^{i_4}$
11	$G_+ G_+ \bar{H}H$	$[12]^2 \delta^{A_1 A_2} \delta_{j_3}^{i_4}$
12	$B_- W_- \bar{H}H$	$\langle 12 \rangle^2 \sigma_{j_3}^{I_2 i_4}$
13	$B_+ W_+ \bar{H}H$	$[12]^2 \sigma_{j_3}^{I_2 i_4}$

Table 4.1: The table shows the thirteen dimension-6 operators and their multiplicity as a result of the Hilbert series method. To each independent operator we associate and enumerate a set of independent minimal amplitudes.

ing to the scattering $pp \rightarrow hW$ and such counting can be performed using Hilbert series method. In Table 4.1 and Table 4.2 we show the content of the various operators and their multiplicities as shown in reference [55] and the corresponding independent minimal amplitudes, respectively for the dimension-six and the dimension-eight effective interactions.

In the following we present the running of the Wilson coefficients defined by

$$\dot{c}_i = 16\pi^2 \mu \frac{\partial}{\partial \mu} c_i, \quad (4.36)$$

we first show the results for dimension six operators, $\dot{c}_i^{(6)}$ and then those for dimension eight $\dot{c}_i^{(8)} = \dot{c}_i^{(8),\text{UV}} - \dot{c}_i^{(8),\text{IR}}$ where IR subtraction has already been performed. In the presented results the dots¹² indicate that the operator associated to the given coefficient mixes with other operators which we are not considering, *i.e.* already at leading order in the couplings the sector we are looking at is not closed. The last term in the RG evolution of each coefficient is needed to isolate the UV contributions from the diagonal IR anomalous dimension. The six-dimensional results fully match with previous calculations in the literature, after a proper change of basis, and have thus provided a useful cross-check for the on-shell techniques discussed so far. While the following pages of renormalisation coefficients may not appear as very enlightening, they provide an idea of the type of the result we were aiming to get for the mixing and should also give a sense of non-triviality (in computational terms) of the calculation of the full dimension-eight case.

First the dimension-six coefficients:

¹²We explicitly display these only for dimension six, for dimension eight they would be present for most coefficients and we omit them.

#	Hilbert series	Minimal amplitude	#	Hilbert series	Minimal amplitude
1	$\bar{H}^4 H^4$	$\mathcal{Y}_{\langle 1234 \rangle} \circ \delta_{j_1}^{i_4} \delta_{j_2}^{i_5} \delta_{j_3}^{i_6} \delta_{j_4}^{i_8}$	34	$2D^2 B_- W_- \bar{H} H$	$\langle 12 \rangle^3 [12] \sigma_{j_1}^{i_2 i_4}$
2	$B_-^2 \bar{H}^2 H^2$	$\mathcal{Y}_{\langle 34 \rangle} \circ \langle 12 \rangle^2 \delta_{j_4}^{i_5} \delta_{j_3}^{i_6}$	35		$\langle 12 \rangle^2 \langle 23 \rangle [23] \sigma_{j_3}^{i_2 i_4}$
3	$B_+^2 \bar{H}^2 H^2$	$\mathcal{Y}_{\langle 34 \rangle} \circ [12]^2 \delta_{j_4}^{i_5} \delta_{j_3}^{i_6}$	36	$2D^2 B_+ W_+ \bar{H} H$	$[12]^3 \langle 12 \rangle \sigma_{j_3}^{i_2 i_4}$
4	$B_- W_- \bar{H}^2 H^2$	$\mathcal{Y}_{\langle 34 \rangle} \circ \mathcal{Y}_{\langle 56 \rangle} \circ \langle 12 \rangle^2 \delta_{j_4}^{i_6} \sigma_{j_3}^{i_2 i_5}$	37		$[12]^2 \langle 23 \rangle [23] \sigma_{j_3}^{i_2 i_4}$
5	$B_+ W_+ \bar{H}^2 H^2$	$\mathcal{Y}_{\langle 34 \rangle} \circ \mathcal{Y}_{\langle 56 \rangle} \circ [12]^2 \delta_{j_4}^{i_6} \sigma_{j_3}^{i_2 i_5}$	38	$D^2 B_- W_+ \bar{H} H$	$\langle 13 \rangle^2 [23]^2 \sigma_{j_3}^{i_2 i_4}$
6	$2W_-^2 \bar{H}^2 H^2$	$\mathcal{Y}_{\langle 34 \rangle} \circ \langle 12 \rangle^2 \delta_{j_1}^{i_2} \delta_{j_2}^{i_3} \delta_{j_3}^{i_4} \delta_{j_4}^{i_5}$	39	$D^2 W_- B_+ \bar{H} H$	$\langle 13 \rangle^2 [23]^2 \sigma_{j_3}^{i_1 i_4}$
7		$\mathcal{Y}_{\langle 12 \rangle} \circ \langle 12 \rangle^2 \sigma_{j_1}^{i_2 i_5} \sigma_{j_3}^{i_4 i_6}$	40	$2D^2 W_- \bar{H}^2 H^2$	$\mathcal{Y}_{\langle 23 \rangle} \circ \mathcal{Y}_{\langle 45 \rangle} \circ \langle 12 \rangle \langle 14 \rangle [24] \epsilon^{i_4 i_5} \sigma_{j_1}^{i_1 i_2} \sigma_{j_2}^{i_3 i_4}$
8		$\mathcal{Y}_{\langle 34 \rangle} \circ [12]^2 \delta_{j_1}^{i_2} \delta_{j_2}^{i_3} \delta_{j_3}^{i_4} \delta_{j_4}^{i_5}$	41		$\mathcal{Y}_{\langle 23 \rangle} \circ \mathcal{Y}_{\langle 45 \rangle} \circ \langle 12 \rangle \langle 13 \rangle [23] \delta_{j_3}^{i_2} \sigma_{j_1}^{i_1 i_4}$
9		$\mathcal{Y}_{\langle 12 \rangle} \circ [12]^2 \sigma_{j_1}^{i_2 i_5} \sigma_{j_3}^{i_4 i_6}$	42	$2D^2 W_+ \bar{H}^2 H^2$	$\mathcal{Y}_{\langle 23 \rangle} \circ \mathcal{Y}_{\langle 45 \rangle} \circ [12] [14] \langle 24 \rangle \epsilon^{i_4 i_5} \sigma_{j_1}^{i_1 i_2} \sigma_{j_2}^{i_3 i_4}$
10	$G_-^2 \bar{H}^2 H^2$	$\mathcal{Y}_{\langle 34 \rangle} \circ \langle 12 \rangle^2 \delta_{j_1}^{i_2} \delta_{j_2}^{i_3} \delta_{j_3}^{i_4} \delta_{j_4}^{i_5}$	43		$\mathcal{Y}_{\langle 23 \rangle} \circ \mathcal{Y}_{\langle 45 \rangle} \circ [12] [13] \langle 23 \rangle \delta_{j_3}^{i_2} \sigma_{j_1}^{i_1 i_4}$
11	$G_+^2 \bar{H}^2 H^2$	$\mathcal{Y}_{\langle 34 \rangle} \circ [12]^2 \delta_{j_1}^{i_2} \delta_{j_2}^{i_3} \delta_{j_3}^{i_4} \delta_{j_4}^{i_5}$	44		$\mathcal{Y}_{\langle 12 \rangle} \circ \langle 12 \rangle^2 [12]^2 \delta_{j_1}^{i_2} \delta_{j_2}^{i_3} \delta_{j_3}^{i_4}$
12	$B_- W_-^2 \bar{H} H$	$\langle 12 \rangle \langle 23 \rangle \langle 13 \rangle \epsilon_{j_1}^{i_2} \epsilon_{j_2}^{i_3} \epsilon_{j_3}^{i_4} \sigma_{j_4}^{i_5 i_6}$	45	$3D^4 \bar{H}^2 H^2$	$\mathcal{Y}_{\langle 12 \rangle} \circ \mathcal{Y}_{\langle 34 \rangle} \circ \langle 13 \rangle^2 [13]^2 \delta_{j_1}^{i_2} \delta_{j_2}^{i_3} \delta_{j_3}^{i_4}$
13	$B_+ W_+^2 \bar{H} H$	$[12] [23] [13] \epsilon_{j_1}^{i_2} \epsilon_{j_2}^{i_3} \epsilon_{j_3}^{i_4} \sigma_{j_4}^{i_5 i_6}$	46		$\mathcal{Y}_{\langle 12 \rangle} \circ \mathcal{Y}_{\langle 34 \rangle} \circ \langle 12 \rangle \langle 13 \rangle [12] [13] \delta_{j_1}^{i_2} \delta_{j_2}^{i_3} \delta_{j_3}^{i_4}$
14	$W_-^3 \bar{H} H$	$\langle 12 \rangle \langle 23 \rangle \langle 13 \rangle \epsilon_{j_1}^{i_2} \epsilon_{j_2}^{i_3} \epsilon_{j_3}^{i_4} \delta_{j_4}^{i_5}$	47		$\mathcal{Y}_{\langle 34 \rangle} \circ \mathcal{Y}_{\langle 56 \rangle} \circ \langle 13 \rangle [23] \epsilon_{j_3}^{i_2} \delta_{j_1}^{i_3} \delta_{j_2}^{i_4} \delta_{j_4}^{i_5}$
15	$W_+^3 \bar{H} H$	$[12] [23] [13] \epsilon_{j_1}^{i_2} \epsilon_{j_2}^{i_3} \epsilon_{j_3}^{i_4} \delta_{j_4}^{i_5}$	48	$4D \bar{Q} \bar{Q} \bar{H}^2 H^2$	$\mathcal{Y}_{\langle 34 \rangle} \circ \mathcal{Y}_{\langle 56 \rangle} \circ \langle 13 \rangle [23] \delta_{j_3}^{i_2} \delta_{j_1}^{i_3} \delta_{j_2}^{i_4} \delta_{j_4}^{i_5}$
16	$G_-^3 \bar{H} H$	$\langle 12 \rangle \langle 23 \rangle \langle 13 \rangle f_{j_1}^{i_2} f_{j_2}^{i_3} f_{j_3}^{i_4} \delta_{j_4}^{i_5}$	49		$\mathcal{Y}_{\langle 34 \rangle} \circ \mathcal{Y}_{\langle 56 \rangle} \circ \langle 15 \rangle [25] \delta_{j_2}^{i_2} \delta_{j_1}^{i_3} \delta_{j_3}^{i_4} \delta_{j_4}^{i_5}$
17	$G_+^3 \bar{H} H$	$[12] [23] [13] f_{j_1}^{i_2} f_{j_2}^{i_3} f_{j_3}^{i_4} \delta_{j_4}^{i_5}$	50		$\mathcal{Y}_{\langle 34 \rangle} \circ \mathcal{Y}_{\langle 56 \rangle} \circ \langle 13 \rangle [23] \delta_{j_3}^{i_2} \delta_{j_1}^{i_3} \delta_{j_2}^{i_4} \delta_{j_4}^{i_5}$
18	$2D^2 \bar{H}^3 H^3$	$\mathcal{Y}_{\langle 123 \rangle} \circ \mathcal{Y}_{\langle 456 \rangle} \circ \langle 12 \rangle [12] \delta_{j_1}^{i_2} \delta_{j_2}^{i_3} \delta_{j_3}^{i_4} \delta_{j_4}^{i_5} \delta_{j_5}^{i_6}$	51		$\langle 12 \rangle^2 [23] \delta_{j_4}^{i_2} \delta_{j_2}^{i_3} \sigma_{j_1}^{i_4 i_5} \sigma_{j_3}^{i_6 i_7}$
19		$\mathcal{Y}_{\langle 123 \rangle} \circ \mathcal{Y}_{\langle 456 \rangle} \circ \langle 14 \rangle [14] \delta_{j_1}^{i_2} \delta_{j_2}^{i_3} \delta_{j_3}^{i_4} \delta_{j_4}^{i_5} \delta_{j_5}^{i_6}$	52		$\langle 12 \rangle \langle 14 \rangle [34] \delta_{j_4}^{i_2} \delta_{j_2}^{i_3} \sigma_{j_1}^{i_4 i_5} \sigma_{j_3}^{i_6 i_7}$
20	$D^2 B_- B_+ \bar{H} H$	$\langle 13 \rangle^2 [23]^2 \delta_{j_3}^{i_4} \delta_{j_4}^{i_5}$	53	$6DW_- \bar{Q} \bar{Q} \bar{H} H$	$\langle 12 \rangle^2 [23] \delta_{j_4}^{i_2} \delta_{j_2}^{i_3} \sigma_{j_1}^{i_4 i_5} \sigma_{j_3}^{i_6 i_7}$
21	$2D^2 W_- W_+ \bar{H} H$	$\langle 13 \rangle^2 [23]^2 \delta_{j_1}^{i_2} \delta_{j_3}^{i_4}$	54		$\langle 12 \rangle \langle 14 \rangle [34] \delta_{j_4}^{i_2} \delta_{j_2}^{i_3} \sigma_{j_1}^{i_4 i_5} \sigma_{j_3}^{i_6 i_7}$
22		$\langle 13 \rangle^2 [23]^2 \epsilon_{j_1}^{i_2} \epsilon_{j_2}^{i_3} \epsilon_{j_3}^{i_4} \sigma_{j_4}^{i_5 i_6}$	55		$\langle 12 \rangle^2 [23] \delta_{j_2}^{i_2} \delta_{j_1}^{i_3} \sigma_{j_3}^{i_4 i_5} \sigma_{j_4}^{i_6 i_7}$
23	$D^2 G_- G_+ \bar{H} H$	$\langle 13 \rangle^2 [23]^2 \delta_{j_1}^{i_2} \delta_{j_3}^{i_4}$	56		$\langle 12 \rangle \langle 14 \rangle [34] \delta_{j_4}^{i_2} \delta_{j_2}^{i_3} \sigma_{j_1}^{i_4 i_5} \sigma_{j_3}^{i_6 i_7}$
24	$D^2 B_- \bar{H}^2 H^2$	$\mathcal{Y}_{\langle 23 \rangle} \circ \mathcal{Y}_{\langle 45 \rangle} \circ \langle 12 \rangle \langle 14 \rangle [24] \delta_{j_3}^{i_2} \delta_{j_2}^{i_3}$	57		$[13]^2 \langle 23 \rangle \delta_{j_4}^{i_2} \delta_{j_2}^{i_3} \sigma_{j_1}^{i_4 i_5} \sigma_{j_3}^{i_6 i_7}$
25	$D^2 B_+ \bar{H}^2 H^2$	$\mathcal{Y}_{\langle 23 \rangle} \circ \mathcal{Y}_{\langle 45 \rangle} \circ [12] [14] \langle 24 \rangle \delta_{j_3}^{i_2} \delta_{j_2}^{i_3}$	58		$[13] [14] \langle 24 \rangle \delta_{j_4}^{i_2} \delta_{j_2}^{i_3} \sigma_{j_1}^{i_4 i_5} \sigma_{j_3}^{i_6 i_7}$
26	$D^2 B_-^2 \bar{H} H$	$\langle 12 \rangle^3 [12] \delta_{j_3}^{i_4} \delta_{j_4}^{i_5}$	59	$6DW_+ \bar{Q} \bar{Q} \bar{H} H$	$[13]^2 \langle 23 \rangle \delta_{j_4}^{i_2} \delta_{j_2}^{i_3} \sigma_{j_1}^{i_4 i_5} \sigma_{j_3}^{i_6 i_7}$
27	$D^2 B_+^2 \bar{H} H$	$[12]^3 \langle 12 \rangle \delta_{j_3}^{i_4} \delta_{j_4}^{i_5}$	60		$[13] [14] \langle 24 \rangle \delta_{j_4}^{i_2} \delta_{j_2}^{i_3} \sigma_{j_1}^{i_4 i_5} \sigma_{j_3}^{i_6 i_7}$
28	$2D^2 W_-^2 \bar{H} H$	$\langle 12 \rangle^3 [12] \delta_{j_1}^{i_2} \delta_{j_2}^{i_3} \delta_{j_3}^{i_4}$	61		$[13]^2 \langle 23 \rangle \delta_{j_2}^{i_2} \delta_{j_1}^{i_3} \sigma_{j_3}^{i_4 i_5} \sigma_{j_4}^{i_6 i_7}$
29		$\mathcal{Y}_{\langle 12 \rangle} \circ \langle 12 \rangle^2 \langle 23 \rangle [23] \epsilon_{j_1}^{i_2} \epsilon_{j_2}^{i_3} \epsilon_{j_3}^{i_4} \sigma_{j_4}^{i_5 i_6} \sigma_{j_5}^{i_7 i_8}$	62		$[13] [14] \langle 24 \rangle \delta_{j_2}^{i_2} \delta_{j_1}^{i_3} \sigma_{j_3}^{i_4 i_5} \sigma_{j_4}^{i_6 i_7}$
30	$2D^2 W_+^2 \bar{H} H$	$[12]^3 \langle 12 \rangle \delta_{j_1}^{i_2} \delta_{j_2}^{i_3} \delta_{j_3}^{i_4}$	63		$\langle 13 \rangle \langle 23 \rangle [23]^2 \delta_{j_3}^{i_2} \delta_{j_1}^{i_3} \delta_{j_2}^{i_4} \delta_{j_4}^{i_5}$
31		$\mathcal{Y}_{\langle 12 \rangle} \circ [12]^2 \langle 23 \rangle [23] \epsilon_{j_1}^{i_2} \epsilon_{j_2}^{i_3} \epsilon_{j_3}^{i_4} \sigma_{j_4}^{i_5 i_6} \sigma_{j_5}^{i_7 i_8}$	64	$4D^3 \bar{Q} \bar{Q} \bar{H} H$	$\langle 12 \rangle \langle 13 \rangle [12] [23] \delta_{j_1}^{i_2} \delta_{j_2}^{i_3} \delta_{j_3}^{i_4} \delta_{j_4}^{i_5} \delta_{j_5}^{i_6}$
32	$D^2 G_-^2 \bar{H} H$	$\langle 12 \rangle^3 [12] \delta_{j_1}^{i_2} \delta_{j_2}^{i_3} \delta_{j_3}^{i_4}$	65		$\langle 13 \rangle \langle 23 \rangle [23]^2 \delta_{j_3}^{i_2} \delta_{j_1}^{i_3} \delta_{j_2}^{i_4} \delta_{j_4}^{i_5}$
33	$D^2 G_+^2 \bar{H} H$	$[12]^3 \langle 12 \rangle \delta_{j_1}^{i_2} \delta_{j_2}^{i_3} \delta_{j_3}^{i_4}$	66		$\langle 12 \rangle \langle 13 \rangle [12] [23] \delta_{j_1}^{i_2} \delta_{j_2}^{i_3} \delta_{j_3}^{i_4} \delta_{j_4}^{i_5} \delta_{j_5}^{i_6}$

Table 4.2: The table shows all the dimension-8 operators, their multiplicity and a set of independent minimal amplitudes.

$$\dot{c}_1^{(6)} = c_1^{(6)} \left(6g_1^2 Y_H^2 + \frac{9g_2^2}{2} + 108\lambda \right) + 6c_1^{(6)} \gamma_{\text{coll}}^H,$$

$$\begin{aligned} \dot{c}_2^{(6)} &= c_5^{(6)} \left(8g_1^2 Y_H Y_Q - 6g_2^2 + 48\mathcal{Y}_1 \bar{\mathcal{Y}}_1 + 24\mathcal{Y}_2 \bar{\mathcal{Y}}_2 \right) + c_2^{(6)} \left(-\frac{8g_1^2 Y_H^2}{3} + 8g_2^2 + 24\lambda \right) \\ &+ c_3^{(6)} \left(2g_1^2 Y_H^2 + \frac{17g_2^2}{2} - 12\lambda \right) + c_4^{(6)} \left(16g_1^2 Y_H Y_Q + 24\mathcal{Y}_1 \bar{\mathcal{Y}}_1 - 24\mathcal{Y}_2 \bar{\mathcal{Y}}_2 \right) + 4c_2^{(6)} \gamma_{\text{coll}}^H + \dots, \end{aligned}$$

$$\begin{aligned} \dot{c}_3^{(6)} &= c_3^{(6)} \left(26g_1^2 Y_H^2 + \frac{33g_2^2}{2} + 12\lambda \right) + c_4^{(6)} \left(32g_1^2 Y_H Y_Q + 48\mathcal{Y}_1 \bar{\mathcal{Y}}_1 - 48\mathcal{Y}_2 \bar{\mathcal{Y}}_2 \right) \\ &+ c_5^{(6)} \left(16g_1^2 Y_H Y_Q + 24\mathcal{Y}_1 \bar{\mathcal{Y}}_1 - 24\mathcal{Y}_2 \bar{\mathcal{Y}}_2 \right) - \frac{40}{3} c_2^{(6)} g_1^2 Y_H^2 \\ &+ 4c_3^{(6)} \gamma_{\text{coll}}^H + \dots, \end{aligned}$$

$$\begin{aligned}
 \dot{c}_4^{(6)} &= c_4^{(6)} \left(\frac{28g_1^2 Y_H^2}{3} + 14g_1^2 Y_Q^2 + \frac{21g_2^2}{2} + 8g_3^2 + 12\mathcal{Y}_1 \bar{\mathcal{Y}}_1 \right) + c_4^{(6)} (2\gamma_{\text{coll}}^H + 2\gamma_{\text{coll}}^Q) \\
 &+ c_5^{(6)} \left(\frac{2g_1^2 Y_H^2}{3} + 4g_1^2 Y_Q^2 + \frac{11g_2^2}{6} - 4\mathcal{Y}_1 \bar{\mathcal{Y}}_1 + 8\mathcal{Y}_2 \bar{\mathcal{Y}}_2 \right) \\
 &+ c_3^{(6)} \left(g_1^2 Y_H Y_Q - \frac{g_2^2}{12} + 2\mathcal{Y}_1 \bar{\mathcal{Y}}_1 - \mathcal{Y}_2 \bar{\mathcal{Y}}_2 \right) + c_2^{(6)} \left(-\frac{1}{3}g_1^2 Y_H Y_Q + \frac{g_2^2}{12} - \mathcal{Y}_1 \bar{\mathcal{Y}}_1 \right) + \dots, \\
 \dot{c}_5^{(6)} &= c_5^{(6)} \left(8g_1^2 Y_H^2 + 6g_1^2 Y_Q^2 + \frac{41g_2^2}{6} + 8g_3^2 - 4\mathcal{Y}_1 \bar{\mathcal{Y}}_1 + 8\mathcal{Y}_2 \bar{\mathcal{Y}}_2 \right) + c_5^{(6)} (2\gamma_{\text{coll}}^H + 2\gamma_{\text{coll}}^Q) \\
 &+ c_2^{(6)} \left(-\frac{g_2^2}{6} + \mathcal{Y}_1 \bar{\mathcal{Y}}_1 + \mathcal{Y}_2 \bar{\mathcal{Y}}_2 \right) + c_3^{(6)} \left(\frac{g_2^2}{6} - \mathcal{Y}_1 \bar{\mathcal{Y}}_1 - \mathcal{Y}_2 \bar{\mathcal{Y}}_2 \right) \\
 &+ c_4^{(6)} (12\mathcal{Y}_2 \bar{\mathcal{Y}}_2 - 12\mathcal{Y}_1 \bar{\mathcal{Y}}_1) + \dots, \\
 \dot{c}_6^{(6)} &= c_6^{(6)} \left(10g_1^2 Y_H^2 + \frac{3g_2^2}{2} + 12\lambda \right) + 6c_{12}^{(6)} g_1 g_2 Y_H + c_6^{(6)} (2\gamma_{\text{coll}}^H + 2\gamma_{\text{coll}}^B) + \dots, \\
 \dot{c}_7^{(6)} &= c_7^{(6)} \left(10g_1^2 Y_H^2 + \frac{3g_2^2}{2} + 12\lambda \right) + 6c_{13}^{(6)} g_1 g_2 Y_H + c_7^{(6)} (2\gamma_{\text{coll}}^H + 2\gamma_{\text{coll}}^B) + \dots, \\
 \dot{c}_8^{(6)} &= c_8^{(6)} \left(2g_1^2 Y_H^2 + \frac{7g_2^2}{2} + 12\lambda \right) + 2c_{12}^{(6)} g_1 g_2 Y_H + c_8^{(6)} (2\gamma_{\text{coll}}^H + 2\gamma_{\text{coll}}^W) + \dots, \\
 \dot{c}_9^{(6)} &= c_9^{(6)} \left(2g_1^2 Y_H^2 + \frac{7g_2^2}{2} + 12\lambda \right) + 2c_{13}^{(6)} g_1 g_2 Y_H + c_9^{(6)} (2\gamma_{\text{coll}}^H + 2\gamma_{\text{coll}}^W) + \dots, \\
 \dot{c}_{10}^{(6)} &= c_{10}^{(6)} \left(2g_1^2 Y_H^2 + \frac{3g_2^2}{2} + 12\lambda \right) + c_{10}^{(6)} (2\gamma_{\text{coll}}^H + 2\gamma_{\text{coll}}^G) + \dots, \\
 \dot{c}_{11}^{(6)} &= c_{11}^{(6)} \left(2g_1^2 Y_H^2 + \frac{3g_2^2}{2} + 12\lambda \right) + c_{11}^{(6)} (2\gamma_{\text{coll}}^H + 2\gamma_{\text{coll}}^G) + \dots, \\
 \dot{c}_{12}^{(6)} &= c_{12}^{(6)} \left(6g_1^2 Y_H^2 + \frac{g_2^2}{2} + 4\lambda \right) + 4c_6^{(6)} g_1 g_2 Y_H + 4c_8^{(6)} g_1 g_2 Y_H \\
 &+ c_{12}^{(6)} (2\gamma_{\text{coll}}^H + \gamma_{\text{coll}}^W + \gamma_{\text{coll}}^B) + \dots, \\
 \dot{c}_{13}^{(6)} &= c_{13}^{(6)} \left(6g_1^2 Y_H^2 + \frac{g_2^2}{2} + 4\lambda \right) + 4c_7^{(6)} g_1 g_2 Y_H + 4c_9^{(6)} g_1 g_2 Y_H \\
 &+ c_{13}^{(6)} (2\gamma_{\text{coll}}^H + \gamma_{\text{coll}}^W + \gamma_{\text{coll}}^B) + \dots,
 \end{aligned}$$

Finally, what follows are the dimension-eight coefficients:

$$\begin{aligned}
 \dot{c}'_1^{(8)} &= \left(6g_2^2 + 8g_1^2 Y_H^2 + 192\lambda\right) c_1^{(8)}, \\
 \dot{c}'_2^{(8)} &= \left(3g_2^2 + 20g_1^2 Y_H^2 + 48\lambda\right) c_2^{(8)} + 8g_1 g_2 Y_H c_4^{(8)}, \\
 \dot{c}'_3^{(8)} &= \left(3g_2^2 + 20g_1^2 Y_H^2 + 48\lambda\right) c_3^{(8)} + 8g_1 g_2 Y_H c_5^{(8)}, \\
 \dot{c}'_4^{(8)} &= 8g_1 g_2 Y_H c_2^{(8)} + \left(13g_2^2 + 12g_1^2 Y_H^2 + 40\lambda\right) c_4^{(8)} + 8g_1 g_2 Y_H c_6^{(8)} + 2g_1 g_2 Y_H c_7^{(8)}, \\
 \dot{c}'_5^{(8)} &= 8g_1 g_2 Y_H c_3^{(8)} + \left(13g_2^2 + 12g_1^2 Y_H^2 + 40\lambda\right) c_5^{(8)} + 8g_1 g_2 Y_H c_8^{(8)} + 2g_1 g_2 Y_H c_9^{(8)}, \\
 \dot{c}'_6^{(8)} &= 4g_1 g_2 Y_H c_4^{(8)} + \left(7g_2^2 + 4g_1^2 Y_H^2 + 48\lambda\right) c_6^{(8)} + \left(4g_2^2 - 4\lambda\right) c_7^{(8)}, \\
 \dot{c}'_7^{(8)} &= \left(31g_2^2 + 4g_1^2 Y_H^2 + 24\lambda\right) c_7^{(8)} + 8g_1 g_2 Y_H c_4^{(8)}, \\
 \dot{c}'_8^{(8)} &= 4g_1 g_2 Y_H c_5^{(8)} + \left(7g_2^2 + 4g_1^2 Y_H^2 + 48\lambda\right) c_8^{(8)} + \left(4g_2^2 - 4\lambda\right) c_9^{(8)}, \\
 \dot{c}'_9^{(8)} &= \left(31g_2^2 + 4g_1^2 Y_H^2 + 24\lambda\right) c_9^{(8)} + 8g_1 g_2 Y_H c_5^{(8)}, \\
 \dot{c}'_{10}^{(8)} &= \left(3g_2^2 + 4g_1^2 Y_H^2 + 48\lambda\right) c_{10}^{(8)}, \\
 \dot{c}'_{11}^{(8)} &= \left(3g_2^2 + 4g_1^2 Y_H^2 + 48\lambda\right) c_{11}^{(8)}, \\
 \dot{c}'_{12}^{(8)} &= \left(\frac{39g_2^2}{2} + 6g_1^2 Y_H^2 + 4\lambda\right) c_{12}^{(8)} + 4g_1 g_2 Y_H c_{14}^{(8)}, \\
 \dot{c}'_{13}^{(8)} &= \left(\frac{39g_2^2}{2} + 6g_1^2 Y_H^2 + 4\lambda\right) c_{13}^{(8)} + 4g_1 g_2 Y_H c_{15}^{(8)}, \\
 \dot{c}'_{14}^{(8)} &= \left(\frac{57g_2^2}{2} + 2g_1^2 Y_H^2 + 12\lambda\right) c_{14}^{(8)} + 3g_1 g_2 Y_H c_{12}^{(8)}, \\
 \dot{c}'_{15}^{(8)} &= \left(\frac{57g_2^2}{2} + 2g_1^2 Y_H^2 + 12\lambda\right) c_{15}^{(8)} + 3g_1 g_2 Y_H c_{13}^{(8)}, \\
 \dot{c}'_{16}^{(8)} &= \left(\frac{3g_2^2}{2} + 36g_3^2 + 2g_1^2 Y_H^2 + 12\lambda\right) c_{16}^{(8)}, \\
 \dot{c}'_{17}^{(8)} &= \left(\frac{3g_2^2}{2} + 36g_3^2 + 2g_1^2 Y_H^2 + 12\lambda\right) c_{17}^{(8)}, \\
 \dot{c}'_{18}^{(8)} &= \left(10g_2^2 + \frac{116g_1^2 Y_H^2}{3} + 72\lambda\right) c_{18}^{(8)} + \left(\frac{17g_2^2}{6} - 26g_1^2 Y_H^2 - 4\lambda\right) c_{19}^{(8)} \\
 &\quad + \left(-18g_2^2 + 108\mathcal{Y}_1 \bar{\mathcal{Y}}_1 + 108\mathcal{Y}_2 \bar{\mathcal{Y}}_2\right) c_{47}^{(8)} \\
 &\quad + \left(18Y_H Y_Q g_1^2 + \frac{45g_2^2}{2} - 108\mathcal{Y}_1 \bar{\mathcal{Y}}_1 - 162\mathcal{Y}_2 \bar{\mathcal{Y}}_2\right) c_{48}^{(8)} \\
 &\quad + \left(-18Y_H Y_Q g_1^2 - \frac{9g_2^2}{2} + 54\mathcal{Y}_2 \bar{\mathcal{Y}}_2\right) c_{49}^{(8)} + \left(36Y_H Y_Q g_1^2 + 54\mathcal{Y}_1 \bar{\mathcal{Y}}_1 - 54\mathcal{Y}_2 \bar{\mathcal{Y}}_2\right) c_{50}^{(8)},
 \end{aligned}$$

$$\begin{aligned}
 \dot{c}_{19}^{(8)} &= \left(-\frac{34g_2^2}{3} - \frac{8g_1^2 Y_H^2}{3} + 16\lambda \right) c_{18}^{(8)} + \left(\frac{145g_2^2}{6} + 2g_1^2 Y_H^2 + 52\lambda \right) c_{19}^{(8)} \\
 &+ \left(-27g_2^2 + 162\mathcal{Y}_1 \bar{\mathcal{Y}}_1 + 162\mathcal{Y}_2 \bar{\mathcal{Y}}_2 \right) c_{47}^{(8)} \\
 &+ \left(-18Y_H Y_Q g_1^2 + \frac{45g_2^2}{2} - 162\mathcal{Y}_1 \bar{\mathcal{Y}}_1 - 108\mathcal{Y}_2 \bar{\mathcal{Y}}_2 \right) c_{48}^{(8)} \\
 &+ \left(18Y_H Y_Q g_1^2 + \frac{9g_2^2}{2} - 54\mathcal{Y}_2 \bar{\mathcal{Y}}_2 \right) c_{49}^{(8)} + \left(-36Y_H Y_Q g_1^2 - 54\mathcal{Y}_1 \bar{\mathcal{Y}}_1 + 54\mathcal{Y}_2 \bar{\mathcal{Y}}_2 \right) c_{50}^{(8)} , \\
 \dot{c}_{20}^{(8)} &= g_1^2 c_{44}^{(8)} Y_H^2 + \frac{1}{3} g_1^2 c_{45}^{(8)} Y_H^2 - \frac{1}{3} g_1^2 c_{46}^{(8)} Y_H^2 + 3g_1 g_2 c_{38}^{(8)} Y_H + 3g_1 g_2 c_{39}^{(8)} Y_H \\
 &+ \left(9g_2^2 + 20g_1^2 Y_H^2 \right) c_{20}^{(8)} - 4g_1^2 Y_Q^2 c_{63}^{(8)} - 8g_1^2 Y_Q^2 c_{65}^{(8)} , \\
 \dot{c}_{21}^{(8)} &= \frac{1}{4} c_{44}^{(8)} g_2^2 + \frac{1}{12} c_{45}^{(8)} g_2^2 - \frac{1}{12} c_{46}^{(8)} g_2^2 - c_{63}^{(8)} g_2^2 - 2c_{65}^{(8)} g_2^2 + g_1 Y_H c_{38}^{(8)} g_2 + g_1 Y_H c_{39}^{(8)} g_2 \\
 &+ \left(\frac{77g_2^2}{3} + 12g_1^2 Y_H^2 \right) c_{21}^{(8)} , \\
 \dot{c}_{22}^{(8)} &= \left(\frac{25g_2^2}{3} + 12g_1^2 Y_H^2 \right) c_{22}^{(8)} - i g_2^2 c_{63}^{(8)} , \\
 \dot{c}_{23}^{(8)} &= -\frac{2}{3} c_{63}^{(8)} g_3^2 - \frac{4}{3} c_{65}^{(8)} g_3^2 + \left(9g_2^2 + 22g_3^2 + 12g_1^2 Y_H^2 \right) c_{23}^{(8)} , \\
 \dot{c}_{24}^{(8)} &= \left(\frac{25g_2^2}{2} + \frac{38g_1^2 Y_H^2}{3} + 12\lambda \right) c_{24}^{(8)} , \\
 \dot{c}_{25}^{(8)} &= \left(\frac{25g_2^2}{2} + \frac{38g_1^2 Y_H^2}{3} + 12\lambda \right) c_{25}^{(8)} , \\
 \dot{c}_{26}^{(8)} &= \left(\frac{3g_2^2}{2} + \frac{10g_1^2 Y_H^2}{3} + 12\lambda \right) c_{26}^{(8)} + g_1 g_2 Y_H c_{34}^{(8)} - \frac{1}{2} g_1 g_2 Y_H c_{35}^{(8)} , \\
 \dot{c}_{27}^{(8)} &= \left(\frac{3g_2^2}{2} + \frac{10g_1^2 Y_H^2}{3} + 12\lambda \right) c_{27}^{(8)} + g_1 g_2 Y_H c_{36}^{(8)} - \frac{1}{2} g_1 g_2 Y_H c_{37}^{(8)} , \\
 \dot{c}_{28}^{(8)} &= -\frac{25}{6} i c_{29}^{(8)} g_2^2 + \frac{1}{3} g_1 Y_H c_{34}^{(8)} g_2 - \frac{1}{6} g_1 Y_H c_{35}^{(8)} g_2 + \left(\frac{11g_2^2}{6} + 2g_1^2 Y_H^2 + 12\lambda \right) c_{28}^{(8)} , \\
 \dot{c}_{29}^{(8)} &= 20i c_{28}^{(8)} g_2^2 - 4i g_1 Y_H c_{34}^{(8)} g_2 + 2i g_1 Y_H c_{35}^{(8)} g_2 + \left(\frac{22g_2^2}{3} + 8g_1^2 Y_H^2 \right) c_{29}^{(8)} , \\
 \dot{c}_{30}^{(8)} &= -\frac{25}{6} i c_{31}^{(8)} g_2^2 - \frac{1}{3} g_1 Y_H c_{36}^{(8)} g_2 + \frac{1}{6} g_1 Y_H c_{37}^{(8)} g_2 + \left(\frac{11g_2^2}{6} + 2g_1^2 Y_H^2 + 12\lambda \right) c_{30}^{(8)} , \\
 \dot{c}_{31}^{(8)} &= 20i c_{30}^{(8)} g_2^2 + 4i g_1 Y_H c_{36}^{(8)} g_2 - 2i g_1 Y_H c_{37}^{(8)} g_2 + \left(\frac{22g_2^2}{3} + 8g_1^2 Y_H^2 \right) c_{31}^{(8)} , \\
 \dot{c}_{32}^{(8)} &= \left(\frac{3g_2^2}{2} + 2g_1^2 Y_H^2 + 12\lambda \right) c_{32}^{(8)} , \\
 \dot{c}_{33}^{(8)} &= \left(\frac{3g_2^2}{2} + 2g_1^2 Y_H^2 + 12\lambda \right) c_{33}^{(8)} ,
 \end{aligned}$$

$$\begin{aligned}
 \dot{c}'_{34}{}^{(8)} &= \frac{2}{3}g_1g_2Y_Hc_{26}^{(8)} + \frac{2}{3}g_1g_2Y_Hc_{28}^{(8)} + \frac{5}{3}ig_1g_2Y_Hc_{29}^{(8)} + \left(-\frac{g_2^2}{3} + \frac{8g_1^2Y_H^2}{3} + 4\lambda\right)c_{34}^{(8)} \\
 &\quad + \left(-\frac{5g_2^2}{12} + \frac{11g_1^2Y_H^2}{3} - 2\lambda\right)c_{35}^{(8)}, \\
 \dot{c}'_{35}{}^{(8)} &= \left(10g_1^2Y_H^2 - \frac{7g_2^2}{6}\right)c_{35}^{(8)}, \\
 \dot{c}'_{36}{}^{(8)} &= \frac{2}{3}g_1g_2Y_Hc_{27}^{(8)} + \frac{2}{3}g_1g_2Y_Hc_{30}^{(8)} + \frac{5}{3}ig_1g_2Y_Hc_{31}^{(8)} + \left(-\frac{g_2^2}{3} + \frac{8g_1^2Y_H^2}{3} + 4\lambda\right)c_{36}^{(8)} \\
 &\quad + \left(-\frac{5g_2^2}{12} + \frac{11g_1^2Y_H^2}{3} - 2\lambda\right)c_{37}^{(8)}, \\
 \dot{c}'_{37}{}^{(8)} &= \left(10g_1^2Y_H^2 - \frac{7g_2^2}{6}\right)c_{37}^{(8)}, \\
 \dot{c}'_{38}{}^{(8)} &= 4g_1g_2Y_Hc_{20}^{(8)} + 4g_1g_2Y_Hc_{21}^{(8)} + \left(16g_1^2Y_H^2 - 2g_2^2\right)c_{38}^{(8)} + \frac{1}{3}g_1g_2Y_Hc_{44}^{(8)} + \frac{1}{3}g_1g_2Y_Hc_{45}^{(8)} \\
 &\quad - \frac{1}{3}g_1g_2Y_Hc_{46}^{(8)} - 4g_1g_2Y_Qc_{63}^{(8)}, \\
 \dot{c}'_{39}{}^{(8)} &= 4g_1g_2Y_Hc_{20}^{(8)} + 4g_1g_2Y_Hc_{21}^{(8)} + \left(16g_1^2Y_H^2 - 2g_2^2\right)c_{39}^{(8)} + \frac{1}{3}g_1g_2Y_Hc_{44}^{(8)} + \frac{1}{3}g_1g_2Y_Hc_{45}^{(8)} \\
 &\quad - \frac{1}{3}g_1g_2Y_Hc_{46}^{(8)} - 4g_1g_2Y_Qc_{63}^{(8)}, \\
 \dot{c}'_{40}{}^{(8)} &= \left(\frac{73g_2^2}{4} + 17g_1^2Y_H^2 + 10\lambda\right)c_{40}^{(8)} + \left(\frac{17g_2^2}{12} + \frac{g_1^2Y_H^2}{3} - 2\lambda\right)c_{41}^{(8)} \\
 &\quad + \left(-4g_2^2 + 24\mathcal{Y}_1\bar{\mathcal{Y}}_1 + 24\mathcal{Y}_2\bar{\mathcal{Y}}_2\right)c_{51}^{(8)} + \left(2g_2^2 - 12\mathcal{Y}_1\bar{\mathcal{Y}}_1 - 12\mathcal{Y}_2\bar{\mathcal{Y}}_2\right)c_{52}^{(8)} \\
 &\quad + \left(8Y_HY_Qg_1^2 + 2g_2^2 - 24\mathcal{Y}_2\bar{\mathcal{Y}}_2\right)c_{53}^{(8)} + \left(-4Y_HY_Qg_1^2 - g_2^2 + 12\mathcal{Y}_2\bar{\mathcal{Y}}_2\right)c_{54}^{(8)} \\
 &\quad + \left(16Y_HY_Qg_1^2 + 24\mathcal{Y}_1\bar{\mathcal{Y}}_1 - 24\mathcal{Y}_2\bar{\mathcal{Y}}_2\right)c_{55}^{(8)} + \left(-8Y_HY_Qg_1^2 - 12\mathcal{Y}_1\bar{\mathcal{Y}}_1 + 12\mathcal{Y}_2\bar{\mathcal{Y}}_2\right)c_{56}^{(8)}, \\
 \dot{c}'_{41}{}^{(8)} &= \left(\frac{17g_2^2}{12} + \frac{g_1^2Y_H^2}{3} - 2\lambda\right)c_{40}^{(8)} + \left(\frac{73g_2^2}{4} + 17g_1^2Y_H^2 + 10\lambda\right)c_{41}^{(8)} \\
 &\quad + \left(4g_2^2 - 24\mathcal{Y}_1\bar{\mathcal{Y}}_1 - 24\mathcal{Y}_2\bar{\mathcal{Y}}_2\right)c_{51}^{(8)} + \left(6g_2^2 - 36\mathcal{Y}_1\bar{\mathcal{Y}}_1 - 36\mathcal{Y}_2\bar{\mathcal{Y}}_2\right)c_{52}^{(8)} \\
 &\quad + \left(-8Y_HY_Qg_1^2 + 6g_2^2 - 48\mathcal{Y}_1\bar{\mathcal{Y}}_1 - 24\mathcal{Y}_2\bar{\mathcal{Y}}_2\right)c_{53}^{(8)} \\
 &\quad + \left(-12Y_HY_Qg_1^2 + 9g_2^2 - 72\mathcal{Y}_1\bar{\mathcal{Y}}_1 - 36\mathcal{Y}_2\bar{\mathcal{Y}}_2\right)c_{54}^{(8)} \\
 &\quad + \left(-16Y_HY_Qg_1^2 - 24\mathcal{Y}_1\bar{\mathcal{Y}}_1 + 24\mathcal{Y}_2\bar{\mathcal{Y}}_2\right)c_{55}^{(8)} + \left(-24Y_HY_Qg_1^2 - 36\mathcal{Y}_1\bar{\mathcal{Y}}_1 + 36\mathcal{Y}_2\bar{\mathcal{Y}}_2\right)c_{56}^{(8)}, \\
 \dot{c}'_{42}{}^{(8)} &= \left(\frac{73g_2^2}{4} + 17g_1^2Y_H^2 + 10\lambda\right)c_{42}^{(8)} + \left(\frac{17g_2^2}{12} + \frac{g_1^2Y_H^2}{3} - 2\lambda\right)c_{43}^{(8)} \\
 &\quad + \left(4g_2^2 - 24\mathcal{Y}_1\bar{\mathcal{Y}}_1 - 24\mathcal{Y}_2\bar{\mathcal{Y}}_2\right)c_{57}^{(8)} + \left(2g_2^2 - 12\mathcal{Y}_1\bar{\mathcal{Y}}_1 - 12\mathcal{Y}_2\bar{\mathcal{Y}}_2\right)c_{58}^{(8)} \\
 &\quad + \left(-8Y_HY_Qg_1^2 - 2g_2^2 + 24\mathcal{Y}_2\bar{\mathcal{Y}}_2\right)c_{59}^{(8)} + \left(-4Y_HY_Qg_1^2 - g_2^2 + 12\mathcal{Y}_2\bar{\mathcal{Y}}_2\right)c_{60}^{(8)} \\
 &\quad + \left(-16Y_HY_Qg_1^2 - 24\mathcal{Y}_1\bar{\mathcal{Y}}_1 + 24\mathcal{Y}_2\bar{\mathcal{Y}}_2\right)c_{61}^{(8)} + \left(-8Y_HY_Qg_1^2 - 12\mathcal{Y}_1\bar{\mathcal{Y}}_1 + 12\mathcal{Y}_2\bar{\mathcal{Y}}_2\right)c_{62}^{(8)},
 \end{aligned}$$

$$\begin{aligned}
 \dot{c}'_{43}^{(8)} &= \left(\frac{17g_2^2}{12} + \frac{g_1^2 Y_H^2}{3} - 2\lambda \right) c_{42}^{(8)} + \left(\frac{73g_2^2}{4} + 17g_1^2 Y_H^2 + 10\lambda \right) c_{43}^{(8)} \\
 &+ \left(-4g_2^2 + 24\mathcal{Y}_1 \bar{\mathcal{Y}}_1 + 24\mathcal{Y}_2 \bar{\mathcal{Y}}_2 \right) c_{57}^{(8)} + \left(6g_2^2 - 36\mathcal{Y}_1 \bar{\mathcal{Y}}_1 - 36\mathcal{Y}_2 \bar{\mathcal{Y}}_2 \right) c_{58}^{(8)} \\
 &+ \left(8Y_H Y_Q g_1^2 - 6g_2^2 + 48\mathcal{Y}_1 \bar{\mathcal{Y}}_1 + 24\mathcal{Y}_2 \bar{\mathcal{Y}}_2 \right) c_{59}^{(8)} \\
 &+ \left(-12Y_H Y_Q g_1^2 + 9g_2^2 - 72\mathcal{Y}_1 \bar{\mathcal{Y}}_1 - 36\mathcal{Y}_2 \bar{\mathcal{Y}}_2 \right) c_{60}^{(8)} \\
 &+ \left(16Y_H Y_Q g_1^2 + 24\mathcal{Y}_1 \bar{\mathcal{Y}}_1 - 24\mathcal{Y}_2 \bar{\mathcal{Y}}_2 \right) c_{61}^{(8)} + \left(-24Y_H Y_Q g_1^2 - 36\mathcal{Y}_1 \bar{\mathcal{Y}}_1 + 36\mathcal{Y}_2 \bar{\mathcal{Y}}_2 \right) c_{62}^{(8)} , \\
 \dot{c}'_{44}^{(8)} &= 12c_{21}^{(8)} g_2^2 - \frac{8}{3} g_1 Y_H c_{38}^{(8)} g_2 - \frac{8}{3} g_1 Y_H c_{39}^{(8)} g_2 + 16g_1^2 Y_H^2 c_{20}^{(8)} \\
 &+ \left(26g_2^2 + \frac{100g_1^2 Y_H^2}{3} + \frac{32\lambda}{3} \right) c_{44}^{(8)} + \left(5g_2^2 + \frac{16\lambda}{3} \right) c_{45}^{(8)} \\
 &+ \left(-\frac{14g_2^2}{3} - \frac{28g_1^2 Y_H^2}{3} - \frac{8\lambda}{3} \right) c_{46}^{(8)} + \left(2g_2^2 + 8\mathcal{Y}_1 \bar{\mathcal{Y}}_1 - 8\mathcal{Y}_2 \bar{\mathcal{Y}}_2 \right) c_{63}^{(8)} \\
 &+ \left(-4g_2^2 + 24\mathcal{Y}_1 \bar{\mathcal{Y}}_1 + 24\mathcal{Y}_2 \bar{\mathcal{Y}}_2 \right) c_{64}^{(8)} + (24\mathcal{Y}_1 \bar{\mathcal{Y}}_1 + 24\mathcal{Y}_2 \bar{\mathcal{Y}}_2) c_{65}^{(8)} , \\
 \dot{c}'_{45}^{(8)} &= 2c_{21}^{(8)} g_2^2 + \frac{2}{3} g_1 Y_H c_{38}^{(8)} g_2 + \frac{2}{3} g_1 Y_H c_{39}^{(8)} g_2 + \frac{8}{3} g_1^2 Y_H^2 c_{20}^{(8)} + \left(-\frac{17g_2^2}{6} - \frac{22g_1^2 Y_H^2}{3} + \frac{40\lambda}{3} \right) c_{44}^{(8)} \\
 &+ \left(\frac{g_2^2}{2} - 6g_1^2 Y_H^2 + \frac{88\lambda}{3} \right) c_{45}^{(8)} + \left(\frac{11g_2^2}{3} + 4g_1^2 Y_H^2 - \frac{28\lambda}{3} \right) c_{46}^{(8)} \\
 &+ \left(-4Y_H Y_Q g_1^2 - g_2^2 + 16\mathcal{Y}_2 \bar{\mathcal{Y}}_2 \right) c_{63}^{(8)} + \left(8Y_H Y_Q g_1^2 + 2g_2^2 - 24\mathcal{Y}_2 \bar{\mathcal{Y}}_2 \right) c_{64}^{(8)} \\
 &+ \left(-8Y_H Y_Q g_1^2 - 8\mathcal{Y}_1 \bar{\mathcal{Y}}_1 + 16\mathcal{Y}_2 \bar{\mathcal{Y}}_2 \right) c_{65}^{(8)} + \left(16Y_H Y_Q g_1^2 + 24\mathcal{Y}_1 \bar{\mathcal{Y}}_1 - 24\mathcal{Y}_2 \bar{\mathcal{Y}}_2 \right) c_{66}^{(8)} , \\
 \dot{c}'_{46}^{(8)} &= 12c_{21}^{(8)} g_2^2 - \frac{28}{3} g_1 Y_H c_{38}^{(8)} g_2 - \frac{28}{3} g_1 Y_H c_{39}^{(8)} g_2 + 16g_1^2 Y_H^2 c_{20}^{(8)} \\
 &+ \left(\frac{41g_2^2}{3} - \frac{28g_1^2 Y_H^2}{3} + \frac{16\lambda}{3} \right) c_{44}^{(8)} \\
 &+ \left(5g_2^2 - 20g_1^2 Y_H^2 + \frac{16\lambda}{3} \right) c_{45}^{(8)} + \left(\frac{23g_2^2}{3} + 20g_1^2 Y_H^2 + \frac{8\lambda}{3} \right) c_{46}^{(8)} \\
 &+ \left(-8Y_H Y_Q g_1^2 + 2g_2^2 + 16\mathcal{Y}_1 \bar{\mathcal{Y}}_1 - 16\mathcal{Y}_2 \bar{\mathcal{Y}}_2 \right) c_{63}^{(8)} + \left(16Y_H Y_Q g_1^2 - 4g_2^2 + 48\mathcal{Y}_1 \bar{\mathcal{Y}}_1 \right) c_{64}^{(8)} \\
 &+ \left(-16Y_H Y_Q g_1^2 + 48\mathcal{Y}_2 \bar{\mathcal{Y}}_2 \right) c_{65}^{(8)} + \left(32Y_H Y_Q g_1^2 + 48\mathcal{Y}_1 \bar{\mathcal{Y}}_1 - 48\mathcal{Y}_2 \bar{\mathcal{Y}}_2 \right) c_{66}^{(8)} , \\
 \dot{c}'_{47}^{(8)} &= \left(\frac{2g_2^2}{27} - \frac{4\mathcal{Y}_1 \bar{\mathcal{Y}}_1}{9} - \frac{4\mathcal{Y}_2 \bar{\mathcal{Y}}_2}{9} \right) c_{18}^{(8)} + \left(-\frac{g_2^2}{27} + \frac{2\mathcal{Y}_1 \bar{\mathcal{Y}}_1}{9} + \frac{2\mathcal{Y}_2 \bar{\mathcal{Y}}_2}{9} \right) c_{19}^{(8)} \\
 &+ \left(\frac{47g_2^2}{3} + 8g_3^2 + \frac{14g_1^2 Y_H^2}{3} + 6g_1^2 Y_Q^2 + 8\mathcal{Y}_1 \bar{\mathcal{Y}}_1 + 8\mathcal{Y}_2 \bar{\mathcal{Y}}_2 + 20\lambda \right) c_{47}^{(8)} \\
 &+ \left(-\frac{17g_2^2}{12} + \frac{19g_1^2 Y_H^2}{3} - 6\mathcal{Y}_1 \bar{\mathcal{Y}}_1 + 6\mathcal{Y}_2 \bar{\mathcal{Y}}_2 + 2\lambda \right) c_{48}^{(8)} \\
 &+ \left(-\frac{17g_2^2}{12} - 7g_1^2 Y_H^2 + 6\mathcal{Y}_1 \bar{\mathcal{Y}}_1 - 6\mathcal{Y}_2 \bar{\mathcal{Y}}_2 + 2\lambda \right) c_{49}^{(8)} + (12\mathcal{Y}_2 \bar{\mathcal{Y}}_2 - 12\mathcal{Y}_1 \bar{\mathcal{Y}}_1) c_{50}^{(8)} ,
 \end{aligned}$$

$$\begin{aligned}
 c'_{48}{}^{(8)} &= \left(\frac{4g_2^2}{27} - \frac{8\mathcal{Y}_1\bar{\mathcal{Y}}_1}{9} - \frac{8\mathcal{Y}_2\bar{\mathcal{Y}}_2}{9} \right) c_{18}^{(8)} + \left(-\frac{g_2^2}{27} + \frac{2\mathcal{Y}_1\bar{\mathcal{Y}}_1}{9} + \frac{2\mathcal{Y}_2\bar{\mathcal{Y}}_2}{9} \right) c_{19}^{(8)} \\
 &+ \left(\frac{103g_2^2}{12} + 8g_3^2 + \frac{49g_1^2Y_H^2}{3} + 6g_1^2Y_Q^2 - 4\mathcal{Y}_1\bar{\mathcal{Y}}_1 + 20\mathcal{Y}_2\bar{\mathcal{Y}}_2 + 30\lambda \right) c_{48}^{(8)} \\
 &+ \left(\frac{17g_2^2}{6} + \frac{2g_1^2Y_H^2}{3} - 4\lambda \right) c_{47}^{(8)} + \left(\frac{17g_2^2}{12} - 13g_1^2Y_H^2 + 12\mathcal{Y}_1\bar{\mathcal{Y}}_1 - 12\mathcal{Y}_2\bar{\mathcal{Y}}_2 - 2\lambda \right) c_{49}^{(8)} \\
 &+ (24\mathcal{Y}_2\bar{\mathcal{Y}}_2 - 24\mathcal{Y}_1\bar{\mathcal{Y}}_1) c_{50}^{(8)} , \\
 c'_{49}{}^{(8)} &= \left(\frac{g_2^2}{27} - \frac{2\mathcal{Y}_1\bar{\mathcal{Y}}_1}{9} - \frac{2\mathcal{Y}_2\bar{\mathcal{Y}}_2}{9} \right) c_{19}^{(8)} + \left(-\frac{17g_2^2}{6} - \frac{2g_1^2Y_H^2}{3} + 4\lambda \right) c_{47}^{(8)} \\
 &+ \left(\frac{205g_2^2}{12} + 8g_3^2 + 5g_1^2Y_H^2 + 6g_1^2Y_Q^2 + 8\mathcal{Y}_1\bar{\mathcal{Y}}_1 + 8\mathcal{Y}_2\bar{\mathcal{Y}}_2 + 18\lambda \right) c_{49}^{(8)} \\
 &+ \left(-\frac{17g_2^2}{12} - \frac{g_1^2Y_H^2}{3} + 2\lambda \right) c_{48}^{(8)} , \\
 c'_{50}{}^{(8)} &= \left(\frac{16}{27}Y_HY_Qg_1^2 - \frac{2g_2^2}{27} + \frac{4\mathcal{Y}_1\bar{\mathcal{Y}}_1}{3} - \frac{4\mathcal{Y}_2\bar{\mathcal{Y}}_2}{9} \right) c_{18}^{(8)} \\
 &+ \left(-\frac{4}{9}Y_HY_Qg_1^2 + \frac{g_2^2}{27} - \frac{8\mathcal{Y}_1\bar{\mathcal{Y}}_1}{9} + \frac{4\mathcal{Y}_2\bar{\mathcal{Y}}_2}{9} \right) c_{19}^{(8)} + \left(-\frac{17g_2^2}{6} - \frac{2g_1^2Y_H^2}{3} + 4\lambda \right) c_{47}^{(8)} \\
 &+ \left(\frac{11g_2^2}{6} + \frac{2g_1^2Y_H^2}{3} + 4g_1^2Y_Q^2 - 4\mathcal{Y}_1\bar{\mathcal{Y}}_1 + 8\mathcal{Y}_2\bar{\mathcal{Y}}_2 \right) c_{48}^{(8)} \\
 &+ (g_2^2 - 4g_1^2Y_Q^2 + 4\mathcal{Y}_1\bar{\mathcal{Y}}_1 - 8\mathcal{Y}_2\bar{\mathcal{Y}}_2 - 4\lambda) c_{49}^{(8)} \\
 &+ \left(\frac{41g_2^2}{3} + 8g_3^2 + 18g_1^2Y_H^2 + 14g_1^2Y_Q^2 + 24\mathcal{Y}_1\bar{\mathcal{Y}}_1 + 28\lambda \right) c_{50}^{(8)} , \\
 c'_{51}{}^{(8)} &= \left(-\frac{g_2^2}{6} + \mathcal{Y}_1\bar{\mathcal{Y}}_1 + \mathcal{Y}_2\bar{\mathcal{Y}}_2 \right) c_{40}^{(8)} \\
 &+ (2Y_H^2g_1^2 + 6Y_Q^2g_1^2 + 4Y_HY_Qg_1^2 + 14g_2^2 + 8g_3^2 + 6\mathcal{Y}_1\bar{\mathcal{Y}}_1 + 2\mathcal{Y}_2\bar{\mathcal{Y}}_2 + 12\lambda) c_{51}^{(8)} \\
 &+ \left(-\frac{11}{3}Y_H^2g_1^2 - 2Y_HY_Qg_1^2 - \frac{11g_2^2}{4} - 2\mathcal{Y}_2\bar{\mathcal{Y}}_2 + 6\lambda \right) c_{52}^{(8)} \\
 &+ \left(-\frac{g_2^2}{6} - 2\mathcal{Y}_1\bar{\mathcal{Y}}_1 + 4\mathcal{Y}_2\bar{\mathcal{Y}}_2 + 4\lambda \right) c_{53}^{(8)} + \left(-\frac{17g_2^2}{12} - \frac{g_1^2Y_H^2}{3} + 2\lambda \right) c_{54}^{(8)} \\
 &+ \left(\frac{16g_2^2}{3} + 4\mathcal{Y}_2\bar{\mathcal{Y}}_2 \right) c_{55}^{(8)} ,
 \end{aligned}$$

$$\begin{aligned}
 \dot{c}'_{52}{}^{(8)} &= \left(\frac{g_2^2}{6} - \mathcal{Y}_1 \bar{\mathcal{Y}}_1 - \mathcal{Y}_2 \bar{\mathcal{Y}}_2 \right) c_{40}^{(8)} + \left(-8Y_H Y_Q g_1^2 - 2g_2^2 - \frac{8\mathcal{Y}_2 \bar{\mathcal{Y}}_2}{3} \right) c_{51}^{(8)} \\
 &+ \left(\frac{28Y_H^2 g_1^2}{3} + 6Y_Q^2 g_1^2 - 4Y_H Y_Q g_1^2 + \frac{33g_2^2}{2} + 8g_3^2 + 6\mathcal{Y}_1 \bar{\mathcal{Y}}_1 + 2\mathcal{Y}_2 \bar{\mathcal{Y}}_2 \right) c_{52}^{(8)} \\
 &+ \left(\frac{8g_2^2}{3} + \frac{2g_1^2 Y_H^2}{3} - 2\mathcal{Y}_1 \bar{\mathcal{Y}}_1 + 4\mathcal{Y}_2 \bar{\mathcal{Y}}_2 \right) c_{54}^{(8)} + \left(-2g_2^2 - 4\mathcal{Y}_1 \bar{\mathcal{Y}}_1 + \frac{4\mathcal{Y}_2 \bar{\mathcal{Y}}_2}{3} \right) c_{55}^{(8)} \\
 &+ \left(\frac{7g_2^2}{3} - 6\mathcal{Y}_1 \bar{\mathcal{Y}}_1 + 6\mathcal{Y}_2 \bar{\mathcal{Y}}_2 \right) c_{56}^{(8)} , \\
 \dot{c}'_{53}{}^{(8)} &= \left(\frac{g_2^2}{6} - \mathcal{Y}_1 \bar{\mathcal{Y}}_1 - \mathcal{Y}_2 \bar{\mathcal{Y}}_2 \right) c_{40}^{(8)} + \left(-2g_2^2 - \frac{20\mathcal{Y}_1 \bar{\mathcal{Y}}_1}{3} + 4\mathcal{Y}_2 \bar{\mathcal{Y}}_2 \right) c_{51}^{(8)} \\
 &+ \left(2Y_H^2 g_1^2 + 6Y_Q^2 g_1^2 + 4Y_H Y_Q g_1^2 + \frac{37g_2^2}{3} + 8g_3^2 - \frac{8\mathcal{Y}_1 \bar{\mathcal{Y}}_1}{3} + 4\mathcal{Y}_2 \bar{\mathcal{Y}}_2 + 4\lambda \right) c_{53}^{(8)} \\
 &+ \left(g_2^2 - \frac{2\mathcal{Y}_1 \bar{\mathcal{Y}}_1}{3} + 2\mathcal{Y}_2 \bar{\mathcal{Y}}_2 \right) c_{52}^{(8)} + \left(-3Y_H^2 g_1^2 - 2Y_H Y_Q g_1^2 + \frac{13g_2^2}{12} - \frac{2\mathcal{Y}_1 \bar{\mathcal{Y}}_1}{3} + 2\lambda \right) c_{54}^{(8)} \\
 &+ \left(-\frac{26g_2^2}{3} - \frac{16\mathcal{Y}_1 \bar{\mathcal{Y}}_1}{3} \right) c_{55}^{(8)} + \left(-g_2^2 + \frac{2\mathcal{Y}_1 \bar{\mathcal{Y}}_1}{3} - 2\mathcal{Y}_2 \bar{\mathcal{Y}}_2 \right) c_{56}^{(8)} , \\
 \dot{c}'_{54}{}^{(8)} &= \left(-\frac{g_2^2}{6} + \mathcal{Y}_1 \bar{\mathcal{Y}}_1 + \mathcal{Y}_2 \bar{\mathcal{Y}}_2 \right) c_{40}^{(8)} + \left(\frac{g_2^2}{6} - \mathcal{Y}_1 \bar{\mathcal{Y}}_1 - \mathcal{Y}_2 \bar{\mathcal{Y}}_2 \right) c_{41}^{(8)} \\
 &+ \left(4g_2^2 + \frac{8\mathcal{Y}_1 \bar{\mathcal{Y}}_1}{3} + \frac{8\mathcal{Y}_2 \bar{\mathcal{Y}}_2}{3} \right) c_{51}^{(8)} + \left(2g_2^2 - \frac{4\mathcal{Y}_1 \bar{\mathcal{Y}}_1}{3} + 4\mathcal{Y}_2 \bar{\mathcal{Y}}_2 \right) c_{52}^{(8)} \\
 &+ \left(8Y_H^2 g_1^2 + 6Y_Q^2 g_1^2 - 4Y_H Y_Q g_1^2 + \frac{79g_2^2}{6} + 8g_3^2 + \frac{8\mathcal{Y}_1 \bar{\mathcal{Y}}_1}{3} + 4\mathcal{Y}_2 \bar{\mathcal{Y}}_2 \right) c_{54}^{(8)} \\
 &+ \left(-8Y_H Y_Q g_1^2 + 2g_2^2 + \frac{8\mathcal{Y}_1 \bar{\mathcal{Y}}_1}{3} \right) c_{53}^{(8)} + \left(\frac{16\mathcal{Y}_1 \bar{\mathcal{Y}}_1}{3} - \frac{16\mathcal{Y}_2 \bar{\mathcal{Y}}_2}{3} \right) c_{55}^{(8)} \\
 &+ \left(-\frac{20g_2^2}{3} + \frac{4\mathcal{Y}_1 \bar{\mathcal{Y}}_1}{3} - 4\mathcal{Y}_2 \bar{\mathcal{Y}}_2 \right) c_{56}^{(8)} , \\
 \dot{c}'_{55}{}^{(8)} &= \left(\frac{1}{3} Y_H Y_Q g_1^2 - \frac{g_2^2}{12} + \mathcal{Y}_1 \bar{\mathcal{Y}}_1 \right) c_{40}^{(8)} + \left(2g_2^2 + \frac{2\mathcal{Y}_1 \bar{\mathcal{Y}}_1}{3} + 2\mathcal{Y}_2 \bar{\mathcal{Y}}_2 \right) c_{51}^{(8)} \\
 &+ \left(-g_2^2 + \frac{2\mathcal{Y}_1 \bar{\mathcal{Y}}_1}{3} - 2\mathcal{Y}_2 \bar{\mathcal{Y}}_2 \right) c_{52}^{(8)} + \left(-\frac{11g_2^2}{6} + 4g_1^2 Y_Q^2 - \frac{4\mathcal{Y}_1 \bar{\mathcal{Y}}_1}{3} + 2\mathcal{Y}_2 \bar{\mathcal{Y}}_2 \right) c_{53}^{(8)} \\
 &+ \left(2Y_H^2 g_1^2 + 14Y_Q^2 g_1^2 + 4Y_H Y_Q g_1^2 + \frac{62g_2^2}{3} + 8g_3^2 + \frac{16\mathcal{Y}_1 \bar{\mathcal{Y}}_1}{3} + 4\mathcal{Y}_2 \bar{\mathcal{Y}}_2 + 4\lambda \right) c_{54}^{(8)} \\
 &+ \left(-g_2^2 + \frac{2\mathcal{Y}_1 \bar{\mathcal{Y}}_1}{3} - 2\mathcal{Y}_2 \bar{\mathcal{Y}}_2 \right) c_{55}^{(8)} + \left(-3Y_H^2 g_1^2 - 2Y_H Y_Q g_1^2 + \frac{13g_2^2}{12} - \frac{2\mathcal{Y}_1 \bar{\mathcal{Y}}_1}{3} + 2\lambda \right) c_{56}^{(8)} ,
 \end{aligned}$$

$$\begin{aligned}
 \dot{c}'_{56}{}^{(8)} &= \left(-\frac{1}{3}Y_H Y_Q g_1^2 + \frac{g_2^2}{12} - \mathcal{Y}_1 \bar{\mathcal{Y}}_1 \right) c_{40}^{(8)} + \left(-\frac{1}{3}Y_H Y_Q g_1^2 - \frac{g_2^2}{12} + \mathcal{Y}_2 \bar{\mathcal{Y}}_2 \right) c_{41}^{(8)} \\
 &+ \left(-4g_2^2 - \frac{8\mathcal{Y}_1 \bar{\mathcal{Y}}_1}{3} - \frac{8\mathcal{Y}_2 \bar{\mathcal{Y}}_2}{3} \right) c_{51}^{(8)} + \left(-2g_2^2 - \frac{14\mathcal{Y}_1 \bar{\mathcal{Y}}_1}{3} + 2\mathcal{Y}_2 \bar{\mathcal{Y}}_2 \right) c_{52}^{(8)} \\
 &+ \left(-2g_2^2 + \frac{4\mathcal{Y}_1 \bar{\mathcal{Y}}_1}{3} - 4\mathcal{Y}_2 \bar{\mathcal{Y}}_2 \right) c_{53}^{(8)} + \left(-\frac{17g_2^2}{6} + 4g_1^2 Y_Q^2 - \frac{2\mathcal{Y}_1 \bar{\mathcal{Y}}_1}{3} \right) c_{54}^{(8)} \\
 &+ \left(8Y_H^2 g_1^2 + 14Y_Q^2 g_1^2 - 4Y_H Y_Q g_1^2 + \frac{37g_2^2}{2} + 8g_3^2 + \frac{14\mathcal{Y}_1 \bar{\mathcal{Y}}_1}{3} + 6\mathcal{Y}_2 \bar{\mathcal{Y}}_2 \right) c_{56}^{(8)} \\
 &+ \left(-8Y_H Y_Q g_1^2 - \frac{4\mathcal{Y}_1 \bar{\mathcal{Y}}_1}{3} + \frac{4\mathcal{Y}_2 \bar{\mathcal{Y}}_2}{3} \right) c_{55}^{(8)}, \\
 \dot{c}'_{57}{}^{(8)} &= \left(2Y_H^2 g_1^2 + 6Y_Q^2 g_1^2 - 4Y_H Y_Q g_1^2 + 14g_2^2 + 8g_3^2 + 2\mathcal{Y}_1 \bar{\mathcal{Y}}_1 + 6\mathcal{Y}_2 \bar{\mathcal{Y}}_2 + 12\lambda \right) c_{57}^{(8)} \\
 &+ \left(\frac{g_2^2}{6} - \mathcal{Y}_1 \bar{\mathcal{Y}}_1 - \mathcal{Y}_2 \bar{\mathcal{Y}}_2 \right) c_{42}^{(8)} + \left(\frac{11Y_H^2 g_1^2}{3} - 2Y_H Y_Q g_1^2 + \frac{11g_2^2}{4} + 2\mathcal{Y}_1 \bar{\mathcal{Y}}_1 - 6\lambda \right) c_{58}^{(8)} \\
 &+ \left(-\frac{11g_2^2}{2} - 2\mathcal{Y}_2 \bar{\mathcal{Y}}_2 + 4\lambda \right) c_{59}^{(8)} + \left(\frac{17g_2^2}{12} + \frac{g_1^2 Y_H^2}{3} - 2\lambda \right) c_{60}^{(8)} \\
 &+ \left(-\frac{16g_2^2}{3} - 4\mathcal{Y}_1 \bar{\mathcal{Y}}_1 \right) c_{61}^{(8)}, \\
 \dot{c}'_{58}{}^{(8)} &= \left(\frac{g_2^2}{6} - \mathcal{Y}_1 \bar{\mathcal{Y}}_1 - \mathcal{Y}_2 \bar{\mathcal{Y}}_2 \right) c_{42}^{(8)} + \left(-8Y_H Y_Q g_1^2 + 2g_2^2 + \frac{8\mathcal{Y}_1 \bar{\mathcal{Y}}_1}{3} \right) c_{57}^{(8)} \\
 &+ \left(\frac{28Y_H^2 g_1^2}{3} + 6Y_Q^2 g_1^2 + 4Y_H Y_Q g_1^2 + \frac{33g_2^2}{2} + 8g_3^2 + 2\mathcal{Y}_1 \bar{\mathcal{Y}}_1 + 6\mathcal{Y}_2 \bar{\mathcal{Y}}_2 \right) c_{58}^{(8)} \\
 &+ \left(-2g_2^2 + \frac{4\mathcal{Y}_1 \bar{\mathcal{Y}}_1}{3} - 4\mathcal{Y}_2 \bar{\mathcal{Y}}_2 \right) c_{59}^{(8)} + \left(\frac{g_2^2}{3} + \frac{2g_1^2 Y_H^2}{3} - 2\mathcal{Y}_1 \bar{\mathcal{Y}}_1 + 4\mathcal{Y}_2 \bar{\mathcal{Y}}_2 \right) c_{60}^{(8)} \\
 &+ \left(-2g_2^2 + \frac{4\mathcal{Y}_1 \bar{\mathcal{Y}}_1}{3} - 4\mathcal{Y}_2 \bar{\mathcal{Y}}_2 \right) c_{61}^{(8)} + \left(-\frac{7g_2^2}{3} - 6\mathcal{Y}_1 \bar{\mathcal{Y}}_1 + 6\mathcal{Y}_2 \bar{\mathcal{Y}}_2 \right) c_{62}^{(8)}, \\
 \dot{c}'_{59}{}^{(8)} &= \left(-\frac{g_2^2}{6} + \mathcal{Y}_1 \bar{\mathcal{Y}}_1 + \mathcal{Y}_2 \bar{\mathcal{Y}}_2 \right) c_{42}^{(8)} + \left(-2g_2^2 + 4\mathcal{Y}_1 \bar{\mathcal{Y}}_1 - \frac{20\mathcal{Y}_2 \bar{\mathcal{Y}}_2}{3} \right) c_{57}^{(8)} \\
 &+ \left(2Y_H^2 g_1^2 + 6Y_Q^2 g_1^2 - 4Y_H Y_Q g_1^2 + 21g_2^2 + 8g_3^2 + 4\mathcal{Y}_1 \bar{\mathcal{Y}}_1 + \frac{8\mathcal{Y}_2 \bar{\mathcal{Y}}_2}{3} + 4\lambda \right) c_{59}^{(8)} \\
 &+ \left(3Y_H^2 g_1^2 - 2Y_H Y_Q g_1^2 - \frac{25g_2^2}{12} - 2\mathcal{Y}_1 \bar{\mathcal{Y}}_1 + \frac{4\mathcal{Y}_2 \bar{\mathcal{Y}}_2}{3} - 2\lambda \right) c_{60}^{(8)} \\
 &+ \left(-g_2^2 - 2\mathcal{Y}_1 \bar{\mathcal{Y}}_1 + \frac{2\mathcal{Y}_2 \bar{\mathcal{Y}}_2}{3} \right) c_{58}^{(8)} + \left(\frac{26g_2^2}{3} + \frac{16\mathcal{Y}_2 \bar{\mathcal{Y}}_2}{3} \right) c_{61}^{(8)} \\
 &+ \left(-g_2^2 - 2\mathcal{Y}_1 \bar{\mathcal{Y}}_1 + \frac{2\mathcal{Y}_2 \bar{\mathcal{Y}}_2}{3} \right) c_{62}^{(8)},
 \end{aligned}$$

$$\begin{aligned}
 \dot{c}'_{60}{}^{(8)} &= \left(-\frac{g_2^2}{6} + \mathcal{Y}_1 \bar{\mathcal{Y}}_1 + \mathcal{Y}_2 \bar{\mathcal{Y}}_2 \right) c_{42}^{(8)} + \left(\frac{g_2^2}{6} - \mathcal{Y}_1 \bar{\mathcal{Y}}_1 - \mathcal{Y}_2 \bar{\mathcal{Y}}_2 \right) c_{43}^{(8)} \\
 &+ \left(-4g_2^2 - \frac{8\mathcal{Y}_1 \bar{\mathcal{Y}}_1}{3} - \frac{8\mathcal{Y}_2 \bar{\mathcal{Y}}_2}{3} \right) c_{57}^{(8)} + \left(2g_2^2 + 4\mathcal{Y}_1 \bar{\mathcal{Y}}_1 - \frac{4\mathcal{Y}_2 \bar{\mathcal{Y}}_2}{3} \right) c_{58}^{(8)} \\
 &+ \left(-8Y_H Y_Q g_1^2 - 2g_2^2 - \frac{16\mathcal{Y}_1 \bar{\mathcal{Y}}_1}{3} + \frac{8\mathcal{Y}_2 \bar{\mathcal{Y}}_2}{3} \right) c_{59}^{(8)} \\
 &+ \left(8Y_H^2 g_1^2 + 6Y_Q^2 g_1^2 + 4Y_H Y_Q g_1^2 + \frac{119g_2^2}{6} + 8g_3^2 + 8\mathcal{Y}_1 \bar{\mathcal{Y}}_1 + \frac{4\mathcal{Y}_2 \bar{\mathcal{Y}}_2}{3} \right) c_{60}^{(8)} \\
 &+ \left(\frac{16\mathcal{Y}_2 \bar{\mathcal{Y}}_2}{3} - \frac{16\mathcal{Y}_1 \bar{\mathcal{Y}}_1}{3} \right) c_{61}^{(8)} + \left(\frac{20g_2^2}{3} + 4\mathcal{Y}_1 \bar{\mathcal{Y}}_1 - \frac{4\mathcal{Y}_2 \bar{\mathcal{Y}}_2}{3} \right) c_{62}^{(8)}, \\
 \dot{c}'_{61}{}^{(8)} &= \left(-\frac{1}{3} Y_H Y_Q g_1^2 + \frac{g_2^2}{12} - \mathcal{Y}_1 \bar{\mathcal{Y}}_1 \right) c_{42}^{(8)} + (6\mathcal{Y}_2 \bar{\mathcal{Y}}_2 - 6\mathcal{Y}_1 \bar{\mathcal{Y}}_1) c_{57}^{(8)} \\
 &+ \left(\frac{3g_2^2}{2} + 4g_1^2 Y_Q^2 - 2\mathcal{Y}_1 \bar{\mathcal{Y}}_1 + 4\mathcal{Y}_2 \bar{\mathcal{Y}}_2 \right) c_{59}^{(8)} \\
 &+ \left(3Y_H^2 g_1^2 - 2Y_H Y_Q g_1^2 - \frac{g_2^2}{12} + 2\mathcal{Y}_1 \bar{\mathcal{Y}}_1 - 2\lambda \right) c_{62}^{(8)} \\
 &+ \left(2Y_H^2 g_1^2 + 14Y_Q^2 g_1^2 - 4Y_H Y_Q g_1^2 + 12g_2^2 + 8g_3^2 + 4\mathcal{Y}_1 \bar{\mathcal{Y}}_1 + 4\lambda \right) c_{61}^{(8)}, \\
 \dot{c}'_{62}{}^{(8)} &= \left(-\frac{1}{3} Y_H Y_Q g_1^2 + \frac{g_2^2}{12} - \mathcal{Y}_1 \bar{\mathcal{Y}}_1 \right) c_{42}^{(8)} + \left(-\frac{1}{3} Y_H Y_Q g_1^2 - \frac{g_2^2}{12} + \mathcal{Y}_2 \bar{\mathcal{Y}}_2 \right) c_{43}^{(8)} \\
 &+ (6\mathcal{Y}_2 \bar{\mathcal{Y}}_2 - 6\mathcal{Y}_1 \bar{\mathcal{Y}}_1) c_{58}^{(8)} + \left(\frac{3g_2^2}{2} + 4g_1^2 Y_Q^2 - 2\mathcal{Y}_1 \bar{\mathcal{Y}}_1 + 4\mathcal{Y}_2 \bar{\mathcal{Y}}_2 \right) c_{60}^{(8)} \\
 &+ \left(8Y_H^2 g_1^2 + 14Y_Q^2 g_1^2 + 4Y_H Y_Q g_1^2 + \frac{71g_2^2}{6} + 8g_3^2 + 2\mathcal{Y}_1 \bar{\mathcal{Y}}_1 + 6\mathcal{Y}_2 \bar{\mathcal{Y}}_2 \right) c_{62}^{(8)} \\
 &+ \left(-8Y_H Y_Q g_1^2 + 4\mathcal{Y}_1 \bar{\mathcal{Y}}_1 - 4\mathcal{Y}_2 \bar{\mathcal{Y}}_2 \right) c_{61}^{(8)}, \\
 \dot{c}'_{63}{}^{(8)} &= \frac{4}{3} i c_{22}^{(8)} g_2^2 - \frac{8}{3} g_1 Y_Q c_{38}^{(8)} g_2 - \frac{8}{3} g_1 Y_Q c_{39}^{(8)} g_2 + \left(\frac{2\mathcal{Y}_2 \bar{\mathcal{Y}}_2}{3} - \frac{2\mathcal{Y}_1 \bar{\mathcal{Y}}_1}{3} \right) c_{44}^{(8)} \\
 &+ \left(\frac{2\mathcal{Y}_2 \bar{\mathcal{Y}}_2}{3} - \frac{2\mathcal{Y}_1 \bar{\mathcal{Y}}_1}{3} \right) c_{45}^{(8)} + \left(\frac{2\mathcal{Y}_1 \bar{\mathcal{Y}}_1}{3} - \frac{2\mathcal{Y}_2 \bar{\mathcal{Y}}_2}{3} \right) c_{46}^{(8)} \\
 &+ \left(12Y_H^2 g_1^2 + \frac{34Y_Q^2 g_1^2}{3} - 4Y_H Y_Q g_1^2 + \frac{19g_2^2}{6} + \frac{136g_3^2}{9} - \frac{16\mathcal{Y}_1 \bar{\mathcal{Y}}_1}{3} + 8\mathcal{Y}_2 \bar{\mathcal{Y}}_2 \right) c_{63}^{(8)} \\
 &+ \left(8Y_H Y_Q g_1^2 + 2g_2^2 + \frac{16\mathcal{Y}_1 \bar{\mathcal{Y}}_1}{3} - \frac{8\mathcal{Y}_2 \bar{\mathcal{Y}}_2}{3} \right) c_{64}^{(8)} + \left(-2g_2^2 - \frac{32\mathcal{Y}_1 \bar{\mathcal{Y}}_1}{3} + 8\mathcal{Y}_2 \bar{\mathcal{Y}}_2 \right) c_{65}^{(8)} \\
 &+ \left(4g_2^2 + \frac{8\mathcal{Y}_1 \bar{\mathcal{Y}}_1}{3} + \frac{8\mathcal{Y}_2 \bar{\mathcal{Y}}_2}{3} \right) c_{66}^{(8)},
 \end{aligned}$$

$$\begin{aligned}
 \dot{c}'_{64}{}^{(8)} &= \frac{2}{3}ic_{22}^{(8)}g_2^2 - \frac{4}{3}g_1Y_Qc_{38}^{(8)}g_2 - \frac{4}{3}g_1Y_Qc_{39}^{(8)}g_2 + \left(-\frac{g_2^2}{6} + \frac{2\mathcal{Y}_1\bar{\mathcal{Y}}_1}{3} + \frac{4\mathcal{Y}_2\bar{\mathcal{Y}}_2}{3}\right)c_{44}^{(8)} \\
 &+ \left(\frac{g_2^2}{6} - \frac{4\mathcal{Y}_1\bar{\mathcal{Y}}_1}{3} - \frac{2\mathcal{Y}_2\bar{\mathcal{Y}}_2}{3}\right)c_{45}^{(8)} + \left(\frac{\mathcal{Y}_1\bar{\mathcal{Y}}_1}{3} - \frac{\mathcal{Y}_2\bar{\mathcal{Y}}_2}{3}\right)c_{46}^{(8)} \\
 &+ \left(2Y_H^2g_1^2 + \frac{8Y_Q^2g_1^2}{3} + 8Y_HY_Qg_1^2 - \frac{13g_2^2}{3} + \frac{32g_3^2}{9} + \frac{8\mathcal{Y}_1\bar{\mathcal{Y}}_1}{3}\right)c_{63}^{(8)} \\
 &+ \left(8Y_H^2g_1^2 + 6Y_Q^2g_1^2 + 4Y_HY_Qg_1^2 + \frac{107g_2^2}{6} + 8g_3^2 + \frac{16\mathcal{Y}_1\bar{\mathcal{Y}}_1}{3}\right)c_{64}^{(8)} \\
 &+ \left(4g_2^2 - \frac{8\mathcal{Y}_1\bar{\mathcal{Y}}_1}{3} + 8\mathcal{Y}_2\bar{\mathcal{Y}}_2\right)c_{65}^{(8)} + \left(2g_2^2 + \frac{8\mathcal{Y}_1\bar{\mathcal{Y}}_1}{3}\right)c_{66}^{(8)}, \\
 \dot{c}'_{65}{}^{(8)} &= -4c_{21}^{(8)}g_2^2 - \frac{2}{3}ic_{22}^{(8)}g_2^2 + \frac{4}{3}g_1Y_Qc_{38}^{(8)}g_2 + \frac{4}{3}g_1Y_Qc_{39}^{(8)}g_2 - \frac{16}{3}g_1^2Y_Q^2c_{20}^{(8)} \\
 &- \frac{64}{9}g_3^2c_{23}^{(8)} + \left(\frac{4\mathcal{Y}_1\bar{\mathcal{Y}}_1}{3} + \frac{2\mathcal{Y}_2\bar{\mathcal{Y}}_2}{3}\right)c_{44}^{(8)} + \frac{2}{3}\mathcal{Y}_1\bar{\mathcal{Y}}_1c_{45}^{(8)} - \frac{2}{3}\mathcal{Y}_1\bar{\mathcal{Y}}_1c_{46}^{(8)} \\
 &+ \left(\frac{17g_2^2}{3} - \frac{8\mathcal{Y}_1\bar{\mathcal{Y}}_1}{3} + 4\mathcal{Y}_2\bar{\mathcal{Y}}_2\right)c_{63}^{(8)} + \left(2g_2^2 - \frac{4\mathcal{Y}_1\bar{\mathcal{Y}}_1}{3} + 4\mathcal{Y}_2\bar{\mathcal{Y}}_2\right)c_{64}^{(8)} \\
 &+ \left(12Y_H^2g_1^2 + \frac{34Y_Q^2g_1^2}{3} - 4Y_HY_Qg_1^2 + \frac{37g_2^2}{2} + \frac{136g_3^2}{9} + \frac{32\mathcal{Y}_1\bar{\mathcal{Y}}_1}{3}\right)c_{65}^{(8)} \\
 &+ \left(8Y_HY_Qg_1^2 - 2g_2^2 - \frac{8\mathcal{Y}_1\bar{\mathcal{Y}}_1}{3}\right)c_{66}^{(8)}, \\
 \dot{c}'_{66}{}^{(8)} &= -2c_{21}^{(8)}g_2^2 - \frac{1}{3}ic_{22}^{(8)}g_2^2 + \frac{2}{3}g_1Y_Qc_{38}^{(8)}g_2 + \frac{2}{3}g_1Y_Qc_{39}^{(8)}g_2 - \frac{8}{3}g_1^2Y_Q^2c_{20}^{(8)} \\
 &- \frac{32}{9}g_3^2c_{23}^{(8)} + \left(-Y_HY_Qg_1^2 + \frac{g_2^2}{12} - \frac{4\mathcal{Y}_1\bar{\mathcal{Y}}_1}{3} + \frac{4\mathcal{Y}_2\bar{\mathcal{Y}}_2}{3}\right)c_{44}^{(8)} \\
 &+ \left(\frac{1}{3}Y_HY_Qg_1^2 - \frac{g_2^2}{12} + \frac{4\mathcal{Y}_1\bar{\mathcal{Y}}_1}{3}\right)c_{45}^{(8)} + \left(\frac{2}{3}Y_HY_Qg_1^2 + \frac{2\mathcal{Y}_1\bar{\mathcal{Y}}_1}{3} - \mathcal{Y}_2\bar{\mathcal{Y}}_2\right)c_{46}^{(8)} \\
 &+ \left(\frac{83g_2^2}{12} - \frac{g_1^2Y_H^2}{3} - 2g_1^2Y_Q^2 - \frac{8\mathcal{Y}_1\bar{\mathcal{Y}}_1}{3} + 8\mathcal{Y}_2\bar{\mathcal{Y}}_2\right)c_{63}^{(8)} \\
 &+ \left(-\frac{13g_2^2}{6} + \frac{2g_1^2Y_H^2}{3} + 4g_1^2Y_Q^2 - \frac{4\mathcal{Y}_1\bar{\mathcal{Y}}_1}{3}\right)c_{64}^{(8)} \\
 &+ \left(\frac{4Y_H^2g_1^2}{3} - \frac{4Y_Q^2g_1^2}{3} + 8Y_HY_Qg_1^2 + \frac{3g_2^2}{2} + \frac{32g_3^2}{9} + \frac{8\mathcal{Y}_1\bar{\mathcal{Y}}_1}{3}\right)c_{65}^{(8)} \\
 &+ \left(\frac{28Y_H^2g_1^2}{3} + 14Y_Q^2g_1^2 + 4Y_HY_Qg_1^2 + \frac{19g_2^2}{2} + 8g_3^2 - \frac{8\mathcal{Y}_1\bar{\mathcal{Y}}_1}{3}\right)c_{66}^{(8)}.
 \end{aligned}$$

Chapter 5

Higher-derivative operators and gravitational observables

The first observation of gravitational waves by the LIGO collaboration [245] at the end of 2015 naturally spiked an interest in the gravitational two-body problem across the board. The amplitudes community in particular saw a major shift in attention towards this topic, and the wide range of tools developed primarily for the sake of collider physics found an ideal ground to flourish and contributed groundbreaking results.

When considering the merger of two galactic objects, the process is usually described in terms of three different phases being an initial inspiral phase, the merger itself and finally the ringdown of the resulting object. During the inspiral phase, in particular in the case of two black holes, as long as the two bodies are far enough apart from each other and since they are separated from us (the observer) by distances on a cosmic scale they can be effectively approximated as point-like particles and described within a quantum theory of gravitationally interacting massive particles. The particular process of interest is usually a two-to-two scattering: in the case of two Schwarzschild black holes for example one considers two scalars $\phi_{m_1}\phi_{m_2} \rightarrow \phi_{m_1}\phi_{m_2}$ but similarly one can describe light deflection of a black hole as $\phi_{m_1}\gamma \rightarrow \phi_{m_1}\gamma$. The aim is clearly not to give a quantum mechanical treatment of the black holes, whose internal structure is in fact completely neglected, rather to extract information about the classical gravitational interaction at high enough precision to give an accurate description of what the experiments are observing. The increased precision comes from extracting the classical information hidden in the higher-loop contributions of such a framework: in quantum field theories featuring massive matter, the mass terms come with an inverse power of \hbar which leads to additional cancellation of the powers of \hbar in the loop expansion and so even arbitrary high loop-orders can feature terms surviving in the classical limit $\hbar \rightarrow 0$ [94–96].

Also in this context on-shell methods prove extremely powerful. In fact the focus is on long-range physics which is encoded in the non-analytic pieces of the amplitude (the analytic part corresponds to local terms in the potential), and since unitarity cuts capture precisely these pieces, loop-level unitarity and generalised unitarity methods prove ideal to extract the relevant contributions from the complete amplitude result. In particular, one wants to consider the external lines of the amplitude as the galactic objects interacting via graviton exchange, narrowing down on the terms that have discontinuities in the \vec{q}^2 channel, corresponding to the momentum transfer \vec{q} of the process [246, 96].

The perturbative expansion with respect to which one computes trees and loops is performed in powers of Newton’s constant G and is called post-Minkowskian (PM) expansion, as opposed to the post-Newtonian (PN) expansion where the perturbative coupling is given by the relative velocity v^2 of the two objects or equivalently (thanks to the virial theorem) by $v^2 \sim Gm/r$ with m the total mass of the binary system and r the relative position. While the PM expansion is relativistic in its nature and thus provides a result complete to all orders in the velocity at each given order in G , in the early inspiral phase the gravitational field is weak and so the system constituents are non-relativistic and the PN expansion might prove better suited in these circumstances. The two approaches can be considered complementary and provide effective cross-checks of one another. In the PN expansion relevant results include the first [247], second [248, 249], third [250–253], fourth [254–266], fifth [267–269] and sixth [270–275] post-Newtonian order. In the post-Minkowskian framework, which is natural in the context of amplitudes, the current state of the art is at 4PM order [30, 276–278] with the previous 3PM order being computed in [29, 279] and confirmed among others in [280].

Scattering amplitudes are naturally organised as a series of powers of G , and it is then convenient to define the effective two-body potential

$$V(p, r) = \sum_{n=1}^{\infty} \left(\frac{G}{|r|} \right)^n c_n(p^2), \quad (5.1)$$

where p and r are the relative momentum and distance. This effective potential is then truncated at a given order in G^1 , and up to this order it reproduces the same physics as the full gravitational theory for two bodies interacting via classical long-range force, and the coefficients of the expansion can be extracted from the amplitudes by an EFT matching procedure [94–98, 246, 281–283, 29]. Such a procedure focusses on the computation of the effective potential which is not a gauge invariant quantity, and thus the matching procedure needs to be performed with some care. On the other hand, one can follow a different route and directly compute gravitational physical observables from the on-shell scattering amplitudes. There are different ways of doing so, one

¹At the time of writing, the highest known PM contribution is to $\mathcal{O}(G^4)$, see [30].

example being pioneered in [26, 28] and further extended in [32, 33], but the one we decided to adopt is the eikonal approach [100–105], in particular for the computation of the time delay and deflection angle of a light particle off a heavy object.

In this approach the relevant amplitudes are evaluated in an approximation where the momentum transfer $|\vec{q}|$ is taken to be much smaller than both the mass m of the heavy scalar and the energy ω of the massless particle, or more precisely taking $m \gg \omega \gg |\vec{q}|$. Crucial for this is a convenient parameterization of spinor helicity variables for the massless particles in the eikonal limit. The amplitudes thus obtained are then transformed to impact parameter space via a two-dimensional Fourier transform. In this space, the amplitudes are expected to exponentiate into an eikonal phase, from which one can extract directly the classical (and, if desired, quantum) deflection angle and time advance/delay. Recent applications of this method to this type of problem include [284] for the deflection angle of massless scalars up to 2PM (namely $\mathcal{O}(G^2)$), [285] for photons and fermions up to 2PM order, and up to 3PM order in [286–289]. We also note that [285] showed the equivalence of the eikonal method and the formalism based on the computation of an intermediate potential/Hamiltonian used for instance in [285, 290–294].

In this chapter we consider effective theories of gravity obtained by adding higher-derivative interactions to the Einstein-Hilbert (EH) action. Higher-derivative operators in gravity have attracted increasing attention and are being studied from a variety of perspectives, including the modifications induced on the potential [293, 294], the effects on gravitational wave observations [295, 106] as well as causality bounds on the associated coefficients [296]. Here in particular we consider terms of the form R^3 , R^4 and FFR with R being the Riemann tensor and F the field strength tensor of the photon, and compute the leading and first subleading contribution in the eikonal formalism. This requires the computation of up to one-loop amplitudes with these operator insertions, from which we extract the deflection angle and time delay from the eikonal phase, considering the deflection of gravitons as well as photons.

Since our computation stops at the first loop order, we make use of an additional simplification stemming from the fact that in the unitarity-based calculation the cuts can be kept in four dimensions, as discrepancies with D -dimensional results only give rise to analytic terms, at this loop order. It is also important to stress that the presence of the higher-derivative couplings allows for helicity-preserving as well as helicity-violating processes to contribute, thus the eikonal *phase* is promoted to an eikonal *phase matrix* in the space of helicities of the external massless particles. In our conventions $(+-)$ and $(-+)$ are the diagonal entries associated to no-flip scattering (recall that we always consider all particles' momenta as outgoing), while $(++)$ and $(--)$ are the off-diagonal entries, with helicity flip. The associated mixing problem has to be resolved in order to

obtain the physical quantities of interest. Whenever the two eigenvalues of the eikonal phase matrix are distinct, a possible violation of causality at small impact parameter arises, as noticed already at tree level in [297]. See also [298–305] for further discussions and resolutions of this issue in UV-complete theories, [103, 297, 306, 307] for earlier appearances of the eikonal operator and [308, 309] for related discussions involving helicity flip and no-flip amplitudes.

In this section we first describe the theory we are working with and give a precise definition of the eikonal limit, providing an explicit parametrisation for all the momenta and spinor-helicity variables we need. We then briefly review the connection between amplitudes in the eikonal limit (Fourier-transformed to impact parameter space) and the eikonal phase matrix, the deflection angle and the time delay. Finally we provide the relevant amplitudes², extract the eikonal phase and compute the modifications of the observables due to the presence of the higher-derivative couplings.

5.1 From amplitudes to the deflection angle and time delay via the eikonal

Gravity with higher-derivative couplings

In this section we study the effects of higher-derivative operators, denoted schematically as R^3 , R^4 and FFR , on the deflection of a light particle by a heavy spin-less object. More precisely, we use the eikonal approximation to compute the corrections to the time delay and deflection angle induced by the following theory

$$S = \int d^4x \sqrt{-g} \left[\frac{1}{2} (D_\mu \phi)(D^\mu \phi) - \frac{1}{2} m^2 \phi^2 - \frac{2}{\kappa^2} R - \frac{2}{\kappa^2} \mathcal{L}_6 + \frac{2}{\kappa^2} \mathcal{L}_8 - \frac{1}{4} F^{\mu\nu} F_{\mu\nu} - \frac{\alpha\gamma}{8} F^{\mu\nu} F^{\rho\sigma} R_{\mu\nu\rho\sigma} \right], \quad (5.2)$$

where in the first line we have the massive scalar particle action mimicking the heavy spin-less object, as well as the Einstein-Hilbert term, then in the second line the purely gravitational interaction terms \mathcal{L}_6 and \mathcal{L}_8 and finally the photon interaction terms. The higher-derivative interactions we consider are

$$\mathcal{L}_6 = \frac{\alpha_1}{48} I_1 + \frac{\alpha_2}{24} G_3 \quad (5.3)$$

²In this and the next chapter through an abuse of notation we often call “amplitude” what technically is only the part of the amplitude with the discontinuity in the kinematic channel related to momentum transfer. In other words, we call amplitude the part of the complete amplitude relevant to our computation.

with

$$I_1 := R^{\alpha\beta}{}_{\mu\nu} R^{\mu\nu}{}_{\rho\sigma} R^{\rho\sigma}{}_{\alpha\beta} , \quad G_3 := I_1 - 2R^{\mu\nu\alpha}{}_{\beta} R^{\beta\gamma}{}_{\nu\sigma} R^{\sigma}{}_{\mu\gamma\alpha} \equiv I_1 - 2I_2 , \quad (5.4)$$

and

$$\mathcal{L}_8 = \beta_1 \mathcal{C}^2 + \beta_2 \mathcal{C} \tilde{\mathcal{C}} + \beta_3 \tilde{\mathcal{C}}^2 , \quad (5.5)$$

where

$$\mathcal{C} := R_{\mu\nu\rho\sigma} R^{\mu\nu\rho\sigma} , \quad \tilde{\mathcal{C}} := \frac{1}{2} R_{\mu\nu\alpha\beta} \epsilon^{\alpha\beta}{}_{\gamma\delta} R^{\gamma\delta\mu\nu} . \quad (5.6)$$

A few comments on the various couplings in (5.2) are in order here.

First, there are two types of R^3 terms, denoted as I_1 and G_3 above. Such terms arise naturally in the low-energy effective description of bosonic string theory where $\alpha_1 = \alpha_2 = \alpha'^2$ which is the value of the couplings we will use in this section. Their effects on gravitational scattering of different matter fields have been discussed in [293, 294]; specifically for the scattering of two massive scalars, both independent structures I_1 and G_3 were found to contribute. On the other hand, for the helicity-preserving deflection of massless particles of spin 0, 1 and 2, it was shown in [293] that the G_3 interaction has no effect. Additional interesting features about the I_1 and G_3 couplings are that I_1 is the only coupling that contributes to pure graviton scattering up to four points [310, 311] and is the two-loop counterterm in pure gravity [312], while G_3 is a topological term in six dimensions. In the following we will be concerned with (helicity-preserving and flipping) scattering of massless gravitons in the background produced by a massive scalar, in which case only the I_1 structure contributes, hence in this section we will refer to it simply as the R^3 term, since no confusion can arise. Note that in the case of photons there is no R^3 contribution to the helicity-flipping process.

The second interaction we study is of the type R^4 . In principle there are 26 independent parity-even quartic contractions of the Riemann tensor [313], but only the seven which do not contain the Ricci scalar or tensor survive on shell in arbitrary dimensions, as can also be seen using field redefinitions [314, 315, 2]. In four dimensions these reduce to two independent parity-even structures [295, 316], plus one parity-odd structure [106], as shown in (5.5).³ In agreement with [316] we find that these interactions induce the following four-point graviton amplitudes: those with all-equal helicities, and the amplitude with two positive- and two negative-helicity gravitons (the MHV configuration). If β_2 in (5.5) is non-vanishing, then the all-plus and all-minus graviton amplitudes are independent. We also note that a particular contraction of four Riemann tensors appears in type-II superstring theories where it is the first higher-derivative curvature correction to the EH theory, and can be determined from four-graviton scattering [318].

³A general approach to find a complete, non-redundant operator basis of dimension six and eight for the effective Standard Model including gravity has been given recently in [317] using the Hilbert series method.

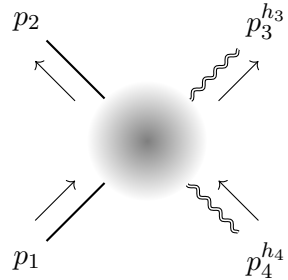
The third interaction we consider is an FFR term, where F is the electromagnetic field strength. It is known to arise in string theory as well as from integrating out massive, charged electrons in the case of electrodynamics coupled to gravity, as discussed in [308, 309], and considered more recently in [298, 299].

We have also introduced in the action a minimally coupled massive scalar to represent a black hole⁴. Note that in (5.2) we have excluded terms quadratic in the curvatures since from an effective field theory/on-shell point of view they have no effect to any order in four dimensions, as shown recently in [2].

Kinematics of the scattering

Here we describe the kinematics of the scattering processes we consider in this section. We denote by p_1 and p_2 the four-momenta of the incoming and outgoing scalars, respectively, with m being their common mass, while the momenta of the incoming and outgoing massless particles (gravitons or photons) are p_4 and p_3 . We stress here that for the graviton scattering process in particular, it is not our goal to describe the specific scattering in order to provide input data for experiment, but rather gain qualitative insights into the theory including higher derivative operators. These insights include for example the necessity of introducing an eikonal phase matrix or the consistency requirements imposed on the couplings by the time delay, as we will see later in this section.

We will work in the centre of mass frame, with the following parameterization:



$$\begin{aligned}
 p_4^\mu &= -(E_4, -\vec{p} + \vec{q}/2), \\
 p_1^\mu &= -(E_1, \vec{p} - \vec{q}/2), \\
 p_2^\mu &= (E_2, \vec{p} + \vec{q}/2), \\
 p_3^\mu &= (E_3, -\vec{p} - \vec{q}/2).
 \end{aligned} \tag{5.7}$$

In our conventions we take all momenta to be outgoing, hence the minus signs in the expressions of p_1 and p_4 since particles 1 and 4 are incoming. We also have

$$\begin{aligned}
 E_1 &= E_2 = \sqrt{m^2 + \vec{p}^2 + \vec{q}^2/4}, \\
 E_3 &= E_4 = \sqrt{\vec{p}^2 + \vec{q}^2/4} := \omega,
 \end{aligned} \tag{5.8}$$

where $\vec{p} \cdot \vec{q} = 0$ due to momentum conservation. Hence \vec{q} lives in a two-dimensional

⁴In order to describe charged black holes the real scalar in (5.2) should be replaced by an electrically charged complex scalar.

space orthogonal to \vec{p} . In this chapter we define the Mandelstam variables as

$$s := (p_1 + p_2)^2 = -\vec{q}^2, \quad t := (p_1 + p_4)^2 = (E_1 + E_4)^2, \quad u := (p_1 + p_3)^2, \quad (5.9)$$

with $s + t + u = 2m^2$. In this notation the spacelike momentum transfer squared is given by s , while t denotes the centre of mass energy squared, and ω is the energy of the scattered massless particle.

In the above parameterization, the kinematic limit we are interested is

$$m \gg \omega \gg |\vec{q}|, \quad (5.10)$$

which implies for the Mandelstam variables

$$t \simeq m^2 + 2m\omega, \quad ut - m^4 \simeq -(2m\omega)^2, \quad (5.11)$$

and for the energies of the massless particles

$$E_3 = E_4 := \omega \simeq |\vec{p}| \left(1 + \frac{\vec{q}^2}{8|\vec{p}|^2} \right). \quad (5.12)$$

For definiteness we choose $\vec{p} = |\vec{p}| \hat{z}$ with $|\vec{p}| \gg |\vec{q}|$, as implied by (5.10). In this approximation we can write the four-momentum p_3 of the massless particle in spinor notation as

$$p_3 = \begin{pmatrix} \frac{\vec{q}^2}{8|\vec{p}|} & -\frac{\bar{q}}{2} \\ -\frac{q}{2} & 2|\vec{p}| \end{pmatrix}, \quad (5.13)$$

with $q := q_1 + iq_2$ and $\bar{q} := q_1 - iq_2$. One can then find an explicit parameterization for the spinors associated to the null momenta $p_i = \lambda_i \tilde{\lambda}_i$, $i = 3, 4$, with the result

$$\begin{aligned} \lambda_3 &= \sqrt{2|\vec{p}|} \begin{pmatrix} -\frac{\bar{q}}{4|\vec{p}|} \\ 1 \end{pmatrix}, & \tilde{\lambda}_3 &= \sqrt{2|\vec{p}|} \begin{pmatrix} -\frac{q}{4|\vec{p}|} & 1 \end{pmatrix}, \\ \lambda_4 &= i\sqrt{2|\vec{p}|} \begin{pmatrix} \frac{\bar{q}}{4|\vec{p}|} \\ 1 \end{pmatrix}, & \tilde{\lambda}_4 &= i\sqrt{2|\vec{p}|} \begin{pmatrix} \frac{q}{4|\vec{p}|} & 1 \end{pmatrix}. \end{aligned} \quad (5.14)$$

Note the extra factors of i due to the negative energy-component of p_4 corresponding to an incoming particle.

Eikonal phase, deflection angle and time delay

In this section we briefly review relevant aspects of the eikonal approximation and the eikonal phase matrix which allows for an efficient extraction of the deflection angle and time delay/advance from scattering amplitudes. This topic was intensively studied in the context of gravity and string theory in the nineties [104, 105]; for related recent work see also [319–321] and references therein.

First, we introduce the amplitude in impact parameter space $\tilde{\mathcal{A}}$. This is defined as a Fourier transform of the amplitude \mathcal{A} with respect to the momentum transfer \vec{q} ,

$$\tilde{\mathcal{A}}(\vec{b}) := \frac{1}{4m\omega} \int \frac{d^{D-2}q}{(2\pi)^{D-2}} e^{i\vec{q}\cdot\vec{b}} \mathcal{A}(\vec{q}) , \quad (5.15)$$

where \vec{b} is the impact parameter, and the number of dimensions will eventually be set to $D = 4 - 2\epsilon$.

In the eikonal approximation the gravitational S -matrix can be written in the form [104, 284]

$$S_{\text{eik}} = e^{i(\delta_0 + \delta_1 + \dots)} , \quad (5.16)$$

where δ_0 is the leading eikonal phase, which is $\mathcal{O}(G)$, δ_1 the first subleading correction, of $\mathcal{O}(G^2)$, and the dots represent subsubleading contributions. Alternatively, one can write the S -matrix in impact parameter space as

$$S_{\text{eik}} = 1 + \tilde{\mathcal{A}}_{\omega}^{(0)} + \tilde{\mathcal{A}}_{\omega^2}^{(1)} + \tilde{\mathcal{A}}_{\omega}^{(1)} + \tilde{\mathcal{A}}_{\omega^3}^{(2)} + \tilde{\mathcal{A}}_{\omega^2}^{(2)} + \tilde{\mathcal{A}}_{\omega}^{(2)} + \dots , \quad (5.17)$$

where the superscript indicates the loop order L and the subscript the power in the energy ω of the massless particle. That the maximal power of ω at a given loop order is $L + 1$ is a well-established fact in (super)gravity and we will see below that the R^3 corrections do not alter this expectation. However, we also find that the R^4 corrections lead to higher powers of ω starting at one loop, which is not surprising since higher-derivative corrections worsen the high-energy behaviour. In the effective field theory approach we adopt, we are not really interested in high-energy physics (or high-energy completions of the theory) – we use the eikonal approximation as an efficient and elegant tool to extract deflection angles and time delay/advances without passing through the computation of non gauge-invariant intermediate quantities such as effective potentials or Hamiltonians. Nevertheless it would be interesting to check if in the R^4 case unitarity can be restored as well through exponentiation.

Equating (5.16) with (5.17) one gets

$$\delta_0 = -i \tilde{\mathcal{A}}_\omega^{(0)} , \quad (5.18)$$

$$\delta_1 = -i \tilde{\mathcal{A}}_\omega^{(1)} , \quad (5.19)$$

as well as the condition

$$-\frac{(\delta_0)^2}{2} = \tilde{\mathcal{A}}_{\omega^2}^{(1)} , \quad (5.20)$$

which implies the consistency condition

$$\tilde{\mathcal{A}}_{\omega^2}^{(1)} = \frac{1}{2} (\tilde{\mathcal{A}}_\omega^{(0)})^2 . \quad (5.21)$$

Thus, the contribution to the one-loop amplitude that is leading in ω , $\tilde{\mathcal{A}}_{\omega^2}^{(1)}$, does not provide any new information about the S -matrix. In general, it is only the term in $\tilde{\mathcal{A}}^{(L)}$ that is linear in ω , $\tilde{\mathcal{A}}_\omega^{(L)}$, that provides new information entering δ_L . We also note that (5.18)–(5.21) hold as matrix equations.

Note that a priori these statements are known to hold for EH gravity. The results in this chapter show that (5.21) also holds for the higher-derivative interactions discussed here at least up to one loop. Of course the work of [104] on the eikonal limit of string amplitudes gives reason to believe that the exponentiation will work for higher-derivative interactions to all orders.

Finally, the particle deflection angle can be obtained from the eigenvalues $\delta^{(i)}$ of the eikonal phase matrix δ . Using a saddle-point approximation [104, 285, 322] one finds, for small θ ,

$$\theta^{(i)} = \frac{1}{\omega} \frac{\partial}{\partial b} \delta^{(i)} , \quad (5.22)$$

where i runs over all eigenvalues of δ and $b = |\vec{b}|$. For the time delay, we will use instead [323–325]

$$t^{(i)} = \frac{\partial \delta^{(i)}}{\partial \omega} . \quad (5.23)$$

5.2 The relevant scattering amplitudes

In this section we compute the relevant amplitudes needed to extract the deflection angle and time delay/advance induced by the various interactions in (5.2). At tree-level we will present exact expressions; at one-loop we only need to compute the part of the amplitude with a discontinuity in the s -channel⁵ and we will write the relevant expressions after expanding them in the eikonal approximation (5.10) – this will be

⁵We recall that $s = -|\vec{q}|^2$ where \vec{q} is the momentum exchange between the classical source and the graviton.

denoted in the following by the \simeq symbol. A direct extraction of the classical part of the deflection angle and time delay can be performed using triple cuts, and in an even more refined way using the holomorphic classical limit [25]. We chose instead to compute the one-loop amplitudes through two-particle cuts, which also determine the quantum part of the amplitude. The latter, despite not being used in the present thesis, becomes essential when considering the exponentiation in the eikonal limit at higher orders [320].

We will begin our discussion with the simple case of EH gravity, quoting from [292] the relevant two-scalar two-graviton amplitude without helicity flip. We also compute the amplitude with helicity flip, and show that it does not contribute in the eikonal approximation, as correctly assumed in previous treatments. We will then move on to compute the relevant tree- and one-loop amplitudes that are necessary in order to compute the corrections induced by the R^3 , R^4 and FFR terms in (5.2).

The two-particle cut diagrams relevant for the R^3 and R^4 cases are shown in Figure 5.1. The corrections induced by the FFR interaction need a separate analysis and we show the corresponding diagrams in Figures 5.2 and 5.3. For the case of the R^n interaction both internal and external particles are gravitons, while in the case of FFR we either have external gravitons and internal photons, or viceversa.

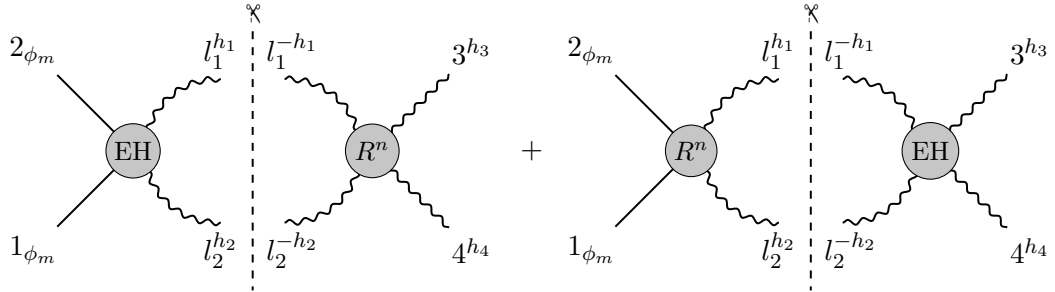


Figure 5.1: The two-particle cut diagrams for the R^n interaction in the $s = -\vec{q}^2$ -channel. In our conventions external momenta are all outgoing and internal loop momenta flow from left to right in the diagram.

A comment is in order here. Focusing on the cuts relevant for R^n depicted in Figure 5.1, the case $h_3 = h_4$ corresponds to the massless particle flipping helicity upon interacting with the scalar, whereas $h_3 = -h_4$ corresponds to the helicity-preserving process, since in our conventions all external particles are outgoing. A simple way to take into account particle statistics is to sum over all values of the internal helicities h_1 and h_2 and divide the result by 2.⁶

⁶If the two particles are identical this introduces the correct Bose symmetry factor of $1/2$; if they are different this takes into account that the internal particles are not colour ordered, hence summing over two possible internal helicity assignments would lead to double counting, compensated by the factor of $1/2$.

5.2.1 Four-point scalar/graviton scattering in EH gravity

The relevant tree-level amplitudes in the EH case are the two-scalar/two-graviton amplitudes in the two helicity configurations for the gravitons:⁷

$$\begin{aligned}\mathcal{A}_{\text{EH}}^{(0)}(1^\phi, 2^\phi, 3^{--}, 4^{++}) &= -\left(\frac{\kappa}{2}\right)^2 \frac{\langle 3|1|4\rangle^4}{s^2} \left[\frac{i}{t-m^2} + \frac{i}{u-m^2} \right], \\ \mathcal{A}_{\text{EH}}^{(0)}(1^\phi, 2^\phi, 3^{++}, 4^{++}) &= -\left(\frac{\kappa}{2}\right)^2 m^4 \frac{[34]^2}{\langle 34\rangle^2} \left[\frac{i}{t-m^2} + \frac{i}{u-m^2} \right],\end{aligned}\tag{5.24}$$

The computation of the four-point one-loop amplitude without helicity flip in the eikonal approximation (5.10) was performed in [292], with the result

$$\begin{aligned}\mathcal{A}_{\text{EH}}^{(1)}(1^\phi, 2^\phi, 3^{--}, 4^{++}) &\simeq \mathcal{N}_h \left(\frac{\kappa}{2}\right)^4 \left[(2m\omega)^4 (I_4(s, t; m) + I_4(s, u; m)) - 15(m^2\omega)^2 I_3(s; m) \right. \\ &\quad \left. + (4m\omega)^2 s I_3(s) - \frac{29}{2}(m\omega)^2 I_2(s) \right],\end{aligned}\tag{5.25}$$

where

$$\mathcal{N}_h := \left(\frac{\langle 3|2|4\rangle}{2m\omega} \right)^4\tag{5.26}$$

is a pure phase, with $\mathcal{N}_h \rightarrow 1$ in the eikonal approximation. We have also computed the new amplitude with helicity flip in the same approximation, with the result

$$\mathcal{A}_{\text{EH}}^{(1)}(1^\phi, 2^\phi, 3^{++}, 4^{++}) \simeq \left(\frac{\kappa}{2}\right)^4 \frac{[34]^2}{\langle 34\rangle^2} (m^2 s)^2 [I_4(s, t; m) + I_4(s, u; m)].\tag{5.27}$$

5.2.2 Four-point scalar/graviton scattering in EH + R³

We now consider the amplitudes with addition of the R^3 interaction in (5.2): the helicity-preserving amplitude at tree-level is vanishing

$$\mathcal{A}_{R^3}^{(0)}(1^\phi, 2^\phi, 3^{--}, 4^{++}) = 0,\tag{5.28}$$

while the helicity-flip amplitude is [293]

$$\mathcal{A}_{R^3}^{(0)}(1^\phi, 2^\phi, 3^{++}, 4^{++}) = i \left(\frac{\kappa}{2}\right)^2 \left(\frac{\alpha'}{4}\right)^2 [34]^4 \frac{(t-m^2)(u-m^2)}{s}.\tag{5.29}$$

⁷See for instance [293, 181].

At one loop, the result of [293] for the no-flip amplitude gives:

$$\mathcal{A}_{R^3}^{(1)}(1^\phi, 2^\phi, 3^{--}, 4^{++}) \simeq \left(\frac{\kappa}{2}\right)^4 \left(\frac{\alpha'}{4}\right)^2 \mathcal{N}_h \left[(ms)^4 (I_4(s, t; m) + I_4(s, u; m)) + (m^2 s \omega)^2 I_3(s; m) + \frac{3}{2} (ms \omega)^2 I_2(s) \right], \quad (5.30)$$

where \mathcal{N}_h is defined in (5.26). The one-loop amplitude with helicity flip requires a new computation and the result in the eikonal approximation is

$$\mathcal{A}_{R^3}^{(1)}(1^\phi, 2^\phi, 3^{++}, 4^{++}) \simeq \left(\frac{\kappa}{2}\right)^4 \left(\frac{\alpha'}{4}\right)^2 [34]^4 \left[(2m\omega)^4 (I_4(s, t; m) + I_4(s, u; m)) - 13(m^2 \omega)^2 I_3(s; m) + 16(m\omega)^2 s I_3(s) + \frac{153}{10} (m\omega)^2 I_2(s) \right]. \quad (5.31)$$

5.2.3 Four-point scalar/graviton scattering in EH + R^4

In this section we consider the addition of an R^4 interaction to the EH action. Such interaction affects the two-scalar two-graviton amplitude at one loop and thus contributes to graviton deflection and time delay at order G^2 . In order to build this amplitude using the unitarity-based method we first need to find the expression for the four-graviton tree-level amplitudes in the R^4 theory. We do it first starting from the Lagrangian in (5.5) in order to make contact with the notation of [295], then we show how to get directly to the result through the approach presented in Section 3 relying only on little-group considerations and dimensional analysis.

Deriving the four-graviton amplitudes from (5.5) is straightforward – we simply have to replace the four Riemann tensors in each term by their linearised form corresponding to the four on-shell gravitons. For particle i the well-known expression in momentum space is

$$R(i)_{\mu\nu\rho\sigma} = \frac{1}{2} F(i)_{\mu\nu} F(i)_{\rho\sigma} \quad (5.32)$$

where

$$F(i)_{\mu\nu} = p_{i\mu} \varepsilon_{i\nu} - p_{i\nu} \varepsilon_{i\mu}. \quad (5.33)$$

Since we are interested in helicity amplitudes, we choose the field strengths $F(i)$ to be selfdual (negative helicity) or anti-selfdual (positive helicity), hence in spinor-helicity formalism their form is

$$F(i)_{\text{SD } \alpha\dot{\alpha}\beta\dot{\beta}} = -\sqrt{2} \lambda_{i\alpha} \lambda_{i\beta} \epsilon_{\dot{\alpha}\dot{\beta}} \quad \text{and} \quad F(i)_{\text{ASD } \alpha\dot{\alpha}\beta\dot{\beta}} = -\sqrt{2} \tilde{\lambda}_{i\dot{\alpha}} \tilde{\lambda}_{i\dot{\beta}} \epsilon_{\alpha\beta}. \quad (5.34)$$

The building blocks in (5.6) are bilinear in Riemann tensors, and take the form

$$\mathcal{C} \simeq \left(F(i)_{(A)SD} \cdot F(j)_{(A)SD} \right)^2, \quad (5.35)$$

and

$$\tilde{\mathcal{C}} \simeq \left(F(i)_{(A)SD} \cdot F(j)_{(A)SD} \right) \left(F(i)_{(A)SD} \cdot \frac{1}{i} * F(j)_{(A)SD} \right), \quad (5.36)$$

where \cdot denotes Lorentz contractions and $*$ denotes the usual Hodge dual which acts on the (anti-)selfdual field strengths as $*F_{SD} = F_{SD}$ and $*F_{ASD} = -F_{ASD}$. Furthermore, given the form (5.34) these expressions are only non-vanishing if both particles i and j have the same helicity. In summary, if both gravitons have negative helicity (SD field strength) we have

$$\mathcal{C} = i\tilde{\mathcal{C}} = \frac{1}{2} \langle ij \rangle^4, \quad (5.37)$$

while if both gravitons have positive helicity (ASD field strength) we have

$$\mathcal{C} = -i\tilde{\mathcal{C}} = \frac{1}{2} [ij]^4. \quad (5.38)$$

With these results one easily arrives at

$$\begin{aligned} \mathcal{A}_{R^4}^{(0)}(1^{++}, 2^{++}, 3^{++}, 4^{++}) &= i\beta^+ \left(\frac{\kappa}{2} \right)^2 \left([12]^4 [34]^4 + [13]^4 [24]^4 + [14]^4 [23]^4 \right), \\ \mathcal{A}_{R^4}^{(0)}(1^{--}, 2^{--}, 3^{--}, 4^{--}) &= i\beta^- \left(\frac{\kappa}{2} \right)^2 \left(\langle 12 \rangle^4 \langle 34 \rangle^4 + \langle 13 \rangle^4 \langle 24 \rangle^4 + \langle 14 \rangle^4 \langle 23 \rangle^4 \right), \\ \mathcal{A}_{R^4}^{(0)}(1^{++}, 2^{++}, 3^{--}, 4^{--}) &= i\tilde{\beta} \left(\frac{\kappa}{2} \right)^2 [12]^4 \langle 34 \rangle^4, \end{aligned} \quad (5.39)$$

with

$$\beta^+ = 4 \left(\beta_1 + \frac{i}{2} \beta_2 - \beta_3 \right), \quad (5.40)$$

$$\beta^- = 4 \left(\beta_1 - \frac{i}{2} \beta_2 - \beta_3 \right), \quad (5.41)$$

$$\tilde{\beta} = 4 \left(\beta_1 + \beta_3 \right). \quad (5.42)$$

Note that if we do not allow the parity-odd coupling ($\beta_2 = 0$), then the coefficient of the all-plus and all-minus amplitudes are the same $\beta^+ = \beta^- := \beta$.

Let us now take the on-shell approach to finding the tree-level amplitudes. We begin by noting that the coupling constant of the four-point amplitude has two powers of κ ($[\kappa] = -1$) and it is proportional to the coupling constant of the R^4 interaction β ($[\beta] = -6$). Furthermore, the nature of the new interaction implies that the four-point amplitude is just a contact term. Mass dimension and scaling under little-group

transformations fix the form of the possible amplitudes completely:

$$\mathcal{A}_{R^4}^{(0)}(1^{++}, 2^{++}, 3^{++}, 4^{++}) \sim i\beta \left(\frac{\kappa}{2}\right)^2 \tilde{\lambda}_1^{\otimes 4} \tilde{\lambda}_2^{\otimes 4} \tilde{\lambda}_3^{\otimes 4} \tilde{\lambda}_4^{\otimes 4}, \quad (5.43)$$

$$\mathcal{A}_{R^4}^{(0)}(1^{++}, 2^{++}, 3^{++}, 4^{--}) = 0, \quad (5.44)$$

$$\mathcal{A}_{R^4}^{(0)}(1^{++}, 2^{++}, 3^{--}, 4^{--}) \sim i\tilde{\beta} \left(\frac{\kappa}{2}\right)^2 \tilde{\lambda}_1^{\otimes 4} \tilde{\lambda}_2^{\otimes 4} \lambda_3^{\otimes 4} \lambda_4^{\otimes 4}. \quad (5.45)$$

Here the $\tilde{\lambda}_i^{\otimes 4}$ and $\lambda_i^{\otimes 4}$ schematically describe the dependence of the amplitude on the spinors: each spinor appears four times and upon taking linear combinations of appropriate pairwise contractions of the spinors gives the desired result. Notice that here the form of the kinematics is entirely fixed by the mass-dimension of the operator (which fixes the dimension of the couplings) combined with the constraints coming from the mass-dimension of the four-point amplitude and the little-group properties which constrain the minimum number of spinors for each external particles. The only freedom we have left is how to contract the spinors among each other, which needs to be done in such a way that Bose-symmetry is satisfied in the final result. For the MHV amplitude (5.45) there is only one possible structure, and we define the corresponding amplitude as

$$\mathcal{A}_{R^4}^{(0)}(1^{++}, 2^{++}, 3^{--}, 4^{--}) = i\tilde{\beta} \left(\frac{\kappa}{2}\right)^2 [12]^4 [34]^4. \quad (5.46)$$

On the other hand, we can now introduce the convenient variables

$$a := [12][34], \quad b := -[13][24], \quad c := [14][23], \quad (5.47)$$

in terms of which the all-plus amplitude can be written in such a way that permutation invariance is manifest. By saturating the spinor indices of (5.43) with the Levi-Civita tensor in all possible ways one gets four distinct combinations:

$$\mathcal{A}_{R^4}^{(0)}(1^{++}, 2^{++}, 3^{++}, 4^{++}) = i\beta \left(\frac{\kappa}{2}\right)^2 \begin{cases} a^4 + b^4 + c^4 \\ a^2 b^2 + a^2 c^2 + b^2 c^2 \\ a^3 b + a b^3 + a^3 c + a c^3 + b^3 c + b c^3 \\ a^2 b c + a b^2 c + a b c^2. \end{cases} \quad (5.48)$$

However, using the Schouten identity, which in terms of these variables reads

$$a + b + c = 0, \quad (5.49)$$

one can show that there is actually only one independent combination, which we will

take to be the first of (5.48). We will then define the all-plus amplitude to be

$$\mathcal{A}_{R^4}^{(0)}(1^{++}, 2^{++}, 3^{++}, 4^{++}) = i\beta \left(\frac{\kappa}{2}\right)^2 \left([12]^4 [34]^4 + [13]^4 [24]^4 + [14]^4 [23]^4 \right). \quad (5.50)$$

In the presence of a parity-invariant theory, the amplitude corresponding to (5.50) with all helicities flipped is simply obtained by replacing $[ji] \rightarrow \langle ij \rangle$, otherwise it should be considered to have an independent normalisation.

Now that we have the tree-level building blocks we can compute the one-loop amplitudes in the eikonal approximation, as done in previous sections. The relevant results are

$$\begin{aligned} \mathcal{A}_{R^4}^{(1)}(1^\phi, 2^\phi, 3^{--}, 4^{++}) &\simeq -\mathcal{N}_h \tilde{\beta} \left(\frac{\kappa}{2}\right)^4 s^2 \left[\frac{35}{4} (m\omega)^4 I_3(s; m) + \frac{93}{8} (m\omega^2)^2 I_2(s) \right], \\ \mathcal{A}_{R^4}^{(1)}(1^\phi, 2^\phi, 3^{++}, 4^{++}) &\simeq -\beta^+ \left(\frac{\kappa}{2}\right)^4 [34]^4 \left[\frac{3}{4} (m\omega)^4 I_3(s; m) + \frac{55}{24} (m\omega^2)^2 I_2(s) \right], \\ \mathcal{A}_{R^4}^{(1)}(1^\phi, 2^\phi, 3^{--}, 4^{--}) &\simeq -\beta^- \left(\frac{\kappa}{2}\right)^4 \langle 34 \rangle^4 \left[\frac{3}{4} (m\omega)^4 I_3(s; m) + \frac{55}{24} (m\omega^2)^2 I_2(s) \right], \end{aligned} \quad (5.51)$$

where \mathcal{N}_h was introduced in (5.26).

5.2.4 Scattering with the *FFR* interaction

The last interaction we wish to consider is the *FFR* term in (5.2). From an on-shell point of view this is the simplest non-minimal modification of the coupling of photons to gravity. As we will show below this leads to new corrections to the bending and time delay/advance of light and graviton propagation in the background of a very massive scalar particle, which mimics a charged black hole when viewed from a distance.

This new interaction modifies the three-point two-photon/one-graviton amplitude:

$$\mathcal{A}_{\text{FFR}}^{(0)}(1^+, 2^+, 3^{++}) = i \left(\frac{\kappa}{2}\right) \left(\frac{\alpha\gamma}{4}\right) [13]^2 [23]^2, \quad (5.52)$$

which we will now use to construct the relevant amplitudes at tree level and one loop to compute deflection angles and time delay in the presence of this interaction. Note that this amplitude is determined once again by its helicity structure and dimensional analysis up to a normalisation which we fixed in order to match the Feynman rule (B.7) following from our action (5.2).

Relevant amplitudes for graviton deflection

Using factorisation and Feynman diagrams we have computed the four-point amplitudes relevant for graviton deflection from a massive *charged* source (such as a charged black hole). The new *FFR* interaction involves two photons and one graviton, hence

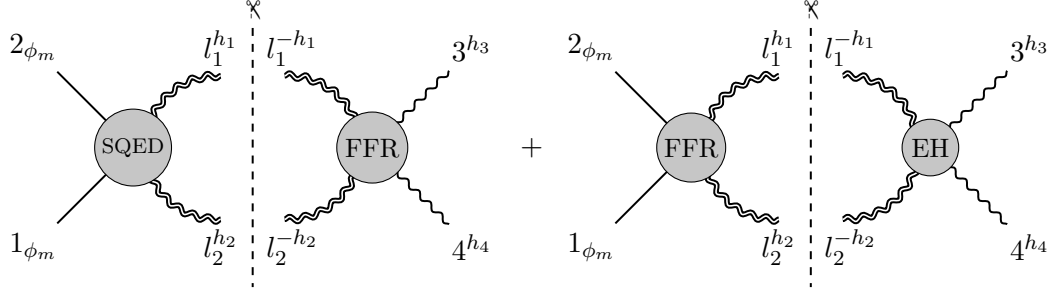


Figure 5.2: The two-particle cut diagrams in the $s = -\vec{q}^2$ -channel of the graviton deflection angle in the presence of an FFR interaction. The internal lines are photons. The first diagram is proportional to $\kappa^2 e^2$ and is only non-vanishing for $h_1 = h_2$ for the internal photons. The second diagram is proportional to κ^4 , it is non-vanishing when $h_4 = -h_3$ and $h_2 = -h_1$ thus it contributes solely to the helicity-preserving configuration. Also, it only produces quantum corrections (bubble integrals) with coefficients that vanish in the case of four-dimensional external kinematics.

one cannot generate a tree-level correction to the amplitude with two scalars and two gravitons. The first corrections arise at one loop, from the cut diagrams in Figure 5.2.

For the cut diagram on the left-hand side of the figure, we need the tree-level scalar QED amplitude with two photons and two massive scalars [23]

$$\mathcal{A}_{\text{SQED}}^{(0)}(1^\phi, 2^\phi, 3^+, 4^+) = Q^2 m^2 \frac{[34]^2}{s} \left(\frac{i}{t - m^2} + \frac{i}{u - m^2} \right), \quad (5.53)$$

along with the modification to the two-graviton/two-photon amplitudes arising from the FFR coupling for both helicity configurations of the graviton

$$\mathcal{A}_{\text{FFR}}^{(0)}(1^+, 2^+, 3^{--}, 4^{++}) = -i \left(\frac{\kappa}{2} \right)^2 \left(\frac{\alpha_\gamma}{4} \right) [12]^2 \frac{\langle 3|1|4 \rangle^4}{stu}, \quad (5.54)$$

and

$$\mathcal{A}_{\text{FFR}}^{(0)}(1^+, 2^+, 3^{++}, 4^{++}) = i \left(\frac{\kappa}{2} \right)^2 \left(\frac{\alpha_\gamma}{4} \right) \left(\frac{[13]^2 [34]^2 [42]^2}{s_{13}} + \frac{[23]^2 [34]^2 [41]^2}{s_{23}} \right). \quad (5.55)$$

Both amplitudes can be computed with on-shell techniques. Specifically, (5.54) can be constructed using BCFW recursion relations [13] by shifting appropriately the graviton momenta, while it is easy to verify [155] that (5.55) can be derived via an (holomorphic) all-line shift.

Note that the cut is non-vanishing only in the singlet configuration (internal photons with the same helicities). This is because the four-point amplitude with two photons and two gravitons induced by the FFR interaction is non-vanishing only for same-helicity photons.

We now move to the cut diagram on the right-hand side of Figure 5.2. The two-

photon/two-graviton EH amplitude only exists in the configuration where the gravitons and the photons have opposite helicity (see for instance [285]),

$$\mathcal{A}_{\text{EH}}^{(0)}(1^+, 2^-, 3^{++}, 4^{--}) = -i \left(\frac{\kappa}{2}\right)^2 [13]^2 \langle 24 \rangle^2 \frac{\langle 4|1|3 \rangle^2}{stu}, \quad (5.56)$$

and thus it contributes only in the helicity-preserving process. Hence, in order to compute the cut we will only need the following two-scalar/two-photon amplitude involving an FFR interaction:

$$\mathcal{A}_{\text{FFR}}^{(0)}(1^\phi, 2^\phi, 3^-, 4^+) = -i \left(\frac{\kappa}{2}\right)^2 \left(\frac{\alpha_\gamma}{4}\right) \langle 3|1|4 \rangle^2. \quad (5.57)$$

Performing the calculation, it turns out that the right-hand side of Figure 5.2 does not produce any non-analytic term with an s -channel discontinuity when external kinematics are considered to be strictly four-dimensional.

Following the above considerations, the one-loop amplitudes in the eikonal limit can be computed entirely from the LHS of Figure 5.2, and are found to be

$$\begin{aligned} \mathcal{A}_{\text{FFR}}^{(1)}(1^\phi, 2^\phi, 3^{--}, 4^{++}) &\simeq -\mathcal{N}_h Q^2 \left(\frac{\kappa}{2}\right)^2 \left(\frac{\alpha_\gamma}{4}\right) s \left[(ms)^2 (I_4(s, t; m) + I_4(s, u; m)) \right. \\ &\quad \left. + (m\omega)^2 I_3(s; m) + \frac{3}{4} \frac{s^3}{\omega^2} I_3(s) + \frac{3}{2} \omega^2 I_2(s) \right], \\ \mathcal{A}_{\text{FFR}}^{(1)}(1^\phi, 2^\phi, 3^{++}, 4^{++}) &= Q^2 \left(\frac{\kappa}{2}\right)^2 \left(\frac{\alpha_\gamma}{4}\right) m^2 [34]^4 I_3(s; m), \end{aligned} \quad (5.58)$$

where again \mathcal{N}_h is the phase defined in (5.26), and Q denotes the charge of the classical source (the black hole).

Relevant amplitudes for photon deflection

It is interesting to study how this new FFR interaction affects the bending and time delay/advance of light. In order to do so, we now review the known two-scalar/two-photon amplitudes for minimally coupled photons [285], and present the new corresponding amplitudes induced by the FFR interaction, both at tree and one-loop level.

In the following we consider processes where the internal legs are gravitons. In the EH theory, for the two-photon two-scalar process, only the helicity-preserving amplitude is

non vanishing⁸, both at tree level

$$\mathcal{A}_{\text{EH}}^{(0)}(1^\phi, 2^\phi, 3^-, 4^+) = i \left(\frac{\kappa}{2}\right)^2 \frac{\langle 3|1|4 \rangle^2}{s}, \quad (5.59)$$

and at one loop [285],

$$\begin{aligned} \mathcal{A}_{\text{EH}}^{(1)}(1^\phi, 2^\phi, 3^-, 4^+) \simeq & -\mathcal{N}_\gamma \left(\frac{\kappa}{2}\right)^4 \left[(2m\omega)^4 (I_4(s, t; m) + I_4(s, u; m)) - 15(m^2\omega)^2 I_3(s; m) \right. \\ & \left. + 3s(2m\omega)^2 I_3(s) - \frac{161}{30}(m\omega)^2 I_2(s) \right], \end{aligned} \quad (5.60)$$

where the phase factor \mathcal{N}_γ is

$$\mathcal{N}_\gamma = \left(\frac{\langle 3|1|4 \rangle}{2m\omega}\right)^2 \simeq -1. \quad (5.61)$$

We now discuss the corrections to the two-scalar two-photon amplitudes arising from one insertion of the *FFR* interaction. These come from a single graviton exchange between a minimally coupled scalar and the *FFR* three-point vertex. At tree level, only the helicity-flip amplitude

$$\mathcal{A}_{\text{FFR}}^{(0)}(1^\phi, 2^\phi, 3^+, 4^+) = -i \left(\frac{\kappa}{2}\right)^2 \left(\frac{\alpha_\gamma}{4}\right) [34]^2 \left[\frac{(t-m^2)(u-m^2)}{s} + m^2 \right], \quad (5.62)$$

contributes in the eikonal approximation, while the no-flip amplitude, already quoted in (5.57), is a contact term that is subleading in the eikonal limit (it does not have a pole in $s = -|\vec{q}|^2$).

Moving to one loop, the relevant two-particle cuts for the $(++)$ configuration are shown in Figure 5.3. We find that the amplitude with photons in the $(++)$ helicity configuration in the eikonal approximation is

$$\begin{aligned} \mathcal{A}_{\text{FFR}}^{(1)}(1^\phi, 2^\phi, 3^+, 4^+) \simeq & -\left(\frac{\kappa}{2}\right)^4 \left(\frac{\alpha_\gamma}{4}\right) [34]^2 \left[(2m\omega)^4 (I_4(s, t; m) + I_4(s, u; m)) \right. \\ & - 15(m^2\omega)^2 I_3(s; m) + 3s(2m\omega)^2 I_3(s) \\ & \left. + \frac{3}{10}(m\omega)^2 I_2(s) \right], \end{aligned} \quad (5.63)$$

⁸Indeed, one can check that in four dimensions the Feynman rule for two same-helicity (on-shell) photons and one off-shell graviton h is zero: $V^{\mu\nu}(1^\pm, 2^\pm, 3^h) = 0$, where $V^{\mu\nu}$ is given in (B.6).

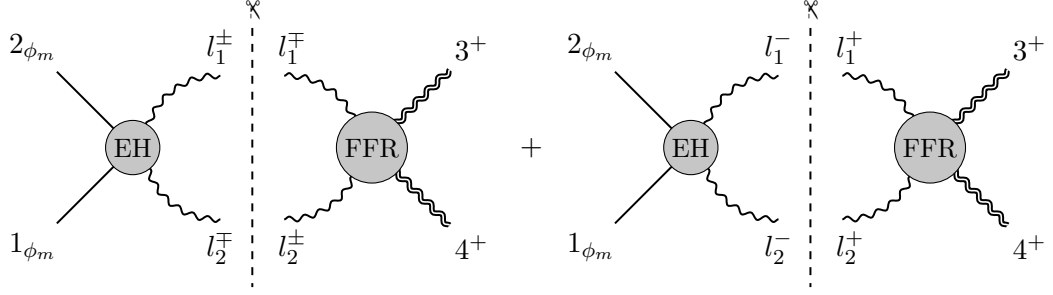


Figure 5.3: The two-particle cut diagrams in the $s = -|\vec{q}|^2$ -channel contributing to photon deflection to first order in the FFR interaction. We only show the helicity-flip configuration since the helicity-preserving cuts vanish. The cut diagram on the RHS of the figure only contributes terms which are subleading in the eikonal limit.

while the amplitude with photons in the $(+-)$ helicity configuration vanishes:

$$\mathcal{A}_{FFR}^{(1)}(1^\phi, 2^\phi, 3^-, 4^+) = 0. \quad (5.64)$$

5.3 Eikonal phase matrix, deflection angle and time delay

In the previous section we have derived the relevant tree and one-loop amplitudes which we will now use to extract the deflection angle and time delay up to 2PM order (or $\mathcal{O}(G^2)$) generated by the addition of the various couplings in (5.2). The key quantity is the eikonal phase matrix δ , to be introduced below, of which we will compute the leading, δ_0 , and subleading contributions, δ_1 . As an important consistency check we will confirm that the leading-energy contribution of the one-loop amplitudes captures the required exponentiation of the leading-order eikonal phase matrix δ_0 .

In the following we focus on the classical contribution to δ . We stress that for the cases we consider, δ will be a 2×2 matrix: the diagonal entries correspond to the two amplitudes $\mathcal{A}(1^\phi, 2^\phi, 3^{h_1}, 4^{h_2})$ where the helicity of the massless particle is not flipped (which in our all-outgoing convention corresponds to $h_1 = -h_2$), while the off-diagonal ones correspond to the two helicity-flip processes (with $h_1 = h_2$).

As a final comment, we note that the combined effect of the interactions in (5.2) is simply the sum of the contributions of each interaction treated independently; hence we will study them separately, and begin our discussion by reviewing the computation in EH gravity.

5.3.1 Graviton deflection angle and time delay in EH gravity

Leading eikonal

The relevant tree-level amplitudes in EH gravity are given in (5.24). In the eikonal approximation (5.10) they become

$$\begin{aligned}\mathcal{A}_{\text{EH}}^{(0)}(1^\phi, 2^\phi, 3^{--}, 4^{++}) &\simeq i \left(\frac{\kappa}{2}\right)^2 \frac{(2m\omega)^2}{\vec{q}^2}, \\ \mathcal{A}_{\text{EH}}^{(0)}(1^\phi, 2^\phi, 3^{++}, 4^{++}) &\simeq i \left(\frac{\kappa}{2}\right)^2 \frac{m^2}{(2\omega)^2} \frac{q^4}{\vec{q}^2} \simeq 0,\end{aligned}\tag{5.65}$$

where the second amplitude is subleading compared to the first.

The amplitudes in impact parameter space are obtained from those in momentum space using (5.15). To compute them, we will use repeatedly the result

$$f(p, d) := \int \frac{d^d q}{(2\pi)^d} e^{i\vec{q}\cdot\vec{b}} |\vec{q}|^p = \frac{2^p \pi^{-d/2} \Gamma\left(\frac{d+p}{2}\right)}{\Gamma\left(-\frac{p}{2}\right)} \frac{1}{b^{d+p}},\tag{5.66}$$

where $b := |\vec{b}|$. We then have

$$\begin{aligned}\tilde{\mathcal{A}}_{\text{EH}}^{(0)}(1^\phi, 2^\phi, 3^{--}, 4^{++})\Big|_\omega &= i \left(\frac{\kappa}{2}\right)^2 \frac{m\omega}{4\pi^{\frac{D-2}{2}}} \Gamma\left(\frac{D}{2} - 2\right) \frac{1}{b^{D-4}}, \\ \tilde{\mathcal{A}}_{\text{EH}}^{(0)}(1^\phi, 2^\phi, 3^{++}, 4^{++})\Big|_\omega &= 0,\end{aligned}\tag{5.67}$$

therefore the leading eikonal phase matrix is

$$\delta_{0,\text{EH}} = \left(\frac{\kappa}{2}\right)^2 (m\omega) f(-2, D-2) \mathbb{1}_2 \simeq - \left(\frac{\kappa}{2}\right)^2 \frac{m\omega}{2\pi} \left[\frac{1}{4-D} + \log b \right] \mathbb{1}_2 + \dots,\tag{5.68}$$

where we omitted terms of $\mathcal{O}(D-4)$ and finite terms which do not depend on \vec{b} .

Next we consider the one-loop amplitudes (5.25) and (5.27). In order to check exponentiation (5.21) we only keep terms that are leading in energy in the eikonal approximation, *i.e.* $\mathcal{O}(\omega^3)$ in momentum space (or $\mathcal{O}(\omega^2)$ in impact parameter space). These are

$$\begin{aligned}\mathcal{A}_{\text{EH}}^{(1)}(1^\phi, 2^\phi, 3^{--}, 4^{++})\Big|_{\omega^3} &= \left(\frac{\kappa}{2}\right)^4 (2m\omega)^4 \left[I_4(s, t; m) + I_4(s, u; m) \right], \\ \mathcal{A}_{\text{EH}}^{(1)}(1^\phi, 2^\phi, 3^{++}, 4^{++})\Big|_{\omega^3} &= 0,\end{aligned}\tag{5.69}$$

where the sum of the box integrals $I_4(s, t; m) + I_4(s, u; m)$ was evaluated in D dimensions

in [321] and is given in (B.4). Transforming to impact parameter space, we have

$$\tilde{\mathcal{A}}_{\text{EH}}^{(1)}(1^\phi, 2^\phi, 3^{--}, 4^{++})\Big|_{\omega^2} = -\left(\frac{\kappa}{2}\right)^4 (m\omega)^2 \frac{2^{D-7}\Gamma(D-4)}{\pi^{\frac{D}{2}}(D-4)\Gamma(3-D/2)} \frac{1}{b^{2D-8}}. \quad (5.70)$$

As expected from (5.21), we find that

$$\tilde{\mathcal{A}}_{\text{EH}}^{(1)}(1^\phi, 2^\phi, 3^{--}, 4^{++})\Big|_{\omega^2} = \frac{1}{2} \left[\tilde{\mathcal{A}}_{\text{EH}}^{(0)}(1^\phi, 2^\phi, 3^{--}, 4^{++})\Big|_{\omega} \right]^2 + \mathcal{O}(D-4). \quad (5.71)$$

Subleading eikonal

In momentum space, the subleading contribution to the eikonal phase matrix is extracted from the $\mathcal{O}(\omega^2)$ contribution to the amplitude in (5.25):⁹

$$\mathcal{A}_{\text{EH}}^{(1)}(1^\phi, 2^\phi, 3^{--}, 4^{++})\Big|_{\omega^2} = \left(\frac{\kappa}{2}\right)^4 (-15 m^4 \omega^2) I_3(s; m), \quad (5.72)$$

where $I_3(s; m)$ is given in (B.3), and as usual $s = -|\vec{q}|^2$. In the following we focus on the first term on the right-hand side of (B.3), since the log term only contributes quantum corrections. Using

$$\int \frac{d^{D-2}q}{(2\pi)^{D-2}} e^{i\vec{q}\cdot\vec{b}} |\vec{q}|^{-1} = \frac{1}{2\pi} \frac{1}{b} + \mathcal{O}(D-4), \quad (5.73)$$

we obtain the subleading part of the amplitude in impact parameter space:

$$\tilde{\mathcal{A}}_{\text{EH}}^{(1)}(1^\phi, 2^\phi, 3^{--}, 4^{++})\Big|_{\omega} = i \left(\frac{\kappa}{2}\right)^4 \frac{15}{256\pi} \frac{m^2\omega}{b}, \quad (5.74)$$

and finally, using (5.19), δ_1 :

$$\delta_{1,\text{EH}} = \left(\frac{\kappa}{2}\right)^4 \frac{15}{256\pi} \frac{m^2\omega}{b} \mathbb{1}_2. \quad (5.75)$$

The eikonal phase matrix up to one loop in EH is then given by

$$\delta_{\text{EH}} = \delta_{0,\text{EH}} + \delta_{1,\text{EH}} + \dots = -\left(\frac{\kappa}{2}\right)^2 \frac{m\omega}{2\pi} \left[\frac{1}{4-D} + \log b - \left(\frac{\kappa}{2}\right)^2 \frac{15}{256\pi} \frac{m}{b} \right] \mathbb{1}_2 + \dots \quad (5.76)$$

Note that this matrix is proportional to the identity, since the polarisation of the gravitons scattered by the classical source is unchanged. The deflection angle can now be extracted using (5.22). While the eigenvalues of δ are divergent in $D = 4$, the

⁹Note that such a contribution is absent in (5.27).

corresponding deflection angle is finite:

$$\theta_{\text{EH}} = -\frac{1}{2\pi} \left(\frac{\kappa}{2}\right)^2 \frac{m}{b} \left[1 + \left(\frac{\kappa}{2}\right)^2 \frac{15}{128} \frac{m}{b}\right] = -\frac{4Gm}{b} \left(1 + G\frac{15\pi m}{16b}\right). \quad (5.77)$$

This result agrees with the derivation of [292], and as expected matches the photon deflection angle [290, 285], first computed by Einstein.¹⁰

Another quantity of interest which can be extracted from the eigenvalues of the eikonal matrix is the time delay. Using (5.23) applied to the leading eikonal phase (5.68), we get

$$t_{\text{EH}} = -\left(\frac{\kappa}{2}\right)^2 \frac{m}{2\pi} \left(\frac{1}{4-D} + \log b\right). \quad (5.78)$$

As is well known, in order to define the time delay in four dimensions we need to take the difference of two time delays as measured by an observer at b and one at a much larger distance $b_0 \gg b$ [297]. Doing so the pole in (5.78) drops out, and neglecting power-suppressed terms in b_0 one gets

$$t_{\text{EH}} = \left(\frac{\kappa}{2}\right)^2 \frac{m}{2\pi} \log \frac{b_0}{b} = 4Gm \log \frac{b_0}{b}, \quad (5.79)$$

in agreement with [327]. Including now also the contribution from δ_1 , we arrive at the result

$$t_{\text{EH}} = \left(\frac{\kappa}{2}\right)^2 \frac{m}{2\pi} \left[\log \frac{b_0}{b} + \left(\frac{\kappa}{2}\right)^2 \frac{15}{128} \frac{m}{b}\right] = 4Gm \left[\log \frac{b_0}{b} + G\frac{15\pi m}{16b}\right]. \quad (5.80)$$

In the next sections we compute the corrections $\Delta\theta_X$ and Δt_X to the deflection angle (5.77) and time delay (5.79) in EH due to the inclusion of an interaction X in (5.2). The complete deflection angle and time delay will then be $\theta_{\text{EH}} + \Delta\theta_X$ and $t_{\text{EH}} + \Delta t_X$.

5.3.2 Graviton deflection angle and time delay in EH + R^3

Leading eikonal

The relevant new amplitudes are obtained by evaluating (5.28) and (5.29) in the eikonal limit (5.10), with the result

$$\begin{aligned} \mathcal{A}_{R^3}^{(0)}(1^\phi, 2^\phi, 3^{--}, 4^{++}) &= 0, \\ \mathcal{A}_{R^3}^{(0)}(1^\phi, 2^\phi, 3^{++}, 4^{++}) &\simeq i \left(\frac{\kappa}{2}\right)^2 \left(\frac{\alpha'}{4}\right)^2 (2m\omega)^2 \frac{q^4}{\bar{q}^2}, \end{aligned} \quad (5.81)$$

¹⁰Initially up to a factor of two [326].

where from (5.13) we have $[34]^4 = q^4$. In order to transform to impact parameter space we rewrite

$$\vec{b} \cdot \vec{q} = \mathfrak{b} \bar{q} + \bar{\mathfrak{b}} q, \quad (5.82)$$

with $\mathfrak{b} := (b_1 + ib_2)/2$, and $\bar{\mathfrak{b}} := (b_1 - ib_2)/2$ (and we recall our previous definitions $q = q_1 + iq_2$, $\bar{q} = q_1 - iq_2$), from which $\mathfrak{b} \bar{\mathfrak{b}} = b^2/4$. Then in \vec{b} -space we have

$$\begin{aligned} \tilde{\mathcal{A}}_{R^3}^{(0)}(1^\phi, 2^\phi, 3^{++}, 4^{++}) \Big|_\omega &= i \left(\frac{\kappa}{2}\right)^2 \left(\frac{\alpha'}{4}\right)^2 (m\omega) \left(\frac{\partial}{\partial \bar{\mathfrak{b}}}\right)^4 f(-2, D-2) \\ &= i \left(\frac{\kappa}{2}\right)^2 \left(\frac{\alpha'}{4}\right)^2 \frac{(m\omega)}{\bar{\mathfrak{b}}^4} \xi f(-2, D-2), \end{aligned} \quad (5.83)$$

where

$$\xi := \left(\frac{D}{2} - 2\right) \left(\frac{D}{2} - 1\right) \left(\frac{D}{2}\right) \left(\frac{D}{2} + 1\right). \quad (5.84)$$

Hence the leading eikonal phase matrix δ_0 , including the first contribution from the R^3 interaction, has the form

$$\delta_0 = \delta_{0,\text{EH}} + \delta_{0,R^3}, \quad (5.85)$$

where $\delta_{0,\text{EH}}$ is given in (5.68), and

$$\delta_{0,R^3} = \left(\frac{\kappa}{2}\right)^2 \left(\frac{\alpha'}{4}\right)^2 (m\omega) [\xi f(-2, D-2)] \begin{pmatrix} 0 & \bar{\mathfrak{b}}^{-4} \\ \mathfrak{b}^{-4} & 0 \end{pmatrix}, \quad (5.86)$$

where we have used (5.18).

Moving on to one loop, from (5.30) and (5.31) we obtain

$$\begin{aligned} \mathcal{A}_{R^3}^{(1)}(1^\phi, 2^\phi, 3^{--}, 4^{++}) \Big|_{\omega^3} &= 0, \\ \mathcal{A}_{R^3}^{(1)}(1^\phi, 2^\phi, 3^{++}, 4^{++}) \Big|_{\omega^3} &= \left(\frac{\kappa}{2}\right)^4 \left(\frac{\alpha'}{4}\right)^2 [34]^4 (2m\omega)^4 [I_4(s, t) + I_4(s, u)]. \end{aligned} \quad (5.87)$$

Transforming to impact parameter space, and using (B.4), we arrive at

$$\begin{aligned} \tilde{\mathcal{A}}_{R^3}^{(1)}(1^\phi, 2^\phi, 3^{++}, 4^{++}) \Big|_{\omega^2} &= - \left(\frac{\kappa}{2}\right)^4 \left(\frac{\alpha'}{4}\right)^2 \frac{(m\omega)^2}{2\pi} \frac{1}{D-4} \left(\frac{\partial}{\partial \bar{\mathfrak{b}}}\right)^4 f(D-6, D-2) \\ &= - \left(\frac{\kappa}{2}\right)^4 \left(\frac{\alpha'}{4}\right)^2 \frac{(m\omega)^2}{2\pi \bar{\mathfrak{b}}^4} \frac{\xi'}{D-4} f(D-6, D-2), \end{aligned} \quad (5.88)$$

where

$$\xi' := (D-4)(D-3)(D-2)(D-1). \quad (5.89)$$

The leading one-loop amplitude matrix in the eikonal approximation is then found to

be

$$\mathcal{A}_{\omega^2}^{(1)} = -\left(\frac{\kappa}{2}\right)^4 (m\omega)^2 \frac{f(D-6, D-2)}{2\pi(D-4)} \begin{pmatrix} 1 & \left(\frac{\alpha'}{4}\right)^2 \frac{\xi'}{\ell^4} \\ \left(\frac{\alpha'}{4}\right)^2 \frac{\xi'}{\ell^4} & 1 \end{pmatrix}. \quad (5.90)$$

One can then check the matrix relation

$$\mathcal{A}_{\omega^2}^{(1)} = -\frac{1}{2}(\delta_0)^2 + \mathcal{O}(D-4), \quad (5.91)$$

in agreement with (5.21). In writing (5.91) we have used that,

$$(\delta_0)^2 = \left(\frac{\kappa}{2}\right)^4 (m\omega)^2 [f(-2, D-2)]^2 \begin{pmatrix} 1 & \left(\frac{\alpha'}{4}\right)^2 \frac{2\xi}{\ell^4} \\ \left(\frac{\alpha'}{4}\right)^2 \frac{2\xi}{\ell^4} & 1 \end{pmatrix}, \quad (5.92)$$

up to and including $\mathcal{O}((\alpha'/4)^2)$.

Finally we compute the eigenvalues of the matrix δ_0 in (5.85). Using

$$\xi f(-2, D-2) = \frac{3}{2\pi} + \mathcal{O}(D-4), \quad (5.93)$$

we can rewrite it as

$$\delta_0 = \left(\frac{\kappa}{2}\right)^2 \frac{m\omega}{2\pi} \begin{pmatrix} -\frac{1}{2\epsilon} - \log b & \left(\frac{\alpha'}{4}\right)^2 \frac{3}{\ell^4} \\ \left(\frac{\alpha'}{4}\right)^2 \frac{3}{\ell^4} & -\frac{1}{2\epsilon} - \log b \end{pmatrix}, \quad (5.94)$$

whose eigenvalues are

$$\delta_0^{(1,2)} = \left(\frac{\kappa}{2}\right)^2 \frac{m\omega}{2\pi} \left[-\frac{1}{2\epsilon} - \log b \pm \left(\frac{\alpha'}{4}\right)^2 \frac{48}{b^4} \right]. \quad (5.95)$$

Following identical steps to those leading from (5.76) to (5.80), one obtains for the time delay at $\mathcal{O}(G)$

$$t_{\text{EH}+R^3} = 4Gm \left[\log \frac{b_0}{b} \pm \left(\frac{\alpha'}{4}\right)^2 \frac{48}{b^4} \right], \quad (5.96)$$

where $G = \kappa^2/(32\pi)$. For sufficiently small b the eigenvalue with the choice of negative sign may become negative, leading to a time advance. We will come back to the time delay computation and add $\mathcal{O}(G^2)$ corrections in Section 5.3.2.

The time advance due to R^3 terms was first discovered in [297], from which it was

argued that the only way to avoid causality violations is to embed the R^3 theory into an appropriate ultraviolet completion – in other words a consistent ultraviolet completion of gravitational theories with an R^3 interaction requires the addition of an infinite tower of massive particles with higher spins. Here we wish to briefly compare our results to theirs.

The authors of [297] considered the interaction of a graviton with the background produced by a coherent state of massless particles, and computed the eikonal phase in order to obtain the Shapiro time delay. The coherent state simulates a large number of successive interactions of the graviton with a single weakly-coupled particle, each instance being considered as independent and contributing with a small amount to the total phase shift. It is then observed that the presence of the R^3 coupling, which modifies the three-point graviton amplitude, leads to non-degenerate eigenvalues of the eikonal phase matrix.

Concretely, it is interesting to compare the eigenvalues (5.95) of the leading eikonal phase matrix (5.85). These eigenvalues turn out to be identical¹¹ to the eigenvalues (3.22) of [297], upon replacing $m\omega \rightarrow \omega^2$. This is due to the fact that we consider a different setup, with massless gravitons moving in the background produced by massive scalar objects of mass m . In both cases the time advance is induced by the novel three-graviton coupling generated by the R^3 interaction.

Before moving on, it is important to stress that the possible time advance which one would observe for small enough values of b in (5.96) would lead to so called asymptotic superluminality [328–330]. While it seems a priori reasonable that in order to satisfy causality superluminal behaviour should be forbidden, this intuition needs to be treated carefully when dealing with curved spacetimes, and indeed it might even lead to contradictions with causality if applied indiscriminately [304, 331]. These subtleties had already been noticed for low-energy effective theory for QED in curved space-time, where group velocity of light is known to be superluminal for certain polarization states [332]. The resolution of the apparent contradiction is requiring superluminal behaviour, if present, to be non-resolvable (*i.e.* non measurable) within the limits of validity of the EFT, which allows to avoid conflicts with causality [333–335].

Subleading eikonal

We now go back to the one-loop amplitudes (5.30) and (5.31) and extract the triangle contributions which are the relevant terms contributing to the subleading eikonal

¹¹Note that in (3.22) of [297] the $1/\epsilon$ pole was not written explicitly. This pole does not affect either the time delay (5.96) or the particle bending angle. Our $1/\epsilon$ pole corresponds to the $\log L$ term in [297], where L is an infrared cutoff.

matrix:

$$\begin{aligned}\mathcal{A}_{R^3}^{(1)}(1^\phi, 2^\phi, 3^{--}, 4^{++})\Big|_{\omega^2} &= \left(\frac{\kappa}{2}\right)^4 \left(\frac{\alpha'}{4}\right)^2 |\vec{q}|^4 m^4 \omega^2 I_3(s; m), \\ \mathcal{A}_{R^3}^{(1)}(1^\phi, 2^\phi, 3^{++}, 4^{++})\Big|_{\omega^2} &= -13 \left(\frac{\kappa}{2}\right)^4 \left(\frac{\alpha'}{4}\right)^2 q^4 m^4 \omega^2 I_3(s; m).\end{aligned}\tag{5.97}$$

We can now transform to impact parameter space, using

$$\int \frac{d^{D-2}q}{(2\pi)^{D-2}} e^{i\vec{q}\vec{b}} |\vec{q}|^3 = \frac{9}{2\pi} \frac{1}{b^5} + \mathcal{O}(D-4),\tag{5.98}$$

$$\left(\frac{\partial}{\partial \vec{b}}\right)^4 \int \frac{d^{D-2}q}{(2\pi)^{D-2}} e^{i\vec{q}\vec{b}} |\vec{q}|^{-1} = \frac{105}{32\pi} \frac{1}{b} \frac{1}{\ell^4} + \mathcal{O}(D-4).\tag{5.99}$$

The amplitudes in impact parameter space then become

$$\begin{aligned}\tilde{\mathcal{A}}_{R^3}^{(1)}(1^\phi, 2^\phi, 3^{--}, 4^{++})\Big|_{\omega} &= -i \left(\frac{\kappa}{2}\right)^4 \left(\frac{\alpha'}{4}\right)^2 \frac{9}{256\pi} \frac{m^2\omega}{b^5}, \\ \tilde{\mathcal{A}}_{R^3}^{(1)}(1^\phi, 2^\phi, 3^{++}, 4^{++})\Big|_{\omega} &= i \left(\frac{\kappa}{2}\right)^4 \left(\frac{\alpha'}{4}\right)^2 \frac{1365}{4096\pi} \frac{m^2\omega}{b} \frac{1}{\ell^4}.\end{aligned}\tag{5.100}$$

Using (5.18), we can extract the contribution of the R^3 interaction to the subleading eikonal matrix δ_1 :

$$\delta_{1,R^3} = \left(\frac{\kappa}{2}\right)^4 \left(\frac{\alpha'}{4}\right)^2 \frac{1}{256\pi} \frac{m^2\omega}{b} \begin{pmatrix} -\frac{9}{b^4} & \frac{1365}{16} \frac{1}{\ell^4} \\ \frac{1365}{16} \frac{1}{\ell^4} & -\frac{9}{b^4} \end{pmatrix}.\tag{5.101}$$

Deflection angle and time delay

We can proceed similarly to the EH case. In the previous sections we showed that the R^3 interaction introduced off-diagonal terms, *i.e.* the helicity of the scattered graviton can change.

The eigenvalues of the leading and subleading eikonal matrices (5.86) and (5.101) are

$$\delta_{0,R^3}^{(1,2)} = \pm \left(\frac{\kappa}{2}\right)^2 \left(\frac{\alpha'}{4}\right)^2 \frac{24}{\pi} \frac{m\omega}{b^4},\tag{5.102}$$

$$\delta_{1,R^3}^{(1,2)} = \left(\frac{\kappa}{2}\right)^4 \left(\frac{\alpha'}{4}\right)^2 \frac{1}{256\pi} \frac{m^2\omega}{b^5} (-9 \pm 1365).\tag{5.103}$$

Next we present the correction to the graviton deflection angle, both in terms of κ and

G :

$$\begin{aligned}\Delta\theta_{R^3}^{(1,2)} &= -\frac{1}{2\pi} \left(\frac{\kappa}{2}\right)^2 \left(\frac{\alpha'}{4}\right)^2 \frac{m}{b} \left[\pm \frac{192}{b^4} + \frac{5}{128} (-9 \pm 1365) \left(\frac{\kappa}{2}\right)^2 \frac{m}{b^5} \right] \\ &= -\frac{4Gm}{b} \left(\frac{\alpha'}{4}\right)^2 \left[\pm \frac{192}{b^4} + \frac{5\pi}{16} (-9 \pm 1365) \frac{Gm}{b^5} \right].\end{aligned}\tag{5.104}$$

Finally, for the time delay, proceeding as in Section 5.3.1, and applying (5.23) to (5.102) and (5.103), we arrive at

$$\begin{aligned}\Delta t_{R^3}^{(1,2)} &= \left(\frac{\kappa}{2}\right)^2 \left(\frac{\alpha'}{4}\right)^2 \frac{m}{2\pi} \left[\pm 48 \frac{1}{b^4} + \left(\frac{\kappa}{2}\right)^2 \frac{1}{128} \frac{m}{b^5} (-9 \pm 1365) \right] \\ &= 4Gm \left(\frac{\alpha'}{4}\right)^2 \left[\pm 48 \frac{1}{b^4} + \frac{\pi}{16} (-9 \pm 1365) \frac{Gm}{b^5} \right].\end{aligned}\tag{5.105}$$

5.3.3 Graviton deflection angle and time delay in $\text{EH} + R^4$

In this section we consider the deflection of gravitons induced by eight-derivative couplings in the Lagrangian, which we collectively denote as R^4 . We will only consider the parity-even interactions in (5.5) in order to present more compact formulae, therefore we set $\beta_2 = 0$, and hence $\beta^+ = \beta^- = \beta$ in (5.39) and (5.51). Furthermore, since these interactions do not produce a three-graviton vertex, it is impossible to build any tree-level two-scalar two-graviton amplitude involving R^4 . Thus there is no tree-level (1PM) bending associated to the new term in the Lagrangian, and one has

$$\delta_{0,R^4} = 0, \tag{5.106}$$

and the leading contribution arises at 2PM order. Furthermore, since the R^4 term only produces a contact term four-graviton interaction, the resulting one-loop amplitude does not contain any box integral. This is consistent with the absence of a tree-level contribution in (5.106) which, in the eikonal approximation, is expected to exponentiate, and would result at one loop in the appearance of box integrals. The same situation occurs for the graviton deflection due to FFR couplings discussed in Section 5.3.4.

The relevant one-loop amplitudes are given in (5.51), and from the massive triangle contributions we extract the following results in the eikonal approximation:

$$\begin{aligned}\mathcal{A}_{R^4}^{(1)}(1^\phi, 2^\phi, 3^{--}, 4^{++})\Big|_{\omega^4} &= i \tilde{\beta} \left(\frac{\kappa}{2}\right)^4 \frac{35}{128} m^3 \omega^4 |\vec{q}|^3, \\ \mathcal{A}_{R^4}^{(1)}(1^\phi, 2^\phi, 3^{++}, 4^{++})\Big|_{\omega^4} &= i \beta \left(\frac{\kappa}{2}\right)^4 \frac{3}{128} m^3 \omega^4 \frac{q^4}{|\vec{q}|},\end{aligned}\tag{5.107}$$

which then translate in impact parameter space into

$$\begin{aligned}\tilde{\mathcal{A}}_{R^4}^{(1)}(1^\phi, 2^\phi, 3^{--}, 4^{++})\Big|_{\omega^3} &= i \tilde{\beta} \left(\frac{\kappa}{2}\right)^4 \frac{315}{512} \frac{m^2 \omega^3}{2\pi b^5}, \\ \tilde{\mathcal{A}}_{R^4}^{(1)}(1^\phi, 2^\phi, 3^{++}, 4^{++})\Big|_{\omega^3} &= i \beta \left(\frac{\kappa}{2}\right)^4 \frac{315}{512} \frac{m^2 \omega^3}{32\pi b} \frac{1}{\ell^4}.\end{aligned}\tag{5.108}$$

The subleading eikonal phase matrix resulting from the previous amplitudes is given by

$$\delta_{1,R^4} = \left(\frac{\kappa}{2}\right)^4 \frac{315}{512} \frac{m^2 \omega^3}{2\pi} \frac{1}{b} \begin{pmatrix} \tilde{\beta} \frac{1}{b^4} & \frac{\beta}{16} \frac{1}{\ell^4} \\ \frac{\beta}{16} \frac{1}{\ell^4} & \tilde{\beta} \frac{1}{b^4} \end{pmatrix},\tag{5.109}$$

whose eigenvalues are easily computed to be

$$\delta_{1,R^4}^{(1,2)} = (\tilde{\beta} \pm \beta) \left(\frac{\kappa}{2}\right)^4 \frac{315}{512} \frac{m^2 \omega^3}{2\pi} \frac{1}{b^5}.\tag{5.110}$$

Using (5.22) we can then extract the deflection angle

$$\Delta\theta_{R^4}^{(1,2)} = -(\tilde{\beta} \pm \beta) \left(\frac{\kappa}{2}\right)^4 \frac{1575}{512} \frac{m^2 \omega^2}{2\pi} \frac{1}{b^6} = -(\tilde{\beta} \pm \beta) (Gm)^2 \frac{1575\pi}{16} \frac{\omega^2}{b^6}.\tag{5.111}$$

Similarly to the EH and the R^3 interaction we can extract the time delay arising from the R^4 interaction in (5.2), which in this case arises entirely from the subleading eikonal phase. Applying (5.23) to (5.110) we find

$$\Delta t_{R^4}^{(1,2)} = (\tilde{\beta} \pm \beta) \left(\frac{\kappa}{2}\right)^4 \frac{945}{512} \frac{m^2 \omega^2}{2\pi} \frac{1}{b^5} = (\tilde{\beta} \pm \beta) (Gm)^2 \frac{945\pi}{16} \frac{\omega^2}{b^5}.\tag{5.112}$$

We can express (5.111) and (5.112) in terms of the couplings introduced in (5.5), using (5.40), (5.41) and (5.42). In the parity-even theory ($\beta_2 = 0$) we get $\beta + \tilde{\beta} = 8\beta_1$, and $\tilde{\beta} - \beta = 8\beta_3$. In order to avoid a potential time-advance and associated causality violation, we need to require

$$\beta_1 > 0 \quad \text{and} \quad \beta_3 > 0.\tag{5.113}$$

Interestingly this positivity constraint is the same as derived from causality considerations in [336] and general S -matrix analyticity properties in [337].

5.3.4 Graviton deflection angle and time delay in EH + FFR

Next we focus our attention on graviton deflection in EH theory with the addition of an FFR coupling. We remind the reader that the contributions computed here

add to the already presented Einstein-Hilbert part $\Delta\theta_{\text{EH}}$ and Δt_{EH} , see Section 5.3.1. As discussed in Section 5.2.4, at tree level there is no new two-scalar two-graviton amplitude generated by this interaction, hence

$$\delta_{0,\text{FFR}} = 0. \quad (5.114)$$

In order to compute the subleading eikonal phase matrix, we look at the massive triangle contribution to the one-loop amplitudes in (5.58),

$$\begin{aligned} \mathcal{A}_{\text{FFR}}^{(1)}(1^\phi, 2^\phi, 3^{--}, 4^{++}) \Big|_{\omega^2} &= -i Q^2 \left(\frac{\kappa}{2}\right)^2 \left(\frac{\alpha_\gamma}{4}\right) \frac{m\omega^2}{32} |\vec{q}|, \\ \mathcal{A}_{\text{FFR}}^{(1)}(1^\phi, 2^\phi, 3^{++}, 4^{++}) \Big|_{\omega^2} &= 0. \end{aligned} \quad (5.115)$$

Using

$$\int \frac{d^{D-2}q}{(2\pi)^{D-2}} e^{i\vec{q}\cdot\vec{b}} |\vec{q}| = -\frac{1}{2\pi} \frac{1}{b^3} + \mathcal{O}(D-4), \quad (5.116)$$

we obtain

$$\begin{aligned} \tilde{\mathcal{A}}_{\text{FFR}}^{(1)}(1^\phi, 2^\phi, 3^{--}, 4^{++}) \Big|_{\omega} &= i Q^2 \left(\frac{\kappa}{2}\right)^2 \left(\frac{\alpha_\gamma}{4}\right) \frac{\omega}{256\pi} \frac{1}{b^3}, \\ \tilde{\mathcal{A}}_{\text{FFR}}^{(1)}(1^\phi, 2^\phi, 3^{++}, 4^{++}) \Big|_{\omega} &= 0, \end{aligned} \quad (5.117)$$

In this case the eikonal phase matrix is diagonal and the subleading contribution $\delta_{1,\text{FFR}}$ is immediately seen to be

$$\delta_{1,\text{FFR}} = Q^2 \left(\frac{\kappa}{2}\right)^2 \left(\frac{\alpha_\gamma}{4}\right) \frac{\omega}{256\pi} \frac{1}{b^3} \mathbf{1}_2. \quad (5.118)$$

The new contribution to the graviton deflection angle due to the *FFR* interaction is then obtained using (5.22):

$$\Delta\theta_{\text{FFR}} = -Q^2 \left(\frac{\kappa}{2}\right)^2 \left(\frac{\alpha_\gamma}{4}\right) \frac{3}{256\pi} \frac{1}{b^4} = -Q^2 G \left(\frac{\alpha_\gamma}{4}\right) \frac{3}{32} \frac{1}{b^4}. \quad (5.119)$$

Applying (5.23) to (5.118) we find the additional contribution to the time delay associated to the bending of a graviton in the *FFR* theory:

$$\Delta t_{\text{FFR}} = Q^2 \left(\frac{\kappa}{2}\right)^2 \left(\frac{\alpha_\gamma}{4}\right) \frac{1}{256\pi} \frac{1}{b^3} = Q^2 G \left(\frac{\alpha_\gamma}{4}\right) \frac{1}{32} \frac{1}{b^3}. \quad (5.120)$$

The bending in this case is due to the electric charge Q of the black hole, not to its mass, which does not appear in either (5.119) or (5.120). We conclude that in order to avoid possible causality violation due to time advance, in the regime of validity of the

EFT and thus up to corrections arising at higher energies, the coefficient of the FFR interaction must obey the positivity constraint

$$\alpha_\gamma > 0. \quad (5.121)$$

5.3.5 Photon deflection angle and time delay in EH + FFR

In this section we consider the photon deflection angle and the time delay/advance arising from the FFR interaction. Compared to the case of graviton bending considered in the previous section, there is a non-vanishing tree-level contribution to the deflection, thus we consider the leading and subleading eikonal cases separately.

Leading eikonal

The first contribution we consider arises from the EH tree-level amplitude (5.59), which in the eikonal approximation becomes¹²

$$\mathcal{A}_{\text{EH}}^{(0)}(1^\phi, 2^\phi, 3^-, 4^+) \simeq i \left(\frac{\kappa}{2}\right)^2 \frac{(2m\omega)^2}{\vec{q}^2}, \quad (5.122)$$

or, upon transforming to impact parameter,

$$\tilde{\mathcal{A}}_{\text{EH}}^{(0)}(1^\phi, 2^\phi, 3^-, 4^+) \simeq i \left(\frac{\kappa}{2}\right)^2 m\omega f(-2, D-2). \quad (5.123)$$

Note that (5.122) has the same form as the two-scalar two-graviton amplitude in the eikonal approximation, first equation in (5.65), as a consequence of the equivalence principle.

At tree-level the helicity-preserving FFR amplitude (5.57) is purely a contact term, while the helicity-flip amplitude is given in (5.62). The leading contribution in the eikonal limit is then

$$\begin{aligned} \mathcal{A}_{\text{FFR}}^{(0)}(1^\phi, 2^\phi, 3^-, 4^+) &\simeq 0, \\ \mathcal{A}_{\text{FFR}}^{(0)}(1^\phi, 2^\phi, 3^+, 4^+) &\simeq i \left(\frac{\kappa}{2}\right)^2 \left(\frac{\alpha_\gamma}{4}\right) (2m\omega)^2 \frac{q^2}{|\vec{q}|^2}, \end{aligned} \quad (5.124)$$

where we used $[34]^2 = -q^2$. Transforming the non-vanishing helicity-flip amplitude to impact parameter space we obtain

$$\tilde{\mathcal{A}}_{\text{FFR}}^{(0)}(1^\phi, 2^\phi, 3^+, 4^+) \simeq i \left(\frac{\kappa}{2}\right)^2 \left(\frac{\alpha_\gamma}{4}\right) \frac{m\omega}{\ell^2} \xi'' f(-2, D-2), \quad (5.125)$$

¹²We recall from Section 5.2.4 that $\mathcal{A}_{\text{EH}}^{(0)}(1^\phi, 2^\phi, 3^+, 4^+) = \mathcal{A}_{\text{EH}}^{(0)}(1^\phi, 2^\phi, 3^-, 4^-) = 0$.

where

$$\xi'' = \left(\frac{D}{2} - 2\right) \left(\frac{D}{2} - 1\right). \quad (5.126)$$

Defining

$$\delta_0^\gamma = \delta_{0,\text{EH}}^\gamma + \delta_{0,\text{FFR}}^\gamma, \quad (5.127)$$

we can combine (5.123) and (5.125) into a single leading eikonal phase matrix¹³

$$\delta_{0,\text{FFR}}^\gamma = \left(\frac{\kappa}{2}\right)^2 m \omega f(-2, D-2) \begin{pmatrix} 1 & \left(\frac{\alpha_\gamma}{4}\right) \frac{\xi''}{\bar{\ell}^2} \\ \left(\frac{\alpha_\gamma}{4}\right) \frac{\xi''}{\bar{\ell}^2} & 1 \end{pmatrix}, \quad (5.128)$$

which, upon expanding around $D = 4$, reduces to

$$\delta_{0,\text{FFR}}^\gamma = -\left(\frac{\kappa}{2}\right)^2 \frac{m \omega}{2\pi} \begin{pmatrix} \frac{1}{4-D} + \log b & -\left(\frac{\alpha_\gamma}{4}\right) \frac{1}{2\bar{\ell}^2} \\ -\left(\frac{\alpha_\gamma}{4}\right) \frac{1}{2\bar{\ell}^2} & \frac{1}{4-D} + \log b \end{pmatrix}. \quad (5.129)$$

Next, in order to test the expected exponentiation property of the leading eikonal phase matrix, we consider the terms of $\mathcal{O}(\omega^2)$ in the one-loop amplitudes. These are given in impact parameter space by

$$\begin{aligned} \tilde{\mathcal{A}}_{\text{EH}}^{(1)}(1^\phi, 2^\phi, 3^-, 4^+) \Big|_{\omega^2} &= -\left(\frac{\kappa}{2}\right)^4 (m\omega)^2 \frac{f(D-6, D-2)}{2\pi(D-4)}, \\ \tilde{\mathcal{A}}_{\text{FFR}}^{(1)}(1^\phi, 2^\phi, 3^+, 4^+) \Big|_{\omega^2} &= -\left(\frac{\kappa}{2}\right)^4 \left(\frac{\alpha_\gamma}{4}\right) \frac{(m\omega)^2}{\bar{\ell}^2} (D-3) \frac{f(D-6, D-2)}{2\pi}, \end{aligned} \quad (5.130)$$

which are obtained from (5.60) and (5.63). In matrix form,

$$\tilde{\mathcal{A}}_{\omega^2}^{(1)} = -\left(\frac{\kappa}{2}\right)^2 \frac{(m\omega)^2}{2\pi} f(D-6, D-2) \begin{pmatrix} \frac{1}{D-4} & \left(\frac{\alpha_\gamma}{4}\right) \frac{D-3}{\bar{\ell}^2} \\ \left(\frac{\alpha_\gamma}{4}\right) \frac{D-3}{\bar{\ell}^2} & \frac{1}{D-4} \end{pmatrix}. \quad (5.131)$$

Expanding around $D = 4$ we find that $\tilde{\mathcal{A}}_{\omega^2}^{(1)}$ satisfies the matrix equation

$$\tilde{\mathcal{A}}_{\omega^2}^{(1)} = -\frac{1}{2}(\delta_0)^2 + \mathcal{O}(D-4), \quad (5.132)$$

as expected.

¹³There is no need here to separate the EH and the FFR contributions, since we consider only photon bending coming from this source.

Subleading eikonal

Next we consider the subleading eikonal phase. The only non-vanishing EH contribution comes from the one-loop massive triangles in the helicity-preserving amplitude (5.60), and reads

$$\tilde{\mathcal{A}}_{\text{EH}}^{(1)}(1^\phi, 2^\phi, 3^-, 4^+) \Big|_\omega = i \left(\frac{\kappa}{2}\right)^4 \frac{15}{256\pi} \frac{m^2\omega}{b}. \quad (5.133)$$

Just as in the case of the leading eikonal phase, the bending angle of photons in pure EH is the same as the graviton bending (5.75) thanks to the equivalence principle.

The contributions coming from the *FFR* interaction are obtained from (5.64) and (5.63), and in impact parameter space are

$$\begin{aligned} \tilde{\mathcal{A}}_{\text{FFR}}^{(1)}(1^\phi, 2^\phi, 3^-, 4^+) \Big|_\omega &= 0, \\ \tilde{\mathcal{A}}_{\text{FFR}}^{(1)}(1^\phi, 2^\phi, 3^+, 4^+) \Big|_\omega &= i \left(\frac{\kappa}{2}\right)^4 \left(\frac{\alpha_\gamma}{4}\right) \frac{45}{1024\pi} \frac{m^2\omega}{b} \frac{1}{\ell^2}. \end{aligned} \quad (5.134)$$

Combining these results into a subleading eikonal phase matrix we get

$$\delta_{1,\text{FFR}}^\gamma = \left(\frac{\kappa}{2}\right)^4 \frac{15}{256\pi} \frac{m^2\omega}{b} \begin{pmatrix} 1 & \left(\frac{\alpha_\gamma}{4}\right) \frac{3}{4\ell^2} \\ \left(\frac{\alpha_\gamma}{4}\right) \frac{3}{4\ell^2} & 1 \end{pmatrix}. \quad (5.135)$$

Deflection angle and time delay

Having computed the eikonal phase matrix at leading and subleading order, we can now extract the light bending angle and time advance/delay. First we compute the eigenvalues of the leading eikonal phase matrix (5.129):

$$\delta_{0,\text{FFR}}^{\gamma(1,2)} = - \left(\frac{\kappa}{2}\right)^2 \frac{m\omega}{2\pi} \left[\left(\frac{1}{4-D} + \log b\right) \mp \left(\frac{\alpha_\gamma}{4}\right) \frac{2}{b^2} \right], \quad (5.136)$$

which match qualitatively the result of photon deflection in a shockwave background (see [301], and [299] for related work), while at subleading order we have

$$\delta_{0,\text{FFR}}^{\gamma(1,2)} = \left(\frac{\kappa}{2}\right)^4 \frac{15}{256\pi} \frac{m^2\omega}{b} \left[1 \pm \left(\frac{\alpha_\gamma}{4}\right) \frac{3}{b^2} \right]. \quad (5.137)$$

Using once again (5.22), we find the light bending angle up to $\mathcal{O}(G^2)$:

$$\begin{aligned}\Delta\theta_{\text{FFR}}^{\gamma(1,2)} &= -\left(\frac{\kappa}{2}\right)^2 \frac{1}{2\pi} \frac{m}{b} \left\{ 1 \pm \left(\frac{\alpha_\gamma}{4}\right) \frac{4}{b^2} + \left(\frac{\kappa}{2}\right)^2 \frac{15}{128} \frac{m}{b} \left[1 \pm \left(\frac{\alpha_\gamma}{4}\right) \frac{9}{b^2} \right] \right\} \\ &= -\frac{4Gm}{b} \left\{ 1 \pm \left(\frac{\alpha_\gamma}{4}\right) \frac{4}{b^2} + \frac{15\pi}{16} \frac{Gm}{b} \left[1 \pm \left(\frac{\alpha_\gamma}{4}\right) \frac{9}{b^2} \right] \right\} .\end{aligned}\tag{5.138}$$

Finally, applying (5.23) to (5.136) and (5.137) we arrive at our result for the time delay:

$$\begin{aligned}\Delta t_{\text{FFR}}^{\gamma(1,2)} &= \left(\frac{\kappa}{2}\right)^2 \frac{m}{2\pi} \left\{ \log \frac{b_0}{b} \pm \left(\frac{\alpha_\gamma}{4}\right) \frac{2}{b^2} + \left(\frac{\kappa}{2}\right)^2 \frac{15}{128} \frac{m}{b} \left[1 \pm \left(\frac{\alpha_\gamma}{4}\right) \frac{3}{b^2} \right] \right\} \\ &= 4Gm \left\{ \log \frac{b_0}{b} \pm \left(\frac{\alpha_\gamma}{4}\right) \frac{2}{b^2} + \frac{15\pi}{16} \frac{Gm}{b} \left[1 \pm \left(\frac{\alpha_\gamma}{4}\right) \frac{3}{b^2} \right] \right\} .\end{aligned}\tag{5.139}$$

We note that the $\mathcal{O}(G\alpha_\gamma)$ part of our result (5.138) is in precise agreement with [309] while it disagrees with [308].¹⁴ Note that (5.139) generically leads to a potential time advance and causality violation independent of the sign of the coupling α_γ . This parallels the situation for the R^3 interaction which requires an appropriate UV completion to restore causality [297].

¹⁴The result of [308] for $\Delta\theta_{\text{FFR}}^\gamma$ was already identified as incorrect in [309] due to an inappropriate definition of the deflection angle.

Chapter 6

Gravitational radiation from R^3 operators

In the previous section we discussed modifications to the bending angle and time delay experienced by a massless particle when deflected off a heavy spinless object, in a theory where additional higher-derivative couplings are present beyond the Einstein-Hilbert action. Here we consider once again these couplings, restricting however to the three-derivative ones, and analyse their effects on the dissipative aspects of the gravitational interaction, namely gravitational radiation from a binary system. This can be done by considering appropriate five-point amplitudes with four massive scalars and one radiated graviton as external states. An effective field theory framework for gravity was advocated in [246], and is ideally suited to study systematically higher-derivative corrections to the EH theory in this context. In [295], this approach was followed to compute the corrections to the gravitational potential between compact objects and their effective mass and current quadrupoles due to perturbations quartic in the Riemann tensor, and the corresponding modifications to the waveforms were then analysed in [106].

Schematically, the strategy consists of considering the binary system from far away as a single object with a small extension in space which emits gravitational waves by the oscillations of its multipoles. The two fundamental ingredients in this framework are the modifications to the potential, which are needed to compute the time-dependence of the multipoles, and the modification to the multipole expansion itself which in our case amounts to the modifications of the quadrupole term. Modifications to the gravitational potential due to cubic interactions in the Riemann tensor were computed in [293, 294], so we will simply quote these results. The quadrupole modifications instead were computed in [4] and we will retrace the steps of the computation in this chapter. The study of radiation is performed in the presence of both cubic modifications to the EH

action and tidal effects. Interestingly, there is an overlap between these two types of corrections which are linked by appropriate field redefinitions [304, 338], while still having possibly very different physical origin – for instance, I_1 and G_3 appear in the low-effective action of bosonic strings, or can be induced by integrating out massive matter [339, 340].

In the presence of scalars and restricting our focus to parity-even interactions, we consider the two independent cubic terms I_1 and I_2 (defined in (5.4)) or equivalently the more natural combination $G_3 := I_1 - 2I_2$, which, as is well known, is topological in six dimensions [341] and has vanishing graviton amplitudes. In [297], it was argued from studying the scattering of polarised gravitons that I_1 potentially leads to superluminal effects/causality violation in the propagation of gravitons for impact parameter $b \lesssim \alpha^{\frac{1}{4}}$. Here $\alpha \sim \Lambda^{-4}$ is the coupling constant of the I_1 interaction, and Λ is the cutoff of the theory. In that paper, α was chosen to be much larger than $G^2 \sim M_{\text{Planck}}^{-4}$. This allows to treat the gravitational scattering in a semiclassical setup, where predictions can be trusted up to $M_{\text{Planck}} (> \Lambda)$. This question was reinvestigated in an EFT framework in [3], where it was found that the I_1 interaction leads to a time advance in the propagation of gravitons (but not photons and scalars) when $b \lesssim \alpha^{\frac{1}{4}}$. Finally, G_3 does not lead to any time advance/delay for massless particles [3], while still correcting the gravitational potential [293, 294]. An identical conclusion for the propagation of massless particles in the background of a black hole was reached in [331], both for the I_1 and G_3 interactions¹.

In this respect, an important observation was made in [333], namely that such superluminality effects (and those observed earlier on in [309, 298, 299]) are unresolvable within the regime of validity of the EFT, and do not lead to violations of causality. In our setup such violations would indeed occur at $b \lesssim \Lambda^{-1}$, which is at the boundary of the regime of validity of our EFT, while the processes we are interested in only probe the regime where the EFT is valid. Above Λ , the only known way to restore causality is to introduce an infinite tower of massive particles [297]. In conclusion, these observations do not rule out cubic interactions for our EFT computation, although they may impose constraints on the cutoff – it needs to be such that possible effects due to the massive modes, required to ensure causality, cannot be resolved with current-day experiments. We also note that, assuming that these interactions can contribute to any classical gravitational scattering ($\Lambda < M_{\text{Planck}}$), then we have $\alpha > G^2$, independently of precise estimates of the cutoff Λ .

In the following, our results for the quadrupole correction, extracted from the appropriate five-point amplitude, are exact to leading order in the perturbations and in the post-Minkowskian expansion. Once we eventually take the PN expansion, we find expressions which are complete at 5PN order for the G_3 and tidal interaction corrections,

¹Note that for G_3 the coefficient $2d_9 + d_{10}$ in Eq. (2.24) of [331] vanishes.

and at 6PN order for the I_1 corrections. We notice that as expected we find that the corrections due to G_3 have the same form as those generated by a particular type of tidal interaction (although we consider the corresponding coefficients in the EFT action as independent). For the PN-expanded result of the tidal corrections to the mass quadrupole we find agreement with [342–344]. The remaining tasks consist in using the corrected quadrupole moment to compute the modifications compared to EH gravity to the power emitted by the radiated gravitational waves, and the corresponding corrections to the waveforms in the Stationary Phase Approximation (SPA)². Here we follow closely [106], and also present a comparison with their result obtained with perturbations that are quartic in the Riemann tensor.

6.1 The EFT action and more about cubic interactions

In this section we consider an EFT describing EH gravity with higher-derivative couplings of mass-dimension six interacting with two massive scalars, which as usual model a spin-less compact object, and we also include the leading tidal interactions which describe finite size effects of the heavy objects. Specifically, the EFT action we consider here is

$$S = S_{\text{eff}} + S_{\phi_1\phi_2} + S_{\text{tidal}} , \quad (6.1)$$

where

$$S_{\text{eff}} = \int d^4x \sqrt{-g} \left[-\frac{2}{\kappa^2} R - \frac{2}{\kappa^2} \mathcal{L}_6 - \dots \right] \quad (6.2)$$

is the effective action for gravity, with \mathcal{L}_6 given in (5.3). The dots in (6.2) stand for higher-derivative interactions that we will not consider here. The two scalars, with masses m_1 and m_2 , couple to gravity with an action

$$S_{\phi_1\phi_2} = \int d^4x \sqrt{-g} \frac{1}{2} \sum_{i=1,2} \left(\partial_\mu \phi_i \partial^\mu \phi_i - m_i^2 \phi_i^2 \right) , \quad (6.3)$$

and in addition we include higher-derivative couplings describing tidal effects of extended heavy objects,

$$S_{\text{tidal}} = \int d^4x \sqrt{-g} \frac{1}{4} R_{\mu\alpha\nu\beta} R^{\rho\alpha\sigma\beta} \sum_{i=1,2} \left(\lambda_i \phi_i^2 \delta_\rho^\mu \delta_\sigma^\nu + \frac{\eta_i}{m_i^4} \nabla^\mu \nabla^\nu \phi_i \nabla_\rho \nabla_\sigma \phi_i \right) + \dots . \quad (6.4)$$

These tidal interactions were studied in [347], and the dots stand for the (Hilbert) series of higher-dimensional operators classified in [338, 348], which will not play any role in this work. We now briefly discuss some properties of the interactions we consider.

Recall that considering I_1 and G_3 , in pure gravity only one of them is independent

²See *e.g.* [345, 346] for details of this approximation.

in four dimensions [349, 350], while in the presence of matter coupled to gravity they become independent. It is well known that, unlike I_1 , the G_3 interaction has a vanishing three-graviton amplitude and does not contribute to graviton scattering up to four particles [341, 311] – and in fact to any number of gravitons. This can be explained by the fact that G_3 is topological in six dimensions [341], and therefore computing tree-level four-dimensional graviton amplitudes from dimensionally reducing the six-dimensional ones automatically gives zero. Combining this observation with unitarity techniques leads to

$$\mathcal{M}_{\text{EH}+G_3}(h_1, \dots, h_n)|_{d<6} = \mathcal{M}_{\text{EH}}(h_1, \dots, h_n)|_{d<6}, \quad (6.5)$$

for any n . Hence the G_3 interaction does not affect the perturbative dynamics in theories of pure gravity. However, if we consider a theory of gravity with matter, *e.g.* massive scalars mimicking black holes or neutron stars, the presence of a G_3 coupling alters their dynamics. In particular the four-point amplitude with two gravitons and two scalars becomes [293, 294]

$$\mathcal{M}_{\text{EH}+G_3}^{(0)}(\phi_1, \phi_2, h_3^{++}, h_4^{++}) = \mathcal{M}_{\text{EH}}^{(0)}(\phi_1, \phi_2, h_3^{++}, h_4^{++}) + i \frac{\alpha_2}{32} \left(\frac{\kappa}{2}\right)^2 [34]^4 (2m^2 + s). \quad (6.6)$$

The non-trivial contribution to the scattering amplitude of two massive scalars and two gravitons from the G_3 interactions modifies the classical potential in the two-body system, as shown in [293, 294]. As we will show below, both G_3 and I_1 produce corrections to the quadrupole moment already at tree level. Specifically we find that the G_3 quadrupole correction is dominant in the post-Newtonian (PN) expansion, which parallels the results found for the corresponding corrections to the gravitational potential quoted earlier in (6.7).

At this point it is once again interesting to take a different approach to the problem and look at dimension-six operators in a purely gravitational context from the on-shell point of view. Classifying all the three-point interactions which involve only gravitons at the given mass-dimension one only finds a single structure proportional to $[12]^2[23]^2[31]^2$ and its parity conjugate³, thus one would expect to only find a single operator in the Lagrangian formalism which contributes to the purely gravitational processes. On the other hand, it is easy to show that the contact term proportional to $[34]^4(2m^2 + s)$ in the amplitude (6.6) is (up to a numerical coefficient) the amplitude arising from a particular tidal interaction of the form $R^{\mu\nu\rho\sigma}R_{\mu\nu\rho\sigma}m^2\phi^2 - \nabla^\alpha R^{\mu\nu\rho\sigma}\nabla_\alpha R_{\mu\nu\rho\sigma}\phi^2$. This suggests that there should exist a link between the two, and indeed one can construct a four-dimensional field redefinition mapping the G_3 interaction into a tidal effect, as

³In a parity-even theory as the one we are considering this obviously still counts as a single interaction.

already noticed in [304, 338]⁴. The explicit construction of such a field redefinition can be found for example in [4]. Despite the fact that the G_3 interaction can be thought of as a tidal effect, we keep it separate from (6.4) and highlight the analogies along the way.

For the sake of the computation of the power radiated by the gravitational waves performed in later sections we need the correction induced by the cubic interactions to the gravitational potential. The full 2PM computation of this quantity was performed in [293, 294], and expanding their result one obtains

$$\begin{aligned}
 V(\vec{r}, |\vec{p}|) = & -\frac{Gm_1m_2}{r} + \frac{3}{8} \frac{\alpha_1 G^2}{r^6} \frac{(m_1 + m_2)^3}{m_1m_2} \vec{p}^2 \\
 & - \frac{3}{4} \frac{\alpha_2 G^2}{r^6} m_1m_2(m_1 + m_2) \left(1 - \frac{m_1^2 + m_2^2}{2m_1^2m_2^2} \vec{p}^2\right) + \dots, \tag{6.7}
 \end{aligned}$$

where the dots indicate higher PN corrections which we do not consider here. Note that the terms proportional to α_1 and α_2 are the result of a one-loop computation. In the PN expansion, the term proportional to α_1 (from the I_1 interaction) is suppressed by a factor of $\vec{p}^2/m_{1,2}^2$ compared to the dominant correction proportional to α_2 (from G_3). Similarly, for the tidal interactions in (6.4) we expand the conservative Hamiltonian computed in [353, 354, 347] up to $\mathcal{O}(\vec{p}^2)$, with the result

$$\begin{aligned}
 V_{\text{tidal}}(\vec{r}, \vec{p}) = & -\frac{3}{2} \frac{G^2 m_2^2}{r^6 m_1} \left[8 \left(1 - \frac{m_1^2 + m_2^2}{2m_1^2m_2^2} \vec{p}^2\right) \lambda_1 + \left(1 + \frac{2m_1^2 + 2m_2^2 + 5m_1m_2}{m_1^2m_2^2} \vec{p}^2\right) \eta_1 \right] \\
 & + 1 \leftrightarrow 2 + \dots, \tag{6.8}
 \end{aligned}$$

where the dots indicate higher PN terms.

6.2 Quadrupole moments in EFTs of gravity

In the PN framework, the conservative and dissipative dynamics of two objects of mass m_1 and m_2 , coupled to the gravity effective action (6.2) is described by the following point-particle effective action [355, 295]:

$$S_{\text{pp}} = \int dt \left[\frac{1}{2} \mu \dot{\vec{r}}^2 - V(\vec{r}, \vec{p}) + \frac{1}{2} Q^{ij}(\vec{r}, \vec{p}) R^{0i0j} + \dots \right], \tag{6.9}$$

where

$$\mu := \frac{m_1m_2}{m_1 + m_2} \tag{6.10}$$

⁴We also observe that black holes in four dimensions have non-vanishing Love numbers when higher-derivative interactions are considered [351, 352].

is the reduced mass, and $\vec{r}(t)$ is the relative position of the two objects. $V(\vec{r}, \vec{p})$ denotes the potential, whose explicit expression to first order in α_1, α_2 [293, 294], and $\lambda_{1,2}, \eta_{1,2}$ [353, 354, 347] is obtained by summing (6.7) and (6.8), and $Q^{ij}(\vec{r}, \vec{p})$ is the quadrupole moment, to be computed below. The dots represent higher-order terms that will be irrelevant in our analysis. This action can be trusted in the inspiral phase before the objects reach relativistic velocities.

We now present the computation of the five-point amplitude $\phi_1\phi_2 \rightarrow \phi_1\phi_2 + \bar{h}(k)$ with four scalars and one radiated soft graviton $\bar{h}(k)$. Its momentum k^μ is on shell, while the momentum of the graviton exchanged between the two objects is purely spacelike (corresponding to an instantaneous interaction), and in our setup is given by $q^\mu = -p_1^\mu - p_2^\mu = (0, \vec{q})$. Furthermore, the energy of the radiated graviton is such that $k^0 \ll |\vec{q}|$, so that k^μ can be ignored for practical purposes, and the radiated graviton enters the amplitude only through its associated Riemann curvature tensor $\bar{R}_{\alpha\beta\mu\nu}$. Finally, because we are only interested in classical contributions (*i.e.* $\mathcal{O}(\hbar^0)$), we keep only the leading terms in \vec{q}^2 .

In the following we first compute fully relativistic scattering amplitudes and then perform the PN expansion to extract the correction to the quadrupole term in the effective action (6.9). In the centre-of-mass frame, the momenta of the particles can be parametrised as

$$\begin{aligned} p_1^\mu &= -\left(E_1, \vec{p} - \frac{\vec{q}}{2}\right), & p_4^\mu &= -\left(E_4, -\vec{p} + \frac{\vec{q}}{2}\right), \\ p_2^\mu &= \left(E_2, \vec{p} + \frac{\vec{q}}{2}\right), & p_3^\mu &= \left(E_3, -\vec{p} - \frac{\vec{q}}{2}\right), \end{aligned} \quad (6.11)$$

with $p_1^2 = p_2^2 = m_1^2, p_3^2 = p_4^2 = m_2^2$. Furthermore, we have

$$E_1 = E_2 = \sqrt{m_1^2 + \vec{p}^2 + \vec{q}^2/4}, \quad E_3 = E_4 = \sqrt{m_2^2 + \vec{p}^2 + \vec{q}^2/4}, \quad (6.12)$$

where $\vec{p} \cdot \vec{q} = 0$ because of momentum conservation. In our all-outgoing convention for the external lines, the four-momenta p_1 and p_4 correspond to the incoming particles, and hence their energies are negative.

6.2.1 The amplitude with cubic interactions

Our next task is to compute the five-point amplitude $\mathcal{A}_\mathcal{O}$ shown in Figure 6.1, with $\mathcal{O} = I_1, I_2$ (which we can then combine to obtain \mathcal{A}_{G_3}). We first obtain its relativistic expression, factoring out a single Riemann tensor associated with the radiated graviton, and then split the Lorentz indices into time and spatial components and isolate the terms contracted into \bar{R}_{0i0j} . Upon Fourier transforming to position space, these components will allow to directly read off Q_{ij} by matching to the Hamiltonian density associated to the point particle effective action (6.9). The classical relativistic results

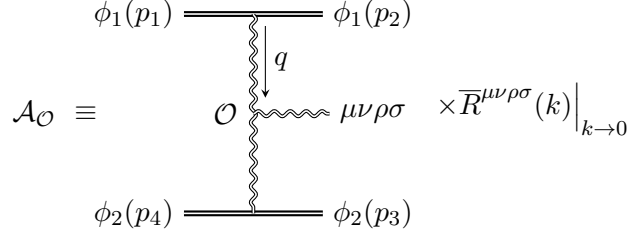


Figure 6.1: The single diagram contributing to the radiation process with an insertion of the operators $\mathcal{O} = I_1, I_2$. All momenta are treated as outgoing and the radiated graviton is taken to be soft.

are, for I_1 :

$$\mathcal{A}_{I_1} = i(\alpha_1 + 2\alpha_2) \left(\frac{\kappa}{2}\right)^2 \frac{q^\mu q^\rho}{q^2} \left[m_1^2 p_3^\nu p_3^\sigma + m_2^2 p_1^\nu p_1^\sigma - 2(p_1 \cdot p_3) p_1^\nu p_3^\sigma \right] \bar{R}_{\mu\nu\rho\sigma}, \quad (6.13)$$

while for I_2 :

$$\mathcal{A}_{I_2} = \frac{i}{2} \alpha_2 \left(\frac{\kappa}{2}\right)^2 \frac{q^\mu q^\rho}{q^2} (m_1^2 p_3^\nu p_3^\sigma + m_2^2 p_1^\nu p_1^\sigma) \bar{R}_{\mu\nu\rho\sigma}. \quad (6.14)$$

Note that the result for the G_3 interaction introduced in (5.3) can be obtained as

$$\mathcal{A}_{G_3} := (\mathcal{A}_{I_1} + \mathcal{A}_{I_2})|_{\alpha_1=0}. \quad (6.15)$$

The terms in the amplitude contributing to the quadrupole radiation are then

$$\mathcal{A}_{I_1}(q) = -i(\alpha_1 + 2\alpha_2) \left(\frac{\kappa}{2}\right)^2 (m_1^2 E_4^2 + m_2^2 E_1^2 - 2E_1^2 E_4^2 - 2\vec{p}^2 E_1 E_4) \frac{q^i q^j}{q^2} \bar{R}_{0i0j} + \dots, \quad (6.16)$$

and

$$\mathcal{A}_{I_2}(q) = -i \frac{\alpha_2}{2} \left(\frac{\kappa}{2}\right)^2 (m_1^2 E_4^2 + m_2^2 E_1^2) \frac{q^i q^j}{q^2} \bar{R}_{0i0j} + \dots, \quad (6.17)$$

where we have used that $E_3 = E_4$ in order to write the result as a function of the energies and momenta of the incoming particles p_1 and p_4 . The dots stand for additional terms proportional to \bar{R}_{0ijk} and \bar{R}_{ijkl} , which can also be extracted from our result.

6.2.2 The amplitude with tidal effects

A calculation similar to the one outlined in the previous section leads to the fully relativistic result

$$\begin{aligned} \mathcal{A}_{\text{tidal}}(q) = & i \left(\frac{\kappa}{2}\right)^2 \frac{q^\mu q^\rho}{q^2} \left\{ 8\lambda_1 p_4^\nu p_4^\sigma + 8\lambda_2 p_1^\nu p_1^\sigma \right. \\ & \left. + \frac{1}{2} \left[(m_1^2 + m_2^2 - t)^2 - 2m_1^2 m_2^2 \right] \left(\frac{\eta_2}{m_2^4} p_4^\nu p_4^\sigma + \frac{\eta_1}{m_1^4} p_1^\nu p_1^\sigma \right) \right\} \bar{R}_{\mu\nu\rho\sigma}, \end{aligned} \quad (6.18)$$

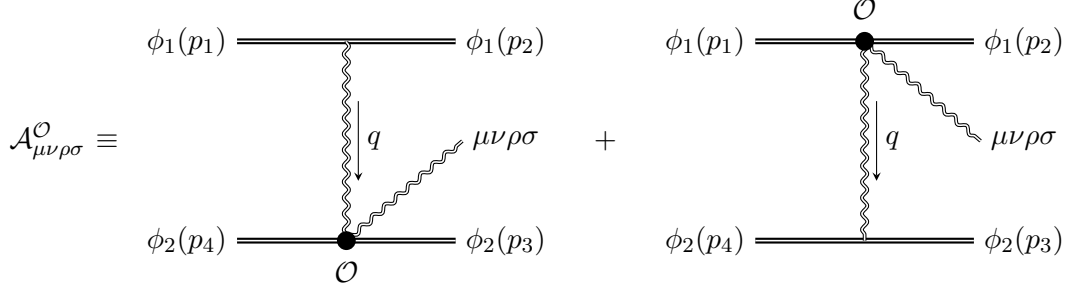


Figure 6.2: The two diagrams contributing to the gravitational radiation, where \mathcal{O} denotes any of the two tidal interactions in (6.4). An overall Riemann tensor of the radiated graviton is factored out, so that $\mathcal{A}^{\mathcal{O}} = \mathcal{A}_{\mu\nu\rho\sigma}^{\mathcal{O}} \bar{R}^{\mu\nu\rho\sigma}(k \rightarrow 0)$.

which, upon expanding in the spatial and time components, reads

$$\begin{aligned} \mathcal{A}_{\text{tidal}}(q) = & -i \left(\frac{\kappa}{2} \right)^2 \left\{ 8\lambda_1 E_4^2 + 8\lambda_2 E_1^2 \right. \\ & \left. + \left[2(E_1 E_4 + \vec{p}^2)^2 - m_1^2 m_2^2 \right] \left(\eta_2 \frac{E_4^2}{m_2^4} + \eta_1 \frac{E_1^2}{m_1^4} \right) \right\} \frac{q^i q^j}{\bar{q}^2} \bar{R}_{0i0j} + \dots, \end{aligned} \quad (6.19)$$

where the ellipses stand once again for terms proportional to \bar{R}_{0ijk} and \bar{R}_{ijkl} which we will not need in the remainder of this section.

6.2.3 The quadrupole corrections

Next we extract the corrections to the mass quadrupole moment Q_{ij} from (6.16), (6.17) and (6.19). To do so we simply match the appropriately normalised and Fourier-transformed $\mathcal{A}_{\mathcal{O}}$, as defined in (6.21) below, to the quadrupole contribution in (6.9)⁵. To begin with, we perform the relevant Fourier transforms using

$$\int dt \int \frac{d^3 q}{(2\pi)^3} \frac{q_i q_j}{|\vec{q}|^2} e^{i\vec{q}\cdot\vec{r}} \bar{R}^{0i0j} = -\frac{3}{4\pi} \int dt \frac{1}{r^5} \left(x_i x_j - \frac{1}{3} r^2 \delta_{ij} \right) \bar{R}^{0i0j}. \quad (6.20)$$

Taking into account the non-relativistic normalisation factor of $-i/4E_1 E_4$, we arrive at the quadrupole-like terms

$$\begin{aligned} \tilde{\mathcal{A}}_{\mathcal{O}}^{\text{quad}}(r) & := -i \frac{\mathcal{A}_{\mathcal{O}}^{\text{quad}}(r)}{4E_1 E_4} \\ & = \frac{1}{2} C_{\mathcal{O}}(E_i, m_i, \vec{p}^2) \int dt \frac{1}{r^5} \left(x_i x_j - \frac{1}{3} r^2 \delta_{ij} \right) \bar{R}^{0i0j}, \end{aligned} \quad (6.21)$$

⁵For further details on the procedure see for example [355, 295].

where $C_{\mathcal{O}}$ are coefficients depending on the energies and masses as well as \vec{p}^2 of the heavy particles, with

$$\begin{aligned} C_{I_1}(E_i, m_i, \vec{p}^2) &= \frac{3}{8\pi} (\alpha_1 + 2\alpha_2) \left(\frac{\kappa}{2}\right)^2 \left(m_1^2 \frac{E_4}{E_1} + m_2^2 \frac{E_1}{E_4} - 2E_1 E_4 - 2\vec{p}^2\right), \\ C_{I_2}(E_i, m_i, \vec{p}^2) &= \frac{3}{16\pi} \alpha_2 \left(\frac{\kappa}{2}\right)^2 \left(m_1^2 \frac{E_4}{E_1} + m_2^2 \frac{E_1}{E_4}\right), \\ C_{\text{tidal}}(E_i, m_i, \vec{p}^2) &= \frac{3}{8\pi} \left(\frac{\kappa}{2}\right)^2 \left\{ 8\lambda_1 \frac{E_4}{E_1} + 8\lambda_2 \frac{E_1}{E_4} + \right. \\ &\quad \left. \left[2(E_1 E_4 + \vec{p}^2)^2 - m_1^2 m_2^2\right] \left(\eta_1 \frac{E_1}{E_4 m_1^4} + \eta_2 \frac{E_4}{E_1 m_2^4}\right) \right\}. \end{aligned} \quad (6.22)$$

Comparing (6.21) with the Hamiltonian density obtained from the action (6.9), we conclude that the modifications to the quadrupole moment arising from the cubic and tidal couplings are given by

$$Q_{\mathcal{O}}^{ij} = \frac{C_{\mathcal{O}}}{\mu r^5} Q_N^{ij}, \quad (6.23)$$

where we have introduced the leading-order quadrupole moment in the EH theory for a binary system with masses m_1 and m_2 ,

$$Q_N^{ij} = \mu \left(x^i x^j - \frac{1}{3} r^2 \delta^{ij} \right), \quad (6.24)$$

with μ being the reduced mass defined in (6.10). Combining the various correction terms, we arrive at

$$Q^{ij} = Q_N^{ij} + Q_{I_1}^{ij} + Q_{I_2}^{ij} + Q_{\text{tidal}}^{ij} = \left(1 + \frac{C_{I_1}}{\mu r^5} + \frac{C_{I_2}}{\mu r^5} + \frac{C_{\text{tidal}}}{\mu r^5} \right) Q_N^{ij}. \quad (6.25)$$

It is interesting to write the three coefficients C_{I_1} , C_{I_2} and C_{tidal} in the PN expansion. Keeping terms up to first order in \vec{p}^2 one has

$$\begin{aligned} C_{I_1}^{\text{PN}} &= -3G (\alpha_1 + 2\alpha_2) M \frac{\vec{p}^2}{\mu}, \\ C_{I_2}^{\text{PN}} &= 3G \alpha_2 m_1 m_2, \\ C_{\text{tidal}}^{\text{PN}} &= 3G \left[8\lambda_1 + \eta_1 + \frac{1}{2M} \left(8(m_1 - m_2)\lambda_1 + (3m_1 + 5m_2)\eta_1 \right) \frac{\vec{p}^2}{\mu^2} \right] \frac{m_2}{m_1} \\ &\quad + 1 \leftrightarrow 2, \end{aligned} \quad (6.26)$$

where

$$M := m_1 + m_2, \quad (6.27)$$

and, as usual, $\kappa^2 := 32\pi G$. For convenience we also quote the contribution due to the G_3 interaction alone – this is given by

$$Q_{G_3}^{ij} = \left(Q_{I_1}^{ij} + Q_{I_2}^{ij} \right) \Big|_{\alpha_1=0} = 3G\alpha_2 \frac{M}{r^5} \left(1 - \frac{2\vec{p}^2}{\mu^2} \right) Q_N^{ij}. \quad (6.28)$$

6.3 Power radiated by the gravitational waves

We can now compute the power radiated by the gravitational waves in the approximation of circular orbits. In the EH theory, the radius of the circular orbit is given by the well-known formula

$$r_N = \left(\frac{GM}{\Omega^2} \right)^{\frac{1}{3}}. \quad (6.29)$$

In the presence of the cubic and tidal interactions, this quantity gets modified as

$$\begin{aligned} r_o &= r_N + \delta r, \\ \delta r &= \Omega^3 \left[-\frac{\alpha_1}{2}v + \left(\frac{\alpha_2}{2} + 8\lambda_{12} \right) \left(\frac{3}{v} + v(2\nu - 1) \right) + \eta_{12} \left(\frac{3}{v} + v(\nu + 2) \right) \right] + \mathcal{O}(g_i^2), \end{aligned} \quad (6.30)$$

where g_i stands for any of the coupling constants of the cubic and tidal perturbations. We also introduced the symmetric mass ratio ν defined as

$$\nu := \frac{m_1 m_2}{M^2}, \quad (6.31)$$

and the parameter

$$v := r_N \Omega = (GM\Omega)^{\frac{1}{3}}, \quad (6.32)$$

as well as the following combinations of the couplings

$$\lambda_{12} := \mu \left(\frac{\lambda_1}{m_1^3} + \frac{\lambda_2}{m_2^3} \right), \quad \eta_{12} := \mu \left(\frac{\eta_1}{m_1^3} + \frac{\eta_2}{m_2^3} \right). \quad (6.33)$$

Finally, Ω denotes the angular velocity on the circular orbit, and the value δr has been computed using (6.30) and (B.30), where the potentials entering (B.30) are given in (6.7) and (6.8). The total energy per unit mass M of the system, to first order in the couplings, is then given by

$$\begin{aligned} E(v) &= -\frac{1}{2}\nu v^2 + \frac{9}{4} \frac{v^{12}}{(GM)^4} \nu (\alpha_2 + 16\lambda_{12} + 2\eta_{12}) + \frac{11}{8} \frac{v^{14}}{(GM)^4} \left[-\nu\alpha_1 \right. \\ &\quad \left. + \nu(2\nu - 1)(\alpha_2 + 16\lambda_{12}) + 4\nu(\nu + 2)\eta_{12} \right]. \end{aligned} \quad (6.34)$$

The above formula is complete at leading order in all of the perturbations (that is $\mathcal{O}(v^{12})$ and at $\mathcal{O}(v^{14})$ for the α_1 correction only. The remaining $\mathcal{O}(v^{14})$ terms have been obtained from a small-velocity expansion of our 2PM result, and in order to get a complete result at that PN order one would need to include also the 3PM corrections to the potential generated by cubic and tidal interactions⁶. We have also compared the contribution to the energy from the $\eta_{1,2}$ corrections to [344], finding agreement (after mapping their coefficients $\mu_A^{(2)}$ to ours)⁷.

Next, we compute the leading-order gravitational-wave flux using the quadrupole formula

$$\mathcal{F}(v) = \frac{G}{5} \langle \ddot{Q}^{ij} \ddot{Q}^{ij} \rangle, \quad (6.35)$$

using the result of our computation for Q^{ij} in (6.25). To first order in the couplings α_1 and α_2 the flux becomes

$$\mathcal{F}(v) = \frac{G}{5} \langle \ddot{Q}_N^{ij} \ddot{Q}_N^{ij} \rangle \left[1 + \frac{2}{\mu r^5} \left(C_{I_1}^{\text{PN}} + C_{I_2}^{\text{PN}} + C_{\text{tidal}}^{\text{PN}} \right) \right] + \mathcal{O}(\alpha_i^2), \quad (6.36)$$

where the PN-expanded coefficients $C_{\mathcal{O}}^{\text{PN}}$ are explicitly given in (6.26).

Two comments are in order here. First, we note that the prefactor $\langle \ddot{Q}_N^{ij} \ddot{Q}_N^{ij} \rangle$ is evaluated on the radius r_o of the circular orbit in the presence of the cubic and tidal interactions, as given in (6.30). Furthermore, the quantity $\vec{p}^2 := p_r^2 + p_\phi^2/r^2$ can be obtained using the fact that $p_r = 0$ on the circular orbit while $p_\phi := l$ is a constant, which can be determined from Hamilton's equations, with the result

$$l := \frac{\mu r_o^2 \Omega}{1 + 2\mu U(r_o)}, \quad (6.37)$$

where r_o is given in (6.30) and $U(r)$ is the part of the potential proportional to \vec{p}^2 , following the conventions of Appendix B.4. Using these relations, \vec{p}^2 is re-expressed as a function of Ω , the masses, and the couplings.

Factoring out the standard power radiated by the gravitational wave in EH,

$$\mathcal{F}_N(v) := \frac{G}{5} \langle \ddot{Q}_N^{ij} \ddot{Q}_N^{ij} \rangle \Big|_{r=r_N} = \frac{32}{5} G \mu^2 r_N^4 \Omega^6 = \frac{32}{5} \frac{\nu^2 v^{10}}{G}, \quad (6.38)$$

⁶Similar considerations apply to our results for the flux in (6.39).

⁷For further details on mapping field-theory to point-particle actions see *e.g.* [27, 356]

we can rewrite the expression for the flux as

$$\begin{aligned} \mathcal{F}(v) = & \frac{32 \nu^2 v^{10}}{5 G} \left[1 + \frac{v^{10}}{(GM)^4} (12 \alpha_2 + 144 \lambda_{12} + 48 \lambda'_{12} + 18 \eta_{12} + 6 \eta'_{12}) \right. \\ & \left. + \frac{v^{12}}{(GM)^4} \left[-8 \alpha_1 + 2(2\nu - 7) \alpha_2 + 8(8\nu - 7) \lambda_{12} + 24 \lambda'_{12} + (8\nu + 31) \eta_{12} + 9 \eta'_{12} \right] \right], \end{aligned} \quad (6.39)$$

with λ_{12} and η_{12} defined in (6.33) and

$$\lambda'_{12} := \frac{1}{M} \left(\frac{\lambda_1}{m_1} + \frac{\lambda_2}{m_2} \right), \quad \eta'_{12} := \frac{1}{M} \left(\frac{\eta_1}{m_1} + \frac{\eta_2}{m_2} \right). \quad (6.40)$$

Similarly to (6.34), the first line and the α_1 term in the second line of (6.39) are complete. We also note that the $\eta_{1,2}$ part of the tidal flux is in agreement with [344].

6.4 Waveforms in EFT of gravity

Following [106] we can also compute the correction induced by the cubic and tidal interactions to the gravitational phase in the saddle point approximation. In this approach, the waveform in the frequency domain is written as⁸

$$\tilde{h}_{\text{SPA}}(f) \sim \exp \left[i \left(\psi_f(t_f) - \frac{\pi}{4} \right) \right], \quad (6.41)$$

where

$$\psi(t) := 2\pi f t - \phi(t). \quad (6.42)$$

Here $\phi(t)$ is the orbital phase, while $\dot{\phi}(t) = \pi F(t)$ defines the instantaneous frequency $F(t)$ of the gravitational wave. t_f is defined as the time where

$$\dot{\psi}(t) \Big|_{t=t_f} = 0, \quad (6.43)$$

implying that $F(t_f) = 2f$. In the adiabatic approximation, the work of [346, 345] provides explicit formulae for $\psi_{\text{SPA}}(t_f)$ and t_f :

$$\psi_{\text{SPA}}(t_f) = 2\pi f t_{\text{ref}} - 2\phi_{\text{ref}} + \frac{2}{G} \int_{v_f}^{v_{\text{ref}}} dv (v_f^3 - v^3) \frac{E'(v)}{\mathcal{F}(v)}, \quad (6.44)$$

$$t_f = t_{\text{ref}} + M \int_{v_f}^{v_{\text{ref}}} dv \frac{E'(v)}{\mathcal{F}(v)}, \quad (6.45)$$

⁸See for example Section III F of [346] for a detailed derivation.

where $v_{\text{ref}} = v(t_{\text{ref}})$ and t_{ref} are integration constants, $v_f := (\pi GM f)^{\frac{1}{3}}$, and $E(v)$ and $\mathcal{F}(v)$ were computed to lowest order in the cubic and tidal perturbations in (6.34) and (6.36), respectively.

We can now compute the correction to $\psi_{\text{SPA}}(t_f)$ due to the presence of the perturbations, expanding the ratio $E'(v)/\mathcal{F}(v)$ at consistent PN order and performing the integration in (6.44). Doing so we arrive at

$$\psi_{\text{SPA}}(t_f) = \psi_{\text{SPA}}^{\text{EH}}(t_f) + \psi_{\text{SPA}}^{I_1+I_2}(t_f) + \psi_{\text{SPA}}^{\text{tidal}}(t_f) . \quad (6.46)$$

Here

$$\psi_{\text{SPA}}^{\text{EH}}(t_f) = 2\pi f t'_{\text{ref}} - 2\phi'_{\text{ref}} + \frac{3}{128 \nu v_f^5} \quad (6.47)$$

is the EH contribution, where we have also included the reference time and phase t'_{ref} and ϕ'_{ref} , which have been redefined in order to absorb terms that depend on v_{ref} ; and

$$\begin{aligned} \psi_{\text{SPA}}^{I_1+I_2}(t_f) &= -\frac{3}{128 \nu v_f^5} \left[156 \frac{\alpha_2}{(GM)^4} v_f^{10} - \frac{545 \alpha_1 + (665 - 850 \nu) \alpha_2}{14(GM)^4} v_f^{12} \right] , \\ \psi_{\text{SPA}}^{\text{tidal}}(t_f) &= -\frac{3}{128 \nu v_f^5} \left\{ 24 \frac{v_f^{10}}{(GM)^4} (8(12\lambda_{12} + \lambda'_{12}) + 12\eta_{12} + \eta'_{12}) \right. \\ &\quad \left. - \frac{10}{7} \frac{v_f^{12}}{(GM)^4} [4((91 - 170\nu)\lambda_{12} - 6\lambda'_{12}) - 5(17\nu + 37)\eta_{12} - 9\eta'_{12}] \right\} , \end{aligned} \quad (6.48)$$

are the new contributions due to cubic and tidal perturbations. Similarly to our comment after (6.34), we note that all the terms at leading order in velocity in (6.48) are complete, while the remaining ones would also receive further modifications from a 3PM computation of the potential and a 2PM computation of the quadrupole.

Finally, it is interesting to compare our results with those of [106]. The perturbations considered in that paper have the form

$$\mathcal{L}_8 = \beta_1 \mathcal{C}^2 + \beta_2 \mathcal{C} \tilde{\mathcal{C}} + \beta_3 \tilde{\mathcal{C}}^2 , \quad (6.49)$$

where

$$\mathcal{C} := R_{\mu\nu\rho\sigma} R^{\mu\nu\rho\sigma} , \quad \tilde{\mathcal{C}} := \frac{1}{2} R_{\mu\nu\alpha\beta} \epsilon^{\alpha\beta}{}_{\gamma\delta} R^{\gamma\delta\mu\nu} . \quad (6.50)$$

The modifications to $\psi_{\text{SPA}}(t_f)$ due to quartic interactions as found in [106] are (reinstating powers of G in the result of that paper, and converting their d_Λ into our β_1 as

defined in (6.49)),

$$\psi_{\text{SPA}}^{\text{quartic}}(t_f) = \psi_{\text{SPA}}^{\text{EH}}(t_f) + \frac{3}{128 \nu v_f^5} \left[\left(\frac{234240}{11} - \frac{522240}{11} \nu \right) \frac{\beta_1}{(GM)^6} v_f^{16} \right]. \quad (6.51)$$

Note the different dependence on v_f in the correction terms in (6.48) and (6.51), which are of $\mathcal{O}(v_f^{10})$ and $\mathcal{O}(v_f^{16})$ in the leading cubic and tidal, and quartic cases, respectively. Comparing also the powers in GM , one is naively tempted to say that the contributions coming from cubic operators as computed in this chapter should be dominant when compared to those in (6.51) stemming from quartic interaction, just as the power counting in the EFT would suggest. In directly comparing these terms however, one implicitly assumes that the cut-off scales and thus the degree of suppression within the EFT, behave in a straight forward manner, with higher powers in Riemann being more and more suppressed. On the other hand, considering the observations of [297], the cubic interactions might actually be suppressed by a higher energy scale than the quartic terms, as pointed out in [295]. It would thus be interesting to perform a comparison of our result in (6.46) to experimental data, as performed in [106] for the case of quartic perturbations in the Riemann tensor, allowing to possibly confirm or reject this suspected stronger suppression, further adding to our understanding of higher derivative interactions in a gravitational context.

Chapter 7

Rational terms from six-dimensional unitarity

The continuous search for new physics at the Large Hadron Collider (LHC) at CERN, and possibly other future collider experiments around the world, fuels a continuous demand for higher precision in the theoretical predictions. Scattering amplitudes represent the basic building blocks for such predictions, and the increasing required precision translates into the need of accessing higher orders (and possibly higher multiplicities) in the perturbative expansion. This endeavour can be roughly divided into two parts: the determination of the analytic expression of the un-integrated amplitude, and the computation of the associated integrals leading to an integrated result entering the cross-sections.

Over the last decades, on-shell methods have established themselves as the go-to technique when addressing the first question while allowing to mitigate the second issue: the systematic determination of multi-loop amplitudes usually leads to an expression in terms of a finite (possibly minimal) set of integrals which constitute an integral basis, knowledge of the basis integrals then entails complete knowledge of the integrated amplitude. However unitarity techniques are blind to a very specific type of contribution which may be present in a loop amplitude. These are the *rational terms*, as opposed to the remainder of the amplitude which we call cut-constructible. Rational terms have no discontinuity in any kinematic channel and thus cannot be probed through a cut in any of the kinematic invariants. An example of such a structure is given in (3.40).

The computation of rational terms has been addressed in several different ways, for example one can make use of factorisation to establish a recursion relation that allows to reconstruct rational terms [178, 224] (see [357, 358] for an elegant applications to two-loop amplitudes in pure Yang-Mills). Another approach is to shift the dimensionality of internal states in the loop away from four dimensions [109, 110] where rational terms

acquire a singularity which can then be detected using unitarity cuts. Multiple cuts have also been used efficiently in this context [179, 359, 226]. This method requires that the internal lines, corresponding to virtual particles, are kept in $d = 4 - 2\epsilon$ dimensions, while momenta and polarisation vectors of external particles live in four dimensions. Keeping the dimensionality of the internal loop-momentum space arbitrary allows to access directly the dependence of the amplitude on d and thus on the regulator ϵ when dimensional regularisation is used, but there are compelling reasons to perform the calculation in fixed integer dimensions instead.

The first reason is that integer dimensions allow for the use of a spinor-helicity formalism, which typically allows to express the tree-level seeds of the multi-loop calculation in a simpler way thus leading to simpler integrands. Furthermore, analytic results are usually preceded by numerical ones, since the latter are where modern-day computers really excel: however it is clear that no numeric computation can be done in an arbitrary non-integer dimension. Nowadays numeric results have acquired an even more important role, since in many instances it is possible to make use of exact numeric results on finite fields to reconstruct full analytic expressions, see [182, 183] for some pioneering work in this regard. The combination of unitarity methods with numerical techniques has led to many notable results [130–134, 136, 360–364].

The key idea we will build upon here to obtain complete loop-level results is that of *dimensional reconstruction* [111–115]. In this approach, one investigates the dependence of the loop amplitudes on the dimensionality of spacetime, which turns out to be polynomial in pure Yang-Mills theory. Then one computes the amplitudes with virtual particles kept in integer dimension $d > 4$ to fix the coefficients in the polynomial by interpolation, which leads by analytic continuation to an expression valid for any non-integer dimension d . The dimensional reconstruction approach can also be effectively combined with the spinor-helicity formalism in six dimensions of [152], which allows for compact expressions of the on-shell building blocks. At higher loops, these techniques were used in [365] to derive the five-point all-plus gluon amplitude integrand in pure Yang-Mills, a generalisation to incorporate fermions was carried out in [366] and then applied in some of the already mentioned results obtained through numerical methods, see for example [132].

In this chapter we study the application of dimensional reconstruction to form factors of operators of the form $\text{Tr } F^n$, for $n = 2, 3, 4$, both for minimal and non-minimal form factors up to four external gluons. Modern amplitude techniques were applied to form factors of $\text{Tr } F^2$, which compute the leading contribution to Higgs + multi-gluon amplitudes in the effective Lagrangian approach, including MHV diagrams [154, 367] at tree level [368, 369] and one loop [370], and a combination of one-loop MHV diagrams and recursion relations [371]. Recent work [372–376] addressed the computation

of the four-dimensional cut-constructible part of Higgs+multi-gluon scattering from operators of mass dimension seven using generalised unitarity [17, 12] applied to form factors [41, 43, 47–49, 374–383]. The key point of this chapter is that we show how to extend dimensional reconstruction to any form factor of operators involving vector fields, which requires the subtraction of form factors of an appropriate class of scalar operators that we identify. Furthermore, we discuss how to generalise the procedure both for amplitudes and form factors beyond two-loop order while still carrying out the computation in a single fixed integer dimension.

7.1 Six-dimensional spinor-helicity formalism

Here we briefly review the six-dimensional spinor-helicity formalism. The construction and applications of the formalism are rather similar to its four-dimensional equivalent, the main difference being that due to the $SO(4)$ little-group structure even the bracket shorthand notation requires the use of additional explicit indices. Since we will be using this formalism essentially as a computational tool, we will not go into too much detail here but focus rather on highlighting key identities and fixing the conventions. For a more complete discussion of the topic we refer the interested reader to [152].

7.1.1 Helicity Spinors in Six Dimensions

In six-dimensional Minkowski spacetime, the Lorentz group is $SO(1,5)$, whose universal covering group is $SL(2, \mathbb{H})$, and we will denote it as $SU^*(4)$. Indeed, its representations are in one-to-one correspondence to those of $SU(4)$, which is the universal covering of $SO(6)$. The six-dimensional little group is $\widetilde{SO}(4) \simeq SU(2) \times SU(2)$.

Let us denote with \square^A and \square_A the objects transforming respectively in the fundamental and anti-fundamental representations of the Lorentz group $SU^*(4)$ and (a, \dot{a}) the indices of the bi-fundamental representations of the two components of the little group. The Clifford algebra is defined by

$$\{\gamma^\mu, \tilde{\gamma}^\nu\}_A{}^B := \gamma_{AC}^\mu \tilde{\gamma}^{\nu CB} + \gamma_{AC}^\nu \tilde{\gamma}^{\mu CB} = 2\eta^{\mu\nu} \delta_A^B, \quad (7.1)$$

where $\mu = 0, \dots, 6$, $\gamma_{AB}^\mu \equiv \gamma_{[AB]}^\mu$ and $\tilde{\gamma}^{\mu AB} \equiv \tilde{\gamma}^{\mu[AB]}$. These gamma matrices transform in the pseudo-real representation $\mathbf{6} = \mathbf{4} \wedge \mathbf{4}$ of $SU^*(4)$ and are related by

$$\tilde{\gamma}^{\mu AB} = (\gamma_{AB}^\mu)^* = \frac{1}{2} \epsilon^{ABCD} \gamma_{AB}^\mu. \quad (7.2)$$

Six-dimensional momenta can be written as

$$p_{AB} := p_\mu \gamma_{AB}^\mu, \quad (7.3)$$

and also transform in the **6** representation. The massless condition on the momenta reads

$$p^2 \sim \epsilon^{ABCD} p_{AB} p_{CD} = 0 , \quad (7.4)$$

which can be solved by expressing the momentum as the bi-spinor

$$p_{AB} = \epsilon^{\dot{a}\dot{b}} \tilde{\lambda}_{\dot{a}A} \tilde{\lambda}_{\dot{b}B} = \tilde{\lambda}_{\dot{a}A} \tilde{\lambda}_{\dot{b}B} , \quad (7.5)$$

where $\tilde{\lambda}_{\dot{a}A}$ is a pseudo-real spinor. Analogously, we can write

$$p^{AB} = \lambda^{aA} \lambda_a^B = -\epsilon^{ab} \lambda_a^A \lambda_b^B , \quad (7.6)$$

which satisfies

$$p^{AB} = (p_{AB})^* = -\frac{1}{2} \epsilon^{ABCD} p_{CD} . \quad (7.7)$$

Notice that, given the above definitions, the spinors λ_{aA} and $\tilde{\lambda}_{\dot{a}A}$ *automatically* satisfy the Dirac equation:

$$p_{AB} \lambda_a^B = -\frac{1}{2} \epsilon_{ABCD} \lambda_a^B \lambda^{bC} \lambda_b^D = -\epsilon_{ABCD} \lambda_a^B \lambda_1^C \lambda_2^D = 0 , \quad (7.8)$$

and similarly for $\tilde{\lambda}_{\dot{a}A}$. The Dirac equation can be also written equivalently as a relation between λ and $\tilde{\lambda}$:

$$0 = \lambda^{aA} \lambda_a^B \tilde{\lambda}_{B\dot{a}} = -\lambda_1^A \lambda_2^B \tilde{\lambda}_{B\dot{a}} + \lambda_2^A \lambda_1^B \tilde{\lambda}_{B\dot{a}} , \quad (7.9)$$

which implies

$$\lambda_a^A \tilde{\lambda}_{A\dot{a}} = 0 . \quad (7.10)$$

Next we need to define polarisation vectors in terms of the spinors, just as in four dimensions one has to introduce a reference spinor to do so, which we call q . Then a good definition is given by

$$\begin{aligned} \varepsilon_{\dot{a}\dot{a}}^{AB}(p, q) &= \frac{\sqrt{2}}{s_{pq}} |p_a\rangle^{[A} [p_{\dot{a}} | q^{B]} , \\ \varepsilon_{a\dot{a}AB}(p, q) &= -\frac{\sqrt{2}}{s_{pq}} [p_{\dot{a}}]_{[A} \langle p_a | q_{B]} , \end{aligned} \quad (7.11)$$

where despite the bracket notation we explicitly display the Lorentz indices A and B which are antisymmetrized.

Before moving to the relation between four- and six-dimensional quantities, we present some useful identities for six-dimensional spinors. We focus on the $SU^*(4)$ structure of

the spinors and keep the little group indices implicit for the sake of clarity, since the latter can be restored at any time being unambiguously related to each spinor.

Consider a certain number of spinors λ_i^A (and $\tilde{\lambda}_{iA}$), with labels $i = 1, \dots, n$. The Lorentz-invariant objects which can be built out of these spinors are of three types:

- Bi-spinor invariant objects:

$$\lambda_i^A \tilde{\lambda}_{jA} := \langle ij \rangle \quad (7.12)$$

- Two distinct four-spinors invariant objects:

$$\epsilon_{ABCD} \lambda_i^A \lambda_j^B \lambda_k^C \lambda_l^D := \langle ijkl \rangle, \quad \epsilon^{ABCD} \tilde{\lambda}_{iA} \tilde{\lambda}_{jB} \tilde{\lambda}_{kC} \tilde{\lambda}_{lD} := [ijkl]. \quad (7.13)$$

The spinors transform in the fundamental representation of $SU^*(4)$, thus $A = 1, \dots, 4$. Two identities (and their two complex conjugate) follow immediately from this:

$$\lambda_1^A \lambda_2^B \lambda_3^C \lambda_4^D \lambda_5^E = 0, \quad (7.14)$$

and

$$\lambda_1^A \lambda_2^B \lambda_3^C \lambda_4^D = \frac{1}{4!} \epsilon^{ABCD} \langle 1234 \rangle, \quad (7.15)$$

and analogous relations hold for $\tilde{\lambda}_{iA}$. Equations (7.14) and (7.15) can be combined to give the six-dimensional Schouten identity:

$$\sum_{\text{cyclic}} \langle 1234 \rangle \lambda_5^A = 0. \quad (7.16)$$

7.1.2 From Six-Dimensional to Four-Dimensional Quantities

For our purposes, we find it convenient to write six-dimensional spinors in terms of four-dimensional ones, allowing amplitudes to be expressed in terms of the more familiar four-dimensional spinors. We can view six-dimensional null vectors as four-dimensional massive ones, by defining the two complex mass parameters

$$m := p_4 + ip_5, \quad \tilde{m} := p_4 - ip_5, \quad (7.17)$$

where p_4 and p_5 are the fifth and the sixth components of the 6D momentum p_μ . The six-dimensional massless condition becomes then

$$p^2 = (p^{(4)})^2 - m\tilde{m} = 0. \quad (7.18)$$

where $(p^{(4)})^2 = p_0^2 - p_1^2 - p_2^2 - p_3^2$ is the four-dimensional massive momentum associated to p_μ . We found it more efficient for our calculation to describe these momenta as a

combination of two massless momenta, as in (2.36). We can decompose six-dimensional helicity spinors in terms of four-dimensional spinors as

$$\lambda_a^A = \begin{pmatrix} -\frac{m}{\langle \lambda \mu \rangle} \mu_\alpha & \lambda_\alpha \\ \tilde{\lambda}^{\dot{\alpha}} & \frac{\tilde{m}}{[\mu \lambda]} \tilde{\mu}^{\dot{\alpha}} \end{pmatrix}, \quad \tilde{\lambda}_{A\dot{a}} = \begin{pmatrix} \frac{\tilde{m}}{\langle \lambda \mu \rangle} \mu^\alpha & \lambda^\alpha \\ -\tilde{\lambda}_{\dot{\alpha}} & \frac{m}{[\mu \lambda]} \tilde{\mu}_{\dot{\alpha}} \end{pmatrix}, \quad (7.19)$$

where the little group indices label the columns and the $SU^*(4)$ indices label the rows. The $SU^*(4)$ index structure can be broken down into two $SL(2, \mathbb{C})$ complex conjugated indices:

$$\square^A = \begin{pmatrix} \square_\alpha \\ \square^{\dot{\alpha}} \end{pmatrix}, \quad \square_A = \begin{pmatrix} \square^\alpha \\ \square_{\dot{\alpha}} \end{pmatrix}. \quad (7.20)$$

This embedding is specific of our choice of gamma matrices: indeed, we choose them such that the γ -matrices restricted to $\mu = 0, \dots, 3$ reduce to the familiar chiral representation in four dimensions¹.

p^{AB} and p_{AB} are invariant under the little group $SU(2) \times SU(2)$ transformations

$$\lambda'^A_a = U_a{}^b \lambda_b^A, \quad \tilde{\lambda}'_{A\dot{a}} = U_{\dot{a}}{}^{\dot{b}} \tilde{\lambda}_{A\dot{b}}, \quad (U_a{}^b, U_{\dot{a}}{}^{\dot{b}}) \in SU(2) \times SU(2). \quad (7.21)$$

The 6D momentum in 4D components reads:

$$p^{AB} = \begin{pmatrix} -m\epsilon_{\alpha\beta} & \lambda_\alpha \tilde{\lambda}^{\dot{\beta}} + \rho \mu_\alpha \tilde{\mu}^{\dot{\beta}} \\ -\tilde{\lambda}^{\dot{\alpha}} \lambda_\beta - \rho \tilde{\mu}^{\dot{\alpha}} \mu_\beta & \tilde{m} \epsilon^{\dot{\alpha}\dot{\beta}} \end{pmatrix}, \quad (7.22)$$

where $\rho = \frac{m\tilde{m}}{\langle \lambda \mu \rangle [\mu \lambda]}$. We notice that m and \tilde{m} completely fix the diagonal components, thus they are little group invariant objects. In our choice of gamma matrices, the off-diagonal components precisely coincide with the 4D massive momentum:

$$p_{\alpha\dot{\alpha}}^{(4)} = \lambda_\alpha \tilde{\lambda}^{\dot{\alpha}} + \rho \mu_\alpha \tilde{\mu}^{\dot{\alpha}}, \quad (p^{(4)})^2 = m\tilde{m}. \quad (7.23)$$

It is easy to see that the two copies of $SU(2)$ of the 6D little group act in an identical way on the 4D momenta and we recover the usual massive little group: indeed, they depend only on the combination $m\tilde{m}$ and we can obtain dotted transformations from the undotted by simply replacing

$$m \longrightarrow -\tilde{m}, \quad \tilde{m} \longrightarrow -m. \quad (7.24)$$

The Lorentz-invariant quantities $\langle i_a j_{\dot{a}} \rangle$, $\langle i_a j_b k_c l_{\dot{d}} \rangle$, $[i_{\dot{a}} j_b k_c l_{\dot{d}}]$ can be written in terms of four-dimensional angle and square brackets, once the helicity indices are fixed ($a, b, c, d = 1, 2$ and $\dot{a}, \dot{b}, \dot{c}, \dot{d} = \dot{1}, \dot{2}$), by using the decomposition given in (7.20) and decompos-

¹For the explicit basis of gamma matrices see Appendix A of [152].

ing $\epsilon_{ABCD} \sim \sum \epsilon^{\alpha\beta} \epsilon_{\dot{\alpha}\dot{\beta}}$ and $\delta_B^A = \text{diag}(\delta_\alpha^\beta, \delta_{\dot{\beta}}^{\dot{\alpha}})$. For a concrete example of how four-dimensional amplitudes are encoded in six-dimensional ones we refer to Appendix C.1, where in particular we discuss how the choice of the little group indices relates to four-dimensional helicity structures.

7.2 The Dimensional Reconstruction Technique

In the first part of the section, we look at the one-loop case from a different perspective which lends itself to a systematic generalisation to form factors. The viewpoint we adopt presents the much desirable advantage that it disentangles the number of dimensions in which amplitudes need to be computed from the loop order. This feature allows for a natural generalisation to any loop order, for both amplitudes and form factors, which will be discussed in the second part of the section.

7.2.1 One-Loop Dimensional Reconstruction

The first step in our study is to identify the dependence of the loop amplitude on the dimensionality of the spacetime. In the literature, a common procedure is to distinguish the two sources of this dependence:

- the first is the number of spin-eigenstates, which is a function of the dimension of the spacetime d_s (for example, gluons have $d_s - 2$ spin degrees of freedom);
- the second is the integration over the loop momentum, which lives in a d -dimensional space.

Specifically, in the following we consider pure Yang-Mills theory

$$\mathcal{L}_{d_s} = -\frac{1}{4}(F_{\mu\nu}^a F^{a\mu\nu})(x), \quad (7.25)$$

where $A^{a\mu}$ is a vector in a spacetime of dimension d_s and x is defined on a spacetime of dimension $d > 4$.

As we mentioned earlier, we are interested in calculating amplitudes (and form factors) involving four-dimensional external gluons. At one loop it is possible to write a general amplitude as

$$\mathcal{A}_{(d_s, d)}^{(1)}(\{p_i, h_i\}) = \int \frac{d^d l}{(2\pi)^d} \frac{\mathcal{N}^{d_s}(\{p_i, h_i\})}{\prod_i D_i}, \quad (7.26)$$

where $\mathcal{N}^{d_s}(\{p_i, h_i\})$ depends on d_s through the number of spin eigenstates and on d through the loop momentum. However, since all external momenta are four-dimensional, the additional components of the loop momentum enter the amplitude only through

its square, which can always be written as

$$l^2 = l_0^2 - l_1^2 - l_2^2 - l_3^2 - \sum_{i=4}^{d-1} l_i^2 := (l^{(4)})^2 - \mu^2. \quad (7.27)$$

The dependence of the amplitude on μ^2 manifests itself in a number of additional integrals with non-trivial numerators, which have to be added to the usual master integral basis. These integrals have the form:

$$\int \frac{d^d l}{(2\pi)^d} \frac{\mu^{2p}}{D_1 \cdots D_n} := I_n^d[\mu^{2p}], \quad (7.28)$$

which can be evaluated as ordinary integrals, but in higher dimensions [110]. The presence of these integrals cannot be probed using four-dimensional unitarity cuts.

Consider now the explicit dependence of the amplitude on d_s . One-loop amplitudes involving only bosons are *linear* in d_s , because it appears only in a closed loop of contracted metric tensors coming from vertices and propagators. Consequently, in order to determine the dependence of the amplitude on d_s , only two constants need to be fixed and these can be obtained by interpolation. Thus it is sufficient to compute the amplitude in two integer dimensions, for example d_0 and $d_1 = d_0 + 1$, and then write the analytic continuation to four dimensions in the Four Dimensional Helicity (FDH) scheme [227, 384]. The result of the interpolation is given by [111]:

$$\mathcal{A}_{(4,d)}^{(1)} = (d_1 - 4)\mathcal{A}_{(d_0,d)}^{(1)} - (d_0 - 4)\mathcal{A}_{(d_1,d)}^{(1)}. \quad (7.29)$$

By definition d are the dynamical dimensions of the theory and we can always choose $d_0 \geq d$. By doing so we can consider the extra dimension in the d_1 -dimensional space as non-dynamical. Then a d_1 -dimensional gluon behaves as a d_0 -dimensional one plus a real scalar $A^{a\mu} = (A^{a\hat{\mu}}, \phi^a)$, and the Lagrangian of the system reads²

$$\mathcal{L}_{d_i} = -\frac{1}{4}F_{\mu\nu}^a F^{a\mu\nu} = -\frac{1}{4}F_{\hat{\mu}\hat{\nu}}^a F^{a\hat{\mu}\hat{\nu}} + \frac{1}{2}D_{\hat{\mu}}\phi^a D^{\hat{\mu}}\phi^a, \quad (7.30)$$

where the hatted quantities refer to d_0 -dimensional Lorentz indices. From the Lagrangian (7.30) we arrive at the conclusion that the one-loop d_i -dimensional amplitude $\mathcal{A}_{(d_i,d)}$ can be expressed as the sum of two contributions: the first contribution is given by the equivalent one-loop gluon amplitude with internal particles living in d_0 dimensions $\mathcal{A}_{(d_0,d)}$; the second one, denoted in the following as $\mathcal{A}_{(d)}^S$, takes into account also scalar interactions coming from the second term on the right-hand side of (7.30). It is also important to stress that $\mathcal{A}_{(d)}^S$ is a gauge-invariant quantity in its own right. As a

²The fields are non-dynamical in the d_1 -dimensional direction of the space-time, thus we can set $\partial_{d_0} A^{a\mu} = 0$ and $\partial_{d_0} \phi^a = 0$ ($\partial_{d_0} = \partial_{d_1-1}$).

result of these observations, (7.29) can be written as:

$$\mathcal{A}_{(4,d)}^{(1)} = \mathcal{A}_{(d_0,d)}^{(1)} - (d_0 - 4)\mathcal{A}_{(d)}^S . \quad (7.31)$$

Since we are considering only the one-loop order, it is easy to see that $\mathcal{A}_{(d)}^S$ can be obtained by trading the gluon loop for a scalar loop.

Up to some additional considerations, the above discussion holds true for form factors as well, and so does (7.31). In particular, the scalar quantity that we have to subtract from the form factor with d_0 -dimensional internal gluons is obtained by trading the gluon loop with a scalar one. However, in contradistinction with the amplitude case, there are two sources for scalars when we are dealing with form factors. Inside the loop, one can have scalars coupled to gluon lines coming from terms of the form $\frac{1}{2}D_\mu\phi^a D^\mu\phi^a$ in the dimensionally-reduced Lagrangian (as in the case of amplitudes), but also scalars coming from the operator inserted in the form factor. This procedure will be clear in the calculation of the non-minimal $\text{Tr } F^2$ form factor, described in Section 7.4.2, where we will emphasise the role of these two distinct contributions (see also [113]).

Finally, what we need is to identify the scalar operator. The procedure we follow is reminiscent of dimensional reduction, which for the operator $\text{Tr } F^2$ was performed in (7.30). From this new point of view, the generalization of the Dimensional Reconstruction technique to other operators is straightforward. In particular, for the only two operators with mass-dimension six involving solely gluons, namely $\text{Tr}(DF)^2$ and $\text{Tr } F^3$, the scalar contribution comes from

$$D_\mu F_{\nu\rho}^a D^\mu F^{a\nu\rho} \mapsto D_\mu D_\nu \phi^a D^\mu D^\nu \phi^a , \quad (7.32)$$

and

$$f^{abc} F^a{}_\mu{}^\nu F^b{}_\nu{}^\rho F^c{}_\rho{}^\mu \mapsto f^{abc} D_\mu \phi^a D_\nu \phi^b F^{c\mu\nu} , \quad (7.33)$$

where scalar operators associated to each operator come from the dimensional reduction from d_1 to d_0 . On the other hand for the $\text{Tr } F^4$ operator, which we will consider later in this chapter, at one-loop we get

$$\text{Tr } F^\mu{}_\nu F^\nu{}_\rho F^\rho{}_\sigma F^\sigma{}_\mu \mapsto \text{Tr } D_\mu \phi D_\nu \phi F^\nu{}_\rho F^{\rho\mu} , \quad (7.34)$$

where in the last equation the trace is in colour space³. The proportionality coefficients are still to be fixed and we will give the right prescription for them within the full tree-level calculation in Section 7.3.

³We emphasise that (7.34) is exactly the scalar operator up to an overall factor, which has still to be fixed. In particular, the two scalars in the previous operator have to be adjacent, because the gluon operator involves only contractions between adjacent field strength.

7.2.2 An L -loop Generalisation

The arguments leading to (7.29) can be extended to arbitrary loop order. Considering pure Yang-Mills theory, any L -loop amplitude can be written as a degree L polynomial in the dimension d_s ⁴,

$$\mathcal{A}_{(d_s,d)}^{(L)} = \sum_{i=0}^L (d_s - 4)^i \mathcal{K}_i, \quad (7.35)$$

where \mathcal{K}_i are quantities to be determined. In particular, note that the four-dimensional amplitude in the FDH scheme [227, 384] coincides with the zero-degree coefficient: $\mathcal{K}_0 = \mathcal{A}_{(4,d)}^{(L)}$. In order to find the coefficients \mathcal{K}_i , we can interpolate the polynomial in $L + 1$ distinct integer dimensions $d_i > 4$. Writing the problem in matrix form, one has

$$\begin{pmatrix} \mathcal{A}_{(d_0,d)}^{(L)} \\ \mathcal{A}_{(d_1,d)}^{(L)} \\ \vdots \\ \mathcal{A}_{(d_L,d)}^{(L)} \end{pmatrix} = \begin{pmatrix} 1 & (d_0 - 4) & (d_0 - 4)^2 & \cdots & (d_0 - 4)^L \\ 1 & (d_1 - 4) & (d_1 - 4)^2 & \cdots & (d_1 - 4)^L \\ \vdots & \vdots & \vdots & \ddots & \vdots \\ 1 & (d_L - 4) & (d_L - 4)^2 & \cdots & (d_L - 4)^L \end{pmatrix} \begin{pmatrix} \mathcal{K}_0 \\ \mathcal{K}_1 \\ \vdots \\ \mathcal{K}_L \end{pmatrix}, \quad (7.36)$$

where we recognise the Vandermonde matrix. Inverting this matrix, it is possible to express the \mathcal{K}_i as functions of the higher-dimensional amplitudes $\mathcal{A}_{(d_i,d)}^{(L)}$ for $i = 0, \dots, L$. In particular \mathcal{K}_0 , which is the four-dimensional amplitude we are interested in, can be written as

$$\mathcal{A}_{(4,d)}^{(L)} = \mathcal{K}_0 = \prod_{j=0}^L (d_j - 4) \sum_{i=0}^L \frac{1}{(d_i - 4)} \prod_{\substack{k=0 \\ k \neq i}}^L \frac{1}{(d_k - d_i)} \mathcal{A}_{(d_i,d)}^{(L)}. \quad (7.37)$$

We can always choose $d_0 > 4$ to be the smallest dimension among the d_i 's, and we also know that at most d dimensions are dynamical, with $4 < d \leq d_0$. Then, we can write the Lagrangian of pure Yang-Mills theory in $d_i > d_0$ dimensions as:

$$\mathcal{L}_{d_i} = -\frac{1}{4} F_{\mu\nu}^a F^{a\mu\nu} + \frac{1}{2} \sum_{i=1}^{d_i-d_0} D_\mu \phi_i^a D^\mu \phi_i^a - \frac{\lambda}{2} f^{abc} f^{ade} \sum_{\substack{i,j=1 \\ j>i}}^{d_i-d_0} \phi_i^b \phi_j^c \phi_i^d \phi_j^e, \quad (7.38)$$

where μ, ν are d_0 -dimensional Lorentz indices, a, b, c are colour indices and f^{abc} are the structure constants of the gauge group. The vector field in d_i dimensions is decomposed in a (d_0 -dimensional) vector A_μ^a and $d_i - d_0$ scalars ϕ_i^a . The coupling of the ϕ^4 interaction is given by

$$\lambda = g^2, \quad (7.39)$$

⁴As already mentioned, the d_s dependence comes from traces of η tensors, and there can be at most L closed loops leading to such a trace.

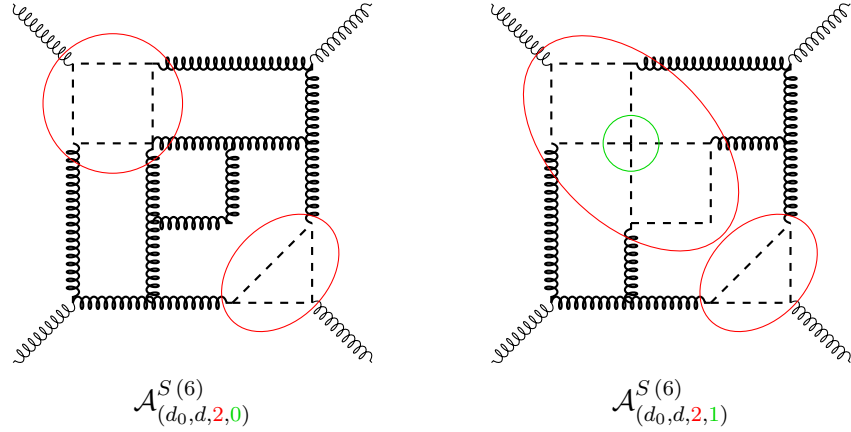


Figure 7.1: Two of the many possible diagrams contributing to the scalar amplitudes at six loops. On the left-hand side an example contribution to $\mathcal{A}_{(d_0, d, 2, 0)}^{S(6)}$ is shown. On the right-hand side the same diagram but with one of the gluon loops involving a four-point interaction replaced by a scalar. The latter diagram contributes to $\mathcal{A}_{(d_0, d, 2, 1)}^{S(6)}$.

and we call it λ for reasons that will be clear in a moment.

From (7.38), we can compute the amplitude with only external gluons⁵

$$\mathcal{A}_{(d_i, d)}^{(L)} = \mathcal{A}_{(d_0, d)}^{(L)} + \sum_{m=0}^{L-1} (d_i - d_0 - 1)^m \sum_{n=1}^{L-m} (d_i - d_0)^n \mathcal{A}_{(d_0, d, n, m)}^{S(L)}, \quad (7.40)$$

where $\mathcal{A}_{(d_0, d)}^{(L)}$ is the complete L -loop amplitude where all the internal legs are vectors and $\mathcal{A}_{(d_0, d, n, m)}^{S(L)}$ are specific combinations of diagrams with at least one scalar loop. Specifically, the diagrams contributing to $\mathcal{A}_{(d_0, d, n, m)}^{S(L)}$ are of order λ^m , *i.e.* they contain m four-scalar interactions, and in addition have n distinct purely scalar subdiagrams.

The coefficients for the scalar contributions in (7.40) can be understood as follows.

1. The number of distinct flavours of scalars is $d_i - d_0$ and they all give the same contribution.
2. Given a set of contiguous scalar propagators inside a diagram, when we draw the first scalar propagator, we need to multiply the diagram by a $d_i - d_0$ factor, corresponding to the distinct possible flavours.
3. Inside the same set of contiguous scalar propagators, each vertex with two scalars and one vector must preserve the scalar flavour, while the four-scalar vertex changes it. Thus each power of λ brings a $d_i - d_0 - 1$ factor.
4. Every distinct set of scalar propagators leads to an additional $d_i - d_0$ factor.

⁵In this section, for the sake of clarity, we reserve the word *vector* only for the d_0 -dimensional vector, whereas we refer to the four-dimensional equivalents as gluons.

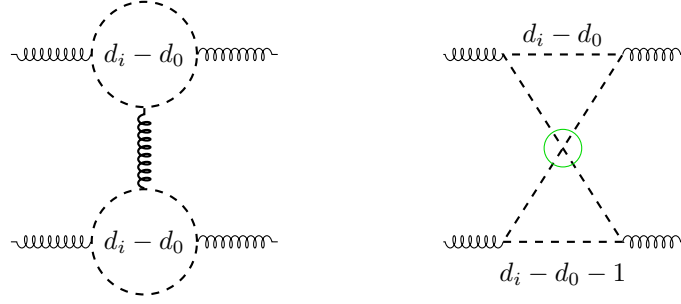


Figure 7.2: Two two-loop diagrams for comparison. In the first case there are two disconnected scalar loops, and every loop admits $d_i - d_0$ different flavours leading to an overall factor $(d_i - d_0)^2$. The second diagram represents two scalar loops connected by a flavour-changing four-scalar vertex (highlighted in green). In this case there are $d_i - d_0$ allowed flavours in one loop but only $d_i - d_0 - 1$ in the second loop, which leads to an overall factor $(d_i - d_0)(d_i - d_0 - 1)$.

5. Since there are no external scalars, the number of distinct sets of scalar propagators plus the number of scalar quartic interactions coincides with the number of scalar loops:

$$n + m = \# \text{ scalar loops} \quad (7.41)$$

6. Clearly the number of scalar loops can be at most L .

We can substitute (7.40) in (7.37) and, for simplicity, we choose

$$d_i = d_0 + i \quad (7.42)$$

with $i = 0, \dots, L$. The final result should not depend on this choice, because the coefficient of a polynomial cannot depend on which point we choose for the fitting. After some manipulations, we find a closed expression which relates complete L -loop four-dimensional amplitudes to the same amplitudes in a higher integer dimension d_0 up to subtractions of scalar contribution:

$$\mathcal{A}_{(4,d)}^{(L)} = \mathcal{A}_{(d_0,d)}^{(L)} + \sum_{m=0}^{L-1} \sum_{n=1}^{L-m} (4 - d_0)^n (3 - d_0)^m \mathcal{A}_{(d_0,d,n,m)}^{S(L)}, \quad (7.43)$$

where, in order to prove this formula, we have used the identity

$$\sum_{i=0}^L \frac{1}{(d_i - 4)} \prod_{\substack{k=0 \\ k \neq i}}^L \frac{1}{(d_k - d_i)} = \prod_{j=0}^L \frac{1}{(d_j - 4)}. \quad (7.44)$$

The whole reasoning can be applied to a more generic scheme where $d_s = 4$ (FHV scheme) is replaced by a generic d_s (e.g. the HV scheme [385] with $d_s = 4 - 2\epsilon$). As long as we keep $d_i > d_s$ and $d_i \geq d$, all the previous steps are still applicable, and we

arrive at

$$\mathcal{A}_{(d_s,d)}^{(L)} = \mathcal{A}_{(d_0,d)}^{(L)} + \sum_{m=0}^{L-1} \sum_{n=1}^{L-m} (d_s - d_0)^n (d_s - d_0 - 1)^m \mathcal{A}_{(d_0,d,n,m)}^{S(L)}, \quad (7.45)$$

which at first sight is identical to (7.40). The non-trivial difference between the two expressions is that $d_s < d_0$, while we need $d_i > d_0$ ($i = 1, \dots, L$) in order to write (7.40). Moreover, as we stressed before, the quantity $(d_i - d_0)$ has a precise physical meaning: it is the number of distinct flavours of scalars in the dimensional reduced theory (7.38). On the other hand, $(d_s - d_0)$ takes into account the number of extra spin degrees of freedom in dimensional regularisation⁶.

A posteriori, the fact that the two expressions are exactly the same is a consequence of our previous considerations. Indeed, one could have recognised the polynomial dependence of the amplitude on the dimensionality d_s already from (7.40), and further identified (7.45) as its analytic continuation for $d_s - d_0 < 0$. Thus, starting from the dimensionally reduced Lagrangian (7.38), the dependence on the dimensionality d_s emerges naturally, and the preceding considerations relating the d_i to d_s through the Vandermonde matrix may appear redundant. However, starting from the analysis of the dimensional dependence of the amplitudes provides a clear physical picture of the relation between d_s , d and d_i .

Our expression reproduces the known results at one loop [111]

$$\mathcal{A}_{(d_s,d)}^{(1)} = \mathcal{A}_{(d_0,d)}^{(1)} + (d_s - d_0) \mathcal{A}_{(d_0,d,0,1)}^{S(1)}, \quad (7.46)$$

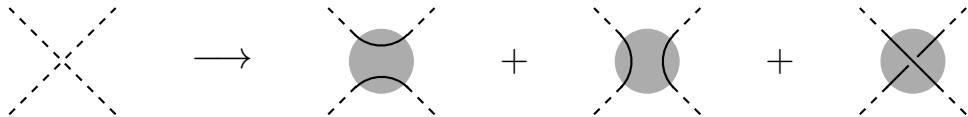
and two loops [365]

$$\mathcal{A}_{(d_s,d)}^{(2)} = \mathcal{A}_{(d_0,d)}^{(2)} + (d_s - d_0) \Delta_{(d_0,d)}^S + (d_s - d_0)^2 \Delta_{(d_0,d)}^{2S}, \quad (7.47)$$

where

$$\Delta_{(d_0,d)}^S = \mathcal{A}_{(d_0,d,0,1)}^{S(2)} - \mathcal{A}_{(d_0,d,1,1)}^{S(2)}, \quad \Delta_{(d_0,d)}^{2S} = \mathcal{A}_{(d_0,d,0,2)}^{S(2)} + \mathcal{A}_{(d_0,d,1,1)}^{S(2)}. \quad (7.48)$$

Considering the two-loop expression in more detail, one sees that in [365] the four-scalar vertex is interpreted in terms of three fictitious flavour contributions:



The two continuous lines in the grey blob represent the colour flow inside the vertex.

⁶There is no dynamics in the dimensions $d_i - d_0$, while this could be not true for the dimensions $d_0 - d_s$.

Considering Figure 7.2 we see that, in our interpretation, the only diagram which at two loops involves this vertex contributes with a factor $(d_s - d_0)(d_s - d_0 - 1)$. However, splitting the vertex according to colour flow as above, the contribution of the same diagram can be attributed to terms containing a factor $(d_s - d_0)^2$ as well as $(d_s - d_0)$. Taking into account this different interpretation of the four-scalar vertex, the two methods perfectly match.

We emphasise that individually each $\mathcal{A}_{(d_0, d, n, m)}^{S(L)}$ is a gauge-invariant quantity: indeed, we know that $\mathcal{A}_{(d_0, d)}^{(L)}$ is gauge invariant and the same is true for $\mathcal{A}_{(4, d)}^{(L)}$, regardless of the choice of d_0 . Since the coefficients of the scalar contributions depend on d_0 , the single $\mathcal{A}_{(d_0, d, n, m)}^{S(L)}$ must be gauge invariant by themselves.

As in the case of the one-loop procedure, (7.43) can be applied also to form factors, as far as we bear in mind that more scalar operators are involved in higher-loop calculations, in addition to those entering already at one loop. These additional terms emerge clearly from (7.38). Indeed, for the operator $\text{Tr } F^2$, beyond one-loop calculations we also need to subtract the scalar contribution from the ϕ^4 operator:

$$F_{\mu\nu}^a F^{a\mu\nu} \mapsto g^2 f^{abd} f^{acd} \phi^b \tilde{\phi}^c \phi^d \tilde{\phi}^e, \quad (7.49)$$

where ϕ and $\tilde{\phi}$ have to be scalars with different flavour. Its contribution has to be carefully taken into account in the subtraction with the right d_s -dependence. In particular, in the form factor equivalent of (7.40), its insertion brings a $(d_i - d_0)(d_i - d_0 - 1)$ coefficient, because of the flavour changing.

An equivalent reasoning is also valid for higher-dimensional operators. For example, from the dimensional reduction procedure of the $\text{Tr } F^3$ operator, we find that the additional scalar operators entering higher-loop calculations are

$$f^{abc} F^a{}_{\mu}{}^{\nu} F^{b\nu}{}_{\rho} F^{c\rho}{}_{\mu} \mapsto \begin{cases} g f^{abc} f^{ade} D_{\mu} \phi^b D^{\mu} \tilde{\phi}^c \phi^d \tilde{\phi}^e \\ g^3 f^{abc} f^{ade} f^{bfg} f^{chi} \phi^d \tilde{\phi}^e \phi^f \hat{\phi}^g \tilde{\phi}^h \hat{\phi}^i \end{cases}, \quad (7.50)$$

where the former enters the calculation at two-loop level, while the latter from three loops. We stress that ϕ , $\tilde{\phi}$ and $\hat{\phi}$ represent three different scalar flavours. Then, in the generalisation of (7.40) to form factors, the insertion of the scalar operators bring a factor of $(d_i - d_0)(d_i - d_0 - 1)$ and $(d_i - d_0)(d_i - d_0 - 1)(d_i - d_0 - 2)$ respectively. Following the same procedure one can recover the scalar operators for $\text{Tr } F^4$, which we do not write explicitly.

In the following we are going to apply this technique to one-loop calculations for form factors. We will always choose $d_0 = 6$, due to the existence of a powerful Spinor Helicity Formalism in six dimensions [152, 115].

A technical comment is in order here. In performing loop calculations, initially we treat the loop momenta as living in $d_0=6$ dimensions, instead of d . This procedure is well defined at the integrand level. Indeed, we know the functional dependence of the integrand on the $d-4$ components of the loop momenta, which appear only through rational combinations of $l_i^{(-2\epsilon)} \cdot l_j^{(-2\epsilon)}$ and μ_i^2 . Then, once we identify these combinations, we can treat the loop momenta as being d -dimensional and integrate over them⁷.

7.3 Tree-Level Form Factors

In this section we will provide all the analytic expressions of the tree-level colour-ordered form factors required for loop calculations.

The tensorial structure of the field strength in four dimensions is given by the antisymmetric product of two vector representations

$$\left(\frac{1}{2}, \frac{1}{2}\right) \wedge \left(\frac{1}{2}, \frac{1}{2}\right) = (1, 0) \oplus (0, 1) , \quad (7.51)$$

where we can choose each component to correspond to the helicity configurations ± 1 . We then define the *self-dual* component of the free field strength as⁸

$$F_{\text{SD},\alpha\dot{\alpha}\beta\dot{\beta}} := \lambda_\alpha \lambda_\beta \epsilon_{\dot{\alpha}\dot{\beta}} , \quad (7.52)$$

which has helicity -1 and transforms in the $(1, 0)$ representation of the Lorentz group⁹. Then, the *anti-self-dual* component, transforming in the $(0, 1)$ representation is

$$F_{\text{ASD},\alpha\dot{\alpha}\beta\dot{\beta}} = \epsilon_{\alpha\beta} \tilde{\lambda}_{\dot{\alpha}} \tilde{\lambda}_{\dot{\beta}} . \quad (7.53)$$

In terms of $\text{SU}^*(4)$ representations, the six-dimensional free field strength transforms in the $\mathbf{6} \wedge \mathbf{6} = \mathbf{15}$, which is the traceless part of $\mathbf{4} \otimes \bar{\mathbf{4}}$. Thus it can be written as [386]

$$F_{a\dot{a}}^{AB}{}_{CD} = \alpha \delta_{[C}^{[A} F_{a\dot{a}}{}^{B]}{}_{D]} , \quad (7.54)$$

where α is a numerical coefficient to be fixed and $F_{a\dot{a}}{}^A{}_B$ is such that $F_{a\dot{a}}{}^A{}_A = 0$ ¹⁰.

⁷It is worth mentioning that in terms of the six-dimensional spinor components the quantity mentioned above reads as follows: $l_i^{(-2\epsilon)} \cdot l_j^{(-2\epsilon)} = \frac{1}{2}(m_i \tilde{m}_j + m_j \tilde{m}_i)$ and $\mu_i^2 = m_i \tilde{m}_i$.

⁸To clarify the abuse of nomenclature, this quantity is the field strength in momentum space corresponding to a polarisation vector of given helicity.

⁹We could have used as definition the following: $F_{\text{SD},\alpha\dot{\alpha}\beta\dot{\beta}} := p_{\alpha\dot{\alpha}} \epsilon_{\beta\dot{\beta}}^- - p_{\beta\dot{\beta}} \epsilon_{\alpha\dot{\alpha}}^- = -\sqrt{2} \lambda_\alpha \lambda_\beta \epsilon_{\dot{\alpha}\dot{\beta}}$. As we can see the only difference is an overall $-\sqrt{2}$ factor.

¹⁰ $A, B, \dots = 1, \dots, 4$ are indices in the (anti)fundamental representation of $\text{SU}^*(4)$ and a, \dot{a} are indices of the six-dimensional little group (for a detailed discussion see Appendix 7.1).

In spinor helicity variables this quantity is [386]

$$F_{a\dot{a}}{}^A{}_B = \lambda_a^A \tilde{\lambda}_{\dot{a}B} , \quad (7.55)$$

which is indeed traceless thanks to the six-dimensional Dirac equation (7.10). Upon dimensionally reducing (7.55) down to four dimensions we match it with (7.52) and (7.53), which fixes the proportionality coefficient to be $\alpha = 2$.

7.3.1 Tr F^2 Form Factors

In this section we consider the operator

$$\mathcal{O}_2 := F_{\mu\nu}^a F^{\mu\nu} . \quad (7.56)$$

In four dimensions \mathcal{O}_2 splits naturally into the sum of the traces of the self-dual and the anti-self-dual components of the field strength:

$$\text{Tr } F^2 = \text{Tr } F_{\text{SD}}^2 + \text{Tr } F_{\text{ASD}}^2 . \quad (7.57)$$

It is trivial to identify these two four-dimensional components of the colour-ordered form factor:

$$\begin{aligned} F_{\mathcal{O}_2}^{(0)}(1^+, 2^+; q) &= 2[1\ 2][2\ 1] , \\ F_{\mathcal{O}_2}^{(0)}(1^-, 2^-; q) &= 2\langle 1\ 2\rangle\langle 2\ 1\rangle . \end{aligned} \quad (7.58)$$

On the other hand, the six-dimensional form factor is

$$F_{\mathcal{O}_2}^{(0)}(1_{a\dot{a}}, 2_{b\dot{b}}; q) = 2\langle 1_a\ 2_b\rangle\langle 2_b\ 1_{\dot{a}}\rangle , \quad (7.59)$$

where the definitions of the spinor brackets can be found in 7.1. Using the particular embedding of the four-dimensional into the six-dimensional space introduced in Appendix 7.1.2 we find that¹¹

$$F_{\mathcal{O}_2}^{(0)}(1_{1\dot{1}}, 2_{1\dot{1}}; q) \Big|_{4\text{D}} = F_{\mathcal{O}_2}^{(0)}(1^+, 2^+; q) , \quad F_{\mathcal{O}_2}^{(0)}(1_{2\dot{2}}, 2_{2\dot{2}}; q) \Big|_{4\text{D}} = F_{\mathcal{O}_2}^{(0)}(1^-, 2^-; q) . \quad (7.60)$$

An analogous statement is true also for amplitudes, where all the four-dimensional helicity configurations can be recovered from the six-dimensional amplitude.¹²

¹¹Four-dimensional limit here means choosing appropriate little-group indices corresponding to the desired helicity configuration in four dimensions, and then taking $m_i, \tilde{m}_i \rightarrow 0$ for any particle i .

¹²Further details on the relation between four and six-dimensional tree-level quantities can be found in Appendix C.1.

The scalar form factor is obtained from (7.30), and we find

$$F_{\mathcal{O}_{2,s}}^{(0)}(1, 2; q) = -\langle 1_a, 2_b \rangle \langle 1^a, 2^b \rangle = 2s_{12} , \quad (7.61)$$

where

$$\mathcal{O}_{2,s} \propto (D\phi)^2 := D_\mu \phi^a D^\mu \phi^a . \quad (7.62)$$

The normalisation of (7.61) has been fixed by matching the four-dimensional limit of this operator with that of the scalar components of (7.59), which must yield the same result. Of course, if one starts from the Lagrangian (7.30) and computes the minimal form factors of the two operators on the right-hand side, the resulting relative normalisation would be the same. The four-dimensional matching prescription is much faster for more complex operators. Let us stress that it would not be possible to implement the scalar subtraction just by excluding the little group components that in four dimensions behave like scalars. Indeed, this would bring us to a result which is not invariant under a little group transformation of the internal six-dimensional legs. In particular, for the subtraction we need a quantity that behaves as a scalar in six dimensions and matches the scalar components of the dimensional-reduced gluon in four dimensions, as shown in Appendix C.1.

Using BCFW recursion relation [12, 13] in six dimensions [152] we have derived the six-dimensional non-minimal form factors with three external legs at tree level, both for the gluon and the scalar operators. The results for \mathcal{O}_2 with three gluons reads

$$\begin{aligned} F_{\mathcal{O}_2}^{(0)}(1_{a\dot{a}}, 2_{b\dot{b}}, 3_{c\dot{c}}; q) &= \frac{2}{s_{23}s_{31}} \langle 1_a 2_b \rangle \langle 2_b 1_{\dot{a}} \rangle \langle 3_c | \not{p}_1 \not{p}_2 | 3_{\dot{c}} \rangle + \text{cyclic} \\ &+ 2 \left(\frac{1}{s_{12}} + \frac{1}{s_{23}} + \frac{1}{s_{31}} \right) (\langle 1_a 2_b \rangle \langle 2_b 3_{\dot{c}} \rangle \langle 3_c 1_{\dot{a}} \rangle - [1_{\dot{a}} 2_b] [2_b 3_c] [3_c 1_a]) , \end{aligned} \quad (7.63)$$

which agrees with the analogous result computed from Feynman diagrams in [113], upon some algebraic manipulation. As a further consistency check we verified that in the four-dimensional limit the different helicity components match the results of [368].

Furthermore, in the scalar subtraction we need to take into account an additional contribution, namely the form factor of the operator \mathcal{O}_2 with two external scalars and one gluon, which is different from zero. Indeed, this is given by:

$$F_{\mathcal{O}_2}^{(0)}(1, 2, 3_{c\dot{c}}; q) = -\frac{2}{s_{12}} \langle 3_c | \not{p}_1 \not{p}_2 | 3_{\dot{c}} \rangle . \quad (7.64)$$

Finally, the non-minimal scalar form factor of $\mathcal{O}_{2,s}$ can be shown to be

$$F_{\mathcal{O}_{2,s}}^{(0)}(1, 2, 3_{c\dot{c}}; q) = -\frac{2q^2}{s_{23}s_{31}} \langle 3_c | \not{p}_1 \not{p}_2 | 3_{\dot{c}} \rangle . \quad (7.65)$$

For a detailed derivation of (7.63)-(7.65) see Appendix C.2. The sum of (7.64) and (7.65) agrees with the result of [113].

7.3.2 Tr F^3 Form Factors

Consider now the operator

$$\mathcal{O}_3 := \text{Tr} F^\mu{}_\nu F^\nu{}_\rho F^\rho{}_\mu . \quad (7.66)$$

Similarly to the case of $\text{Tr} F^2$, this operator splits, in four dimensions, into a self-dual and anti-self dual part

$$\mathcal{O}_3 := \text{Tr} F^3 = \text{Tr} F_{\text{SD}}^3 + \text{Tr} F_{\text{ASD}}^3 . \quad (7.67)$$

Consequently, the only possible helicity configurations of the minimal tree-level form factors are all-plus and all-minus:

$$\begin{aligned} F_{\mathcal{O}_3}^{(0)}(1^+, 2^+, 3^+; q) &= -2[12][23][31] , \\ F_{\mathcal{O}_3}^{(0)}(1^-, 2^-, 3^-; q) &= 2\langle 12 \rangle \langle 23 \rangle \langle 31 \rangle . \end{aligned} \quad (7.68)$$

In six dimensions the minimal form factor is given by

$$\begin{aligned} F_{\mathcal{O}_3}^{(0)}(1_{a\dot{a}}, 2_{b\dot{b}}, 3_{c\dot{c}}) &= F_{1_{a\dot{a}}}^{AB}{}_{CD} F_{2_{b\dot{b}}}^{CD}{}_{EF} F_{3_{c\dot{c}}}^{EF}{}_{AB} \\ &= -\langle 1_a 2_{\dot{b}} \rangle \langle 2_b 3_{\dot{c}} \rangle \langle 3_c 1_{\dot{a}} \rangle + [1_{\dot{a}} 2_b] [2_{\dot{b}} 3_c] [3_{\dot{c}} 1_a] , \end{aligned} \quad (7.69)$$

where $F_{a\dot{a}}^{AB}{}_{CD}$ is defined in (7.54). We can obtain the corresponding scalar operator from (7.33), which states that

$$\mathcal{O}_{3,s} \propto \text{Tr}(D\phi)^2 F := \text{Tr} D_\mu \phi D_\nu \phi F^{\mu\nu} . \quad (7.70)$$

Thus

$$F_{\mathcal{O}_{3,s}}^{(0)}(1, 2, 3_{c\dot{c}}) := \frac{1}{2} p_1^{AB} p_{2CD} F_{3_{c\dot{c}}}^{CD}{}_{AB} = \langle 3_c | \not{p}_1 \not{p}_2 | 3_{\dot{c}} \rangle , \quad (7.71)$$

where, once again, the normalisation is fixed by matching the four-dimensional limits of this quantity with the scalar configuration of (7.69).

As a final remark, we point out that \mathcal{O}_3 is not the only mass-dimension six operator which appears in the Yang-Mills theories (also with matter). One also has a contribution from

$$\tilde{\mathcal{O}}_3 := D^\alpha F^{a\mu\nu} D_\alpha F_{\mu\nu}^a . \quad (7.72)$$

However, it is easy to see that the minimal form factor for $\tilde{\mathcal{O}}_3$ can be related to the one of \mathcal{O}_2 as

$$F_{\tilde{\mathcal{O}}_3}^{(0)}(1_{a\dot{a}}, 2_{b\dot{b}}; q) = s_{12} F_{\mathcal{O}_2}^{(0)}(1_{a\dot{a}}, 2_{b\dot{b}}; q) . \quad (7.73)$$

Further Lorentz contractions of two covariant derivatives and two field strengths, such as $D^\mu F_\mu^{\alpha\nu} D^\rho F_{\rho\nu}^a$, are ruled out or expressed in terms of the operators previously mentioned thanks to the equations of motion. In particular, in the case of pure Yang-Mills theory $\tilde{\mathcal{O}}_3$ can be expressed as a linear combination of \mathcal{O}_2 and \mathcal{O}_3 through the equations of motion. For a detailed discussion, see [387].

Finally, we provide the tree-level expressions needed for the one-loop computation of the non-minimal form factor of \mathcal{O}_3 which are:

- the non-minimal tree-level form factor of \mathcal{O}_3 with four gluons

$$F_{\mathcal{O}_3}^{(0)}(1_{a\dot{a}}, 2_{b\dot{b}}, 3_{c\dot{c}}, 4_{d\dot{d}}; q) = \mathcal{B}_{a\dot{a}b\dot{b}c\dot{c}d\dot{d}} + \mathcal{C}_{a\dot{a}b\dot{b}c\dot{c}d\dot{d}} + \mathcal{D}_{a\dot{a}b\dot{b}c\dot{c}d\dot{d}} , \quad (7.74)$$

with

$$\begin{aligned} \mathcal{B}_{a\dot{a}b\dot{b}c\dot{c}d\dot{d}} &= (-\langle 1_a 2_b \rangle \langle 2_b 3_c \rangle \langle 3_c 1_a \rangle + [1_{\dot{a}} 2_{\dot{b}}] [2_{\dot{b}} 3_{\dot{c}}] [3_{\dot{c}} 1_{\dot{a}}]) \frac{\langle 4_d | \not{p}_1 \not{p}_3 | 4_d \rangle}{s_{34} s_{41}} + \text{cyclic} , \\ \mathcal{C}_{a\dot{a}b\dot{b}c\dot{c}d\dot{d}} &= \frac{\langle 1_a 2_b \rangle \langle 2_b 4_d \rangle \langle 4_d 3_c \rangle \langle 3_c 1_a \rangle + [1_{\dot{a}} 2_{\dot{b}}] [2_{\dot{b}} 4_{\dot{d}}] [4_{\dot{d}} 3_{\dot{c}}] [3_{\dot{c}} 1_{\dot{a}}]}{s_{34}} + \text{cyclic} , \\ \mathcal{D}_{a\dot{a}b\dot{b}c\dot{c}d\dot{d}} &= - \left(\sum_{i=1}^4 \frac{1}{s_{i i+1}} \right) (\langle 1_a 2_b \rangle \langle 2_b 3_c \rangle \langle 3_c 4_d \rangle \langle 4_d 1_a \rangle + [1_{\dot{a}} 2_{\dot{b}}] [2_{\dot{b}} 3_{\dot{c}}] [3_{\dot{c}} 4_{\dot{d}}] [4_{\dot{d}} 1_{\dot{a}}]) \end{aligned} \quad (7.75)$$

- the non-minimal tree-level form factor of \mathcal{O}_3 with two external scalars

$$F_{\mathcal{O}_3}^{(0)}(1, 2, 3_{c\dot{c}}, 4_{d\dot{d}}; q) = \frac{1}{s_{12}} \left(\langle 3_c 4_d \rangle \langle 4_d | \not{p}_1 \not{p}_2 | 3_c \rangle - \langle 4_d 3_c \rangle \langle 3_c | \not{p}_1 \not{p}_2 | 4_d \rangle \right) \quad (7.76)$$

- the non-minimal tree-level form factor of $\mathcal{O}_{3,s}$ with two external scalars

$$\begin{aligned} F_{\mathcal{O}_{3,s}}^{(0)}(1, 2, 3_{c\dot{c}}, 4_{d\dot{d}}; q) &= \frac{\langle 3_c | \not{p}_4 \not{p}_2 | 3_c \rangle \langle 4_d | \not{p}_1 \not{p}_2 | 4_d \rangle}{s_{23} s_{34}} + \frac{\langle 4_d | \not{p}_1 \not{p}_3 | 4_d \rangle \langle 3_c | \not{p}_1 \not{p}_2 | 3_c \rangle}{s_{34} s_{41}} \\ &+ \langle 3_c | \not{p}_2 \not{p}_1 | 4_d \rangle \langle 4_d 3_c \rangle \left(\frac{1}{s_{34}} + \frac{1}{s_{23}} + \frac{1}{s_{41}} \right) \\ &- \langle 4_d | \not{p}_2 \not{p}_1 | 3_c \rangle \langle 3_c 4_d \rangle \frac{1}{s_{34}} + \langle 3_c | \not{p}_2 | 4_d \rangle [3_c | \not{p}_1 | 4_d] \left(\frac{1}{s_{23}} + \frac{1}{s_{41}} \right) . \end{aligned} \quad (7.77)$$

These formulas have been obtained by requiring the six-dimensional form factor to match, upon taking the four-dimensional limit, the known four-dimensional expressions

in different helicity configurations [372, 388, 389, 311]. The resulting ansatz was then numerically compared with the results from Feynman diagrams and a complete match was found.

7.3.3 $\text{Tr } F^4$ and Higher Dimensional Form Factors

The fourth power in the field strength can be considered as a turning point in the general behaviour of the operators, for reasons which will become clear in a moment. The first study of renormalisation properties of gluonic operators of dimension up to eight was carried out in [390] and with more recent techniques in [391]. It turns out that we can have four possible independent operators involving different contractions of four field strengths:

$$\begin{aligned} \text{Tr } F^\mu{}_\nu F^\nu{}_\rho F^\rho{}_\sigma F^\sigma{}_\mu, & \quad \text{Tr } F^{\mu\nu} F_{\mu\nu} F^{\rho\sigma} F_{\rho\sigma}, \\ \text{Tr } F^\mu{}_\nu F^\rho{}_\sigma F^\nu{}_\rho F^\sigma{}_\mu, & \quad \text{Tr } F^{\mu\nu} F^{\rho\sigma} F_{\mu\nu} F_{\rho\sigma}. \end{aligned} \quad (7.78)$$

In pure gauge theories, which we are considering in this work, all these operators can appear with independent coefficients, while they are no more independent in the low energy effective action from the superstring theory [392–394]. In this section we will focus only on the first operator, which we will refer to as $\text{Tr } F^4$:

$$\mathcal{O}_4 := \text{Tr } F^4 := \text{Tr } F^\mu{}_\nu F^\nu{}_\rho F^\rho{}_\sigma F^\sigma{}_\mu. \quad (7.79)$$

This encloses all the main features of the operators with higher powers in the field strength, and at the end of this section we will be able to generalise some results to a peculiar operator involving a consecutive chain of n field strengths.

In four dimensions the main difference between $\text{Tr } F^4$ and the lower-power cases is that the structure of this operator allows the mixing of the self- and anti-self-dual components, *i.e.* schematically

$$\text{Tr } F^4 \simeq \text{Tr } F_{\text{SD}}^4 + \text{Tr} \left(F_{\text{SD}}^2 F_{\text{ASD}}^2 \right) + \text{Tr } F_{\text{ASD}}^4. \quad (7.80)$$

Thus the usual all-plus (all-minus) minimal form factors appear along with MHV-like quantities:

$$\begin{aligned} F_{\mathcal{O}_4}^{(0)}(1^+, 2^+, 3^+, 4^+; q) &= 2[1\ 2][2\ 3][3\ 4][4\ 1], \\ F_{\mathcal{O}_4}^{(0)}(1^+, 2^+, 3^-, 4^-; q) &= [1\ 2]^2 \langle 3\ 4 \rangle^2, \\ F_{\mathcal{O}_4}^{(0)}(1^+, 2^-, 3^+, 4^-; q) &= [1\ 3]^2 \langle 2\ 4 \rangle^2, \end{aligned} \quad (7.81)$$

and all the other configurations can be obtained by symmetry and parity arguments.

In six dimensions the minimal form factor is

$$\begin{aligned}
 F_{\mathcal{O}_4}^{(0)}(1_{a\dot{a}}, 2_{b\dot{b}}, 3_{c\dot{c}}, 4_{d\dot{d}}; q) &= F_{1a\dot{a}}^{AB} F_{CD} F_{2b\dot{b}}^{CD} F_{EF} F_{3c\dot{c}}^{EF} F_{GH} F_{4d\dot{d}}^{GH} F_{AB} \\
 &\stackrel{(7.14)}{=} \langle 1_a 2_{\dot{b}} \rangle \langle 2_b 3_{\dot{c}} \rangle \langle 3_c 4_{\dot{d}} \rangle \langle 4_d 1_{\dot{a}} \rangle + [1_{\dot{a}} 2_b] [2_{\dot{b}} 3_c] [3_{\dot{c}} 4_d] [4_{\dot{d}} 1_a] \\
 &\quad + \langle 1_a 2_b 3_c 4_d \rangle [1_{\dot{a}} 2_{\dot{b}} 3_{\dot{c}} 4_{\dot{d}}] ,
 \end{aligned} \tag{7.82}$$

where we notice that at this power of the field strength the new structure $\langle \dots \rangle [\dots]$ involving four-spinor invariants appears, which is very reminiscent of the four-point amplitude. This new structure gives us the MHV-like components in (7.81) when we consider the appropriate little-group configurations in the four-dimensional limit (see Appendix C.1).

We have already identified the scalar operator associated to $\text{Tr } F^4$ in (7.34) and we define

$$\mathcal{O}_{4,s} \propto \text{Tr } D_\mu \phi D_\nu \phi F^\nu{}_\rho F^{\rho\mu} \tag{7.83}$$

such that its minimal form factor is

$$\begin{aligned}
 F_{\mathcal{O}_{4,s}}(1, 2, 3_{c\dot{c}}, 4_{d\dot{d}}; q) &= \frac{1}{2} p_1^{AB} p_{2CD} F_{3c\dot{c}}^{CD} F_{EF} F_{4d\dot{d}}^{EF} F_{AB} \\
 &= -\langle 3_c | \not{p}_2 \not{p}_1 | 4_{\dot{d}} \rangle \langle 4_d 3_{\dot{c}} \rangle + \frac{1}{4} \langle 2^a 2_a 3_c 4_d \rangle [1_{\dot{a}} 1^{\dot{a}} 3_{\dot{c}} 4_{\dot{d}}] .
 \end{aligned} \tag{7.84}$$

The expression of $\text{Tr } F^4$ gives us some insight about the operators involving the n^{th} power of the field strength, where the Lorentz indices are contracted between adjacent field strengths, which we will refer to as $\text{Tr } F^n$:

$$\mathcal{O}_n := \text{Tr } F^n = \text{Tr } F_{\mu_1}{}^{\mu_2} F_{\mu_2}{}^{\mu_3} \dots F_{\mu_{n-1}}{}^{\mu_n} F_{\mu_n}{}^{\mu_1} . \tag{7.85}$$

It is easy to show that this operator can be decomposed in a sum of double traces (in the Lorentz indices) on the self-dual and anti-self-dual parts, schematically¹³:

$$\text{Tr } F^n \simeq \sum_{i=0}^n \text{Tr} \left(F_{\text{SD}}^{n-i} F_{\text{ASD}}^i \right) . \tag{7.86}$$

Take two disjoint and ordered subsets of labels $S_+ = \{p_k\}_{k=1\dots i}$ and $S_- = \{q_k\}_{k=1\dots n-i}$, with $S_+ \cup S_- = \{1, \dots, n\}$. Then all tree level form factors, for any helicity configura-

¹³We stress that this general structure was hidden by lower power-operators because the field strength is traceless: $\text{Tr } F_{\text{SD}}^{n-1} F_{\text{ASD}} = \text{Tr } F_{\text{SD}} F_{\text{ASD}}^{n-1} = 0$.

tion, can be written in a very compact way:

$$F_{\mathcal{O}_n}^{(0)}(1^{h_1}, \dots, n^{h_n}; q) = c_{n,i} \prod_{k=1}^i [p_k p_{k+1}] \prod_{k=i+1}^n \langle q_k q_{k+1} \rangle, \quad (7.87)$$

where the overall coefficient is

$$c_{n,i} = \begin{cases} 2 & i = 0 \\ (-1)^{n-i} & i \neq 0, n \\ (-1)^n 2 & i = n \end{cases} \quad (7.88)$$

An explicit example of this general formula is given by

$$F_{\mathcal{O}_5}^{(0)}(1^-, 2^+, 3^-, 4^-, 5^+; q) = -\langle 13 \rangle \langle 34 \rangle \langle 41 \rangle [25] [52]. \quad (7.89)$$

The structure of $\text{Tr } F^n$ form factors in six dimensions is much more complicated than the four-dimensional one, the number of terms grows very fast, but nonetheless some general pattern can be observed. In particular if we restrict to a kinematic configuration for which only some of the legs are truly six dimensional and the others are defined on the embedded four-dimensional subspace, the formulae are much easier and compact. In principle, this is all we need in order to calculate rational terms with the dimensional reconstruction technique, since we need to consider only the limited number of internal loop legs as six dimensional. As an example, consider the minimal form factor of $\text{Tr } F^n$ with two six-dimensional legs and $n - 2$ four-dimensional legs in the all-plus helicity configuration. The general expression is given by

$$\begin{aligned} \text{Tr } F^n(1_{a\dot{a}}, 2_{b\dot{b}}, 3^+, \dots, n^+) &= (\langle 1_a 2_{\dot{b}} \rangle \langle 2_b 3_{\dot{1}} \rangle [34] \langle n_1 1_{\dot{a}} \rangle + [1_{\dot{a}} 2_b] \langle 2_{\dot{b}} 3_1 \rangle [34] [n_{\dot{1}} 1_a] + \\ &+ \langle 1_a 2_b n_1 3_1 \rangle [1_{\dot{a}} 2_{\dot{b}} 3_{\dot{1}} 4_{\dot{1}}]) \prod_{i=4}^{n-1} [i i + 1]. \end{aligned} \quad (7.90)$$

This result can be found by observing that the combination $\lambda_{i_a}^A \tilde{\lambda}_{i_{B\dot{a}}}$ appears only once for each six-dimensional leg, which allows to write an ansatz comprising every possible combination with arbitrary coefficients to be fixed. The coefficients can then be determined by taking the four-dimensional limit of the six-dimensional gluons and requiring the form factor to match (7.87). For the sake of comparison, if we take $n = 6$ the three terms of (7.90) come from a fully six-dimensional expression of 39 terms which has already been reduced from initial 52 terms using Schouten identity.

7.4 One-Loop Form Factors

In this section we will consider a number of one-loop applications of the dimensional reconstruction procedure discussed so far. The results obtained for the minimal form factors of $\text{Tr } F^2$ and $\text{Tr } F^3$ were already known in the literature. We prove that the latter has no rational terms, as it has also been argued by [388]. These calculations will be useful to set the stage and give an example of the procedure before dealing with more involved operators and kinematic configurations. In particular, we reproduce the known non-minimal form factor of $\text{Tr } F^2$ with three positive-helicity external gluons. Finally, we compute the complete minimal form factor of $\text{Tr } F^n$ with $n = 4$ at one loop and generalise some of the results to arbitrary n .

7.4.1 The Minimal $\text{Tr } F^2$ Form Factors

As a first proof of concept of the method we will confirm the well known statement that the minimal form factor of the operator $\text{Tr } F^2$ in pure Yang-Mills does not have any rational terms. In particular, we will consider the all-plus helicity configuration.

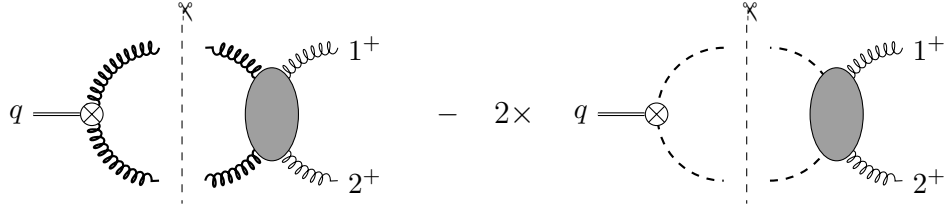


Figure 7.3: Two-particle cut of the one-loop form factor $\text{Tr } F^2$ in six dimensions.

The quantity we want to compute can be written as

$$\begin{aligned} F_{\mathcal{O}_2}^{(1)}(1^+, 2^+; q) &:= F_{\mathcal{O}_2}^{(0)}(1^+, 2^+; q) \cdot f^{(2)}(s_{12}) \\ &= 2[1\ 2][2\ 1] \cdot f^{(2)}(s_{12}) , \end{aligned} \quad (7.91)$$

where we factored out all the helicity dependence in the tree-level prefactor, and $f^{(2)}(s_{12})$ is a function only of the Mandelstam variable s_{12} . As explained in Section 7.2 this quantity can be computed using (7.31):

$$f^{(2)}(s_{12}) = f_{6\text{D}}^{(2)}(s_{12}) - 2f_{\phi}^{(2)}(s_{12}) , \quad (7.92)$$

where $f_{6\text{D}}^{(2)}(s_{12})$ and $f_{\phi}^{(2)}(s_{12})$ are the form factors with six-dimensional internal gluons or scalars respectively, normalised by the corresponding tree-level quantity.

At one loop, the two-particle cut represented in Figure 7.3 is¹⁴

¹⁴The explicit expression of \mathcal{A}_g can be found in Appendix C.1.

$$f_{6D}^{(2)}(s_{12})\Big|_{2\text{-cut}} = \frac{1}{2[1\ 2][2\ 1]} \int d\text{LIPS } F_{\mathcal{O}_2}^{(0)}(-l_1^{a\dot{a}}, -l_2^{b\dot{b}}) \mathcal{A}_g^{(0)}(l_2^{b\dot{b}}, l_1^{a\dot{a}}, 1_{1\dot{1}}, 2_{2\dot{2}}) , \quad (7.93)$$

where dLIPS is a short-hand notation for the one-loop Lorentz phase space integration, more explicitly one could set $d\text{LIPS} = d^D l / (2\pi)^D$ with $l \equiv l_1$ and $l_2 = q - l_1$, or equivalently swapping l_1 and l_2 . In order to simplify this expression we decompose the six-dimensional quantities in terms of four-dimensional ones, as explained in detail in Section 7.1.2. These calculations are rather lengthy and have been dealt with through the use of a `Mathematica` package devised during the preparation of [1] and described therein. In general, we write six-dimensional expressions in terms of $\{\lambda_{i\alpha}, \tilde{\lambda}_{i\dot{\alpha}}, \mu_{i\alpha}, \tilde{\mu}_{i\dot{\alpha}}, m_i, \tilde{m}_i\}$ with $i = 1, 2, l_1, l_2$, as explained in Appendix 7.1.2. Imposing that the external legs are defined in four dimensions is equivalent to setting $m_j = 0$ and $\tilde{m}_j = 0$ for $j = 1, 2$, which automatically removes any dependence of $f^{(2)}$ on $\mu_{j\alpha}$ and $\tilde{\mu}_{j\dot{\alpha}}$. From (7.22), momentum conservation implies

$$\sum_i m_i = 0 , \quad \sum_i \tilde{m}_i = 0 . \quad (7.94)$$

Only the two internal legs l_1 and l_2 have to be kept in six dimensions, in other words $p_i^5, p_i^6 \neq 0$ for $i = l_1, l_2$, which implies

$$m_{l_2} = -m_{l_1} := -m , \quad \tilde{m}_{l_2} = -\tilde{m}_{l_1} := -\tilde{m} , \quad (7.95)$$

where

$$\mu^2 = m\tilde{m} , \quad (7.96)$$

with μ^2 defined in (7.27). The result for the complete integrand in (7.93) is, schematically,

$$\mathcal{I} = \frac{i\langle l_1 l_2 \rangle^2 [l_2 l_1]^2}{s_{12}s_{2l_2}} + \mu^2 (4 \text{ terms}) + \mu^4 (17 \text{ terms}) + \mu^6 (5 \text{ terms}) + \mu^8 (1 \text{ term}), \quad (7.97)$$

where the Mandelstam invariants are defined in terms of six-dimensional momenta. It is important to note that the dependence on μ_i and $\tilde{\mu}_i$ is spurious and we can choose these “reference momenta” in order to cancel as many terms as possible from our result. After doing so one has to be careful in identifying the loop momenta and Mandelstam invariants consistently with this choice. A particularly convenient choice is

$$\mu_{l_1} \rightarrow \lambda_{l_2} , \quad \mu_{l_2} \rightarrow \lambda_{l_1} , \quad \tilde{\mu}_{l_2} \rightarrow \tilde{\mu}_{l_1} . \quad (7.98)$$

Doing so, we immediately arrive at

$$f_{6D}^{(2)}(s_{12})\Big|_{2\text{-cut}} = \int d\text{LIPS} \left(-i \frac{s_{12}}{s_{2l_2}} + 2i \frac{\mu^2}{s_{2l_2}} \right). \quad (7.99)$$

Next we repeat a similar computation for the two-particle cut with internal gluons replaced by scalars:

$$\begin{aligned} f_{\phi}^{(2)}(s_{12})\Big|_{2\text{-cut}} &= \frac{1}{2[1\ 2][2\ 1]} \int d\text{LIPS} F_{\mathcal{O}_{2,s}}^{(0)}(-l_1, -l_2) \mathcal{A}^{(0)}(l_2, l_1, 1_{a\dot{a}}, 2_{b\dot{b}}) \\ &= \int d\text{LIPS} i \frac{\mu^2}{s_{2l_2}}. \end{aligned} \quad (7.100)$$

Taking the difference between (7.99) and twice (7.100) leads to the desired four-dimensional result

$$f^{(2)}(s_{12})\Big|_{2\text{-cut}} = -is_{12} \int d\text{LIPS} \frac{1}{s_{2l_2}}. \quad (7.101)$$

It is important to stress that in order to perform the scalar subtraction consistently, one needs first to write both $f_{6D}^{(2)}$ and $f_{\phi}^{(2)}$ as functions of the full d -dimensional momenta and Mandelstam invariants, in order to eliminate any dependence on the choice of the arbitrary helicity spinors μ_i and $\tilde{\mu}_i$. We can directly read off the one-loop result from (7.101):

$$f^{(2)}(s_{12}) = -is_{12} \cdot q \quad \text{---} \quad \begin{array}{c} p_1 \\ \diagup \quad \diagdown \\ \quad \quad \quad | \\ \quad \quad \quad l \\ \quad \quad \quad | \\ \diagdown \quad \diagup \\ p_2 \end{array} \quad (7.102)$$

where the triangle integral with outgoing momenta (p_1, p_2, q) is defined in Appendix C.3.

As anticipated, our result (7.102) does not contain any μ^2 term *i.e.* any rational term, and is thus in agreement with the very well known result. An equivalent result holds for the all-minus helicity configuration.

7.4.2 The Non-Minimal $\text{Tr } F^2$ Form Factor

In this section we address the computation of the one-loop non-minimal form factor of the operator $\text{Tr } F^2$. As usual we begin by defining the normalised quantity $f^{(2;3)}$ as

$$F_{\mathcal{O}_2}^{(1)}(1^+, 2^+, 3^+; q) := 2[1\ 2][2\ 3][3\ 1] \cdot f^{(2;3)}(s_{12}, s_{23}, s_{13}), \quad (7.103)$$

with

$$f^{(2;3)}(s_{12}, s_{23}, s_{13}) = f_{6D}^{(2;3)}(s_{12}, s_{23}, s_{13}) - 2f_{\phi}^{(2;3)}(s_{12}, s_{23}, s_{13}), \quad (7.104)$$

Notice that we decided not to normalise by the corresponding tree-level form-factor, which carries additional non-trivial dependence on the Mandelstam variables, but simply by a factor $[1\ 2][2\ 3][3\ 1]$ which only captures the complete helicity dependence of the operator. Computing the discontinuity in the s_{12} -channel we have

$$f_{6\text{D}}^{(3)}(\{s_{ij}\})\Big|_{s_{12}\text{-cut}} = \frac{1}{2[1\ 2][2\ 3][3\ 1]} \int \text{dLIPS } F_{\mathcal{O}_2}^{(0)}(l_1^{a\dot{a}}, l_2^{b\dot{b}}, 3_{1\dot{1}}) \mathcal{A}^{(0)}(-l_2^{a\dot{a}}, -l_1^{b\dot{b}}, 1_{1\dot{1}}, 2_{2\dot{2}}), \quad (7.105)$$

which, upon making use of momentum conservation in the form of (7.95), is a 356-term expression. We make use of the redundant degrees of freedom to simplify the expression by choosing

$$\mu_{l_1} \mapsto \lambda_{l_2}, \quad \tilde{\mu}_{l_1} \mapsto \tilde{\lambda}_3, \quad \mu_{l_2} \mapsto \lambda_{l_1}, \quad \tilde{\mu}_{l_2} \mapsto \tilde{\lambda}_3, \quad (7.106)$$

which leads to

$$f_{6\text{D}}^{(3)}(\{s_{ij}\})\Big|_{s_{12}\text{-cut}} \propto \int \text{dLIPS } [3\ l_1] \langle l_1\ l_2 \rangle [l_2\ 3]. \quad (7.107)$$

Note that, after using (7.106), the last expression apparently is no longer invariant with respect to little-group transformations of l_1 and l_2 , since these transformations mix the λ and μ . In other words, looking at the numerator of (7.107), l_1 and l_2 appear as four-dimensional massless momenta, whereas they should really be massive. Hence in order to further manipulate the expression in a consistent manner we have to restore the masses, *i.e.* restore explicit little-group invariance. This is achieved by the replacement

$$\lambda_i^\alpha \tilde{\lambda}_i^{\dot{\alpha}} \mapsto \underbrace{\left(\lambda_i^\alpha \tilde{\lambda}_i^{\dot{\alpha}} + \frac{\mu^2}{\langle \lambda_i\ \mu_i \rangle [\tilde{\mu}_i\ \tilde{\lambda}_i]} \mu_i^\alpha \tilde{\mu}_i^{\dot{\alpha}} \right)}_{p_i^{(4)\ \alpha\dot{\alpha}}} - \frac{\mu^2}{\langle \lambda_i\ \mu_i \rangle [\tilde{\mu}_i\ \tilde{\lambda}_i]} \mu_i^\alpha \tilde{\mu}_i^{\dot{\alpha}}, \quad (7.108)$$

which in the particular case of (7.107) becomes

$$|l_1\rangle [l_1] \mapsto I_1^{(4)} - \frac{\mu^2}{\langle l_1\ l_2 \rangle [3\ l_1]} |l_2\rangle [3], \quad |l_2\rangle [l_2] \mapsto I_2^{(4)} - \frac{\mu^2}{\langle l_2\ l_1 \rangle [3\ l_2]} |l_1\rangle [3], \quad (7.109)$$

where the replacements (7.106) have already been applied. After this substitution and some further manipulation, (7.107) becomes

$$f_{6\text{D}}^{(2;3)}(s_{12}, s_{23}, s_{13})\Big|_{s_{12}\text{-cut}} = i \frac{[1\ 2]}{[2\ 3][3\ 1]} \int \text{dLIPS } [3] I_1^{(4)} I_2^{(4)} [3] \mathcal{I}_{6\text{D}}^{(2;3)}, \quad (7.110)$$

where

$$\mathcal{I}_{6\text{D}}^{(2;3)} = \frac{q^4 s_{12} - 2\mu^2 q^2 s_{12} - 4\mu^2 s_{3l_1} s_{3l_2}}{s_{12}^2 s_{2,-l_2} s_{3l_1} s_{3l_2}}. \quad (7.111)$$

Performing the appropriate scalar subtraction for the non-minimal configuration of the operator $\text{Tr } F^2$ is more subtle than in the minimal case. The double cut one needs to compute is represented in Figure 7.4. There are two different tree-level form factors to

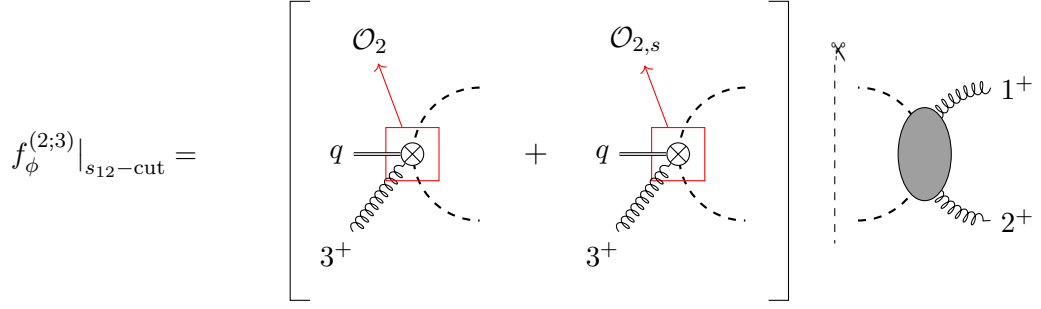


Figure 7.4: A double cut of the scalar contribution to $\text{Tr } F^2$ non-minimal. The red boxes highlight the two different operator insertions.

be inserted into the cut: the non-minimal form factors with two external scalars and one gluon of the operators $\text{Tr } F^2$ and $(D\phi)^2$. The tree-level expression for these form factors are given in (7.64) and (7.65) respectively. Computing the complete result for the double-cut of the scalar contribution leads to

$$f_\phi^{(2;3)}(s_{12}, s_{23}, s_{13})|_{s_{12}\text{-cut}} = i \frac{[1\ 2]}{[2\ 3][3\ 1]} \int \text{dLIPS} [3|I_1^{(4)} I_2^{(4)}|3] \mathcal{I}_\phi^{(2;3)}, \quad (7.112)$$

with

$$\mathcal{I}_\phi^{(2;3)} = -\mu^2 \frac{q^2 s_{12} + s_{3l_1} s_{3l_2}}{s_{12}^2 s_{2,-l_2} s_{3l_1} s_{3l_2}}. \quad (7.113)$$

Upon subtracting twice (7.112) from (7.110), uplifting the cut and performing some algebraic manipulations on the numerator, one ends up with the final expression:

$$\begin{aligned} f^{(2,3)}(s_{12}, s_{23}, s_{13})|_{s_{12}\text{-disc}} = & -\frac{iq^4}{2s_{31}} \begin{array}{c} q \quad p_1 \\ \diagdown \quad \diagup \\ \square \\ \diagup \quad \diagdown \\ p_3 \quad p_2 \end{array} - \frac{iq^4}{2s_{23}} \begin{array}{c} q \quad p_3 \\ \diagdown \quad \diagup \\ \square \\ \diagup \quad \diagdown \\ p_2 \quad p_1 \end{array} \\ & - \frac{iq^4(s_{31}+s_{23})}{s_{12}s_{23}s_{31}} \cdot \left(\begin{array}{c} p_1 \\ \diagdown \quad \diagup \\ \triangle \\ \diagup \quad \diagdown \\ p_3 \end{array} + \begin{array}{c} p_3 \\ \diagdown \quad \diagup \\ \triangle \\ \diagup \quad \diagdown \\ p_1 \end{array} \right) \\ & + \frac{4i}{s_{12}^2} \cdot \begin{array}{c} q \quad p_1 \\ \diagdown \quad \diagup \\ \circ \mu^2 \\ \diagup \quad \diagdown \\ p_3 \quad p_2 \end{array} + \frac{2i}{s_{12}} \cdot \begin{array}{c} q \quad p_1 \\ \diagdown \quad \diagup \\ \triangle \mu^2 \\ \diagup \quad \diagdown \\ p_3 \quad p_2 \end{array} \end{aligned} \quad (7.114)$$

where all integrals can be found in Appendix C.3.

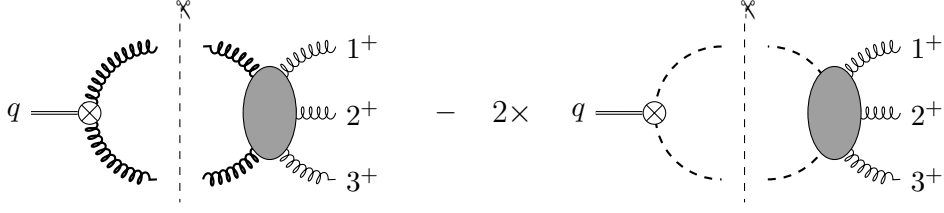


Figure 7.5: Two-particle cut of the one-loop form factor $\text{Tr } F^2$ in the s_{123} channel in six dimensions.

Clearly the double cuts in the channels s_{23} and s_{13} can be derived from (7.114) by symmetry arguments, thus the only invariant channel left to compute would be s_{123} , see Figure 7.5. This double-cut involves the use of the five-point amplitudes in six dimensions with five gluons as well as with three gluons and two scalars¹⁵, combined with the minimal form factor of \mathcal{O}_2 and $\mathcal{O}_{2,s}$ respectively. The only topology probed by this cut, which is not probed by any of the previous cuts, is the bubble with the form factor in one of the two vertices and all the momenta in the other. Performing the calculation the associated coefficient turns out to be zero. Thus (7.114) and its permutations give the complete result, which matches the one given in [395, 113].

7.4.3 The Minimal $\text{Tr } F^3$ Form Factors

We now consider the $\text{Tr } F^3$ form factor in the all-plus helicity configuration. The procedure we follow is exactly the same as in the $\text{Tr } F^2$ case. First we factor out the helicity dependence as an overall tree-level prefactor:

$$\begin{aligned} F_{\mathcal{O}_3}^{(1)}(1^+, 2^+, 3^+; q) &:= F_{\mathcal{O}_3}^{(0)}(1^+, 2^+, 3^+; q) \cdot f^{(3)}(s_{12}, s_{23}, s_{13}) \\ &= -2[12][23][31] \cdot f^{(3)}(s_{12}, s_{23}, s_{13}) , \end{aligned} \quad (7.115)$$

then we compute $f^{(3)}$ as the difference $f_{6\text{D}}^{(3)} - 2f_{\phi}^{(3)}$. We start with the two-particle cut in the s_{12} channel represented in Figure 7.6, which reads

$$f_{6\text{D}}^{(3)}(s_{12}) \Big|_{s_{12}\text{-cut}} = -\frac{1}{2[12][23][31]} \int \text{dLIPS } F_{\mathcal{O}_3}^{(0)}(-l_1^{a\dot{a}}, -l_2^{b\dot{b}}, 3_{1\dot{1}}) \mathcal{A}^{(0)}(l_2 a\dot{a}, l_1 b\dot{b}, 1_{1\dot{1}}, 2_{2\dot{2}}) . \quad (7.116)$$

Upon expanding the six-dimensional invariants we get a 168-term expression. This can be considerably simplified using momentum conservation as in (7.95) and choosing the μ s to be

$$\mu_{l_1} \mapsto \lambda_{l_2} , \quad \tilde{\mu}_{l_1} \mapsto \tilde{\lambda}_3 , \quad \mu_{l_2} \mapsto \lambda_{l_1} , \quad \tilde{\mu}_{l_2} \mapsto \tilde{\lambda}_3 . \quad (7.117)$$

¹⁵Their analytic expression is given in Appendix C.1.

Doing so, we arrive at the compact expression

$$f_{6D}^{(3)}(s_{12}, s_{23}, s_{13})|_{s_{12}\text{-cut}} = i \int d\text{LIPS} \left(\frac{[1\ 2][3|\not{l}_1^{(4)}\not{l}_2^{(4)}|3]}{s_{2l_2}[2\ 3][3\ 1]} + \mu^2 \frac{[3|\not{l}_1^{(4)}\not{l}_2^{(4)}|3]}{[3|\not{p}_1\not{p}_2|3]} \right), \quad (7.118)$$

where we have already reconstructed the full d -dimensional momenta. Computing the scalar contribution in a similar fashion¹⁶ leads to

$$f_{\phi}^{(3)}(s_{12}, s_{23}, s_{13})|_{s_{12}\text{-cut}} = \frac{i}{2} \int d\text{LIPS} \mu^2 \frac{[3|\not{l}_1^{(4)}\not{l}_2^{(4)}|3]}{[3|\not{p}_1\not{p}_2|3]}, \quad (7.119)$$

and finally

$$f^{(3)}(s_{12}, s_{23}, s_{13})|_{s_{12}\text{-cut}} = i \frac{[1\ 2]}{[2\ 3][3\ 1]} \int d\text{LIPS} \frac{[3|\not{l}_1^{(4)}\not{l}_2^{(4)}|3]}{s_{2l_2}}. \quad (7.120)$$

After using (7.117), it is possible to write $f^{(3)}$ in terms of Mandelstam invariants:

$$f^{(3)}(s_{12}, s_{23}, s_{13})|_{s_{12}\text{-cut}} = -i \int d\text{LIPS} \left(\frac{s_{12}}{s_{2l_2}} + 2 \right) \quad (7.121)$$

modulo terms which integrate to zero. Uplifting this result leads to:

$$f^{(3)}(s_{12}, s_{23}, s_{13})|_{s_{12}\text{-disc}} = -i s_{12} \cdot \begin{array}{c} p_1 \\ \diagup \quad \diagdown \\ q \quad \quad l \\ \diagdown \quad \diagup \\ p_3 \quad \quad p_2 \end{array} - 2i \cdot \begin{array}{c} p_1 \\ \diagup \quad \diagdown \\ q \quad \quad l \\ \diagdown \quad \diagup \\ p_3 \quad \quad p_2 \end{array}. \quad (7.122)$$

Combining the discontinuities in the three channels s_{12} , s_{23} and s_{31} we arrive at the complete one-loop form factor

$$f^{(3)}(\{s_{ij}\}) = \sum_{k=1}^n f^{(3)}(\{s_{ij}\})|_{s_{k\ k+1}\text{-disc}}, \quad (7.123)$$

where every term in the sum can be obtained from (7.122) by relabelling the external legs.

¹⁶For the case of the scalar contribution it turns out that the most convenient choice for the μ is the same as in the gluon case. Notice that it is for this particular reason that we would have been allowed to perform the subtraction between the two contributions without writing them in terms of full d -dimensional quantities first. Indeed, if this were not the case, we would have had to reconstruct the form of the loop momenta in terms of general μ s before doing the subtraction.

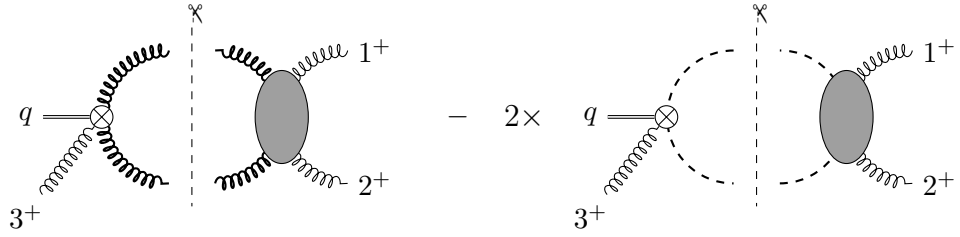
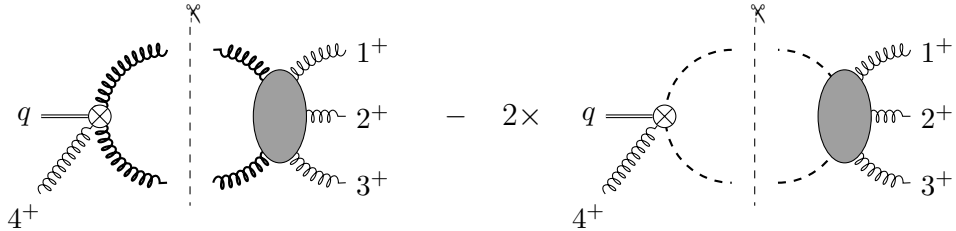


Figure 7.6: Two-particle cut of the one-loop form factor $\text{Tr } F^3$ in the s_{12} channel in six dimensions.

7.4.4 The Non-Minimal $\text{Tr } F^3$ Form Factor

In the last sections we showed how the dimensional reconstruction can be applied to form factors. In this section we derive the complete form factor of the operator $\text{Tr } F^3$ with four gluons in the all-plus helicity configuration.

The procedure we follow has been described in detail earlier, hence we now only sketch the relevant derivations and provide the main results. Up to cyclic permutations there are two independent unitarity cuts to be computed, say in the s_{12} -channel and s_{123} -channel. Starting from the s_{123} -cut, one needs to evaluate the following difference to obtain the complete result:



where the tree-level form factor in the scalar subtraction term (second term in the figure above) is the minimal form factor of the operator $\text{Tr } (D_\mu \phi D_\nu \phi F^{\mu\nu})$. The Passarino-Veltman reductions of the resulting tensor integrals have been performed using the *Mathematica* package *FeynCalc* [396, 397]. From the two-particle cuts in the s_{123} -

channel we obtain the following functions:

$$\begin{aligned}
 F_{\mathcal{O}_3}^{(1)}(1^+, 2^+, 3^+, 4^+; q)|_{s_{123}\text{-disc}} = & D_0^{[0]} \text{ (box diagram) } + C_0^{[0]} \text{ (triangle diagram) } \\
 & + C_1^{[0]} \text{ (triangle diagram) } + B_0^{[0]} \text{ (bubble diagram) } ,
 \end{aligned} \tag{7.124}$$

with the coefficients

$$\begin{aligned}
 D_0^{[0]} &= -i F(1, 2, 3; 4) , \\
 C_0^{[0]} &= -i \frac{s_{12} + s_{31}}{s_{12}s_{23}} F(1, 2, 3; 4) , \\
 C_1^{[0]} &= -i \frac{s_{23} + s_{31}}{s_{12}s_{23}} F(1, 2, 3; 4) ,
 \end{aligned} \tag{7.125}$$

where

$$F(1, 2, 3; 4) := \frac{s_{123}}{s_{31}^2} (s_{12}[13][24] + s_{31}[12][34]) (s_{23}[13][24] + s_{31}[23][14]) . \tag{7.126}$$

Finally the coefficient of the bubble can be written as

$$B_0^{[0]} = 2i[12][23][34][41] b_0^{[0]} , \tag{7.127}$$

where the helicity-blind function $b_0^{[0]}$ is defined as

$$b_0^{[0]} = \frac{s_{123}^2}{s_{12}s_{23}} \left(\frac{1}{s_{12} + s_{31}} + \frac{1}{s_{23} + s_{31}} \right) + \frac{[13][24]}{[12][34]} \frac{s_{123}^2}{s_{23}s_{31}} \cdot \frac{1}{s_{12} + s_{31}} + \frac{[13][24]}{[14][23]} \frac{s_{123}^2}{s_{12}s_{31}} \cdot \frac{1}{s_{23} + s_{31}} . \tag{7.128}$$

The result also contains a box integral with a μ^2 numerator, which after integration is of $\mathcal{O}(\epsilon)$. For completeness we quote its coefficient:

$$D_0^{[2]} = -2is_{123} \left(\frac{[12]^2[34]^2}{s_{12}} + \frac{[23]^2[41]^2}{s_{23}} + \frac{[13]^2[24]^2}{s_{31}} \right) . \tag{7.129}$$

Next we consider the two-particle cut in the s_{12} -channel and, as discussed in earlier sections, the discontinuity of the complete form factor is determined from the difference

$$F_{6D}^{(1)}(1^+, 2^+, 3^+, 4^+; q)|_{s_{12}\text{-cut}} - 2F_{\phi}^{(1)}(1^+, 2^+, 3^+, 4^+; q)|_{s_{12}\text{-cut}} , \tag{7.130}$$

where the second term is the scalar subtraction. As in the case of the non-minimal form factor of $\text{Tr } F^2$, there are two contributions to the scalar quantity $F_\phi^{(1)}(1^+, 2^+, 3^+, 4^+; q)$, which are represented in Figure 7.7. The first contribution comes from the operator $\text{Tr } F^3$ with two scalars and two gluons, whereas the second one comes from the scalar operator $\text{Tr } D_\mu \phi D_\nu \phi F^{\mu\nu}$.

$$F_\phi^{(1)}(1^+, 2^+, 3^+, 4^+; q)|_{s_{12}\text{-cut}} = \left[\begin{array}{c} \mathcal{O}_3 \\ \text{Diagram 1} \\ \mathcal{O}_{3,s} \\ \text{Diagram 2} \end{array} \right] \times \text{Diagram 3}$$

Figure 7.7: A two-particle cut of the scalar contribution to the non-minimal $\text{Tr } F^3$ form factor. The red boxes highlight the two different operator insertions.

After tensor reductions, we find

$$F_{\mathcal{O}_3}^{(1)}(1^+, 2^+, 3^+, 4^+; q)|_{s_{12}\text{-disc}} = D_0^{[0]} \text{Diagram 1} + D_1^{[0]} \text{Diagram 2} + C_1^{[0]} \text{Diagram 3} + C_2^{[0]} \text{Diagram 4} + C_3^{[0]} \text{Diagram 5} + C_3^{[2]} \text{Diagram 6} + B_1^{[0]} \text{Diagram 7} + B_1^{[2]} \text{Diagram 8}, \quad (7.131)$$

where we checked that the coefficients $D_0^{[p]}$, $D_1^{[p]}$, $C_0^{[p]}$ and $C_2^{[p]}$ match the ones found in

the previous calculation, up to relabelling. The other coefficients for the triangles are

$$\begin{aligned} C_3^{[0]} &= i[1\ 2][2\ 3][3\ 4][4\ 1] c_3^{[0]} , \\ C_3^{[2]} &= \frac{4i}{s_{12}}[1\ 2][3\ 4][1\ 3][2\ 4] , \end{aligned} \quad (7.132)$$

where

$$\begin{aligned} c_3^{[0]} &= \frac{s_{12} + s_{31}}{s_{23}} + \frac{s_{12}}{s_{34}} \left(1 + \frac{s_{13}}{s_{14}} + \frac{s_{24}}{s_{23}} \right) - \frac{[1\ 3][2\ 4]}{[1\ 4][2\ 3]} \left[\frac{s_{123}(s_{12} + s_{31}) - s_{13}^2}{s_{13}^2} - \frac{s_{12}}{s_{34}} \right] \\ &\quad - \frac{[1\ 3][2\ 4]}{[1\ 2][3\ 3]} \frac{s_{12}}{s_{13}^2 s_{23}} \left[s_{123}(s_{23} + s_{31}) - 2s_{31}^2 \right] + (1, 4) \longleftrightarrow (2, 3) , \end{aligned} \quad (7.133)$$

while for the bubbles

$$\begin{aligned} B_1^{[0]} &= 2i[1\ 3]^2[2\ 4]^2 \left(\frac{1}{s_{31}} - \frac{1}{s_{23}} + \frac{s_{12}}{s_{23}s_{31}} \right) + 2i[1\ 2]^2[3\ 4]^2 \left(\frac{2}{s_{23}} - \frac{2s_{12}}{s_{23}(s_{13} + s_{23})} \right) \\ &\quad + 2i[1\ 2][3\ 4][1\ 3][2\ 4] \left(\frac{1}{s_{12}} + \frac{4}{s_{23}} - \frac{2}{s_{34}} - \frac{4s_{24}}{s_{23}s_{34}} \right) + (1, 4) \longleftrightarrow (2, 3) , \end{aligned} \quad (7.134)$$

and

$$B_1^{[2]} = \frac{4i}{s_{12}^2} [1\ 2][3\ 4] ([1\ 3][2\ 4] + [2\ 3][1\ 4]) . \quad (7.135)$$

We have checked that our result satisfies the expected infrared consistency conditions. In particular, using the results for the coefficients D_0 , C_0 and C_1 , one immediately finds that the coefficient of $\frac{(-s_{123})^{-\epsilon}}{\epsilon^2}$ vanishes, as required. We have also confirmed that the coefficient of $\frac{(-s_{12})^{-\epsilon}}{\epsilon^2}$ is proportional to the corresponding tree-level non-minimal form factor derived in [372],

$$F_{O_3}^{(0)}(1^+, 2^+, 3^+, 4^+; q) = -2 \frac{[1\ 2][2\ 3][3\ 4][4\ 1]}{s_{12}} \left(1 + \frac{[1\ 3][2\ 4]}{[2\ 3][4\ 1]} - \frac{s_{24}}{s_{41}} \right) + \text{cyclic} . \quad (7.136)$$

7.4.5 The Minimal $\text{Tr } F^4$ Form Factors

In this section we consider the form factors of $\text{Tr } F^4$ in all possible helicity configurations. The case where all particles have the same helicity is interesting since it admits an immediate generalisation to the minimal form factors of operators of the form $\text{Tr } F^n$ defined in (7.85). In this family, $\text{Tr } F^4$ is the first operator whose minimal form factor contains rational terms. We are going to consider the quantities in the planar limit of the theory, *i.e.* at one loop we will probe only the discontinuities in the Mandelstam invariants of adjacent momenta in the colour-ordered form factor. At this point it is important to stress that non-planar contributions behave differently: as one can

see from (7.34) there is no non-planar scalar contribution, because in the operator the scalars can only appear next to each other, and then the complete four-dimensional contribution coincides with the diagrams with purely six-dimensional internal gluons.

All-Plus Helicity Configuration

We begin by defining

$$F_{\mathcal{O}_4}^{(1)}(1^+, 2^+, 3^+, 4^+; q) := 2[1\ 2][2\ 3][3\ 4][4\ 1] \cdot f^{(4)}(\{s_{ij}\}) . \quad (7.137)$$

At one loop, we can make the following observations:

- The cut-constructible part, coming from the form factor involving only gluons, has the same structure as $F_{\mathcal{O}_3}^{(1)}(1^+, 2^+, 3^+; q)$, with both UV and IR divergences.
- Terms proportional to μ^2 and μ^4 now appear. As already mentioned, these could not arise for $n < 4$ because of the limited kinematic, as we will show below. The new integrals are two triangles with μ^2 and μ^4 numerators¹⁷ and when expanded in powers of the dimensional regulator ϵ give a finite contribution in the $\epsilon \rightarrow 0$ limit. They are exactly the rational terms that cannot be seen by the completely four-dimensional cut construction, where clearly $\mu^2 = 0$.

Following the procedure outlined in the previous sections, we find

$$\begin{aligned} f^4(\{s_{ij}\})|_{s_{12}\text{-disc}} = & -i \left(1 + \frac{[1\ 3][2\ 4]}{[1\ 4][2\ 3]} \right) \cdot \begin{array}{c} q \\ \nearrow \\ \text{---} \text{---} \text{---} \\ \searrow \\ l \\ \text{---} \text{---} \text{---} \\ p_1 \\ \nearrow \\ p_2 \\ \searrow \\ p_3 \end{array} - i s_{12} \cdot \begin{array}{c} q \\ \nearrow \\ \text{---} \text{---} \text{---} \\ \searrow \\ l \\ \text{---} \text{---} \text{---} \\ p_1 \\ \nearrow \\ p_2 \\ \searrow \\ p_3 \end{array} \\ & + i \frac{[1\ 2][3\ 4]}{[2\ 3][4\ 1]} \cdot \begin{array}{c} q \\ \nearrow \\ \text{---} \text{---} \text{---} \\ \searrow \\ l \\ \text{---} \text{---} \text{---} \\ p_1 \\ \nearrow \\ p_2 \\ \searrow \\ p_3 \end{array} - i \frac{[3\ 4]}{[3]p_2 p_1 [4]} \cdot \begin{array}{c} q \\ \nearrow \\ \text{---} \text{---} \text{---} \\ \searrow \\ l \\ \text{---} \text{---} \text{---} \\ p_1 \\ \nearrow \\ p_2 \\ \searrow \\ p_3 \end{array} \end{aligned} \quad (7.138)$$

Notice that in the final result the integral $I_3^4[\mu^4]$ appears. In general, in a renormalizable gauge theory one would expect triangle integrals to appear with at most a third power of the loop momentum in the numerator, which allows for at most a μ^2 triangle contribution. However we are considering an effective field theory with an operator of mass-dimension eight, hence the possibility of having also an $I_3^4[\mu^4]$ term. The last step of the calculation is the sum over all the possible channel discontinuities, as we did in (7.123) for $\text{Tr } F^3$.

The above result can be immediately generalized to $\text{Tr } F^n$ for arbitrary n in the all-plus helicity configurations, where we define

¹⁷For analytic expressions of such integrals see for example Appendix C.3.

$$\text{Tr } F^n(1^+, \dots, n^+; q)|_{1\text{-loop}} := (-)^n 2 \prod_{k=1}^n [k k + 1] \cdot f^{(n)}(\{s_{ij}\}) , \quad (7.139)$$

and

$$\begin{aligned} f^{(n)}(\{s_{ij}\})|_{s_{12}\text{-disc}} = & -i \left(1 + \frac{[13][2n]}{[1n][23]} \right) \cdot \begin{array}{c} q \\ \vdots \\ p_3 \end{array} \begin{array}{c} \diagup \\ \diagdown \end{array} \begin{array}{c} p_1 \\ l \\ p_2 \end{array} - i s_{12} \cdot \begin{array}{c} q \\ \vdots \\ p_3 \end{array} \begin{array}{c} \diagup \\ \diagdown \end{array} \begin{array}{c} p_1 \\ l \\ p_2 \end{array} \\ & + i \frac{[12][3n]}{[23][n1]} \cdot \begin{array}{c} q \\ \vdots \\ p_3 \end{array} \begin{array}{c} \diagup \\ \diagdown \end{array} \begin{array}{c} p_1 \\ \mu^2 \\ p_2 \end{array} - i \frac{[3n]}{[3]p_2 p_1 [n]} \cdot \begin{array}{c} q \\ \vdots \\ p_3 \end{array} \begin{array}{c} \diagup \\ \diagdown \end{array} \begin{array}{c} p_1 \\ \mu^4 \\ p_2 \end{array} \end{aligned} \quad (7.140)$$

This simple generalisation is due to the fact that, upon properly normalising with the corresponding four-dimensional quantities, the six-dimensional minimal tree-level form factor of $\text{Tr } F^n$ is identical to that of $\text{Tr } F^4$ up to the replacement $4 \mapsto n$, as can be seen from (7.90). As a final remark, notice that we can a posteriori explain the absence of rational terms for $\text{Tr } F^3$: indeed we can recover (7.122) by simply replacing $n \mapsto 3$ in (7.140). Then, rational terms vanish since they are proportional to $[3n]$.

MHV Configuration: the Alternate and Split-Helicity Colour Ordered Form Factors

We define the MHV colour-ordered form factor with alternate-helicity gluons as follows:

$$F_{O_4}^{(1)}(1^+, 2^-, 3^+, 4^-; q) := \langle 24 \rangle^2 [13]^2 \cdot f_a^{(4)}(\{s_{ij}\}) . \quad (7.141)$$

Since this case presents some peculiarities in the calculations, we will give more details about it. In particular, the cut of the form factor with six-dimensional internal gluons in the s_{12} -channel is given by

$$\begin{aligned} f_{a,6D}^{(4)}(\{s_{ij}\})|_{s_{12}\text{-cut}} &= - \int \text{dLIPS} \frac{i}{s_{12}s_{2l_2}} \frac{\mathcal{I}_{6D}^2}{\langle 24 \rangle^2 [13]^2} \\ &= - \int \text{dLIPS} \frac{i}{s_{12}s_{2l_2}} (2k \cdot l_2)^2 , \end{aligned} \quad (7.142)$$

where

$$\mathcal{I}_{6D} = 2\mu^2 \langle 24 \rangle [13] + \langle 2|l_1^{(4)}|3\rangle \langle 4|l_2^{(4)}|1\rangle + \langle 2|l_2^{(4)}|3\rangle \langle 4|l_1^{(4)}|1\rangle \quad (7.143)$$

and in the last step we removed terms proportional to $\langle 2|l_2^{(4)}|1\rangle$ that vanish upon

integration. Also k_μ is a massive momentum defined by

$$k_{\alpha\dot{\alpha}} = \frac{[12]}{[13]} \lambda_{2\alpha} \tilde{\lambda}_{3\dot{\alpha}} - \frac{\langle 12 \rangle}{\langle 24 \rangle} \lambda_{4\alpha} \tilde{\lambda}_{1\dot{\alpha}} , \quad (7.144)$$

and it is easy to prove that it satisfies the following relations:

$$k^2 = 2p_1 \cdot k = 2p_2 \cdot k = s_{12} . \quad (7.145)$$

Surprisingly, the scalar contribution is identically zero after integration:

$$f_{a,\phi}^{(4)}(\{s_{ij}\})|_{s_{12}\text{-cut}} = \int \text{dLIPS} \frac{i}{s_{12}s_{2l_2}} \frac{\langle 4|l_1^{(4)}|3\rangle\langle 4|l_2^{(4)}|3\rangle\langle 2|l_2^{(4)}|1\rangle^2}{\langle 24\rangle^2[13]^2} = 0 , \quad (7.146)$$

because of the presence of the term $\langle 2|l_2^{(4)}|1\rangle^2$. Thus the discontinuity in the s_{12} -channel is completely given by the pure six-dimensional contribution (7.142), which after the integral reduction can be written as

$$f_a^{(4)}(\{s_{ij}\})|_{s_{12}\text{-disc}} = -is_{12} \cdot \begin{array}{c} p_1 \\ \diagup \quad \diagdown \\ q \quad \quad l \\ \diagdown \quad \diagup \\ p_3 \quad p_2 \end{array} . \quad (7.147)$$

It is worth stressing that all the other planar contributions can be obtained from the previous one easily by symmetry arguments.

As usual, for the split-helicity configuration we factorise the tree-level form factor:

$$F_{\mathcal{O}_4}^{(1)}(1^+, 3^+, 2^-, 4^-; q) := [13]^2 \langle 24 \rangle^2 \cdot f_s^{(4)}(\{s_{ij}\}) . \quad (7.148)$$

Unlike the previous case, in the planar limit we have two different cuts which cannot be related by symmetry: in particular, we can perform the cut in channels with same or opposite helicity gluons. The discontinuity in the s_{12} -channel, after the scalar subtraction, is given by

$$f_s^{(4)}(\{s_{ij}\})|_{s_{13}\text{-disc}} = -is_{13} \cdot \begin{array}{c} p_1 \\ \diagup \quad \diagdown \\ q \quad \quad l \\ \diagdown \quad \diagup \\ p_2 \quad p_3 \end{array} . \quad (7.149)$$

The cut in the s_{23} -channel is reminiscent of the alternate-helicity case, with vanishing

scalar contribution up to integration:

$$f_s^{(4)}(\{s_{ij}\})|_{s_{23}\text{-cut}} \simeq - \int \text{dLIPS} \frac{i}{s_{13}s_3l_2} (2k \cdot l_2)^2, \quad (7.150)$$

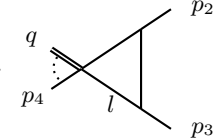
where the momentum k_μ is defined by

$$k_{\alpha\dot{\alpha}} = \frac{[23]}{[13]} \lambda_{2\alpha} \tilde{\lambda}_{1\dot{\alpha}} + \frac{\langle 23 \rangle}{\langle 24 \rangle} \lambda_{4\alpha} \tilde{\lambda}_{3\dot{\alpha}}, \quad (7.151)$$

and it satisfies the following relations:

$$k^2 = 2p_2 \cdot k = 2p_3 \cdot k = s_{23}. \quad (7.152)$$

The cut in the s_{23} channel is

$$f_s^{(4)}(\{s_{ij}\})|_{s_{23}\text{-disc}} = -i s_{23} \cdot \text{Diagram} \quad (7.153)$$


Let us emphasise some relevant features of the result:

- The final result is free of rational terms. Thus we would have found the same, complete, quantity even with four-dimensional unitarity-cuts.
- The only operator that contributes in four dimensions is $\text{Tr}(F_{\text{SD}}^2 F_{\text{ASD}}^2)$, which is a descendant of $\text{Tr} \phi^4$ in $\mathcal{N} = 4$ SYM¹⁸.
- We note the absence of bubbles in the final result for this (unrenormalized) form factor. This may be related to the independence of the bare quantity on the matter content of the theory. One could then regard the computation as if it was performed in $\mathcal{N} = 4$ SYM, where the operator under consideration belongs to a protected multiplet.
- An unrelated observation is that the colour-ordered form factors with alternate and split-helicity configurations are the same:

$$F_{\mathcal{O}_4}^{(1)}(1^+, 2^-, 3^+, 4^-; q) = F_{\mathcal{O}_4}^{(1)}(1^+, 3^+, 2^-, 4^-; q). \quad (7.154)$$

This is an accident due to the simple topology of the integral basis combined with the fact that bubbles do not appear. At first, the equality (7.154) could appear as a consequence of the photon decoupling identities which hold in Yang-Mills theory. However these identities are no longer valid when one considers interactions with higher powers of the field strength.

¹⁸See for example Table 7 in [398].

Chapter 8

Conclusions

In this thesis we discussed some of the many applications of on-shell techniques in the context of high-energy physics. As we saw in Chapter 2, for what analytic expressions of tree-level amplitudes are concerned an on-shell recursion like BCFW appears far more desirable than an off-shell one like Berends-Giele. On-shell expressions are typically more compact, and taking advantage of the factorization properties of tree-amplitudes on physical poles also drastically reduces issues related to combinatoric complexity usually associated to diagrammatic or off-shell methods. On the other hand, we saw that in order to apply these BCFW-like recursions to a wider range of theories, the use of unphysical reference spinors may be required. This motivated the search for a general algorithm combining the best of both on-shell and off-shell worlds: a recursive approach making use of on-shell seeds, taking advantage of unitarity through factorization but at the same time incorporating the information on the pole structure provided by locality, reproducing compact results of simple physical interpretation.

In Chapter 3 we presented a first attempt at such an algorithm, but various improvements are clearly desirable. In particular, it would be interesting to better understand the way external vector bosons contribute to the singularity structure of the tree-amplitude. When writing the latter in terms of spinor structures carrying the helicity weights and Mandelstam invariants in the pole structures, the presence of vector bosons leads to additional poles which do not come simply from intermediate particle propagation but also from external polarization. These mix in non-trivial ways but always miraculously produce at most additional simple poles compatible with locality of the final result. A better understanding of how this recombination happens from an on-shell point of view would be greatly beneficial to our algorithm, and it would also be an interesting problem in its own right.

Equipped with the tree-level machinery we saw how to recombine this information in order to obtain loop-level results. In Chapter 4 we discussed applications to the com-

putation of the anomalous dimension matrix for operators in the Standard Model EFT. The parametrization of Beyond Standard Model physics through SMEFT has become increasingly popular over recent years, due to the fact that no a priori information on the complete UV theory is required in this setup [51, 52]. In this context it is important to compute the anomalous dimension matrix which is usually non-vanishing and non-diagonal, implying that the Wilson coefficients at the energy scales accessible to the colliders differ from those at the high-energy matching scale, and furthermore they mix among each other. Unitarity techniques crucially simplify the computation of the anomalous dimension matrix [237] and provide insights in the deeper structure of the zeros appearing in it [34–36]. We addressed the computation of the mixing of all the mass-dimension eight operators in the complete SMEFT, at linear order in the Wilson coefficients, extending previous partial results and pushing ahead the study of this class of operators which start to attract more and more attention due to their contribution to specific processes of experimental interest [73–77]. Immediate extensions of our results include the computation of the mixing when more than one fermion family is considered, or when we allow for subleading contributions of the Wilson coefficients, both of which could be achieved with some modifications of the computational machinery already at our disposal. Additionally, it would also be interesting to repeat the two-loop computation in [37] with dimension-six operators but in the complete Standard Model instead of the simplified $SU(N)$ theory considered in that paper. The hope would be that combining such a computation with the knowledge of the SMEFT mixing matrix at one loop for dimension eight operators, would allow to spot new patterns in the zeroes previously hidden by the sole focus on one-loop dimension six operators [84–86].

Unitarity methods find interesting applications also in EFTs of gravity. Considering theories with massive matter classical effects can be found also at the loop level [94–96]. In other words, computing higher-order contributions in the perturbative expansion around the gravitational coupling G leads to terms which are non-vanishing in the $\hbar \rightarrow 0$ limit and thus contribute for example to the classical gravitational potential. Loop-level on-shell methods are particularly well suited for the task of extracting relevant information without the need of computing the complete amplitude, since taking unitarity cuts in the appropriate kinematic channel immediately isolates the contributions corresponding to graviton exchange between two external scalars mimicking the heavy galactic objects. Furthermore, taking the cuts in four dimensions automatically discards the terms corresponding to local interactions in the potential, *i.e.* the rational terms.

In Chapter 5 we looked at the effect of higher-derivative operators on the bending angle and the time delay experienced by a light particle when interacting with a heavy object. Modifications to the action were incorporated as new tree-amplitudes in the construction, and modifications to the observables directly extracted through the eikonal

approach [100–105]. Due to the non-minimal interactions we considered, the eikonal phase was promoted to a matrix, from which we extracted related phases through diagonalization. This leads to different values of the deflection angle and time delay for different helicities and allows to find some consistency conditions of the theory which replicate conditions already found in the literature [297, 336, 337]. In this context it would be particularly interesting to explore the sub-sub-leading corrections to the eikonal phase due to the R^4 operator: in the eikonal approach, successive contributions in the perturbative expansion are expected to re-sum into an exponential. We explicitly find exponentiation for R^3 , however for R^4 one-loop provides the leading contribution to the eikonal phase, thus additional two-loop results would be required to check exponentiation.

In Chapter 6, we performed the study of R^3 operators discussing the interplay with tidal effects and in particular we compute the quadrupole corrections for these terms. These corrections are extracted from a five-point amplitude which, beyond the massive scalar states, also features a soft graviton representing the emitted radiation. Considering the binary system from afar as a small extended object which emits gravitational radiation through a multipole expansion, we extract the quadrupole contributions from the computed amplitude and use it along with the already known potential [293, 294] to extract the radiated power. In this regard, it would be interesting to perform a study similar to what was done for the R^4 operators in [106] but for R^3 , based on the results here presented.

To conclude the thesis, in Chapter 7 we took a look at some technical aspects of the multi-loop unitarity methods. Since these methods rely on the discontinuities which are present in the amplitude in order to reconstruct its analytic form, terms which do not present discontinuities in the kinematic channels cannot be detected. While one way of solving this issue is to move away from four dimensions and perform the unitarity cuts in $D = 4 - 2\epsilon$ dimensions [109, 110], this presents some drawbacks, including the fact that one loses the possibility of making use of the powerful spinor-helicity formalism as well as of numerical evaluations. To bypass this issue in the case of Yang-Mills theory, it has been found that the dependence on space-time of the amplitude is polynomial and the complete amplitude can be obtained by evaluating the associated coefficients from amplitudes in integer dimensions [111–115]. We have seen how to extend this method from amplitudes to form factors and furthermore how to generalise it beyond two loops in such a way that still only evaluations in a single higher-dimension are required. A first task would be to perform a proof-of-concept calculation at a higher loop order, which in turn would also require possibly additional six-dimensional building blocks to be fed into the unitarity cuts. Obtaining these tree-level amplitudes/form factors in six-dimensions can be cumbersome, so another direction worth exploring would be the generalisation of the algorithm presented in Chapter 3 to six-dimensions, which

should only present a technical rather than conceptual challenge. In this thesis we only considered pure Yang-Mills theory, but theories including fermions clearly should be addressed too. Doing so should lead to an extension for form factors of [366] which then would allow to address any general theory and obtain complete four-dimensional results from six-dimensional amplitudes.

The applications discussed in this thesis are only the tip of the iceberg of what unitarity considerations, or in other words simple conservation of probability, can tell us about amplitudes and form factors. These insights manifest in terms of the on-shell unitarity methods which nowadays gain widespread interest and study, and surely will produce further outstanding results for decades to come.

Appendix A

SMEFT auxiliary material

A.1 The Standard Model gauge group

In Table A.1 we write explicitly the representations under which each particle in the infrared spectrum of the Standard Model transforms, for the gauge group $U(1) \times SU(2) \times SU(3)$.

	$U(1)$	$SU(2)$	$SU(3)$
B_{\pm}	0	1	1
W_{\pm}	0	3	1
G_{\pm}	0	1	8
Q	$-\frac{1}{6}$	2	3
\bar{u}	$+\frac{2}{3}$	1	3
\bar{d}	$-\frac{1}{3}$	1	3
L	$+\frac{1}{2}$	2	1
\bar{e}	-1	1	1
Q	$+\frac{1}{6}$	2	3
u	$-\frac{2}{3}$	1	3
d	$+\frac{1}{3}$	1	3
L	$-\frac{1}{2}$	2	1
e	+1	1	1
\bar{H}	$-\frac{1}{2}$	2	1
H	$+\frac{1}{2}$	2	1

Table A.1: The spectrum of the Standard Model and the transformation properties of all the fields.

Our convention on the colour factor are completely specified by the decomposition of the contraction of two generators for both the $SU(N)$ and $SU(2)$ groups respectively:

$$\tau^A{}_c \tau^B{}_b = \frac{1}{2N} \delta^{AB} \delta_b^a + \frac{i}{2} f^{ABC} \tau^C{}_b{}^a + \frac{1}{2} d^{ABC} \tau^C{}_b{}^a, \quad (\text{A.1})$$

where f^{ABC} are the structure constants and d^{ABC} is the traceless completely symmetry d -tensor, and

$$\sigma^I i_k \sigma^J k_j = \frac{1}{4} \delta^{IJ} \delta_j^i + \frac{i}{2} \epsilon^{IJK} \sigma^K i_j. \quad (\text{A.2})$$

For the $SU(2)$ group we also need to specify how indices in the fundamental are raised and lowered by the ϵ -tensor:

$$x_i = \epsilon_{ij} x^j = \epsilon_{ij} \epsilon^{jk} x_k. \quad (\text{A.3})$$

A.2 Three-point amplitudes in the Standard Model

In this section we present the complete set of non-vanishing three-point amplitudes in the Standard Model. As already mentioned in Section 3.1.1, consistent factorisation of the four-point amplitudes imposes constraints which not only fix the colour structures but also relate the couplings of the various three-point amplitudes among each other. Once these constraints are taken into account a small set of the numerical coefficients in front of the amplitudes is still arbitrary and up to convention.

$$\mathcal{A}(W_-^I, W_-^J, W_+^K) = g_2 \epsilon^{IJK} \frac{\langle 12 \rangle^3}{\langle 23 \rangle \langle 31 \rangle}, \quad \mathcal{A}(W_-^I, W_+^J, W_+^K) = -g_2 \epsilon^{IJK} \frac{[23]^3}{[12][31]},$$

$$\mathcal{A}(G_-^A, G_-^B, G_+^C) = g_3 f^{ABC} \frac{\langle 12 \rangle^3}{\langle 23 \rangle \langle 31 \rangle}, \quad \mathcal{A}(G_-^A, G_+^B, G_+^C) = -g_3 f^{ABC} \frac{[23]^3}{[12][31]},$$

$$\mathcal{A}(B_-, \bar{e}_m, e_n) = i g_1 \delta_{nm} \frac{\langle 12 \rangle^2}{\langle 23 \rangle}, \quad \mathcal{A}(B_+, \bar{e}_m, e_n) = i g_1 \delta_{nm} \frac{[13]^2}{[23]},$$

$$\mathcal{A}(B_-, \bar{L}_m^i, L_n^j) = -i \frac{g_1}{2} \delta_{mn} \delta_i^j \frac{\langle 12 \rangle^2}{\langle 23 \rangle}, \quad \mathcal{A}(B_+, \bar{L}_m^i, L_n^j) = -i \frac{g_1}{2} \delta_{mn} \delta_i^j \frac{[13]^2}{[23]},$$

$$\mathcal{A}(B_-, \bar{u}_m^a, u_n^b) = -i \frac{2g_1}{3} \delta_{nm} \delta_b^a \frac{\langle 12 \rangle^2}{\langle 23 \rangle}, \quad \mathcal{A}(B_+, \bar{u}_m^a, u_n^b) = -i \frac{2g_1}{3} \delta_{nm} \delta_b^a \frac{[13]^2}{[23]},$$

$$\mathcal{A}(B_-, \bar{d}_m^a, d_n^b) = i \frac{g_1}{3} \delta_{nm} \delta_b^a \frac{\langle 12 \rangle^2}{\langle 23 \rangle}, \quad \mathcal{A}(B_+, \bar{d}_m^a, d_n^b) = i \frac{g_1}{3} \delta_{nm} \delta_b^a \frac{[13]^2}{[23]},$$

$$\mathcal{A}(B_-, \bar{Q}_m^{a,i}, Q_n^{b,j}) = i \frac{g_1}{6} \delta_{mn} \delta_i^j \delta_b^a \frac{\langle 12 \rangle^2}{\langle 23 \rangle}, \quad \mathcal{A}(B_+, \bar{Q}_m^{a,i}, Q_n^{b,j}) = i \frac{g_1}{6} \delta_{mn} \delta_i^j \delta_b^a \frac{[13]^2}{[23]}$$

$$\mathcal{A}(B_-, \bar{H}^i, H^j) = i \frac{g_1}{2} \delta_i^j \frac{\langle 12 \rangle \langle 31 \rangle}{\langle 23 \rangle}, \quad \mathcal{A}(B_+, \bar{H}^i, H^j) = -i \frac{g_1}{2} \delta_i^j \frac{[12][31]}{[23]},$$

$$\mathcal{A}(W_-^I, \bar{L}_m^i, L_n^j) = i g_2 \delta_{mn} \sigma^I j_i \frac{\langle 12 \rangle^2}{\langle 23 \rangle}, \quad \mathcal{A}(W_+^I, \bar{L}_m^i, L_n^j) = i g_2 \delta_{mn} \sigma^I j_i \frac{[13]^2}{[23]},$$

$$\begin{aligned}
 \mathcal{A}(W_-^I, \bar{Q}_m^{a,i}, Q_n^{b,j}) &= i g_2 \delta_{mn} \sigma^{Ij}_i \delta_a^b \frac{\langle 12 \rangle^2}{\langle 23 \rangle}, & \mathcal{A}(W_+^I, \bar{Q}_m^{a,i}, Q_n^{b,j}) &= i g_2 \delta_{mn} \sigma^{Ij}_i \delta_a^b \frac{[13]^2}{[23]}, \\
 \mathcal{A}(W_-^I, \bar{H}^i, H^j) &= i g_2 \sigma^{Ij}_i \frac{\langle 12 \rangle \langle 31 \rangle}{\langle 23 \rangle}, & \mathcal{A}(W_+^I, \bar{H}^i, H^j) &= -i g_2 \sigma^{Ij}_i \frac{[12][31]}{[23]}, \\
 \mathcal{A}(G_-^A, \bar{u}_m^a, u_n^b) &= -i g_3 \delta_{nm} \tau^{Aa}_b \frac{\langle 12 \rangle^2}{\langle 23 \rangle}, & \mathcal{A}(G_+^A, \bar{u}_m^a, u_n^b) &= -i g_3 \delta_{nm} \tau^{Aa}_b \frac{[13]^2}{[23]}, \\
 \mathcal{A}(G_-^A, \bar{d}_m^a, d_n^b) &= -i g_3 \delta_{nm} \tau^{Aa}_b \frac{\langle 12 \rangle^2}{\langle 23 \rangle}, & \mathcal{A}(G_+^A, \bar{d}_m^a, d_n^b) &= -i g_3 \delta_{nm} \delta_i^j \tau^{Aa}_b \frac{[13]^2}{[23]}, \\
 \mathcal{A}(G_-^A, \bar{Q}_m^{a,i}, Q_n^{b,j}) &= i g_3 \delta_{mn} \tau^{Ab}_a \delta_i^j \frac{\langle 12 \rangle^2}{\langle 23 \rangle}, & \mathcal{A}(G_+^A, \bar{Q}_m^{a,i}, Q_n^{b,j}) &= i g_3 \delta_{mn} \delta_i^j \tau^{Ab}_a \frac{[13]^2}{[23]}, \\
 \\
 \mathcal{A}(\bar{Q}_m^{a,i}, \bar{u}_n^b, \bar{H}^j) &= i \mathcal{Y}_{mn}^{(1)} \epsilon_{ij} \delta_a^b \langle 12 \rangle, & \mathcal{A}(Q_m^{a,i}, u_n^b, H^j) &= -i \bar{\mathcal{Y}}_{nm}^{(1)} \epsilon^{ij} \delta_b^a [12], \\
 \mathcal{A}(Q_m^{a,i}, d_n^b, \bar{H}^j) &= i \mathcal{Y}_{nm}^{(2)} \delta_j^i \delta_b^a [12], & \mathcal{A}(\bar{Q}_m^{a,i}, \bar{d}_n^b, H^j) &= i \bar{\mathcal{Y}}_{mn}^{(2)} \delta_i^j \delta_b^a \langle 12 \rangle, \\
 \mathcal{A}(\bar{L}_m^i, e_n, \bar{H}^j) &= i \mathcal{Y}_{nm}^{(3)} \delta_j^i [12], & \mathcal{A}(\bar{L}_m^i, \bar{e}_n, H^j) &= i \bar{\mathcal{Y}}_{mn}^{(3)} \delta_i^j \langle 12 \rangle.
 \end{aligned}$$

A.3 Infrared collinear anomalous dimensions in the Standard Model

In this section we are going to show an example of the computation of the collinear anomalous dimension for the W bosons in the Standard Model and we will give the result for all the particles in the spectrum of the theory.

We start by giving the stress-tensor form factor [127] following the normalisation procedure given in [237] for generic complex scalars, fermions and vectors respectively¹:

$$\begin{aligned}
 \langle \bar{\phi}^{\mathbb{A}} \phi^{\mathbb{B}} | T^{\alpha\dot{\alpha}\beta\dot{\beta}} | 0 \rangle &= \frac{1}{3} \delta_{\mathbb{A}}^{\mathbb{B}} \left(\lambda_1^\alpha \lambda_1^\beta \tilde{\lambda}_1^{\dot{\alpha}} \tilde{\lambda}_1^{\dot{\beta}} - \lambda_1^\alpha \lambda_2^\beta \tilde{\lambda}_1^{\dot{\alpha}} \tilde{\lambda}_2^{\dot{\beta}} - \lambda_1^\alpha \lambda_2^\beta \tilde{\lambda}_2^{\dot{\alpha}} \tilde{\lambda}_1^{\dot{\beta}} - \lambda_2^\alpha \lambda_1^\beta \tilde{\lambda}_1^{\dot{\alpha}} \tilde{\lambda}_2^{\dot{\beta}} \right. \\
 &\quad \left. - \lambda_2^\alpha \lambda_1^\beta \tilde{\lambda}_2^{\dot{\alpha}} \tilde{\lambda}_1^{\dot{\beta}} + \lambda_2^\alpha \lambda_2^\beta \tilde{\lambda}_2^{\dot{\alpha}} \tilde{\lambda}_2^{\dot{\beta}} \right) \\
 \langle \bar{\psi}^{\mathbb{A}} \psi^{\mathbb{B}} | T^{\alpha\dot{\alpha}\beta\dot{\beta}} | 0 \rangle &= \frac{1}{2} \delta_{\mathbb{A}}^{\mathbb{B}} \left(\lambda_1^\alpha \lambda_1^\beta \tilde{\lambda}_2^{\dot{\alpha}} \tilde{\lambda}_1^{\dot{\beta}} + \lambda_1^\alpha \lambda_1^\beta \tilde{\lambda}_1^{\dot{\alpha}} \tilde{\lambda}_2^{\dot{\beta}} - \lambda_1^\alpha \lambda_2^\beta \tilde{\lambda}_2^{\dot{\alpha}} \tilde{\lambda}_2^{\dot{\beta}} - \lambda_2^\alpha \lambda_1^\beta \tilde{\lambda}_2^{\dot{\alpha}} \tilde{\lambda}_2^{\dot{\beta}} \right) \\
 \langle v_-^{\mathbb{I}} v_+^{\mathbb{J}} | T^{\alpha\dot{\alpha}\beta\dot{\beta}} | 0 \rangle &= -2 \delta^{\mathbb{I}\mathbb{J}} \lambda_1^\alpha \lambda_1^\beta \tilde{\lambda}_2^{\dot{\alpha}} \tilde{\lambda}_2^{\dot{\beta}},
 \end{aligned} \tag{A.4}$$

where $\mathbb{A}, \mathbb{B}, \mathbb{I}, \mathbb{J}$ are generic colour indices. Once we fix the minimal form factor for the

¹The different overall minus sign with respect to [237] comes from our different convention choice for $\lambda_{-k}^\alpha = i\lambda_k^\alpha$ and $\tilde{\lambda}_{-k}^{\dot{\alpha}} = i\tilde{\lambda}_k^{\dot{\alpha}}$, while the authors in [237] chose $\lambda_{-k}^\alpha = \lambda_k^\alpha$ and $\tilde{\lambda}_{-k}^{\dot{\alpha}} = -\tilde{\lambda}_k^{\dot{\alpha}}$.

stress tensor, we can apply the formula (4.35):

$$\langle W_-^I W_+^J | T^{\mu\nu} | 0 \rangle \cdot \sum_{l=1}^2 \frac{\gamma_{\text{coll}}^{(l)}}{16\pi^2} = \frac{1}{\pi} \sum_{\{l_1, l_2\}} \int \frac{d\Omega_2}{32\pi^2} \left[\mathcal{A}_4(p_{l_1}^{h_{l_1}} p_{l_2}^{h_{l_2}} \rightarrow W_-^I W_+^J) - \sum_{k=1}^3 \frac{g_k^2}{\cos^2 \theta \sin^2 \theta} T_{k, l_1} \cdot T_{k, l_2} \right] \cdot \langle p_{l_1}^{h_{l_1}} p_{l_2}^{h_{l_2}} | T^{\mu\nu} | 0 \rangle, \quad (\text{A.5})$$

where the sum over $\{l_1, l_2\}$ runs over the pairs

$$\left\{ \{W_-, W_+\}, \{W_+, W_-\}, \{\bar{Q}, Q\}, \{Q, \bar{Q}\}, \{\bar{L}, L\}, \{L, \bar{L}\}, \{\bar{H}, H\}, \{H, \bar{H}\} \right\}. \quad (\text{A.6})$$

Considering that $\gamma_{\text{coll}}^{W_-} = \gamma_{\text{coll}}^{W_+} := \gamma_{\text{coll}}^W$, we can rewrite (A.5) as

$$\gamma_{\text{coll}}^W = 8\pi \sum_{\{l_1, l_2\}} \int \frac{d\Omega_2}{32\pi^2} \left[\mathcal{A}_4(p_{l_1}^{h_{l_1}} p_{l_2}^{h_{l_2}} \rightarrow W_-^I W_+^J) - \sum_{k=1}^3 \frac{g_k^2}{\cos^2 \theta \sin^2 \theta} T_{k, l_1} \cdot T_{k, l_2} \right] \cdot \frac{\langle p_{l_1}^{h_{l_1}} p_{l_2}^{h_{l_2}} | T^{\mu\nu} | 0 \rangle}{\langle W_-^I W_+^J | T^{\mu\nu} | 0 \rangle}, \quad (\text{A.7})$$

We will list now the different contributions from the W bosons (which need the infrared divergence subtraction), the quarks, the leptons and the Higgs doublet, respectively:

$$\gamma_{\text{coll}}^W = -g_2^2 \left(\frac{11}{3} \times 2 - \frac{N_f}{3} \times 3 - \frac{N_f}{3} - \frac{1}{6} \right), \quad (\text{A.8})$$

where the factor of $\times 2$ in the first term is the Casimir of the adjoint representation of $SU(2)$, while the factor of $\times 3$ in the second term comes from the sum on different colour of the quarks. This is the usual result for the $SU(2)$ beta function with N_f Weyl fermions and 1 scalar, both transforming in the fundamental of the gauge group.

Finally, we give the explicit results for the other states in the Standard Model. We start from the vector bosons

$$\gamma_{\text{coll}}^B = \frac{2}{3} g_1^2 \left[\left(Y_Q^2 \times 2 + Y_u^2 + Y_d^2 \right) \times 3 + \left(Y_L^2 \times 2 + Y_e^2 \right) + Y_H^2 \right], \quad (\text{A.9})$$

$$\gamma_{\text{coll}}^G = -g_3^2 \left(\frac{11}{3} \times 3 - \frac{N_f}{3} \times 2 \times 2 \right), \quad (\text{A.10})$$

where the first $\times 2$ in the second term of γ_{coll}^G comes from the sum over $SU(2)$ indices (or equivalently over d and u) and the second $\times 2$ factor comes from the fact that $SU(3)$ is not a chiral theory and the quarks behave as a doublet of Dirac fermions. Then we

have the collinear anomalous dimensions for the fermions

$$\left(\gamma_{\text{coll}}^Q\right)_{mn} = -3 \left(g_1^2 Y_Q^2 + \frac{3}{4} g_2^2 + \frac{8}{6} g_3^2 \right) \delta_{mn} + \mathcal{Y}_{mp}^{(1)} \bar{\mathcal{Y}}_{pn}^{(1)} + \mathcal{Y}_{mp}^{(2)} \bar{\mathcal{Y}}_{pn}^{(2)}, \quad (\text{A.11})$$

$$\left(\gamma_{\text{coll}}^u\right)_{mn} = -3 \left(g_1^2 Y_u^2 + \frac{8}{6} g_3^2 \right) \delta_{mn} + 2 \bar{\mathcal{Y}}_{np}^{(1)} \mathcal{Y}_{pm}^{(1)}, \quad (\text{A.12})$$

$$\left(\gamma_{\text{coll}}^d\right)_{mn} = -3 \left(g_1^2 Y_d^2 + \frac{8}{6} g_3^2 \right) \delta_{mn} + 2 \bar{\mathcal{Y}}_{np}^{(2)} \mathcal{Y}_{pm}^{(2)}, \quad (\text{A.13})$$

$$\left(\gamma_{\text{coll}}^L\right)_{mn} = -3 \left(g_1^2 Y_L^2 + \frac{3}{4} g_2^2 \right) \delta_{mn} + \mathcal{Y}_{mp}^{(3)} \bar{\mathcal{Y}}_{pn}^{(3)}, \quad (\text{A.14})$$

$$\left(\gamma_{\text{coll}}^e\right)_{mn} = -3 g_1^2 Y_e^2 \delta_{mn} + 2 \bar{\mathcal{Y}}_{np}^{(3)} \mathcal{Y}_{pm}^{(3)}, \quad (\text{A.15})$$

and, finally, the Higgs

$$\gamma_{\text{coll}}^H = -4 g_1^2 Y_H^2 - 4 g_2^2 \times \frac{3}{4} + 2 \text{Tr } \mathcal{Y}^{(1)} \cdot \bar{\mathcal{Y}}^{(1)} \times 3 + 2 \text{Tr } \mathcal{Y}^{(2)} \cdot \bar{\mathcal{Y}}^{(2)} \times 3 + 2 \text{Tr } \mathcal{Y}^{(3)} \cdot \bar{\mathcal{Y}}^{(3)}, \quad (\text{A.16})$$

where $\frac{3}{4}$ and $\frac{8}{6}$ are the Casimir of the fundamental representation of $SU(2)$ and $SU(3)$, respectively.

Appendix B

Gravity EFTs auxiliary material

B.1 Some relevant integrals

In this section we give the explicit expression for the integral functions appearing in some our results, in particular in Section 5. These expressions are expanded in ϵ up to the relevant orders, and only terms with an s -channel discontinuity are kept.

$$I_2(s) \simeq \frac{i}{16\pi^2} \left[\frac{1}{\epsilon} - \log(-s) \right], \quad (\text{B.1})$$

$$I_3(s) \simeq \frac{i}{16\pi^2 s} \left[\frac{1}{\epsilon^2} - \frac{\log(-s)}{\epsilon} + \frac{1}{2} \log^2(-s) \right], \quad (\text{B.2})$$

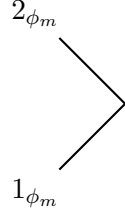
$$I_3(s; m) \simeq -\frac{i}{32} \left[\frac{1}{m\sqrt{-s}} + \frac{\log(-s/m^2)}{\pi^2 m^2} \right], \quad (\text{B.3})$$

$$\begin{aligned} I_4(s, t; m) + I_4(s, u; m) &\simeq -\frac{1}{8\pi} \frac{1}{m\omega} \frac{1}{D-4} (-s)^{\frac{D-6}{2}} \\ &\simeq -\frac{1}{16\pi s (m\omega)} \left[\frac{1}{\epsilon} - \log\left(-\frac{s}{m^2}\right) \right]. \end{aligned} \quad (\text{B.4})$$

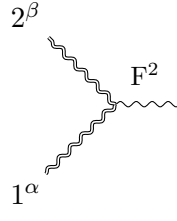
B.2 Feynman rules

Below we list some of the Feynman rules used to obtain the tree-level amplitudes needed in Section 5. Note that 1_{ϕ_m} represents a massive scalar with momentum p_1 , 1^α represents a photon with momentum p_1 , and $3^{\mu\nu}$ represents a graviton with momentum

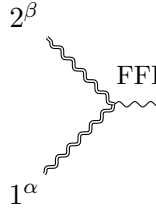
p_3 :



$$3^{\mu\nu} = i \left(\frac{\kappa}{2} \right) \left[-\eta^{\mu\nu} (p_1 \cdot p_2 + m^2) + p_1^\mu p_2^\nu + p_2^\mu p_1^\nu \right] \quad (\text{B.5})$$



$$3^{\mu\nu} = i \left(\frac{\kappa}{2} \right) \left[\frac{1}{2} \eta^{\alpha\beta} \eta^{\mu\nu} s_{12} - \eta^{\alpha(\mu} \eta^{\nu)\beta} s_{12} - 2 \eta^{\alpha\beta} p_1^{(\mu} p_2^{\nu)} \right. \\ \left. + 2 \eta^{\alpha(\mu} p_2^{\nu)} p_1^\beta + 2 \eta^{\beta(\mu} p_1^{\nu)} p_2^\alpha - \eta^{\mu\nu} p_1^\beta p_2^\alpha \right] \quad (\text{B.6})$$



$$3^{\mu\nu} = i \left(\frac{\kappa}{2} \right) \left(\frac{\alpha_\gamma}{4} \right) \left[\eta^{\alpha(\mu} \eta^{\nu)\beta} s_{13} s_{23} - 2 \eta^{\alpha(\mu} p_2^{\nu)} p_3^\beta s_{13} \right. \\ \left. - 2 \eta^{\beta(\mu} p_1^{\nu)} p_3^\alpha s_{23} + 4 p_1^{(\mu} p_2^{\nu)} p_3^\alpha p_3^\beta \right] \quad (\text{B.7})$$

B.3 The tree-level amplitudes

In this appendix we collect for the reader's convenience all the tree-level amplitudes we have used in our derivations. All are consistent with the normalisations of (5.2), also we assume all momenta to be outgoing.

$$\mathcal{A}_{\text{SQED}}^{(0)}(1^\phi, 2^\phi, 3^+, 4^+) = e^2 m^2 \frac{[34]^2}{s} \left(\frac{i}{t-m^2} + \frac{i}{u-m^2} \right), \quad (\text{B.8})$$

$$\mathcal{A}_{\text{EH}}^{(0)}(1^+, 2^-, 3^{++}, 4^{--}) = -i \left(\frac{\kappa}{2} \right)^2 [13]^2 \langle 24 \rangle^2 \frac{\langle 4|1|3 \rangle^2}{stu}, \quad (\text{B.9})$$

$$\mathcal{A}_{\text{EH}}^{(0)}(1^\phi, 2^\phi, 3^{--}, 4^{++}) = - \left(\frac{\kappa}{2} \right)^2 \frac{\langle 3|1|4 \rangle^4}{s^2} \left[\frac{i}{t-m^2} + \frac{i}{u-m^2} \right], \quad (\text{B.10})$$

$$\mathcal{A}_{\text{EH}}^{(0)}(1^{++}, 2^{++}, 3^{--}, 4^{--}) = i \left(\frac{\kappa}{2} \right)^2 \frac{s_{12}s_{13}}{s_{14}} \frac{\langle 34 \rangle^8}{\langle 12 \rangle^4 \langle 23 \rangle^4 \langle 34 \rangle^4 \langle 41 \rangle^4}, \quad (\text{B.11})$$

$$\mathcal{A}_{\text{EH}}^{(0)}(1^\phi, 2^\phi, 3^{++}, 4^{++}) = - \left(\frac{\kappa}{2} \right)^2 m^4 \frac{[34]^2}{\langle 34 \rangle^2} \left[\frac{i}{t-m^2} + \frac{i}{u-m^2} \right], \quad (\text{B.12})$$

$$\mathcal{A}_{\text{EH}}^{(0)}(1^\phi, 2^\phi, 3^-, 4^+) = i \left(\frac{\kappa}{2} \right)^2 \frac{\langle 3|1|4 \rangle^2}{s}, \quad (\text{B.13})$$

$$\mathcal{A}_{\text{EH}}^{(0)}(1^\phi, 2^\phi, 3^+, 4^+) = 0, \quad (\text{B.14})$$

$$\mathcal{A}_{R^3}^{(0)}(1^{++}, 2^{++}, 3^{++}, 4^{--}) = -i \left(\frac{\kappa}{2} \right)^2 \left(\frac{\alpha'}{4} \right)^2 (\langle 41 \rangle [13] \langle 34 \rangle)^2 \frac{[12][23][31]}{\langle 12 \rangle \langle 23 \rangle \langle 31 \rangle}, \quad (\text{B.15})$$

$$\mathcal{A}_{R^3}^{(0)}(1^\phi, 2^\phi, 3^{--}, 4^{++}) = 0, \quad (\text{B.16})$$

$$\mathcal{A}_{R^3}^{(0)}(1^\phi, 2^\phi, 3^{++}, 4^{++}) = i \left(\frac{\kappa}{2} \right)^2 \left(\frac{\alpha'}{4} \right)^2 [34]^4 \frac{(t-m^2)(u-m^2)}{s}, \quad (\text{B.17})$$

$$\mathcal{A}_{R^4}^{(0)}(1^{++}, 2^{++}, 3^{++}, 4^{++}) = i\beta \left(\frac{\kappa}{2} \right)^2 \left([12]^4 [34]^4 + [13]^4 [24]^4 + [14]^4 [23]^4 \right), \quad (\text{B.18})$$

$$\mathcal{A}_{R^4}^{(0)}(1^{++}, 2^{++}, 3^{--}, 4^{--}) = i\tilde{\beta} \left(\frac{\kappa}{2} \right)^2 [12]^4 \langle 34 \rangle^4, \quad (\text{B.19})$$

$$\mathcal{A}_{R^4}^{(0)}(1^\phi, 2^\phi, 3^{h_3}, 4^{h_4}) = 0 \quad \text{with} \quad h_3, h_4 \in \{+, -, ++, --\}, \quad (\text{B.20})$$

$$\mathcal{A}_{\text{FFR}}^{(0)}(1^+, 2^+, 3^{++}) = i \left(\frac{\kappa}{2} \right) \left(\frac{\alpha_\gamma}{4} \right) [13]^2 [23]^2, \quad (\text{B.21})$$

$$\mathcal{A}_{\text{FFR}}^{(0)}(1^+, 2^+, 3^{--}, 4^{++}) = -i \left(\frac{\kappa}{2} \right)^2 \left(\frac{\alpha_\gamma}{4} \right) [12]^2 \frac{\langle 3|1|4 \rangle^4}{stu}, \quad (\text{B.22})$$

$$\mathcal{A}_{\text{FFR}}^{(0)}(1^+, 2^+, 3^{++}, 4^{++}) = i \left(\frac{\kappa}{2} \right)^2 \left(\frac{\alpha_\gamma}{4} \right) \left(\frac{[13]^2 [34]^2 [42]^2}{s_{13}} + \frac{[23]^2 [34]^2 [41]^2}{s_{23}} \right), \quad (\text{B.23})$$

$$\mathcal{A}_{\text{FFR}}^{(0)}(1^\phi, 2^\phi, 3^-, 4^+) = -i \left(\frac{\kappa}{2} \right)^2 \left(\frac{\alpha_\gamma}{4} \right) \langle 3|1|4 \rangle^2, \quad (\text{B.24})$$

$$\mathcal{A}_{\text{FFR}}^{(0)}(1^\phi, 2^\phi, 3^+, 4^+) = -i \left(\frac{\kappa}{2} \right)^2 \left(\frac{\alpha_\gamma}{4} \right) [34]^2 \left[\frac{(t-m^2)(u-m^2)}{s} + m^2 \right]. \quad (\text{B.25})$$

B.4 Hamiltonians with momentum-dependent potentials

The expressions presented here have been used in Section 6.

Consider a momentum-dependent Hamiltonian of the form

$$H = \frac{\vec{p}^2}{2\mu} [1 + 2\mu U(r)] + V(r) , \quad (\text{B.26})$$

where $\vec{p}^2 = p_r^2 + \frac{p_\phi^2}{r^2}$. From Hamilton's equations we learn that $p_\phi := l$ is constant, as well as $\dot{\phi} = \frac{l}{\mu r^2} [1 + 2\mu U(r)]$. The latter equation can be used to re-express l as a function of Ω . We also have

$$\dot{r} = \frac{p_r}{\mu} [1 + 2\mu U(r)] , \quad (\text{B.27})$$

and, for circular orbits, we see that $p_r = 0$ and hence $\dot{p}_r = 0$. In this case, the Hamilton equation $\dot{p}_r = -\frac{\partial H}{\partial r}$ simplifies to

$$V'(r_\circ) - \frac{l^2}{\mu r_\circ^3} [1 + 2\mu U(r_\circ)] + \frac{l^2}{r_\circ^2} U'(r_\circ) = 0 , \quad (\text{B.28})$$

where r_\circ is the radius of the circular orbit. We will also set $\Omega := \dot{\phi}(r = r_\circ)$, or

$$\Omega := \frac{l}{\mu r_\circ^2} [1 + 2\mu U(r_\circ)] . \quad (\text{B.29})$$

Using this to eliminate l in favour of Ω , we finally get

$$V'(r_\circ) - \frac{\mu r_\circ \Omega^2}{1 + 2\mu U(r_\circ)} \left[1 - \frac{\mu r_\circ U'(r_\circ)}{1 + 2\mu U(r_\circ)} \right] = 0 . \quad (\text{B.30})$$

This equation determines r_\circ as a function of Ω . In the absence of a perturbation, we have

$$\Omega_N = \frac{l}{\mu r_N^2} , \quad (\text{B.31})$$

where r_N is the radius of the circular orbit in the EH theory, given in (6.29).

Appendix C

Some six-dimensional results

In this section we present some six-dimensional tree-level results, both for amplitudes and non-minimal form factors, needed for the unitarity calculations in Section 7.

C.1 Six-Dimensional Scattering Amplitudes

As we already mentioned, in six dimensions the notion of helicity is encoded in a tensorial structure, which must be reflected by the amplitudes. The advantage of this tensorial nature of helicity is that a single (tensorial) expression of the amplitude contains all the possible four-dimensional helicity configurations, when dimensional reduced. The drawback however is that one loses some of the simplicity which was peculiar to specific helicity configurations. In particular there is no concept of MHV amplitudes.

In Section 7.1.2 we have chosen the embedding of the four dimensions into the six-dimensional space. Thus the four-dimensional helicity structure is embedded in the six-dimensional amplitudes. In general this represents a good consistency check for six-dimensional results. In fact for an appropriate limit these results must return their four-dimensional counterparts. More specifically, accordingly to our embedding, it turns out that states characterised by little-group indices $(1, 1)$ and $(2, 2)$ correspond to the positive and the negative helicity states in the four-dimensional limit $(m, \tilde{m} \rightarrow 0)$, because of representation we chose for the gamma matrices. On the other hand, in four dimensions the additional $(1, 2)$ and $(2, 1)$ components coincide with two 4D scalars.

The four-gluon amplitude, computed in [152], is

$$\mathcal{A}_g(1_{a\dot{a}}, 2_{b\dot{b}}, 3_{c\dot{c}}, 4_{d\dot{d}}) = \begin{array}{c} 1_{a\dot{a}} \\ \text{wavy} \\ \text{tree} \\ \text{wavy} \\ 4_{d\dot{d}} \end{array} \begin{array}{c} 2_{b\dot{b}} \\ \text{wavy} \\ \text{tree} \\ \text{wavy} \\ 3_{c\dot{c}} \end{array} = -\frac{i}{s_{12}s_{23}} \langle 1_a 2_b 3_c 4_d \rangle [1_{\dot{a}}, 2_{\dot{b}}, 3_{\dot{c}}, 4_{\dot{d}}]. \quad (\text{C.1})$$

According to our embedding, we expect $\mathcal{A}_g(1_{22}, 2_{22}, 3_{11}, 4_{11})$ to reproduce the MHV amplitude $\mathcal{A}(1^-, 2^-, 3^+, 4^+)$ in the limit $m_i, \tilde{m}_i \rightarrow 0$ for $i = 1, \dots, 4$, which is indeed the case:

$$\mathcal{A}_g(1_{22}, 2_{22}, 3_{11}, 4_{11}) \Big|_{4D} = i \frac{\langle 12 \rangle^4}{\langle 12 \rangle \langle 23 \rangle \langle 34 \rangle \langle 41 \rangle}. \quad (\text{C.2})$$

While $\mathcal{A}_g(1_{12}, 2_{21}, 3_{11}, 4_{22})$ reproduces the four-point amplitude with two scalars and two opposite-helicity gluons $\mathcal{A}(1_\phi, 2_{\bar{\phi}}, 3^+, 4^-)$:

$$\mathcal{A}_g(1_{12}, 2_{21}, 3_{11}, 4_{22}) = i \frac{\langle 14 \rangle^2 \langle 24 \rangle^2}{\langle 12 \rangle \langle 23 \rangle \langle 34 \rangle \langle 41 \rangle}. \quad (\text{C.3})$$

Another amplitude of which we make frequent use is the six-dimensional four-point amplitude with two gluons and two scalars [113]

$$\mathcal{A}_s(1_{a\dot{a}}, 2_{b\dot{b}}, 3, 4) = \begin{array}{c} 1_{a\dot{a}} \\ \text{wavy} \\ \text{tree} \\ \text{dashed} \\ 4 \end{array} \begin{array}{c} 2_{b\dot{b}} \\ \text{wavy} \\ \text{tree} \\ \text{dashed} \\ 3 \end{array} = -\frac{i}{4s_{12}s_{23}} \langle 1_a 2_b 3_c 3^c \rangle [1_{\dot{a}}, 2_{\dot{b}}, 4^d, 4_d]. \quad (\text{C.4})$$

The massless scalars in six dimensions behave as massive scalars when reduced to four dimensions. Taking the limits $m_1, m_2, \tilde{m}_1, \tilde{m}_2 \rightarrow 0$ and choosing the helicity components we find the four-point amplitudes for gluons and massive scalars in four dimensions:

$$\begin{aligned} \mathcal{A}_s(1_{22}, 2_{11}, 3, 4) \Big|_{4D} &= -i \frac{\langle 1 | \not{p}_3^{(4)} | 2 \rangle}{s_{12}s_{23}}, \\ \mathcal{A}_s(1_{11}, 2_{11}, 3, 4) \Big|_{4D} &= i\mu^2 \frac{[12]^2}{s_{12}s_{23}}, \end{aligned} \quad (\text{C.5})$$

where μ^2 coincides in this case with the mass of the scalar squared.

Finally, the last amplitude one needs is the five-point tree-level amplitude. The ampli-

tude with five-gluons has first been computed in [152]. In [386, 115] this result has been extended to the five-point superamplitude in the $\mathcal{N} = (1, 1)$ theory. This superamplitude also contains information about the amplitude with scalar fields which is needed for the scalar subtraction when doing dimensional reconstruction. The amplitude with five gluons is

$$\mathcal{A}_g(1_{a\dot{a}}, 2_{b\dot{b}}, 3_{c\dot{c}}, 4_{d\dot{d}}, 5_{e\dot{e}}) = \frac{i}{s_{12}s_{23}s_{34}s_{45}s_{51}} (-\mathcal{M}_{a\dot{a}b\dot{b}c\dot{c}d\dot{d}e\dot{e}} + \mathcal{D}_{a\dot{a}b\dot{b}c\dot{c}d\dot{d}e\dot{e}}) \quad (\text{C.6})$$

with

$$\mathcal{M}_{a\dot{a}b\dot{b}c\dot{c}d\dot{d}e\dot{e}} = \langle 1_a | \not{p}_2 \not{p}_3 \not{p}_4 \not{p}_5 | 1_{\dot{a}} \rangle \langle 2_b 3_c 4_d 5_e \rangle [2_{\dot{b}} 3_{\dot{c}} 4_{\dot{d}} 5_{\dot{e}}] + \text{cyclic}, \quad (\text{C.7})$$

and

$$\begin{aligned} 2\mathcal{D}_{a\dot{a}b\dot{b}c\dot{c}d\dot{d}e\dot{e}} = & \langle 1_a \tilde{\Sigma}_{2\dot{b}} \rangle \langle 2_b 3_c 4_d 5_e \rangle [1_{\dot{a}} 3_{\dot{c}} 4_{\dot{d}} 5_{\dot{e}}] + \langle 3_c \tilde{\Sigma}_{4\dot{d}} \rangle \langle 1_a 2_b 4_d 5_e \rangle [1_{\dot{a}} 2_{\dot{b}} 3_{\dot{c}} 5_{\dot{e}}] \\ & + \langle 4_d \tilde{\Sigma}_{5\dot{e}} \rangle \langle 1_a 2_b 3_c 5_e \rangle [1_{\dot{a}} 2_{\dot{b}} 3_{\dot{c}} 4_{\dot{d}}] - \langle 3_c \tilde{\Sigma}_{5\dot{e}} \rangle \langle 1_a 2_b 4_d 5_e \rangle [1_{\dot{a}} 2_{\dot{b}} 3_{\dot{c}} 4_{\dot{d}}] \\ & - [1_{\dot{a}} \Sigma_{2b}] \langle 1_a 3_c 4_d 5_e \rangle [2_{\dot{b}} 3_{\dot{c}} 4_{\dot{d}} 5_{\dot{e}}] - [3_{\dot{c}} \Sigma_{4d}] \langle 1_a 2_b 3_c 5_e \rangle [1_{\dot{a}} 2_{\dot{b}} 4_{\dot{d}} 5_{\dot{e}}] \\ & - [4_{\dot{d}} \Sigma_{5e}] \langle 1_a 2_b 3_c 4_d \rangle [1_{\dot{a}} 2_{\dot{b}} 3_{\dot{c}} 5_{\dot{e}}] + [3_{\dot{c}} \tilde{\Sigma}_{5e}] \langle 1_a 2_b 3_c 4_d \rangle [1_{\dot{a}} 2_{\dot{b}} 4_{\dot{d}} 5_{\dot{e}}]. \end{aligned} \quad (\text{C.8})$$

The amplitude with two scalars and three gluons is

$$\mathcal{A}_g(1_\phi, 2_{\bar{\phi}}, 3_{c\dot{c}}, 4_{d\dot{d}}, 5_{e\dot{e}}) = -\frac{i}{s_{12}s_{23}s_{34}s_{45}s_{51}} (\mathcal{M}_{c\dot{c}d\dot{d}e\dot{e}}^s + \mathcal{D}_{c\dot{c}d\dot{d}e\dot{e}}^s), \quad (\text{C.9})$$

with

$$\begin{aligned} \mathcal{M}_{c\dot{c}d\dot{d}e\dot{e}}^s = & \langle 3_c | \not{p}_1 | 4_d \rangle [3_{\dot{c}} | \not{p}_2 | 4_{\dot{d}}] \langle 5_e | \not{p}_1 \not{p}_2 \not{p}_3 \not{p}_4 | 5_{\dot{e}} \rangle + \langle 4_d | \not{p}_1 | 5_e \rangle [4_{\dot{d}} | \not{p}_2 | 5_{\dot{e}}] \langle 3_c | \not{p}_4 \not{p}_5 \not{p}_1 \not{p}_2 | 3_{\dot{c}} \rangle \\ & + \langle 3_c | \not{p}_1 | 5_e \rangle [3_{\dot{c}} | \not{p}_2 | 5_{\dot{e}}] \langle 4_d | \not{p}_5 \not{p}_1 \not{p}_2 \not{p}_3 | 4_{\dot{d}} \rangle + \frac{1}{2} \langle 3_c 4_d 5_e 1^a \rangle [3_{\dot{c}} 4_{\dot{d}} 5_{\dot{e}} 2_b] \langle 1_a \tilde{\Sigma}_{2\dot{b}}^b \rangle, \end{aligned} \quad (\text{C.10})$$

and

$$\begin{aligned} 2\mathcal{D}_{c\dot{c}d\dot{d}e\dot{e}}^s = & -\langle 4_d | \not{p}_1 | 5_e \rangle [3_{\dot{c}} | \not{p}_2 | 5_{\dot{e}}] \langle 3_c \tilde{\Sigma}_{4\dot{d}} \rangle + \langle 4_d | \not{p}_1 | 5_e \rangle [3_{\dot{c}} | \not{p}_2 | 4_{\dot{d}}] \langle 3_c \tilde{\Sigma}_{5\dot{e}} \rangle \\ & - \langle 3_c | \not{p}_1 | 5_e \rangle [3_{\dot{c}} | \not{p}_2 | 4_{\dot{d}}] \langle 4_d \tilde{\Sigma}_{5\dot{e}} \rangle + \langle 3_c | \not{p}_1 | 5_e \rangle [4_{\dot{d}} | \not{p}_2 | 5_{\dot{e}}] [3_{\dot{c}} \Sigma_{4d}] \\ & - \langle 3_c | \not{p}_1 | 4_d \rangle [4_{\dot{d}} | \not{p}_2 | 5_{\dot{e}}] [3_{\dot{c}} \Sigma_{5e}] + \langle 3_c | \not{p}_1 | 4_d \rangle [3_{\dot{c}} | \not{p}_2 | 5_{\dot{e}}] [4_{\dot{d}} \Sigma_{5e}]. \end{aligned} \quad (\text{C.11})$$

The Σ and $\tilde{\Sigma}$ that appear in the previous formulae are defined as

$$\begin{aligned} |\Sigma_{ia}\rangle &= \left(\not{p}_i \not{p}_{i+1} \not{p}_{i+2} \not{p}_{i+3} - \not{p}_i \not{p}_{i+3} \not{p}_{i+2} \not{p}_{i+1} \right) |i_a\rangle \\ |\tilde{\Sigma}_{ia}\rangle &= \left(\not{p}_i \not{p}_{i+1} \not{p}_{i+2} \not{p}_{i+3} - \not{p}_i \not{p}_{i+3} \not{p}_{i+2} \not{p}_{i+1} \right) |i_a\rangle \end{aligned} \quad (\text{C.12})$$

where we define $\not{p}_6 \equiv \not{p}_1$.

C.2 Non-Minimal Form Factors

In this section we will address the computation of six-dimensional tree-level building blocks using BCFW recursion relations¹. In particular we briefly comment on the main steps of the calculation of $\text{Tr } F^2$ in the non-minimal configuration.

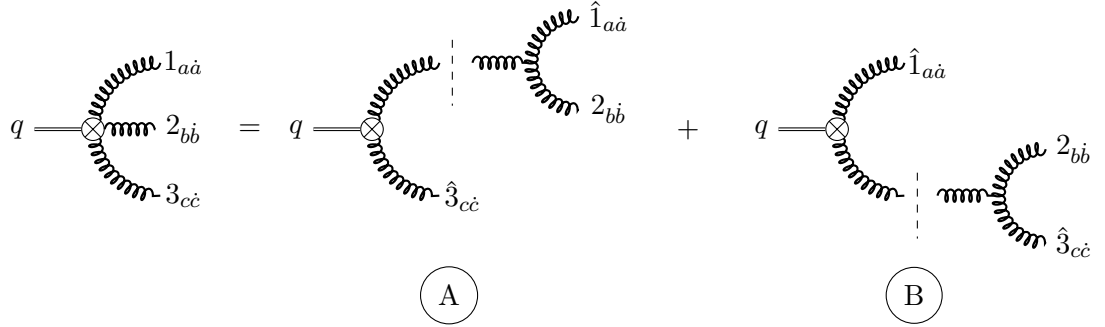


Figure C.1: BCFW construction of the tree-level non-minimal $\text{Tr } F^2$ form factor in six dimensions.

Diagrammatically the terms we need to compute are represented in Figure C.1. In this computation one needs to make use of the three-point on-shell amplitudes in six-dimensions. These are most conveniently defined in terms of a set of auxiliary $\text{SU}(2)$ spinors which we denote by $u_a, \tilde{u}_{\hat{a}}, w_a$ and $\tilde{w}_{\hat{a}}$, following the conventions of [152]. These objects are not Lorentz-invariants in six dimensions and thus are not allowed to appear in the final expression, however they enjoy useful properties which simplify the calculation. The on-shell three-point amplitude cleanly expressed in terms of the above mentioned spinors:

$$\mathcal{A}_3(1_{a\hat{a}}, 2_{b\hat{b}}, 3_{c\hat{c}}) = i \Gamma_{abc}(1, 2, 3) \tilde{\Gamma}_{\hat{a}\hat{b}\hat{c}}(1, 2, 3), \quad (\text{C.13})$$

with

$$\begin{aligned} \Gamma_{abc}(1, 2, 3) &= u_{1a} u_{2b} w_{3c} + u_{1a} w_{2b} u_{3c} + w_{1a} u_{2b} u_{3c}, \\ \tilde{\Gamma}_{\hat{a}\hat{b}\hat{c}}(1, 2, 3) &= \tilde{u}_{1\hat{a}} \tilde{u}_{2\hat{b}} \tilde{w}_{3\hat{c}} + \tilde{u}_{1\hat{a}} \tilde{w}_{2\hat{b}} \tilde{u}_{3\hat{c}} + \tilde{w}_{1\hat{a}} \tilde{u}_{2\hat{b}} \tilde{u}_{3\hat{c}}. \end{aligned} \quad (\text{C.14})$$

Consider now applying six-dimensional BCFW as in Figure C.1. The hatted momenta are shifted by a quantity proportional to the complex parameter z as

$$\begin{aligned} \hat{p}_1 &= p_1 + z X^{a\hat{a}} \varepsilon_{1a\hat{a}}, \\ \hat{p}_3 &= p_3 - z X^{a\hat{a}} \varepsilon_{1a\hat{a}}, \end{aligned} \quad (\text{C.15})$$

¹For a more detailed account of six-dimensional BCFW see [152].

where $X^{a\dot{a}}$ is an arbitrary tensor needed to saturate the little group indices. This tensor, which also multiplies C.19, will be removed at the end of the calculation. The on-shell condition $\hat{p}_{1,2}^2 = 0$ implies $\det X = 0$, which allows to express X as

$$X^{a\dot{a}} = x^a \tilde{x}^{\dot{a}}. \quad (\text{C.16})$$

Furthermore we can define the quantities

$$y^b = \tilde{x}^{\dot{a}} \langle 3_b 1^{\dot{a}} \rangle^{-1}, \quad \tilde{y}_{\dot{b}} = x^a \langle 1^a 3^{\dot{b}} \rangle^{-1}, \quad (\text{C.17})$$

which allow us to rewrite the momentum shift C.15 in terms of the spinor shifts

$$\begin{aligned} |\hat{1}^a\rangle &= |1^a\rangle + z x^a y_b |3^b\rangle, \\ |\hat{3}^b\rangle &= |3^b\rangle + z y^b x_a |1^a\rangle, \\ |\hat{1}^{\dot{a}}\rangle &= |1^{\dot{a}}\rangle - z \tilde{x}^{\dot{a}} \tilde{y}_{\dot{b}} |3^{\dot{b}}\rangle, \\ |\hat{3}^{\dot{b}}\rangle &= |3^{\dot{b}}\rangle - z \tilde{y}^{\dot{b}} \tilde{x}_{\dot{a}} |1^{\dot{a}}\rangle. \end{aligned} \quad (\text{C.18})$$

Considering now for example term A in Figure C.1 one has

$$\begin{aligned} (\text{A}) &= X^{a\dot{a}} \mathcal{A}_3(\hat{1}_{a\dot{a}}, 2_{b\dot{b}}, \hat{k}_{d\dot{d}}) \frac{-i}{s_{12}} F_{\mathcal{O}_2}^{(0)}(-\hat{k}^{d\dot{d}}, \hat{3}_{c\dot{c}}; q) \\ &= \frac{i}{s_{12}} X^{a\dot{a}} \Gamma_{abd}(\hat{1}, 2, \hat{k}) \tilde{\Gamma}_{\dot{a}\dot{b}\dot{d}}(\hat{1}, 2, \hat{k}) \langle \hat{k}^d \hat{3}_{\dot{c}} \rangle \langle \hat{3}_{\dot{c}} \hat{k}^{\dot{d}} \rangle. \end{aligned} \quad (\text{C.19})$$

Before substituting the definitions (C.18) in (C.19), we make use of the properties of $u, \tilde{u}, w, \tilde{w}$ to simplify this expression. The most useful identities are

$$\begin{aligned} u_{i\dot{a}} w_{i\dot{b}} - u_{i\dot{b}} w_{i\dot{a}} &= \epsilon_{\dot{a}\dot{b}}, \quad \tilde{u}_{i\dot{a}} \tilde{w}_{i\dot{b}} - \tilde{u}_{i\dot{b}} \tilde{w}_{i\dot{a}} = \epsilon_{\dot{a}\dot{b}}, \\ |u_i \cdot i\rangle &= |u_j \cdot j\rangle, \quad |\tilde{u}_i \cdot i\rangle = |\tilde{u}_j \cdot j\rangle \quad \forall i, j = 1, 2, k, \\ |w_1 \cdot 1\rangle + |w_2 \cdot 2\rangle + |w_k \cdot k\rangle &= 0, \\ |\tilde{w}_1 \cdot 1\rangle + |\tilde{w}_2 \cdot 2\rangle + |\tilde{w}_k \cdot k\rangle &= 0, \end{aligned} \quad (\text{C.20})$$

where we used the shorthand notation $u_{i\dot{a}} |i^{\dot{a}}\rangle = |u_i \cdot i\rangle$ and $\tilde{u}_{i\dot{a}} |\dot{i}^{\dot{a}}\rangle = |\tilde{u}_i \cdot i\rangle$. These identities allow us to rewrite

$$\begin{aligned} \Gamma_{abd}(\hat{1}, 2, \hat{k}) \langle \hat{k}^d \rangle &= \langle \hat{1}_a | u_{2b} + \langle 2_b | u_{\hat{1}a}, \\ \tilde{\Gamma}_{\dot{a}\dot{b}\dot{d}}(\hat{1}, 2, \hat{k}) |\hat{k}^{\dot{d}}\rangle &= |\hat{1}_{\dot{a}}\rangle \tilde{u}_{2\dot{b}} + |2_{\dot{b}}\rangle \tilde{u}_{\hat{1}\dot{a}}, \end{aligned} \quad (\text{C.21})$$

which in turn leads to

$$(A) = \frac{i}{s_{12}} X^{a\dot{a}} \left(\langle \hat{1}_a \hat{3}_{\dot{c}} \rangle \langle \hat{3}_c \hat{1}_{\dot{a}} \rangle u_{2b} \tilde{u}_{2\dot{b}} + \langle \hat{1}_a \hat{3}_{\dot{c}} \rangle \langle \hat{3}_c 2_b \rangle u_{2b} \tilde{u}_{1\dot{a}} \right. \\ \left. + \langle 2_b \hat{3}_{\dot{c}} \rangle \langle \hat{3}_c \hat{1}_{\dot{a}} \rangle u_{\hat{1}_a} \tilde{u}_{2\dot{b}} + \langle 2_b \hat{3}_{\dot{c}} \rangle \langle \hat{3}_c 2_b \rangle u_{\hat{1}_a} \tilde{u}_{\hat{1}_{\dot{a}}} \right). \quad (C.22)$$

To further simplify the result, and to eliminate the residual SU(2) spinors, we make the following observations:

- pairs of u_i, \tilde{u}_j with $i \neq j$ can be immediately rewritten in terms of six-dimensional invariants as

$$u_{1_a} \tilde{u}_{2\dot{b}} = \langle 1_a 2_b \rangle, \quad u_{2_b} \tilde{u}_{1\dot{a}} = -\langle 2_b 1_a \rangle, \\ u_{2_b} \tilde{u}_{k\dot{c}} = \langle 2_b k_{\dot{c}} \rangle, \quad u_{k_c} \tilde{u}_{2\dot{b}} = -\langle k_c 2_b \rangle. \quad (C.23)$$

- pairs of u_i, \tilde{u}_j with $i = j$ can be rewritten using the identity [386]

$$u_{i_a} \tilde{u}_{i\dot{a}} = \frac{(-1)^{\mathcal{P}_{ij}}}{s_{iP}} \langle i_a | p_j P | i_{\dot{a}} \rangle, \quad (C.24)$$

where p_j is any other momentum belonging to the same three-point amplitude as p_i , and $\mathcal{P}_{ij} = +1$ for clockwise ordering of the states (i, j) . Also P is any given arbitrary momentum.

Repeating a similar reasoning on term (B) one gets

$$(B) = \frac{i}{s_{23}} X^{a\dot{a}} \left(\langle \hat{1}_a \hat{3}_{\dot{c}} \rangle \langle \hat{3}_c \hat{1}_{\dot{a}} \rangle u_{2b} \tilde{u}_{2\dot{b}} + \langle \hat{1}_a \hat{3}_{\dot{c}} \rangle \langle 2_b \hat{1}_{\dot{a}} \rangle u_{3c} \tilde{u}_{2\dot{b}} \right. \\ \left. + \langle \hat{1}_a 2_b \rangle \langle \hat{3}_c \hat{1}_{\dot{a}} \rangle u_{2b} \tilde{u}_{3\dot{c}} + \langle \hat{1}_a 2_b \rangle \langle 2_b \hat{1}_{\dot{a}} \rangle u_{3c} \tilde{u}_{3\dot{c}} \right). \quad (C.25)$$

The on-shell condition for the intermediate propagators in (A) and (B) defines two different BCFW shift parameters, which we label z_A and z_B respectively. By computing z_A and z_B one can see that they are related by

$$z_B = -\frac{s_{23}}{s_{12}} z_A. \quad (C.26)$$

Thanks to this relation multiple cancellations happen between terms in (A) and terms in (B). With some further algebra and removing the $X^{a\dot{a}}$ tensor, one arrives at (7.63).

The analytic expression of the six-dimensional form factor $F_{\mathcal{O}_2}^{(0)}(1_{a\dot{a}}, 2_{b\dot{b}}, 3_{c\dot{c}}; q)$ could also be computed using Feynman diagrams, see for example [113]. Due to the low multiplicity of this form factor, there is just a small number of contributing Feynman diagrams. The diagrammatic approach may thus be considered as equivalently viable as BCFW in this case, the latter method however leads to a far more compact expression with all the symmetries manifest.

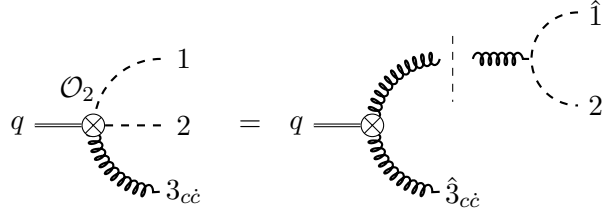


Figure C.2: BCFW construction of the tree-level non-minimal $\text{Tr } F^2$ form factor with two scalars.

In a similar way but with much less involved calculation, we can find both the non-minimal form factors with two scalars and one gluon (7.64) and (7.65). In Figure C.2 and Figure C.3 we show the BCFW factorization channels for these calculations. The only missing ingredient is the three-point amplitude with two scalars and one gluon in six dimensions, which turns out to be very simple:

$$\mathcal{A}(1_{a\hat{a}}, 2, 3) = i u_{1a} \tilde{u}_{1\hat{a}} . \tag{C.27}$$

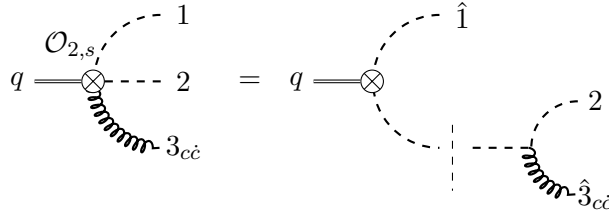


Figure C.3: BCFW construction of the tree-level non-minimal $D\phi^2$ form factor.

C.3 Integral Expressions

The integrals needed in the calculations of Section 7 are:

$$\begin{aligned}
 \text{Diagram 1} &= \int \frac{d^{4-2\epsilon}l}{(2\pi)^{4-2\epsilon}} \frac{1}{l^2 (l+p_1+p_2)^2} = i \frac{c_\Gamma}{(4\pi)^{2-\epsilon}} \frac{(-s_{12})^{-\epsilon}}{\epsilon(1-2\epsilon)}, \\
 \text{Diagram 2} &= \int \frac{d^{4-2\epsilon}l}{(2\pi)^{4-2\epsilon}} \frac{1}{l^2 (l+p_2)^2 (l+p_1+p_2)^2} = -\frac{i c_\Gamma}{(4\pi)^{2-\epsilon}} \frac{(-s_{12})^{-1-\epsilon}}{\epsilon^2}, \\
 \text{Diagram 3} &= -\frac{i c_\Gamma}{(4\pi)^{2-\epsilon}} \frac{1}{\epsilon^2} \left[\frac{(-q^2)^{-\epsilon} - (-p^2)^{-\epsilon}}{q^2 - p^2} \right],
 \end{aligned} \tag{C.28}$$

and

$$\begin{aligned}
 \text{Diagram 4} &= \int \frac{d^{4-2\epsilon}l}{(2\pi)^{4-2\epsilon}} \frac{1}{l^2 (l+p_1)^2 (l+p_1+p_2)^2 (l+p_1+p_2+p_3)^2} \\
 &= -\frac{2 i c_\Gamma}{(4\pi)^{2-\epsilon}} \frac{1}{s_{12}s_{23}} \left\{ -\frac{1}{\epsilon^2} \left[(-s_{12})^{-\epsilon} + (-s_{23})^{-\epsilon} - (-q^2)^{-\epsilon} \right] + \right. \\
 &\quad \left. + \text{Li}_2 \left(1 - \frac{s_{12}}{q^2} \right) + \text{Li}_2 \left(1 - \frac{s_{23}}{q^2} \right) + \frac{1}{2} \log^2 \left(\frac{s_{12}}{s_{23}} \right) + \frac{\pi^2}{6} \right\} + \mathcal{O}(\epsilon),
 \end{aligned} \tag{C.29}$$

where

$$c_\Gamma = \frac{\Gamma[1+\epsilon] \Gamma[1-\epsilon]^2}{\Gamma[1-2\epsilon]} . \tag{C.30}$$

This results are exact to all orders in ϵ , and the expression of the corresponding integral functions in a different number of dimensions can be obtained by simply replacing ϵ with the appropriate value, for instance $\epsilon \mapsto \epsilon - 1$ and $\epsilon \mapsto \epsilon - 2$ for $d = 6 - 2\epsilon$ and $d = 8 - 2\epsilon$, respectively. In particular it turns out that all the integrals which give the rational terms, *i.e.* those with a non-trivial numerator written in (7.28), can always be expressed as integrals in higher dimensions [110]. Indeed consider the general integral function

$$I_n^d[\mu^{2p}] = \int \frac{d^{4-2\epsilon}l}{(2\pi)^{4-2\epsilon}} (\mu^2)^p f_n(\{p_i\}, l) = \int \frac{d^4l^{(4)}}{(2\pi)^4} \int \frac{d^{-2\epsilon}\mu}{(2\pi)^{-2\epsilon}} (\mu^2)^p f_n(\{p_i\}, l), \tag{C.31}$$

and the μ -measure can be rewritten as

$$\begin{aligned} \int d^{-2\epsilon} \mu (\mu^2)^p &= \frac{1}{2} \int d\Omega_{-1-2\epsilon} \int_0^{+\infty} d\mu^2 (\mu^2)^{-1-\epsilon+p} \\ &= \frac{\int \Omega_{-1-2\epsilon}}{\int d\Omega_{2p-1-2\epsilon}} \int d^{2p-2\epsilon} \mu . \end{aligned} \quad (\text{C.32})$$

Then (C.31) can be written as

$$\begin{aligned} I_n^d[\mu^{2p}] &= \frac{(2\pi)^{2p} \int d\Omega_{-1-2\epsilon}}{\int d\Omega_{2p-1-2\epsilon}} \int \frac{d^{4+2p-2\epsilon} l}{(2\pi)^{4+2p-2\epsilon}} f_n(\{p_i\}, l) \\ &= -\epsilon(1-\epsilon)(2-\epsilon) \cdots (p-1-\epsilon) (4\pi)^p I_n^{d+2p}[1] , \end{aligned} \quad (\text{C.33})$$

where

$$\int d\Omega_x = \frac{2\pi^{\frac{x+1}{2}}}{\Gamma[\frac{x+1}{2}]} . \quad (\text{C.34})$$

We can then obtain the following values of the integrals involving the mass term μ :

$$\begin{aligned} \text{Diagram 1} &= \frac{-i}{(4\pi)^2} \cdot \frac{s_{12}}{6} + \mathcal{O}(\epsilon) , & \text{Diagram 2} &= \mathcal{O}(\epsilon) , \\ \text{Diagram 3} &= \frac{i}{(4\pi)^2} \cdot \frac{1}{2} + \mathcal{O}(\epsilon) , & \text{Diagram 4} &= \frac{-i}{(4\pi)^2} \cdot \frac{1}{6} + \mathcal{O}(\epsilon) , \\ \text{Diagram 5} &= \frac{i}{(4\pi)^2} \cdot \frac{s_{12}}{24} + \mathcal{O}(\epsilon) , & & \end{aligned}$$

Bibliography

- [1] M. Accettulli Huber, A. Brandhuber, S. De Angelis, and G. Travaglini, “Complete Form Factors in Yang-Mills from Unitarity and Spinor Helicity in Six Dimensions,” *Phys. Rev. D* **101** no. 2, (2020) 026004, [arXiv:1910.04772 \[hep-th\]](#).
- [2] M. Accettulli Huber, A. Brandhuber, S. De Angelis, and G. Travaglini, “Note on the absence of R^2 corrections to Newton’s potential,” *Phys. Rev. D* **101** no. 4, (2020) 046011, [arXiv:1911.10108 \[hep-th\]](#).
- [3] M. Accettulli Huber, A. Brandhuber, S. De Angelis, and G. Travaglini, “Eikonal phase matrix, deflection angle and time delay in effective field theories of gravity,” *Phys. Rev. D* **102** no. 4, (2020) 046014, [arXiv:2006.02375 \[hep-th\]](#).
- [4] M. Accettulli Huber, A. Brandhuber, S. De Angelis, and G. Travaglini, “From amplitudes to gravitational radiation with cubic interactions and tidal effects,” *Phys. Rev. D* **103** no. 4, (2021) 045015, [arXiv:2012.06548 \[hep-th\]](#).
- [5] M. Accettulli Huber and S. De Angelis, “Standard Model EFTs via on-shell methods,” *JHEP* **11** (2021) 221, [arXiv:2108.03669 \[hep-th\]](#).
- [6] M. A. Huber, A. Correia, S. Ramgoolam, and M. Sadrzadeh, “Permutation invariant matrix statistics and computational language tasks,” [arXiv:2202.06829 \[cs.CL\]](#).
- [7] **CMS** Collaboration, S. Chatrchyan *et al.*, “Observation of a New Boson at a Mass of 125 GeV with the CMS Experiment at the LHC,” *Phys. Lett. B* **716** (2012) 30–61, [arXiv:1207.7235 \[hep-ex\]](#).
- [8] G. Aad, T. Abajyan, B. Abbott, J. Abdallah, S. Abdel Khalek, A. Abdelalim, O. Abdinov, R. Aben, B. Abi, M. Abolins, and O. AbouZeid, “Observation of a new particle in the search for the standard model higgs boson with the atlas detector at the lhc,” *Physics Letters B* **716** no. 1, (2012) 1–29. <https://www.sciencedirect.com/science/article/pii/S037026931200857X>.

-
- [9] R. P. Feynman, “Space-time approach to quantum electrodynamics,” *Phys. Rev.* **76** (Sep, 1949) 769–789. <https://link.aps.org/doi/10.1103/PhysRev.76.769>.
- [10] Z. Bern, L. J. Dixon, D. C. Dunbar, and D. A. Kosower, “One loop n point gauge theory amplitudes, unitarity and collinear limits,” *Nucl. Phys.* **B425** (1994) 217–260, [arXiv:hep-ph/9403226](https://arxiv.org/abs/hep-ph/9403226) [hep-ph].
- [11] Z. Bern, L. J. Dixon, D. C. Dunbar, and D. A. Kosower, “Fusing gauge theory tree amplitudes into loop amplitudes,” *Nucl. Phys.* **B435** (1995) 59–101, [arXiv:hep-ph/9409265](https://arxiv.org/abs/hep-ph/9409265) [hep-ph].
- [12] R. Britto, F. Cachazo, and B. Feng, “Generalized unitarity and one-loop amplitudes in N=4 super-Yang-Mills,” *Nucl. Phys.* **B725** (2005) 275–305, [arXiv:hep-th/0412103](https://arxiv.org/abs/hep-th/0412103) [hep-th].
- [13] R. Britto, F. Cachazo, B. Feng, and E. Witten, “Direct proof of tree-level recursion relation in Yang-Mills theory,” *Phys. Rev. Lett.* **94** (2005) 181602, [arXiv:hep-th/0501052](https://arxiv.org/abs/hep-th/0501052) [hep-th].
- [14] M. L. Mangano and S. J. Parke, “Multiparton amplitudes in gauge theories,” *Phys. Rept.* **200** (1991) 301–367, [arXiv:hep-th/0509223](https://arxiv.org/abs/hep-th/0509223) [hep-th].
- [15] S. J. Parke and T. R. Taylor, “An Amplitude for n Gluon Scattering,” *Phys. Rev. Lett.* **56** (1986) 2459.
- [16] M. L. Mangano, S. J. Parke, and Z. Xu, “Duality and Multi - Gluon Scattering,” *Nucl. Phys. B* **298** (1988) 653–672.
- [17] Z. Bern, L. J. Dixon, and D. A. Kosower, “One loop amplitudes for $e^+ e^-$ to four partons,” *Nucl. Phys.* **B513** (1998) 3–86, [arXiv:hep-ph/9708239](https://arxiv.org/abs/hep-ph/9708239) [hep-ph].
- [18] Z. Bern, L. J. Dixon, and D. A. Kosower, “Two-loop $g \rightarrow gg$ splitting amplitudes in QCD,” *JHEP* **08** (2004) 012, [arXiv:hep-ph/0404293](https://arxiv.org/abs/hep-ph/0404293).
- [19] R. K. Ellis, K. Melnikov, and G. Zanderighi, “W+3 jet production at the Tevatron,” *Phys. Rev. D* **80** (2009) 094002, [arXiv:0906.1445](https://arxiv.org/abs/0906.1445) [hep-ph].
- [20] C. F. Berger, Z. Bern, L. J. Dixon, F. Febres Cordero, D. Forde, T. Gleisberg, H. Ita, D. A. Kosower, and D. Maitre, “Precise Predictions for W + 4 Jet Production at the Large Hadron Collider,” *Phys. Rev. Lett.* **106** (2011) 092001, [arXiv:1009.2338](https://arxiv.org/abs/1009.2338) [hep-ph].
- [21] Z. Bern, J. J. M. Carrasco, W.-M. Chen, H. Johansson, R. Roiban, and M. Zeng, “Five-loop four-point integrand of $N = 8$ supergravity as a generalized double copy,” *Phys. Rev. D* **96** no. 12, (2017) 126012, [arXiv:1708.06807](https://arxiv.org/abs/1708.06807) [hep-th].

-
- [22] Z. Bern, J. J. Carrasco, W.-M. Chen, A. Edison, H. Johansson, J. Parra-Martinez, R. Roiban, and M. Zeng, “Ultraviolet Properties of $\mathcal{N} = 8$ Supergravity at Five Loops,” *Phys. Rev. D* **98** no. 8, (2018) 086021, [arXiv:1804.09311 \[hep-th\]](#).
- [23] N. E. J. Bjerrum-Bohr, J. F. Donoghue, and P. Vanhove, “On-shell Techniques and Universal Results in Quantum Gravity,” *JHEP* **02** (2014) 111, [arXiv:1309.0804 \[hep-th\]](#).
- [24] F. Cachazo and A. Guevara, “Leading Singularities and Classical Gravitational Scattering,” [arXiv:1705.10262 \[hep-th\]](#).
- [25] A. Guevara, “Holomorphic Classical Limit for Spin Effects in Gravitational and Electromagnetic Scattering,” *JHEP* **04** (2019) 033, [arXiv:1706.02314 \[hep-th\]](#).
- [26] D. A. Kosower, B. Maybee, and D. O’Connell, “Amplitudes, Observables, and Classical Scattering,” *JHEP* **02** (2019) 137, [arXiv:1811.10950 \[hep-th\]](#).
- [27] M.-Z. Chung, Y.-T. Huang, J.-W. Kim, and S. Lee, “The simplest massive S-matrix: from minimal coupling to Black Holes,” *JHEP* **04** (2019) 156, [arXiv:1812.08752 \[hep-th\]](#).
- [28] B. Maybee, D. O’Connell, and J. Vines, “Observables and amplitudes for spinning particles and black holes,” [arXiv:1906.09260 \[hep-th\]](#).
- [29] Z. Bern, C. Cheung, R. Roiban, C.-H. Shen, M. P. Solon, and M. Zeng, “Scattering Amplitudes and the Conservative Hamiltonian for Binary Systems at Third Post-Minkowskian Order,” *Phys. Rev. Lett.* **122** no. 20, (2019) 201603, [arXiv:1901.04424 \[hep-th\]](#).
- [30] Z. Bern, J. Parra-Martinez, R. Roiban, M. S. Ruf, C.-H. Shen, M. P. Solon, and M. Zeng, “Scattering Amplitudes and Conservative Binary Dynamics at $\mathcal{O}(G^4)$,” *Phys. Rev. Lett.* **126** no. 17, (2021) 171601, [arXiv:2101.07254 \[hep-th\]](#).
- [31] E. Herrmann, J. Parra-Martinez, M. S. Ruf, and M. Zeng, “Radiative classical gravitational observables at $\mathcal{O}(G^3)$ from scattering amplitudes,” *JHEP* **10** (2021) 148, [arXiv:2104.03957 \[hep-th\]](#).
- [32] A. Cristofoli, R. Gonzo, D. A. Kosower, and D. O’Connell, “Waveforms from Amplitudes,” [arXiv:2107.10193 \[hep-th\]](#).
- [33] R. Britto, R. Gonzo, and G. R. Jehu, “Graviton particle statistics and coherent states from classical scattering amplitudes,” *JHEP* **03** (2022) 214, [arXiv:2112.07036 \[hep-th\]](#).

- [34] C. Cheung and C.-H. Shen, “Nonrenormalization Theorems without Supersymmetry,” *Phys. Rev. Lett.* **115** no. 7, (2015) 071601, [arXiv:1505.01844 \[hep-ph\]](#).
- [35] Z. Bern, J. Parra-Martinez, and E. Sawyer, “Nonrenormalization and Operator Mixing via On-Shell Methods,” *Phys. Rev. Lett.* **124** no. 5, (2020) 051601, [arXiv:1910.05831 \[hep-ph\]](#).
- [36] M. Jiang, J. Shu, M.-L. Xiao, and Y.-H. Zheng, “Partial Wave Amplitude Basis and Selection Rules in Effective Field Theories,” *Phys. Rev. Lett.* **126** no. 1, (2021) 011601, [arXiv:2001.04481 \[hep-ph\]](#).
- [37] Z. Bern, J. Parra-Martinez, and E. Sawyer, “Structure of two-loop SMEFT anomalous dimensions via on-shell methods,” *JHEP* **10** (2020) 211, [arXiv:2005.12917 \[hep-ph\]](#).
- [38] N. Arkani-Hamed and J. Trnka, “The Amplituhedron,” *JHEP* **10** (2014) 030, [arXiv:1312.2007 \[hep-th\]](#).
- [39] S. Caron-Huot, L. J. Dixon, F. Dulat, M. von Hippel, A. J. McLeod, and G. Papathanasiou, “Six-Gluon amplitudes in planar $\mathcal{N} = 4$ super-Yang-Mills theory at six and seven loops,” *JHEP* **08** (2019) 016, [arXiv:1903.10890 \[hep-th\]](#).
- [40] S. Caron-Huot, L. J. Dixon, J. M. Drummond, F. Dulat, J. Foster, O. Gürdoğan, M. von Hippel, A. J. McLeod, and G. Papathanasiou, “The Steinmann Cluster Bootstrap for $N = 4$ Super Yang-Mills Amplitudes,” *PoS CORFU2019* (2020) 003, [arXiv:2005.06735 \[hep-th\]](#).
- [41] A. Brandhuber, B. Spence, G. Travaglini, and G. Yang, “Form Factors in $\mathcal{N} = 4$ Super Yang-Mills and Periodic Wilson Loops,” *JHEP* **01** (2011) 134, [arXiv:1011.1899 \[hep-th\]](#).
- [42] L. V. Bork, D. I. Kazakov, and G. S. Vartanov, “On form factors in $N=4$ sym,” *JHEP* **02** (2011) 063, [arXiv:1011.2440 \[hep-th\]](#).
- [43] A. Brandhuber, O. Gurdogan, R. Mooney, G. Travaglini, and G. Yang, “Harmony of Super Form Factors,” *JHEP* **10** (2011) 046, [arXiv:1107.5067 \[hep-th\]](#).
- [44] L. V. Bork, D. I. Kazakov, and G. S. Vartanov, “On MHV Form Factors in Superspace for $\mathcal{N} = 4$ SYM Theory,” *JHEP* **10** (2011) 133, [arXiv:1107.5551 \[hep-th\]](#).
- [45] L. V. Bork, “On NMHV form factors in $N=4$ SYM theory from generalized unitarity,” *JHEP* **01** (2013) 049, [arXiv:1203.2596 \[hep-th\]](#).

- [46] R. H. Boels, B. A. Kniehl, O. V. Tarasov, and G. Yang, “Color-kinematic Duality for Form Factors,” *JHEP* **02** (2013) 063, [arXiv:1211.7028 \[hep-th\]](#).
- [47] B. Penante, B. Spence, G. Travaglini, and C. Wen, “On super form factors of half-BPS operators in N=4 super Yang-Mills,” *JHEP* **1404** (2014) 083, [arXiv:1402.1300 \[hep-th\]](#).
- [48] L. Bianchi, A. Brandhuber, R. Panerai, and G. Travaglini, “Form factor recursion relations at loop level,” *JHEP* **02** (2019) 182, [arXiv:1812.09001 \[hep-th\]](#).
- [49] L. Bianchi, A. Brandhuber, R. Panerai, and G. Travaglini, “Dual conformal invariance for form factors,” *JHEP* **02** (2019) 134, [arXiv:1812.10468 \[hep-th\]](#).
- [50] L. J. Dixon, A. J. McLeod, and M. Wilhelm, “A Three-Point Form Factor Through Five Loops,” *JHEP* **04** (2021) 147, [arXiv:2012.12286 \[hep-th\]](#).
- [51] W. Buchmuller and D. Wyler, “Effective Lagrangian Analysis of New Interactions and Flavor Conservation,” *Nucl. Phys.* **B268** (1986) 621–653.
- [52] I. Brivio and M. Trott, “The Standard Model as an Effective Field Theory,” *Phys. Rept.* **793** (2019) 1–98, [arXiv:1706.08945 \[hep-ph\]](#).
- [53] L. Lehman and A. Martin, “Hilbert Series for Constructing Lagrangians: expanding the phenomenologist’s toolbox,” *Phys. Rev. D* **91** (2015) 105014, [arXiv:1503.07537 \[hep-ph\]](#).
- [54] B. Henning, X. Lu, T. Melia, and H. Murayama, “Hilbert series and operator bases with derivatives in effective field theories,” *Commun. Math. Phys.* **347** no. 2, (2016) 363–388, [arXiv:1507.07240 \[hep-th\]](#).
- [55] B. Henning, X. Lu, T. Melia, and H. Murayama, “2, 84, 30, 993, 560, 15456, 11962, 261485, ...: Higher dimension operators in the SM EFT,” *JHEP* **08** (2017) 016, [arXiv:1512.03433 \[hep-ph\]](#). [Erratum: *JHEP* 09, 019 (2019)].
- [56] Y. Shadmi and Y. Weiss, “Effective Field Theory Amplitudes the On-Shell Way: Scalar and Vector Couplings to Gluons,” *JHEP* **02** (2019) 165, [arXiv:1809.09644 \[hep-ph\]](#).
- [57] T. Ma, J. Shu, and M.-L. Xiao, “Standard Model Effective Field Theory from On-shell Amplitudes,” [arXiv:1902.06752 \[hep-ph\]](#).
- [58] R. Aoude and C. S. Machado, “The Rise of SMEFT On-shell Amplitudes,” *JHEP* **12** (2019) 058, [arXiv:1905.11433 \[hep-ph\]](#).

-
- [59] G. Durieux, T. Kitahara, Y. Shadmi, and Y. Weiss, “The electroweak effective field theory from on-shell amplitudes,” *JHEP* **01** (2020) 119, [arXiv:1909.10551 \[hep-ph\]](#).
- [60] A. Falkowski, “Bases of massless EFTs via momentum twistors,” [arXiv:1912.07865 \[hep-ph\]](#).
- [61] G. Durieux and C. S. Machado, “Enumerating higher-dimensional operators with on-shell amplitudes,” *Phys. Rev. D* **101** no. 9, (2020) 095021, [arXiv:1912.08827 \[hep-ph\]](#).
- [62] A. Falkowski, G. Isabella, and C. S. Machado, “On-shell effective theory for higher-spin dark matter,” *SciPost Phys.* **10** no. 5, (2021) 101, [arXiv:2011.05339 \[hep-ph\]](#).
- [63] G. Durieux, T. Kitahara, C. S. Machado, Y. Shadmi, and Y. Weiss, “Constructing massive on-shell contact terms,” *JHEP* **12** (2020) 175, [arXiv:2008.09652 \[hep-ph\]](#).
- [64] H.-L. Li, Z. Ren, J. Shu, M.-L. Xiao, J.-H. Yu, and Y.-H. Zheng, “Complete Set of Dimension-8 Operators in the Standard Model Effective Field Theory,” [arXiv:2005.00008 \[hep-ph\]](#).
- [65] H.-L. Li, Z. Ren, M.-L. Xiao, J.-H. Yu, and Y.-H. Zheng, “Complete Set of Dimension-9 Operators in the Standard Model Effective Field Theory,” [arXiv:2007.07899 \[hep-ph\]](#).
- [66] B. Henning, X. Lu, and H. Murayama, “How to use the Standard Model effective field theory,” *JHEP* **01** (2016) 023, [arXiv:1412.1837 \[hep-ph\]](#).
- [67] I. Brivio, Y. Jiang, and M. Trott, “The SMEFTsim package, theory and tools,” *JHEP* **12** (2017) 070, [arXiv:1709.06492 \[hep-ph\]](#).
- [68] I. Brivio, T. Corbett, and M. Trott, “The Higgs width in the SMEFT,” *JHEP* **10** (2019) 056, [arXiv:1906.06949 \[hep-ph\]](#).
- [69] S. Dawson, S. Homiller, and S. D. Lane, “Putting standard model EFT fits to work,” *Phys. Rev. D* **102** no. 5, (2020) 055012, [arXiv:2007.01296 \[hep-ph\]](#).
- [70] A. David and G. Passarino, “Use and reuse of SMEFT,” [arXiv:2009.00127 \[hep-ph\]](#).
- [71] J. Ellis, M. Madigan, K. Mimasu, V. Sanz, and T. You, “Top, Higgs, Diboson and Electroweak Fit to the Standard Model Effective Field Theory,” *JHEP* **04** (2021) 279, [arXiv:2012.02779 \[hep-ph\]](#).

- [72] M. Trott, “A methodology for theory uncertainties in the SMEFT,” [arXiv:2106.13794 \[hep-ph\]](#).
- [73] J. Ellis, N. E. Mavromatos, and T. You, “Light-by-Light Scattering Constraint on Born-Infeld Theory,” *Phys. Rev. Lett.* **118** no. 26, (2017) 261802, [arXiv:1703.08450 \[hep-ph\]](#).
- [74] J. Ellis and S.-F. Ge, “Constraining Gluonic Quartic Gauge Coupling Operators with $gg \rightarrow \gamma\gamma$,” *Phys. Rev. Lett.* **121** no. 4, (2018) 041801, [arXiv:1802.02416 \[hep-ph\]](#).
- [75] J. Ellis, H.-J. He, and R.-Q. Xiao, “Probing new physics in dimension-8 neutral gauge couplings at e+e- colliders,” *Sci. China Phys. Mech. Astron.* **64** no. 2, (2021) 221062, [arXiv:2008.04298 \[hep-ph\]](#).
- [76] N. Arkani-Hamed and K. Harigaya, “Naturalness and the muon magnetic moment,” [arXiv:2106.01373 \[hep-ph\]](#).
- [77] C. Hays, A. Martin, V. Sanz, and J. Setford, “On the impact of dimension-eight SMEFT operators on Higgs measurements,” *JHEP* **02** (2019) 123, [arXiv:1808.00442 \[hep-ph\]](#).
- [78] T. Corbett, A. Martin, and M. Trott, “Consistent higher order $\sigma(\mathcal{G}\mathcal{G} \rightarrow h)$, $\Gamma(h \rightarrow \mathcal{G}\mathcal{G})$ and $\Gamma(h \rightarrow \gamma\gamma)$ in geoSMEFT,” [arXiv:2107.07470 \[hep-ph\]](#).
- [79] S. Alioli, R. Boughezal, E. Mereghetti, and F. Petriello, “Novel angular dependence in Drell-Yan lepton production via dimension-8 operators,” *Phys. Lett. B* **809** (2020) 135703, [arXiv:2003.11615 \[hep-ph\]](#).
- [80] R. Boughezal, E. Mereghetti, and F. Petriello, “Dilepton production in the SMEFT at $\mathcal{O}(1/\Lambda^4)$,” [arXiv:2106.05337 \[hep-ph\]](#).
- [81] T. Corbett, A. Helset, A. Martin, and M. Trott, “EWPD in the SMEFT to dimension eight,” *JHEP* **06** (2021) 076, [arXiv:2102.02819 \[hep-ph\]](#).
- [82] T. Corbett, “The one-loop tadpole in the geoSMEFT,” [arXiv:2106.10284 \[hep-ph\]](#).
- [83] A. Martin and M. Trott, “The ggh variations,” [arXiv:2109.05595 \[hep-ph\]](#).
- [84] E. E. Jenkins, A. V. Manohar, and M. Trott, “Renormalization Group Evolution of the Standard Model Dimension Six Operators I: Formalism and lambda Dependence,” *JHEP* **10** (2013) 087, [arXiv:1308.2627 \[hep-ph\]](#).
- [85] E. E. Jenkins, A. V. Manohar, and M. Trott, “Renormalization Group Evolution of the Standard Model Dimension Six Operators II: Yukawa Dependence,” *JHEP* **01** (2014) 035, [arXiv:1310.4838 \[hep-ph\]](#).

- [86] R. Alonso, E. E. Jenkins, A. V. Manohar, and M. Trott, “Renormalization Group Evolution of the Standard Model Dimension Six Operators III: Gauge Coupling Dependence and Phenomenology,” *JHEP* **04** (2014) 159, [arXiv:1312.2014 \[hep-ph\]](#).
- [87] S. Antusch, M. Drees, J. Kersten, M. Lindner, and M. Ratz, “Neutrino mass operator renormalization revisited,” *Phys. Lett. B* **519** (2001) 238–242, [arXiv:hep-ph/0108005](#).
- [88] R. Alonso, H.-M. Chang, E. E. Jenkins, A. V. Manohar, and B. Shotwell, “Renormalization group evolution of dimension-six baryon number violating operators,” *Phys. Lett. B* **734** (2014) 302–307, [arXiv:1405.0486 \[hep-ph\]](#).
- [89] Y. Liao and X.-D. Ma, “Renormalization Group Evolution of Dimension-seven Baryon- and Lepton-number-violating Operators,” *JHEP* **11** (2016) 043, [arXiv:1607.07309 \[hep-ph\]](#).
- [90] S. Davidson, M. Gorbahn, and M. Leak, “Majorana neutrino masses in the renormalization group equations for lepton flavor violation,” *Phys. Rev. D* **98** no. 9, (2018) 095014, [arXiv:1807.04283 \[hep-ph\]](#).
- [91] Y. Liao and X.-D. Ma, “Renormalization Group Evolution of Dimension-seven Operators in Standard Model Effective Field Theory and Relevant Phenomenology,” *JHEP* **03** (2019) 179, [arXiv:1901.10302 \[hep-ph\]](#).
- [92] M. Chala and A. Titov, “Neutrino masses in the Standard Model effective field theory,” [arXiv:2104.08248 \[hep-ph\]](#).
- [93] M. Chala, G. Guedes, M. Ramos, and J. Santiago, “Towards the renormalisation of the Standard Model effective field theory to dimension eight: Bosonic interactions I,” [arXiv:2106.05291 \[hep-ph\]](#).
- [94] Y. Iwasaki, “Fourth-order gravitational potential based on quantum field theory,” *Lett. Nuovo Cim.* **1S2** (1971) 783–786. [*Lett. Nuovo Cim.*1,783(1971)].
- [95] Y. Iwasaki, “Quantum theory of gravitation vs. classical theory - fourth-order potential,” *Prog. Theor. Phys.* **46** (1971) 1587–1609.
- [96] B. R. Holstein and J. F. Donoghue, “Classical physics and quantum loops,” *Phys. Rev. Lett.* **93** (2004) 201602, [arXiv:hep-th/0405239 \[hep-th\]](#).
- [97] C. Cheung, I. Z. Rothstein, and M. P. Solon, “From Scattering Amplitudes to Classical Potentials in the Post-Minkowskian Expansion,” *Phys. Rev. Lett.* **121** no. 25, (2018) 251101, [arXiv:1808.02489 \[hep-th\]](#).
- [98] D. Neill and I. Z. Rothstein, “Classical Space-Times from the S Matrix,” *Nucl. Phys.* **B877** (2013) 177–189, [arXiv:1304.7263 \[hep-th\]](#).

-
- [99] Z. Bern, D. Kosmopoulos, and A. Zhiboedov, “Gravitational Effective Field Theory Islands, Low-Spin Dominance, and the Four-Graviton Amplitude,” [arXiv:2103.12728 \[hep-th\]](#).
- [100] H. Cheng and T. T. Wu, “High-energy elastic scattering in quantum electrodynamics,” *Phys. Rev. Lett.* **22** (1969) 666.
- [101] M. Lévy and J. Sucher, “Eikonal approximation in quantum field theory,” *Phys. Rev.* **186** (Oct, 1969) 1656–1670.
<https://link.aps.org/doi/10.1103/PhysRev.186.1656>.
- [102] H. D. Abarbanel and C. Itzykson, “Relativistic eikonal expansion,” *Phys. Rev. Lett.* **23** (1969) 53.
- [103] D. Amati, M. Ciafaloni, and G. Veneziano, “Superstring Collisions at Planckian Energies,” *Phys. Lett. B* **197** (1987) 81.
- [104] D. Amati, M. Ciafaloni, and G. Veneziano, “Higher Order Gravitational Deflection and Soft Bremsstrahlung in Planckian Energy Superstring Collisions,” *Nucl. Phys.* **B347** (1990) 550–580.
- [105] D. N. Kabat and M. Ortiz, “Eikonal quantum gravity and Planckian scattering,” *Nucl. Phys. B* **388** (1992) 570–592, [arXiv:hep-th/9203082](#).
- [106] N. Sennett, R. Brito, A. Buonanno, V. Gorbenko, and L. Senatore, “Gravitational-Wave Constraints on an Effective-Field-Theory Extension of General Relativity,” [arXiv:1912.09917 \[gr-qc\]](#).
- [107] R. Ellis and J. Sexton, “Qcd radiative corrections to parton-parton scattering,” *Nuclear Physics B* **269** no. 2, (1986) 445–484.
<https://www.sciencedirect.com/science/article/pii/0550321386902324>.
- [108] Z. Bern, L. J. Dixon, and D. A. Kosower, “One loop corrections to five gluon amplitudes,” *Phys. Rev. Lett.* **70** (1993) 2677–2680, [arXiv:hep-ph/9302280 \[hep-ph\]](#).
- [109] W. L. van Neerven, “Dimensional Regularization of Mass and Infrared Singularities in Two Loop On-shell Vertex Functions,” *Nucl. Phys.* **B268** (1986) 453–488.
- [110] Z. Bern and A. G. Morgan, “Massive loop amplitudes from unitarity,” *Nucl. Phys. B* **467** (1996) 479–509, [arXiv:hep-ph/9511336](#).
- [111] W. T. Giele, Z. Kunszt, and K. Melnikov, “Full one-loop amplitudes from tree amplitudes,” *JHEP* **04** (2008) 049, [arXiv:0801.2237 \[hep-ph\]](#).

-
- [112] R. Boughezal, K. Melnikov, and F. Petriello, “The four-dimensional helicity scheme and dimensional reconstruction,” *Phys. Rev.* **D84** (2011) 034044, [arXiv:1106.5520 \[hep-ph\]](#).
- [113] S. Davies, “One-Loop QCD and Higgs to Partons Processes Using Six-Dimensional Helicity and Generalized Unitarity,” *Phys. Rev.* **D84** (2011) 094016, [arXiv:1108.0398 \[hep-ph\]](#).
- [114] R. K. Ellis, W. T. Giele, Z. Kunszt, and K. Melnikov, “Masses, fermions and generalized D -dimensional unitarity,” *Nucl. Phys.* **B822** (2009) 270–282, [arXiv:0806.3467 \[hep-ph\]](#).
- [115] Z. Bern, J. J. Carrasco, T. Dennen, Y.-t. Huang, and H. Ita, “Generalized Unitarity and Six-Dimensional Helicity,” *Phys. Rev.* **D83** (2011) 085022, [arXiv:1010.0494 \[hep-th\]](#).
- [116] F. Wilczek, “Decays of Heavy Vector Mesons Into Higgs Particles,” *Phys. Rev. Lett.* **39** (1977) 1304.
- [117] M. A. Shifman, A. I. Vainshtein, M. B. Voloshin, and V. I. Zakharov, “Low-Energy Theorems for Higgs Boson Couplings to Photons,” *Sov. J. Nucl. Phys.* **30** (1979) 711–716. [*Yad. Fiz.*30,1368(1979)].
- [118] S. Dawson, “Radiative corrections to Higgs boson production,” *Nucl. Phys.* **B359** (1991) 283–300.
- [119] W. R. Inc., “Mathematica, Version 12.3.” <https://www.wolfram.com/mathematica>. Champaign, IL, 2021.
- [120] L. J. Dixon, “Calculating scattering amplitudes efficiently,” in *Theoretical Advanced Study Institute in Elementary Particle Physics (TASI 95): QCD and Beyond*, pp. 539–584. 1, 1996. [arXiv:hep-ph/9601359](#).
- [121] H. Elvang and Y.-t. Huang, “Scattering Amplitudes,” [arXiv:1308.1697 \[hep-th\]](#).
- [122] J. M. Henn and J. C. Plefka, *Scattering Amplitudes in Gauge Theories*, vol. 883. Springer, Berlin, 2014.
- [123] A. Brandhuber, J. Plefka, and G. Travaglini, “The SAGEX Review on Scattering Amplitudes, Chapter 1: Modern Fundamentals of Amplitudes,” [arXiv:2203.13012 \[hep-th\]](#).
- [124] E. Witten, “Perturbative gauge theory as a string theory in twistor space,” *Commun. Math. Phys.* **252** (2004) 189–258, [arXiv:hep-th/0312171 \[hep-th\]](#).

-
- [125] M. E. Peskin, “Simplifying Multi-Jet QCD Computation,” in *13th Mexican School of Particles and Fields*. 1, 2011. [arXiv:1101.2414 \[hep-ph\]](#).
- [126] D. A. Kosower, “Next-to-maximal helicity violating amplitudes in gauge theory,” *Phys. Rev.* **D71** (2005) 045007, [arXiv:hep-th/0406175 \[hep-th\]](#).
- [127] N. Arkani-Hamed, T.-C. Huang, and Y.-t. Huang, “Scattering Amplitudes For All Masses and Spins,” [arXiv:1709.04891 \[hep-th\]](#).
- [128] P. Benincasa and F. Cachazo, “Consistency Conditions on the S-Matrix of Massless Particles,” [arXiv:0705.4305 \[hep-th\]](#).
- [129] F. A. Berends and W. T. Giele, “Recursive Calculations for Processes with n Gluons,” *Nucl. Phys.* **B306** (1988) 759–808.
- [130] S. Abreu, F. Febres Cordero, H. Ita, B. Page, and M. Zeng, “Planar Two-Loop Five-Gluon Amplitudes from Numerical Unitarity,” *Phys. Rev. D* **97** no. 11, (2018) 116014, [arXiv:1712.03946 \[hep-ph\]](#).
- [131] S. Abreu, F. Febres Cordero, H. Ita, M. Jaquier, and B. Page, “Subleading Poles in the Numerical Unitarity Method at Two Loops,” *Phys. Rev. D* **95** no. 9, (2017) 096011, [arXiv:1703.05255 \[hep-ph\]](#).
- [132] S. Abreu, F. Febres Cordero, H. Ita, B. Page, and V. Sotnikov, “Planar Two-Loop Five-Parton Amplitudes from Numerical Unitarity,” *JHEP* **11** (2018) 116, [arXiv:1809.09067 \[hep-ph\]](#).
- [133] S. Abreu, J. Dormans, F. Febres Cordero, H. Ita, and B. Page, “Analytic Form of Planar Two-Loop Five-Gluon Scattering Amplitudes in QCD,” *Phys. Rev. Lett.* **122** no. 8, (2019) 082002, [arXiv:1812.04586 \[hep-ph\]](#).
- [134] S. Abreu, J. Dormans, F. Febres Cordero, H. Ita, B. Page, and V. Sotnikov, “Analytic Form of the Planar Two-Loop Five-Parton Scattering Amplitudes in QCD,” *JHEP* **05** (2019) 084, [arXiv:1904.00945 \[hep-ph\]](#).
- [135] S. Badger, D. Chicherin, T. Gehrmann, G. Heinrich, J. M. Henn, T. Peraro, P. Wasser, Y. Zhang, and S. Zoia, “Analytic form of the full two-loop five-gluon all-plus helicity amplitude,” *Phys. Rev. Lett.* **123** no. 7, (2019) 071601, [arXiv:1905.03733 \[hep-ph\]](#).
- [136] S. Abreu, H. Ita, F. Moriello, B. Page, W. Tschernow, and M. Zeng, “Two-Loop Integrals for Planar Five-Point One-Mass Processes,” *JHEP* **11** (2020) 117, [arXiv:2005.04195 \[hep-ph\]](#).
- [137] J. Henn, T. Peraro, Y. Xu, and Y. Zhang, “A first look at the function space for planar two-loop six-particle Feynman integrals,” *JHEP* **03** (2022) 056, [arXiv:2112.10605 \[hep-th\]](#).

-
- [138] R. Britto, F. Cachazo, and B. Feng, “New recursion relations for tree amplitudes of gluons,” *Nucl. Phys. B* **715** (2005) 499–522, [arXiv:hep-th/0412308](#).
- [139] N. Arkani-Hamed and J. Kaplan, “On Tree Amplitudes in Gauge Theory and Gravity,” *JHEP* **04** (2008) 076, [arXiv:0801.2385 \[hep-th\]](#).
- [140] M. Bianchi, H. Elvang, and D. Z. Freedman, “Generating Tree Amplitudes in N=4 SYM and N = 8 SG,” *JHEP* **09** (2008) 063, [arXiv:0805.0757 \[hep-th\]](#).
- [141] A. Brandhuber, P. Heslop, and G. Travaglini, “A Note on dual superconformal symmetry of the N=4 super Yang-Mills S-matrix,” *Phys.Rev.* **D78** (2008) 125005, [arXiv:0807.4097 \[hep-th\]](#).
- [142] N. Arkani-Hamed, F. Cachazo, and J. Kaplan, “What is the Simplest Quantum Field Theory?,” *JHEP* **09** (2010) 016, [arXiv:0808.1446 \[hep-th\]](#).
- [143] H. Elvang, D. Z. Freedman, and M. Kiermaier, “Recursion Relations, Generating Functions, and Unitarity Sums in N=4 SYM Theory,” *JHEP* **04** (2009) 009, [arXiv:0808.1720 \[hep-th\]](#).
- [144] R. Boels, K. J. Larsen, N. A. Obers, and M. Vonk, “MHV, CSW and BCFW: Field theory structures in string theory amplitudes,” *JHEP* **11** (2008) 015, [arXiv:0808.2598 \[hep-th\]](#).
- [145] C. Cheung, D. O’Connell, and B. Wecht, “BCFW Recursion Relations and String Theory,” *JHEP* **09** (2010) 052, [arXiv:1002.4674 \[hep-th\]](#).
- [146] S. Badger, E. Glover, and V. V. Khoze, “Recursion relations for gauge theory amplitudes with massive vector bosons and fermions,” *JHEP* **01** (2006) 066, [arXiv:hep-th/0507161](#).
- [147] S. Badger, E. Glover, V. Khoze, and P. Svrcek, “Recursion relations for gauge theory amplitudes with massive particles,” *JHEP* **07** (2005) 025, [arXiv:hep-th/0504159](#).
- [148] D. Forde and D. A. Kosower, “All-multiplicity amplitudes with massive scalars,” *Phys. Rev. D* **73** (2006) 065007, [arXiv:hep-th/0507292](#).
- [149] C. F. Berger, V. Del Duca, and L. J. Dixon, “Recursive Construction of Higgs-Plus-Multiparton Loop Amplitudes: The Last of the Phi-nite Loop Amplitudes,” *Phys. Rev. D* **74** (2006) 094021, [arXiv:hep-ph/0608180](#). [Erratum: *Phys.Rev.D* 76, 099901 (2007)].
- [150] C. Schwinn and S. Weinzierl, “On-shell recursion relations for all Born QCD amplitudes,” *JHEP* **04** (2007) 072, [arXiv:hep-ph/0703021](#).

-
- [151] A. Hall, “Massive Quark-Gluon Scattering Amplitudes at Tree Level,” *Phys. Rev. D* **77** (2008) 025011, [arXiv:0710.1300 \[hep-ph\]](#).
- [152] C. Cheung and D. O’Connell, “Amplitudes and Spinor-Helicity in Six Dimensions,” *JHEP* **07** (2009) 075, [arXiv:0902.0981 \[hep-th\]](#).
- [153] K. Risager, “A Direct proof of the CSW rules,” *JHEP* **12** (2005) 003, [arXiv:hep-th/0508206 \[hep-th\]](#).
- [154] F. Cachazo, P. Svrcek, and E. Witten, “MHV vertices and tree amplitudes in gauge theory,” *JHEP* **09** (2004) 006, [arXiv:hep-th/0403047 \[hep-th\]](#).
- [155] T. Cohen, H. Elvang, and M. Kiermaier, “On-shell constructibility of tree amplitudes in general field theories,” *JHEP* **04** (2011) 053, [arXiv:1010.0257 \[hep-th\]](#).
- [156] C. Cheung, C.-H. Shen, and J. Trnka, “Simple Recursion Relations for General Field Theories,” *JHEP* **06** (2015) 118, [arXiv:1502.05057 \[hep-th\]](#).
- [157] C. Cheung, K. Kampf, J. Novotny, C.-H. Shen, and J. Trnka, “On-Shell Recursion Relations for Effective Field Theories,” *Phys. Rev. Lett.* **116** no. 4, (2016) 041601, [arXiv:1509.03309 \[hep-th\]](#).
- [158] C. Cheung, K. Kampf, J. Novotny, C.-H. Shen, and J. Trnka, “A Periodic Table of Effective Field Theories,” *JHEP* **02** (2017) 020, [arXiv:1611.03137 \[hep-th\]](#).
- [159] D. Chicherin, T. Gehrmann, J. M. Henn, P. Wasser, Y. Zhang, and S. Zoia, “Analytic result for a two-loop five-particle amplitude,” *Phys. Rev. Lett.* **122** no. 12, (2019) 121602, [arXiv:1812.11057 \[hep-th\]](#).
- [160] L. J. Dixon, O. Gürdogan, A. J. McLeod, and M. Wilhelm, “Bootstrapping a Stress-Tensor Form Factor through Eight Loops,” [arXiv:2204.11901 \[hep-th\]](#).
- [161] C.-N. Yang and R. L. Mills, “Conservation of Isotopic Spin and Isotopic Gauge Invariance,” *Phys. Rev.* **96** (1954) 191–195.
- [162] M. E. Peskin and D. V. Schroeder, *An Introduction to quantum field theory*. Addison-Wesley, Reading, USA, 1995.
- [163] B. Grzadkowski, M. Iskrzynski, M. Misiak, and J. Rosiek, “Dimension-Six Terms in the Standard Model Lagrangian,” *JHEP* **10** (2010) 085, [arXiv:1008.4884 \[hep-ph\]](#).

- [164] L. Lehman, “Extending the Standard Model Effective Field Theory with the Complete Set of Dimension-7 Operators,” *Phys. Rev. D* **90** no. 12, (2014) 125023, [arXiv:1410.4193 \[hep-ph\]](#).
- [165] C. W. Murphy, “Dimension-8 operators in the Standard Model Effective Field Theory,” *JHEP* **10** (2020) 174, [arXiv:2005.00059 \[hep-ph\]](#).
- [166] Y. Liao and X.-D. Ma, “An explicit construction of the dimension-9 operator basis in the standard model effective field theory,” *JHEP* **11** (2020) 152, [arXiv:2007.08125 \[hep-ph\]](#).
- [167] S. De Angelis, “Amplitude bases in generic EFTs,” [arXiv:2202.02681 \[hep-th\]](#).
- [168] P. Dittner, “Invariant tensors in $\mathfrak{su}(3)$,” *Commun. Math. Phys.* **22** (1971) 238–252.
- [169] P. Dittner, “Invariant tensors in $\mathfrak{su}(3)$. 2.,” *Commun. Math. Phys.* **27** (1972) 44–52.
- [170] J. A. de Azcarraga, A. J. Macfarlane, A. J. Mountain, and J. C. Perez Bueno, “Invariant tensors for simple groups,” *Nucl. Phys. B* **510** (1998) 657–687, [arXiv:physics/9706006](#).
- [171] D. Littlewood and A. Richardson, “Philos. trans. roy. soc. london ser. a,” *Group characters and algebra* **233** (1934) 99–141.
- [172] G. de B. Robinson, “On the representations of the symmetric group,” *American Journal of Mathematics* **60** no. 3, (1938) 745–760.
- [173] R. M. Fonseca, “Enumerating the operators of an effective field theory,” *Phys. Rev. D* **101** no. 3, (2020) 035040, [arXiv:1907.12584 \[hep-ph\]](#).
- [174] N. Arkani-Hamed and J. Kaplan, “On Tree Amplitudes in Gauge Theory and Gravity,” *JHEP* **04** (2008) 076, [arXiv:0801.2385 \[hep-th\]](#).
- [175] K. Kampf, J. Novotny, and J. Trnka, “Recursion relations for tree-level amplitudes in the $SU(N)$ nonlinear sigma model,” *Phys. Rev. D* **87** no. 8, (2013) 081701, [arXiv:1212.5224 \[hep-th\]](#).
- [176] C. Cheung, K. Kampf, J. Novotny, and J. Trnka, “Effective Field Theories from Soft Limits of Scattering Amplitudes,” *Phys. Rev. Lett.* **114** no. 22, (2015) 221602, [arXiv:1412.4095 \[hep-th\]](#).
- [177] Z. Bern, L. J. Dixon, D. C. Dunbar, and D. A. Kosower, “One loop selfdual and $N=4$ superYang-Mills,” *Phys. Lett.* **B394** (1997) 105–115, [arXiv:hep-th/9611127 \[hep-th\]](#).

-
- [178] Z. Bern, L. J. Dixon, and D. A. Kosower, “On-shell recurrence relations for one-loop QCD amplitudes,” *Phys. Rev.* **D71** (2005) 105013, [arXiv:hep-th/0501240](#) [hep-th].
- [179] A. Brandhuber, S. McNamara, B. J. Spence, and G. Travaglini, “Loop amplitudes in pure Yang-Mills from generalised unitarity,” *JHEP* **10** (2005) 011, [arXiv:hep-th/0506068](#) [hep-th].
- [180] S. D. Badger, “Direct Extraction Of One Loop Rational Terms,” *JHEP* **01** (2009) 049, [arXiv:0806.4600](#) [hep-ph].
- [181] D. Nandan, J. Plefka, and G. Travaglini, “All rational one-loop Einstein-Yang-Mills amplitudes at four points,” *JHEP* **09** (2018) 011, [arXiv:1803.08497](#) [hep-th].
- [182] A. von Manteuffel and R. M. Schabinger, “A novel approach to integration by parts reduction,” *Phys. Lett. B* **744** (2015) 101–104, [arXiv:1406.4513](#) [hep-ph].
- [183] T. Peraro, “Scattering amplitudes over finite fields and multivariate functional reconstruction,” *JHEP* **12** (2016) 030, [arXiv:1608.01902](#) [hep-ph].
- [184] A. Hodges, “Eliminating spurious poles from gauge-theoretic amplitudes,” *JHEP* **05** (2013) 135, [arXiv:0905.1473](#) [hep-th].
- [185] S. Badger, “Automating QCD amplitudes with on-shell methods,” *J. Phys. Conf. Ser.* **762** no. 1, (2016) 012057, [arXiv:1605.02172](#) [hep-ph].
- [186] F. Berends and W. Giele, “Recursive calculations for processes with n gluons,” *Nuclear Physics B* **306** no. 4, (1988) 759–808. <https://www.sciencedirect.com/science/article/pii/0550321388904427>.
- [187] R. Lidl and H. Niederreiter, *Introduction to Finite Fields and their Applications*. Cambridge University Press, 2 ed., 1994.
- [188] T. Peraro, “FiniteFlow: multivariate functional reconstruction using finite fields and dataflow graphs,” *JHEP* **07** (2019) 031, [arXiv:1905.08019](#) [hep-ph].
- [189] P. Wang, “A p-adic algorithm for univariate partial fractions.”
- [190] Y.-t. Huang and D. McGady, “Consistency Conditions for Gauge Theory S Matrices from Requirements of Generalized Unitarity,” *Phys. Rev. Lett.* **112** no. 24, (2014) 241601, [arXiv:1307.4065](#) [hep-th].
- [191] W.-M. Chen, Y.-t. Huang, and D. A. McGady, “Anomalies without an action,” [arXiv:1402.7062](#) [hep-th].

- [192] A. Azatov, R. Contino, C. S. Machado, and F. Riva, “Helicity selection rules and noninterference for BSM amplitudes,” *Phys. Rev. D* **95** no. 6, (2017) 065014, [arXiv:1607.05236 \[hep-ph\]](#).
- [193] A. Adams, N. Arkani-Hamed, S. Dubovsky, A. Nicolis, and R. Rattazzi, “Causality, analyticity and an IR obstruction to UV completion,” *JHEP* **10** (2006) 014, [arXiv:hep-th/0602178](#).
- [194] Z. Bern, L. J. Dixon, and D. A. Kosower, “On-Shell Methods in Perturbative QCD,” *Annals Phys.* **322** (2007) 1587–1634, [arXiv:0704.2798 \[hep-ph\]](#).
- [195] Z. Bern and Y.-t. Huang, “Basics of Generalized Unitarity,” *J. Phys. A* **44** (2011) 454003, [arXiv:1103.1869 \[hep-th\]](#).
- [196] G. Ossola, C. G. Papadopoulos, and R. Pittau, “Reducing full one-loop amplitudes to scalar integrals at the integrand level,” *Nucl. Phys. B* **763** (2007) 147–169, [arXiv:hep-ph/0609007](#).
- [197] P. Mastrolia and G. Ossola, “On the Integrand-Reduction Method for Two-Loop Scattering Amplitudes,” *JHEP* **11** (2011) 014, [arXiv:1107.6041 \[hep-ph\]](#).
- [198] S. Badger, H. Frellesvig, and Y. Zhang, “Hepta-Cuts of Two-Loop Scattering Amplitudes,” *JHEP* **04** (2012) 055, [arXiv:1202.2019 \[hep-ph\]](#).
- [199] Y. Zhang, “Integrand-Level Reduction of Loop Amplitudes by Computational Algebraic Geometry Methods,” *JHEP* **09** (2012) 042, [arXiv:1205.5707 \[hep-ph\]](#).
- [200] P. Mastrolia, E. Mirabella, G. Ossola, and T. Peraro, “Scattering Amplitudes from Multivariate Polynomial Division,” *Phys. Lett. B* **718** (2012) 173–177, [arXiv:1205.7087 \[hep-ph\]](#).
- [201] P. Mastrolia, E. Mirabella, G. Ossola, and T. Peraro, “Integrand-Reduction for Two-Loop Scattering Amplitudes through Multivariate Polynomial Division,” *Phys. Rev. D* **87** no. 8, (2013) 085026, [arXiv:1209.4319 \[hep-ph\]](#).
- [202] P. Mastrolia, E. Mirabella, G. Ossola, and T. Peraro, “Multiloop Integrand Reduction for Dimensionally Regulated Amplitudes,” *Phys. Lett. B* **727** (2013) 532–535, [arXiv:1307.5832 \[hep-ph\]](#).
- [203] P. Mastrolia, T. Peraro, and A. Primo, “Adaptive Integrand Decomposition in parallel and orthogonal space,” *JHEP* **08** (2016) 164, [arXiv:1605.03157 \[hep-ph\]](#).
- [204] K. Chetyrkin and F. Tkachov, “Integration by parts: The algorithm to calculate beta-functions in 4 loops,” *Nuclear Physics B* **192** no. 1, (1981) 159–204. <https://www.sciencedirect.com/science/article/pii/0550321381901991>.

-
- [205] S. Laporta, “High precision calculation of multiloop Feynman integrals by difference equations,” *Int. J. Mod. Phys. A* **15** (2000) 5087–5159, [arXiv:hep-ph/0102033](#).
- [206] J. M. Henn, “Multiloop integrals in dimensional regularization made simple,” *Phys. Rev. Lett.* **110** (2013) 251601, [arXiv:1304.1806 \[hep-th\]](#).
- [207] J. M. Henn, “Lectures on differential equations for Feynman integrals,” *J. Phys. A* **48** (2015) 153001, [arXiv:1412.2296 \[hep-ph\]](#).
- [208] H. Frellesvig, F. Gasparotto, S. Laporta, M. K. Mandal, P. Mastrolia, L. Mattiazzi, and S. Mizera, “Decomposition of Feynman Integrals on the Maximal Cut by Intersection Numbers,” *JHEP* **05** (2019) 153, [arXiv:1901.11510 \[hep-ph\]](#).
- [209] H. Frellesvig, F. Gasparotto, M. K. Mandal, P. Mastrolia, L. Mattiazzi, and S. Mizera, “Vector Space of Feynman Integrals and Multivariate Intersection Numbers,” *Phys. Rev. Lett.* **123** no. 20, (2019) 201602, [arXiv:1907.02000 \[hep-th\]](#).
- [210] H. Frellesvig, F. Gasparotto, S. Laporta, M. K. Mandal, P. Mastrolia, L. Mattiazzi, and S. Mizera, “Decomposition of Feynman Integrals by Multivariate Intersection Numbers,” *JHEP* **03** (2021) 027, [arXiv:2008.04823 \[hep-th\]](#).
- [211] S. Caron-Huot and A. Pokraka, “Duals of Feynman integrals. Part I. Differential equations,” *JHEP* **12** (2021) 045, [arXiv:2104.06898 \[hep-th\]](#).
- [212] S. Caron-Huot and A. Pokraka, “Duals of Feynman Integrals. Part II. Generalized unitarity,” *JHEP* **04** (2022) 078, [arXiv:2112.00055 \[hep-th\]](#).
- [213] C. Duhr, “Mathematical aspects of scattering amplitudes,” in *Theoretical Advanced Study Institute in Elementary Particle Physics: Journeys Through the Precision Frontier: Amplitudes for Colliders*, pp. 419–476. 2015. [arXiv:1411.7538 \[hep-ph\]](#).
- [214] Y. Zhang, “Lecture Notes on Multi-loop Integral Reduction and Applied Algebraic Geometry,” 12, 2016. [arXiv:1612.02249 \[hep-th\]](#).
- [215] S. Weinzierl, “Feynman Integrals,” [arXiv:2201.03593 \[hep-th\]](#).
- [216] S. Abreu, R. Britto, and C. Duhr, “The SAGEX Review on Scattering Amplitudes, Chapter 3: Mathematical structures in Feynman integrals,” [arXiv:2203.13014 \[hep-th\]](#).
- [217] J. Blümlein and C. Schneider, “The SAGEX Review on Scattering Amplitudes, Chapter 4: Multi-loop Feynman Integrals,” [arXiv:2203.13015 \[hep-th\]](#).

- [218] G. Passarino and M. J. G. Veltman, “One Loop Corrections for $e^+ e^-$ Annihilation Into $\mu^+ \mu^-$ in the Weinberg Model,” *Nucl. Phys.* **B160** (1979) 151–207.
- [219] W. L. van Neerven and J. A. M. Vermaseren, “Large Loop Integrals,” *Phys. Lett.* **137B** (1984) 241–244.
- [220] T. Binoth, J. P. Guillet, and G. Heinrich, “Algebraic evaluation of rational polynomials in one-loop amplitudes,” *JHEP* **02** (2007) 013, [arXiv:hep-ph/0609054](#) [hep-ph].
- [221] Z.-G. Xiao, G. Yang, and C.-J. Zhu, “The rational parts of one-loop QCD amplitudes I: The general formalism,” *Nucl. Phys.* **B758** (2006) 1–34, [arXiv:hep-ph/0607015](#) [hep-ph].
- [222] X. Su, Z. Xiao, G. Yang, and C.-J. Zhu, “The Rational Part of QCD Amplitude. II. The Five-Gluon,” *Nucl. Phys.* **B758** (2006) 35–52, [arXiv:hep-ph/0607016](#) [hep-ph].
- [223] Z. Xiao, G. Yang, and C.-J. Zhu, “The Rational Part of QCD Amplitude. III. The Six-Gluon,” *Nucl. Phys.* **B758** (2006) 53–89, [arXiv:hep-ph/0607017](#) [hep-ph].
- [224] Z. Bern, L. J. Dixon, and D. A. Kosower, “The last of the finite loop amplitudes in QCD,” *Phys. Rev.* **D72** (2005) 125003, [arXiv:hep-ph/0505055](#) [hep-ph].
- [225] Z. Bern, L. J. Dixon, and D. A. Kosower, “Bootstrapping multi-parton loop amplitudes in QCD,” *Phys. Rev.* **D73** (2006) 065013, [arXiv:hep-ph/0507005](#) [hep-ph].
- [226] C. Anastasiou, R. Britto, B. Feng, Z. Kunszt, and P. Mastrolia, “Unitarity cuts and Reduction to master integrals in d dimensions for one-loop amplitudes,” *JHEP* **03** (2007) 111, [arXiv:hep-ph/0612277](#) [hep-ph].
- [227] Z. Bern and D. A. Kosower, “The Computation of loop amplitudes in gauge theories,” *Nucl. Phys.* **B379** (1992) 451–561.
- [228] Z. Bern and A. De Freitas, “Two-loop helicity amplitudes for fermion-fermion scattering,” *Nuclear Physics B - Proceedings Supplements* **135** (2004) 51–55. <https://www.sciencedirect.com/science/article/pii/S092056320400369X>. Loops and Legs in Quantum Field Theory. Proceedings of the 7th DESY Workshop on Elementary Particle Theory.
- [229] D. Forde, “Direct extraction of one-loop integral coefficients,” *Phys. Rev.* **D75** (2007) 125019, [arXiv:0704.1835](#) [hep-ph].

- [230] P. Mastrolia, “On Triple-cut of scattering amplitudes,” *Phys. Lett. B* **644** (2007) 272–283, [arXiv:hep-th/0611091](#).
- [231] P. Mastrolia, G. Ossola, C. G. Papadopoulos, and R. Pittau, “Optimizing the Reduction of One-Loop Amplitudes,” *JHEP* **06** (2008) 030, [arXiv:0803.3964 \[hep-ph\]](#).
- [232] J. L. Bourjaily, E. Herrmann, and J. Trnka, “Prescriptive Unitarity,” *JHEP* **06** (2017) 059, [arXiv:1704.05460 \[hep-th\]](#).
- [233] J. L. Bourjaily, E. Herrmann, C. Langer, A. J. McLeod, and J. Trnka, “Prescriptive Unitarity for Non-Planar Six-Particle Amplitudes at Two Loops,” *JHEP* **12** (2019) 073, [arXiv:1909.09131 \[hep-th\]](#).
- [234] J. L. Bourjaily, N. Kalyanapuram, C. Langer, and K. Patatoukos, “Prescriptive unitarity with elliptic leading singularities,” *Phys. Rev. D* **104** no. 12, (2021) 125009, [arXiv:2102.02210 \[hep-th\]](#).
- [235] S. L. Adler, “Axial-vector vertex in spinor electrodynamics,” *Phys. Rev.* **177** (Jan, 1969) 2426–2438. <https://link.aps.org/doi/10.1103/PhysRev.177.2426>.
- [236] J. S. Bell and R. Jackiw, “A PCAC puzzle: $\pi^0 \rightarrow \gamma\gamma$ in the σ model,” *Nuovo Cim. A* **60** (1969) 47–61.
- [237] S. Caron-Huot and M. Wilhelm, “Renormalization group coefficients and the S-matrix,” *JHEP* **12** (2016) 010, [arXiv:1607.06448 \[hep-th\]](#).
- [238] C. G. Callan, Jr., S. R. Coleman, J. Wess, and B. Zumino, “Structure of phenomenological Lagrangians. 2.,” *Phys. Rev.* **177** (1969) 2247–2250.
- [239] K. Symanzik, “Small distance behavior in field theory and power counting,” *Commun. Math. Phys.* **18** (1970) 227–246.
- [240] K. Symanzik, “Small distance behavior analysis and Wilson expansion,” *Commun. Math. Phys.* **23** (1971) 49–86.
- [241] B. I. Zwiebel, “From Scattering Amplitudes to the Dilatation Generator in N=4 SYM,” *J.Phys.* **A45** (2012) 115401, [arXiv:1111.0083 \[hep-th\]](#).
- [242] J. Elias-Miro, J. R. Espinosa, E. Masso, and A. Pomarol, “Higgs windows to new physics through d=6 operators: constraints and one-loop anomalous dimensions,” *JHEP* **11** (2013) 066, [arXiv:1308.1879 \[hep-ph\]](#).
- [243] J. Elias Miró, J. Ingoldby, and M. Riembau, “EFT anomalous dimensions from the S-matrix,” *JHEP* **09** (2020) 163, [arXiv:2005.06983 \[hep-ph\]](#).

-
- [244] P. Baratella, C. Fernandez, and A. Pomarol, “Renormalization of Higher-Dimensional Operators from On-shell Amplitudes,” *Nucl. Phys. B* **959** (2020) 115155, [arXiv:2005.07129 \[hep-ph\]](#).
- [245] **LIGO Scientific, Virgo** Collaboration, B. P. Abbott *et al.*, “Observation of Gravitational Waves from a Binary Black Hole Merger,” *Phys. Rev. Lett.* **116** no. 6, (2016) 061102, [arXiv:1602.03837 \[gr-qc\]](#).
- [246] J. F. Donoghue, “General relativity as an effective field theory: The leading quantum corrections,” *Phys. Rev.* **D50** (1994) 3874–3888, [arXiv:gr-qc/9405057 \[gr-qc\]](#).
- [247] A. Einstein, L. Infeld, and B. Hoffmann, “The Gravitational equations and the problem of motion,” *Annals Math.* **39** (1938) 65–100.
- [248] T. Damour and G. Schäfer, “Lagrangians for point masses at the second post-Newtonian approximation of general relativity,” *Gen. Rel. Grav.* **17** (1985) 879–905.
- [249] J. B. Gilmore and A. Ross, “Effective field theory calculation of second post-Newtonian binary dynamics,” *Phys. Rev.* **D78** (2008) 124021, [arXiv:0810.1328 \[gr-qc\]](#).
- [250] T. Damour, P. Jaranowski, and G. Schäfer, “Dimensional regularization of the gravitational interaction of point masses,” *Phys. Lett.* **B513** (2001) 147–155, [arXiv:gr-qc/0105038 \[gr-qc\]](#).
- [251] L. Blanchet, T. Damour, and G. Esposito-Farese, “Dimensional regularization of the third post-Newtonian dynamics of point particles in harmonic coordinates,” *Phys. Rev.* **D69** (2004) 124007, [arXiv:gr-qc/0311052 \[gr-qc\]](#).
- [252] Y. Itoh and T. Futamase, “New derivation of a third post-Newtonian equation of motion for relativistic compact binaries without ambiguity,” *Phys. Rev.* **D68** (2003) 121501, [arXiv:gr-qc/0310028 \[gr-qc\]](#).
- [253] S. Foffa and R. Sturani, “Effective field theory calculation of conservative binary dynamics at third post-Newtonian order,” *Phys. Rev.* **D84** (2011) 044031, [arXiv:1104.1122 \[gr-qc\]](#).
- [254] P. Jaranowski and G. Schäfer, “Towards the 4th post-Newtonian Hamiltonian for two-point-mass systems,” *Phys. Rev.* **D86** (2012) 061503, [arXiv:1207.5448 \[gr-qc\]](#).
- [255] T. Damour, P. Jaranowski, and G. Schäfer, “Nonlocal-in-time action for the fourth post-Newtonian conservative dynamics of two-body systems,” *Phys. Rev.* **D89** no. 6, (2014) 064058, [arXiv:1401.4548 \[gr-qc\]](#).

-
- [256] C. R. Galley, A. K. Leibovich, R. A. Porto, and A. Ross, “Tail effect in gravitational radiation reaction: Time nonlocality and renormalization group evolution,” *Phys. Rev. D* **93** (2016) 124010, [arXiv:1511.07379 \[gr-qc\]](#).
- [257] T. Damour, P. Jaranowski, and G. Schäfer, “Fourth post-Newtonian effective one-body dynamics,” *Phys. Rev.* **D91** no. 8, (2015) 084024, [arXiv:1502.07245 \[gr-qc\]](#).
- [258] T. Damour, P. Jaranowski, and G. Schäfer, “Conservative dynamics of two-body systems at the fourth post-Newtonian approximation of general relativity,” *Phys. Rev.* **D93** no. 8, (2016) 084014, [arXiv:1601.01283 \[gr-qc\]](#).
- [259] L. Bernard, L. Blanchet, A. Bohé, G. Faye, and S. Marsat, “Fokker action of nonspinning compact binaries at the fourth post-Newtonian approximation,” *Phys. Rev.* **D93** no. 8, (2016) 084037, [arXiv:1512.02876 \[gr-qc\]](#).
- [260] L. Bernard, L. Blanchet, A. Bohé, G. Faye, and S. Marsat, “Energy and periastron advance of compact binaries on circular orbits at the fourth post-Newtonian order,” *Phys. Rev.* **D95** no. 4, (2017) 044026, [arXiv:1610.07934 \[gr-qc\]](#).
- [261] S. Foffa and R. Sturani, “Dynamics of the gravitational two-body problem at fourth post-Newtonian order and at quadratic order in the Newton constant,” *Phys. Rev.* **D87** no. 6, (2013) 064011, [arXiv:1206.7087 \[gr-qc\]](#).
- [262] S. Foffa, P. Mastrolia, R. Sturani, and C. Sturm, “Effective field theory approach to the gravitational two-body dynamics, at fourth post-Newtonian order and quintic in the Newton constant,” *Phys. Rev.* **D95** no. 10, (2017) 104009, [arXiv:1612.00482 \[gr-qc\]](#).
- [263] R. A. Porto and I. Z. Rothstein, “Apparent ambiguities in the post-Newtonian expansion for binary systems,” *Phys. Rev. D* **96** no. 2, (2017) 024062, [arXiv:1703.06433 \[gr-qc\]](#).
- [264] R. A. Porto, “Lamb shift and the gravitational binding energy for binary black holes,” *Phys. Rev. D* **96** no. 2, (2017) 024063, [arXiv:1703.06434 \[gr-qc\]](#).
- [265] S. Foffa, R. A. Porto, I. Rothstein, and R. Sturani, “Conservative dynamics of binary systems to fourth Post-Newtonian order in the EFT approach II: Renormalized Lagrangian,” *Phys. Rev. D* **100** no. 2, (2019) 024048, [arXiv:1903.05118 \[gr-qc\]](#).
- [266] J. Bluemlein, A. Maier, P. Marquard, and G. Schaefer, “Fourth post-Newtonian Hamiltonian dynamics of two-body systems from an effective field theory approach,” *Nucl. Phys. B* **955** (2020) 115041, [arXiv:2003.01692 \[gr-qc\]](#).

-
- [267] S. Foffa, P. Mastrolia, R. Sturani, C. Sturm, and W. J. Torres Bobadilla, “Static two-body potential at fifth post-Newtonian order,” *Phys. Rev. Lett.* **122** no. 24, (2019) 241605, [arXiv:1902.10571 \[gr-qc\]](#).
- [268] J. Bluemlein, A. Maier, and P. Marquard, “Five-Loop Static Contribution to the Gravitational Interaction Potential of Two Point Masses,” *Phys. Lett. B* **800** (2020) 135100, [arXiv:1902.11180 \[gr-qc\]](#).
- [269] D. Bini, T. Damour, and A. Geralico, “Binary dynamics at the fifth and fifth-and-a-half post-Newtonian orders,” *Phys. Rev. D* **102** no. 2, (2020) 024062, [arXiv:2003.11891 \[gr-qc\]](#).
- [270] J. Bluemlein, A. Maier, P. Marquard, and G. Schaefer, “Testing binary dynamics in gravity at the sixth post-Newtonian level,” [arXiv:2003.07145 \[gr-qc\]](#).
- [271] J. Blümlein, A. Maier, P. Marquard, and G. Schäfer, “The 6th post-Newtonian potential terms at $O(G_N^4)$,” *Phys. Lett. B* **816** (2021) 136260, [arXiv:2101.08630 \[gr-qc\]](#).
- [272] D. Bini, T. Damour, and A. Geralico, “Sixth post-Newtonian local-in-time dynamics of binary systems,” *Phys. Rev. D* **102** no. 2, (2020) 024061, [arXiv:2004.05407 \[gr-qc\]](#).
- [273] D. Bini, T. Damour, and A. Geralico, “Sixth post-Newtonian nonlocal-in-time dynamics of binary systems,” *Phys. Rev. D* **102** no. 8, (2020) 084047, [arXiv:2007.11239 \[gr-qc\]](#).
- [274] D. Bini, T. Damour, A. Geralico, S. Laporta, and P. Mastrolia, “Gravitational dynamics at $O(G^6)$: perturbative gravitational scattering meets experimental mathematics,” [arXiv:2008.09389 \[gr-qc\]](#).
- [275] D. Bini, T. Damour, A. Geralico, S. Laporta, and P. Mastrolia, “Gravitational scattering at the seventh order in G : nonlocal contribution at the sixth post-Newtonian accuracy,” *Phys. Rev. D* **103** no. 4, (2021) 044038, [arXiv:2012.12918 \[gr-qc\]](#).
- [276] Z. Bern, J. Parra-Martinez, R. Roiban, M. S. Ruf, C.-H. Shen, M. P. Solon, and M. Zeng, “Scattering Amplitudes, the Tail Effect, and Conservative Binary Dynamics at $O(G^4)$,” *Phys. Rev. Lett.* **128** no. 16, (2022) 161103, [arXiv:2112.10750 \[hep-th\]](#).
- [277] C. Dlapa, G. Kälin, Z. Liu, and R. A. Porto, “Dynamics of binary systems to fourth Post-Minkowskian order from the effective field theory approach,” *Phys. Lett. B* **831** (2022) 137203, [arXiv:2106.08276 \[hep-th\]](#).

- [278] C. Dlapa, G. Kälin, Z. Liu, and R. A. Porto, “Conservative Dynamics of Binary Systems at Fourth Post-Minkowskian Order in the Large-Eccentricity Expansion,” *Phys. Rev. Lett.* **128** no. 16, (2022) 161104, [arXiv:2112.11296 \[hep-th\]](#).
- [279] Z. Bern, C. Cheung, R. Roiban, C.-H. Shen, M. P. Solon, and M. Zeng, “Black Hole Binary Dynamics from the Double Copy and Effective Theory,” *JHEP* **10** (2019) 206, [arXiv:1908.01493 \[hep-th\]](#).
- [280] A. Brandhuber, G. Chen, G. Travaglini, and C. Wen, “Classical gravitational scattering from a gauge-invariant double copy,” *JHEP* **10** (2021) 118, [arXiv:2108.04216 \[hep-th\]](#).
- [281] V. Vaidya, “Gravitational spin Hamiltonians from the S matrix,” *Phys. Rev.* **D91** no. 2, (2015) 024017, [arXiv:1410.5348 \[hep-th\]](#).
- [282] M. Carrillo-González, C. de Rham, and A. J. Tolley, “Scattering amplitudes for binary systems beyond GR,” *JHEP* **11** (2021) 087, [arXiv:2107.11384 \[hep-th\]](#).
- [283] T. Damour, “High-energy gravitational scattering and the general relativistic two-body problem,” *Phys. Rev.* **D97** no. 4, (2018) 044038, [arXiv:1710.10599 \[gr-qc\]](#).
- [284] R. Akhouri, R. Saotome, and G. Sterman, “High Energy Scattering in Perturbative Quantum Gravity at Next to Leading Power,” [arXiv:1308.5204 \[hep-th\]](#).
- [285] N. E. J. Bjerrum-Bohr, J. F. Donoghue, B. R. Holstein, L. Plante, and P. Vanhove, “Light-like Scattering in Quantum Gravity,” *JHEP* **11** (2016) 117, [arXiv:1609.07477 \[hep-th\]](#).
- [286] Z. Bern, H. Ita, J. Parra-Martinez, and M. S. Ruf, “Universality in the classical limit of massless gravitational scattering,” [arXiv:2002.02459 \[hep-th\]](#).
- [287] Z. Bern, A. Luna, R. Roiban, C.-H. Shen, and M. Zeng, “Spinning Black Hole Binary Dynamics, Scattering Amplitudes and Effective Field Theory,” [arXiv:2005.03071 \[hep-th\]](#).
- [288] J. Parra-Martinez, M. S. Ruf, and M. Zeng, “Extremal black hole scattering at $O(G^3)$: graviton dominance, eikonal exponentiation, and differential equations,” [arXiv:2005.04236 \[hep-th\]](#).
- [289] P. Di Vecchia, C. Heissenberg, R. Russo, and G. Veneziano, “The eikonal approach to gravitational scattering and radiation at $\mathcal{O}(G^3)$,” *JHEP* **07** (2021) 169, [arXiv:2104.03256 \[hep-th\]](#).

- [290] N. E. J. Bjerrum-Bohr, J. F. Donoghue, B. R. Holstein, L. Plante, and P. Vanhove, “Bending of Light in Quantum Gravity,” *Phys. Rev. Lett.* **114** no. 6, (2015) 061301, [arXiv:1410.7590 \[hep-th\]](#).
- [291] D. Bai and Y. Huang, “More on the Bending of Light in Quantum Gravity,” *Phys. Rev.* **D95** no. 6, (2017) 064045, [arXiv:1612.07629 \[hep-th\]](#).
- [292] H.-H. Chi, “Graviton Bending in Quantum Gravity from One-Loop Amplitudes,” *Phys. Rev.* **D99** no. 12, (2019) 126008, [arXiv:1903.07944 \[hep-th\]](#).
- [293] A. Brandhuber and G. Travaglini, “On higher-derivative effects on the gravitational potential and particle bending,” *JHEP* **01** (2020) 010, [arXiv:1905.05657 \[hep-th\]](#).
- [294] W. T. Emond and N. Moynihan, “Scattering Amplitudes, Black Holes and Leading Singularities in Cubic Theories of Gravity,” *JHEP* **12** (2019) 019, [arXiv:1905.08213 \[hep-th\]](#).
- [295] S. Endlich, V. Gorbenko, J. Huang, and L. Senatore, “An effective formalism for testing extensions to General Relativity with gravitational waves,” *JHEP* **09** (2017) 122, [arXiv:1704.01590 \[gr-qc\]](#).
- [296] C. de Rham, A. J. Tolley, and J. Zhang, “Causality Constraints on Gravitational Effective Field Theories,” *Phys. Rev. Lett.* **128** no. 13, (2022) 131102, [arXiv:2112.05054 \[gr-qc\]](#).
- [297] X. O. Camanho, J. D. Edelstein, J. Maldacena, and A. Zhiboedov, “Causality Constraints on Corrections to the Graviton Three-Point Coupling,” *JHEP* **02** (2016) 020, [arXiv:1407.5597 \[hep-th\]](#).
- [298] T. J. Hollowood and G. M. Shore, “The Refractive index of curved spacetime: The Fate of causality in QED,” *Nucl. Phys. B* **795** (2008) 138–171, [arXiv:0707.2303 \[hep-th\]](#).
- [299] G. Goon and K. Hinterbichler, “Superluminality, black holes and EFT,” *JHEP* **02** (2017) 134, [arXiv:1609.00723 \[hep-th\]](#).
- [300] T. J. Hollowood and G. M. Shore, “Causality and Micro-Causality in Curved Spacetime,” *Phys. Lett. B* **655** (2007) 67–74, [arXiv:0707.2302 \[hep-th\]](#).
- [301] T. J. Hollowood and G. M. Shore, “Causality Violation, Gravitational Shockwaves and UV Completion,” *JHEP* **03** (2016) 129, [arXiv:1512.04952 \[hep-th\]](#).

-
- [302] K. Benakli, S. Chapman, L. Darmé, and Y. Oz, “Superluminal graviton propagation,” *Phys. Rev. D* **94** no. 8, (2016) 084026, [arXiv:1512.07245 \[hep-th\]](#).
- [303] T. J. Hollowood and G. M. Shore, “Causality, Renormalizability and Ultra-High Energy Gravitational Scattering,” *J. Phys. A* **49** no. 21, (2016) 215401, [arXiv:1601.06989 \[hep-th\]](#).
- [304] C. de Rham and A. J. Tolley, “Speed of gravity,” *Phys. Rev. D* **101** no. 6, (2020) 063518, [arXiv:1909.00881 \[hep-th\]](#).
- [305] C. de Rham, J. Francfort, and J. Zhang, “Black Hole Gravitational Waves in the Effective Field Theory of Gravity,” [arXiv:2005.13923 \[hep-th\]](#).
- [306] D. Amati, M. Ciafaloni, and G. Veneziano, “Classical and Quantum Gravity Effects from Planckian Energy Superstring Collisions,” *Int. J. Mod. Phys. A* **3** (1988) 1615–1661.
- [307] G. D’Appollonio, P. Vecchia, R. Russo, and G. Veneziano, “Microscopic unitary description of tidal excitations in high-energy string-brane collisions,” *JHEP* **11** (2013) 126, [arXiv:1310.1254 \[hep-th\]](#).
- [308] F. A. Berends and R. Gastmans, “Quantum Electrodynamical Corrections to Graviton-Matter Vertices,” *Annals Phys.* **98** (1976) 225.
- [309] I. Drummond and S. Hathrell, “QED Vacuum Polarization in a Background Gravitational Field and Its Effect on the Velocity of Photons,” *Phys. Rev. D* **22** (1980) 343.
- [310] P. van Nieuwenhuizen and C. C. Wu, “On integral relations for invariants constructed from three riemann tensors and their applications in quantum gravity,” *Journal of Mathematical Physics* **18** no. 1, (1977) 182–186, <https://doi.org/10.1063/1.523128>. <https://doi.org/10.1063/1.523128>.
- [311] J. Broedel and L. J. Dixon, “Color-kinematics duality and double-copy construction for amplitudes from higher-dimension operators,” *JHEP* **10** (2012) 091, [arXiv:1208.0876 \[hep-th\]](#).
- [312] M. H. Goroff and A. Sagnotti, “Quantum gravity at two loops,” *Phys. Lett.* **160B** (1985) 81–86.
- [313] S. Fulling, R. C. King, B. Wybourne, and C. Cummins, “Normal forms for tensor polynomials. 1: The Riemann tensor,” *Class. Quant. Grav.* **9** (1992) 1151–1197.
- [314] A. A. Tseytlin, “Ambiguity in the Effective Action in String Theories,” *Phys. Lett.* **B176** (1986) 92–98.

-
- [315] R. R. Metsaev and A. A. Tseytlin, “Order alpha-prime (Two Loop) Equivalence of the String Equations of Motion and the Sigma Model Weyl Invariance Conditions: Dependence on the Dilaton and the Antisymmetric Tensor,” *Nucl. Phys. B* **293** (1987) 385–419.
- [316] D. C. Dunbar, J. H. Godwin, G. R. Jehu, and W. B. Perkins, “Loop Amplitudes in an Extended Gravity Theory,” *Phys. Lett. B* **780** (2018) 41–47, [arXiv:1711.05526 \[hep-th\]](#).
- [317] M. Ruhdorfer, J. Serra, and A. Weiler, “Effective Field Theory of Gravity to All Orders,” [arXiv:1908.08050 \[hep-ph\]](#).
- [318] D. J. Gross and E. Witten, “Superstring Modifications of Einstein’s Equations,” *Nucl. Phys. B* **277** (1986) 1.
- [319] P. Di Vecchia, A. Luna, S. G. Naculich, R. Russo, G. Veneziano, and C. D. White, “A tale of two exponentiations in $\mathcal{N} = 8$ supergravity,” *Phys. Lett. B* **798** (2019) 134927, [arXiv:1908.05603 \[hep-th\]](#).
- [320] P. Di Vecchia, S. G. Naculich, R. Russo, G. Veneziano, and C. D. White, “A tale of two exponentiations in $\mathcal{N} = 8$ supergravity at subleading level,” [arXiv:1911.11716 \[hep-th\]](#).
- [321] A. Koemans Collado, P. Di Vecchia, and R. Russo, “Revisiting the 2PM eikonal and the dynamics of binary black holes,” [arXiv:1904.02667 \[hep-th\]](#).
- [322] N. E. J. Bjerrum-Bohr, B. R. Holstein, J. F. Donoghue, L. Plante, and P. Vanhove, “Illuminating Light Bending,” *PoS CORFU2016* (2017) 077, [arXiv:1704.01624 \[gr-qc\]](#).
- [323] L. Eisenbud, *The formal properties of nuclear collisions*. PhD thesis, Princeton U., 1948.
- [324] D. Bohm, *Quantum Theory*. New York: Prentice Hall, 1951.
- [325] E. P. Wigner, “Lower Limit for the Energy Derivative of the Scattering Phase Shift,” *Phys. Rev.* **98** (1955) 145–147.
- [326] A. Einstein, “On The influence of gravitation on the propagation of light,” *Annalen Phys.* **35** (1911) 898–908.
- [327] M. Ciafaloni and D. Colferai, “Rescattering corrections and self-consistent metric in Planckian scattering,” *JHEP* **10** (2014) 085, [arXiv:1406.6540 \[hep-th\]](#).

-
- [328] K. Hinterbichler, A. Joyce, and R. A. Rosen, “Massive Spin-2 Scattering and Asymptotic Superluminality,” *JHEP* **03** (2018) 051, [arXiv:1708.05716 \[hep-th\]](#).
- [329] J. Bonifacio, K. Hinterbichler, A. Joyce, and R. A. Rosen, “Massive and Massless Spin-2 Scattering and Asymptotic Superluminality,” *JHEP* **06** (2018) 075, [arXiv:1712.10020 \[hep-th\]](#).
- [330] K. Hinterbichler, A. Joyce, and R. A. Rosen, “Eikonal scattering and asymptotic superluminality of massless higher spin fields,” *Phys. Rev. D* **97** no. 12, (2018) 125019, [arXiv:1712.10021 \[hep-th\]](#).
- [331] C. de Rham, J. Francfort, and J. Zhang, “Black Hole Gravitational Waves in the Effective Field Theory of Gravity,” *Phys. Rev. D* **102** no. 2, (2020) 024079, [arXiv:2005.13923 \[hep-th\]](#).
- [332] I. T. Drummond and S. J. Hathrell, “Qed vacuum polarization in a background gravitational field and its effect on the velocity of photons,” *Phys. Rev. D* **22** (Jul, 1980) 343–355. <https://link.aps.org/doi/10.1103/PhysRevD.22.343>.
- [333] C. de Rham and A. J. Tolley, “Causality in curved spacetimes: The speed of light and gravity,” *Phys. Rev. D* **102** no. 8, (2020) 084048, [arXiv:2007.01847 \[hep-th\]](#).
- [334] C. Y. R. Chen, C. de Rham, A. Margalit, and A. J. Tolley, “A cautionary case of casual causality,” *JHEP* **03** (2022) 025, [arXiv:2112.05031 \[hep-th\]](#).
- [335] M. Carrillo Gonzalez, C. de Rham, V. Pozsgay, and A. J. Tolley, “Causal Effective Field Theories,” [arXiv:2207.03491 \[hep-th\]](#).
- [336] A. Gruzinov and M. Kleban, “Causality Constrains Higher Curvature Corrections to Gravity,” *Class. Quant. Grav.* **24** (2007) 3521–3524, [arXiv:hep-th/0612015 \[hep-th\]](#).
- [337] B. Bellazzini, C. Cheung, and G. N. Remmen, “Quantum Gravity Constraints from Unitarity and Analyticity,” *Phys. Rev. D* **93** no. 6, (2016) 064076, [arXiv:1509.00851 \[hep-th\]](#).
- [338] Z. Bern, J. Parra-Martinez, R. Roiban, E. Sawyer, and C.-H. Shen, “Leading Nonlinear Tidal Effects and Scattering Amplitudes,” [arXiv:2010.08559 \[hep-th\]](#).
- [339] I. G. Avramidi, *Covariant methods for the calculation of the effective action in quantum field theory and investigation of higher derivative quantum gravity*. PhD thesis, Moscow State U., 1986. [arXiv:hep-th/9510140 \[hep-th\]](#).

-
- [340] I. G. Avramidi, “The Covariant Technique for Calculation of One Loop Effective Action,” *Nucl. Phys.* **B355** (1991) 712–754. [Erratum: Nucl. Phys.B509,557(1998)].
- [341] P. van Nieuwenhuizen and C. C. Wu, “On Integral Relations for Invariants Constructed from Three Riemann Tensors and their Applications in Quantum Gravity,” *J. Math. Phys.* **18** (1977) 182.
- [342] Q. Henry, G. Faye, and L. Blanchet, “Tidal effects in the equations of motion of compact binary systems to next-to-next-to-leading post-Newtonian order,” *Phys. Rev. D* **101** no. 6, (2020) 064047, [arXiv:1912.01920 \[gr-qc\]](#).
- [343] T. Marchand, Q. Henry, F. Larrouturou, S. Marsat, G. Faye, and L. Blanchet, “The mass quadrupole moment of compact binary systems at the fourth post-Newtonian order,” *Class. Quant. Grav.* **37** no. 21, (2020) 215006, [arXiv:2003.13672 \[gr-qc\]](#).
- [344] Q. Henry, G. Faye, and L. Blanchet, “Tidal effects in the gravitational-wave phase evolution of compact binary systems to next-to-next-to-leading post-Newtonian order,” *Phys. Rev. D* **102** no. 4, (2020) 044033, [arXiv:2005.13367 \[gr-qc\]](#).
- [345] T. Damour, B. R. Iyer, and B. Sathyaprakash, “Improved filters for gravitational waves from inspiralling compact binaries,” *Phys. Rev. D* **57** (1998) 885–907, [arXiv:gr-qc/9708034](#).
- [346] A. Buonanno, B. Iyer, E. Ochsner, Y. Pan, and B. Sathyaprakash, “Comparison of post-Newtonian templates for compact binary inspiral signals in gravitational-wave detectors,” *Phys. Rev. D* **80** (2009) 084043, [arXiv:0907.0700 \[gr-qc\]](#).
- [347] C. Cheung and M. P. Solon, “Tidal Effects in the Post-Minkowskian Expansion,” [arXiv:2006.06665 \[hep-th\]](#).
- [348] K. Haddad and A. Helset, “Gravitational tidal effects in quantum field theory,” [arXiv:2008.04920 \[hep-th\]](#).
- [349] D. Lovelock, “Dimensionally dependent identities,” *Mathematical Proceedings of the Cambridge Philosophical Society* **68** no. 2, (1970) 345?350.
- [350] S. Edgar and A. Hoglund, “Dimensionally dependent tensor identities by double antisymmetrization,” *J. Math. Phys.* **43** (2002) 659–677, [arXiv:gr-qc/0105066](#).
- [351] V. Cardoso, M. Kimura, A. Maselli, and L. Senatore, “Black Holes in an Effective Field Theory Extension of General Relativity,” *Phys. Rev. Lett.* **121** no. 25, (2018) 251105, [arXiv:1808.08962 \[gr-qc\]](#).

-
- [352] S. Cai and K.-D. Wang, “Non-vanishing of tidal Love numbers,” [arXiv:1906.06850 \[hep-th\]](#).
- [353] D. Bini, T. Damour, and A. Geralico, “Scattering of tidally interacting bodies in post-Minkowskian gravity,” *Phys. Rev. D* **101** no. 4, (2020) 044039, [arXiv:2001.00352 \[gr-qc\]](#).
- [354] G. Kälin and R. A. Porto, “Post-Minkowskian Effective Field Theory for Conservative Binary Dynamics,” [arXiv:2006.01184 \[hep-th\]](#).
- [355] W. D. Goldberger and I. Z. Rothstein, “An Effective field theory of gravity for extended objects,” *Phys. Rev. D* **73** (2006) 104029, [arXiv:hep-th/0409156 \[hep-th\]](#).
- [356] J.-W. Kim and M. Shim, “Sum rule for Love,” [arXiv:2011.03337 \[hep-th\]](#).
- [357] D. C. Dunbar and W. B. Perkins, “Two-loop five-point all plus helicity Yang-Mills amplitude,” *Phys. Rev. D* **93** no. 8, (2016) 085029, [arXiv:1603.07514 \[hep-th\]](#).
- [358] D. C. Dunbar, G. R. Jehu, and W. B. Perkins, “Two-loop six gluon all plus helicity amplitude,” *Phys. Rev. Lett.* **117** no. 6, (2016) 061602, [arXiv:1605.06351 \[hep-th\]](#).
- [359] C. Anastasiou, R. Britto, B. Feng, Z. Kunszt, and P. Mastrolia, “D-dimensional unitarity cut method,” *Phys. Lett. B* **645** (2007) 213–216, [arXiv:hep-ph/0609191 \[hep-ph\]](#).
- [360] S. Badger, C. Brønnum-Hansen, H. B. Hartanto, and T. Peraro, “First look at two-loop five-gluon scattering in QCD,” *Phys. Rev. Lett.* **120** no. 9, (2018) 092001, [arXiv:1712.02229 \[hep-ph\]](#).
- [361] H. B. Hartanto, S. Badger, C. Brønnum-Hansen, and T. Peraro, “A numerical evaluation of planar two-loop helicity amplitudes for a W-boson plus four partons,” *JHEP* **09** (2019) 119, [arXiv:1906.11862 \[hep-ph\]](#).
- [362] S. Badger, C. Brønnum-Hansen, D. Chicherin, T. Gehrmann, H. B. Hartanto, J. Henn, M. Marcoli, R. Moodie, T. Peraro, and S. Zoia, “Virtual QCD corrections to gluon-initiated diphoton plus jet production at hadron colliders,” *JHEP* **11** (2021) 083, [arXiv:2106.08664 \[hep-ph\]](#).
- [363] S. Abreu, F. Febres Cordero, H. Ita, B. Page, and V. Sotnikov, “Leading-color two-loop QCD corrections for three-jet production at hadron colliders,” *JHEP* **07** (2021) 095, [arXiv:2102.13609 \[hep-ph\]](#).

-
- [364] S. Abreu, F. Febres Cordero, H. Ita, M. Klinkert, B. Page, and V. Sotnikov, “Leading-color two-loop amplitudes for four partons and a W boson in QCD,” *JHEP* **04** (2022) 042, [arXiv:2110.07541 \[hep-ph\]](#).
- [365] S. Badger, H. Frellesvig, and Y. Zhang, “A Two-Loop Five-Gluon Helicity Amplitude in QCD,” *JHEP* **12** (2013) 045, [arXiv:1310.1051 \[hep-ph\]](#).
- [366] F. R. Anger and V. Sotnikov, “On the Dimensional Regularization of QCD Helicity Amplitudes With Quarks,” [arXiv:1803.11127 \[hep-ph\]](#).
- [367] A. Brandhuber, B. J. Spence, and G. Travaglini, “One-loop gauge theory amplitudes in $\mathcal{N}=4$ super Yang-Mills from MHV vertices,” *Nucl. Phys.* **B706** (2005) 150–180, [arXiv:hep-th/0407214 \[hep-th\]](#).
- [368] L. J. Dixon, E. W. N. Glover, and V. V. Khoze, “MHV rules for Higgs plus multi-gluon amplitudes,” *JHEP* **12** (2004) 015, [arXiv:hep-th/0411092 \[hep-th\]](#).
- [369] S. D. Badger, E. W. N. Glover, and V. V. Khoze, “MHV rules for Higgs plus multi-parton amplitudes,” *JHEP* **03** (2005) 023, [arXiv:hep-th/0412275 \[hep-th\]](#).
- [370] S. D. Badger, E. W. N. Glover, and K. Risager, “One-loop phi-MHV amplitudes using the unitarity bootstrap,” *JHEP* **07** (2007) 066, [arXiv:0704.3914 \[hep-ph\]](#).
- [371] S. Badger, E. W. Nigel Glover, P. Mastrolia, and C. Williams, “One-loop Higgs plus four gluon amplitudes: Full analytic results,” *JHEP* **01** (2010) 036, [arXiv:0909.4475 \[hep-ph\]](#).
- [372] A. Brandhuber, M. Kostacinska, B. Penante, and G. Travaglini, “Higgs amplitudes from $\mathcal{N} = 4$ super Yang-Mills theory,” *Phys. Rev. Lett.* **119** no. 16, (2017) 161601, [arXiv:1707.09897 \[hep-th\]](#).
- [373] Q. Jin and G. Yang, “Analytic Two-Loop Higgs Amplitudes in Effective Field Theory and the Maximal Transcendentality Principle,” *Phys. Rev. Lett.* **121** no. 10, (2018) 101603, [arXiv:1804.04653 \[hep-th\]](#).
- [374] A. Brandhuber, M. Kostacinska, B. Penante, and G. Travaglini, “ $\text{Tr}(F^3)$ supersymmetric form factors and maximal transcendentality Part I: $\mathcal{N} = 4$ super Yang-Mills,” [arXiv:1804.05703 \[hep-th\]](#).
- [375] A. Brandhuber, M. Kostacinska, B. Penante, and G. Travaglini, “ $\text{Tr}(F^3)$ supersymmetric form factors and maximal transcendentality Part II: $0 < \mathcal{N} < 4$ super Yang-Mills,” [arXiv:1804.05828 \[hep-th\]](#).

- [376] Q. Jin and G. Yang, “Hidden Analytic Relations for Two-Loop Higgs Amplitudes in QCD,” [arXiv:1904.07260 \[hep-th\]](#).
- [377] T. Gehrmann, J. M. Henn, and T. Huber, “The three-loop form factor in $N=4$ super Yang-Mills,” *JHEP* **03** (2012) 101, [arXiv:1112.4524 \[hep-th\]](#).
- [378] A. Brandhuber, G. Travaglini, and G. Yang, “Analytic two-loop form factors in $\mathcal{N}=4$ SYM,” *JHEP* **05** (2012) 082, [arXiv:1201.4170 \[hep-th\]](#).
- [379] A. Brandhuber, B. Penante, G. Travaglini, and C. Wen, “The last of the simple remainders,” *JHEP* **1408** (2014) 100, [arXiv:1406.1443 \[hep-th\]](#).
- [380] D. Nandan, C. Sieg, M. Wilhelm, and G. Yang, “Cutting through form factors and cross sections of non-protected operators in $\mathcal{N} = 4$ SYM,” *JHEP* **06** (2015) 156, [arXiv:1410.8485 \[hep-th\]](#).
- [381] F. Loebbert, D. Nandan, C. Sieg, M. Wilhelm, and G. Yang, “On-Shell Methods for the Two-Loop Dilatation Operator and Finite Remainders,” *JHEP* **10** (2015) 012, [arXiv:1504.06323 \[hep-th\]](#).
- [382] A. Brandhuber, M. Kostacínska, B. Penante, G. Travaglini, and D. Young, “The $SU(2|3)$ dynamic two-loop form factors,” *JHEP* **08** (2016) 134, [arXiv:1606.08682 \[hep-th\]](#).
- [383] F. Loebbert, C. Sieg, M. Wilhelm, and G. Yang, “Two-Loop $SL(2)$ Form Factors and Maximal Transcendentality,” *JHEP* **12** (2016) 090, [arXiv:1610.06567 \[hep-th\]](#).
- [384] Z. Bern, A. De Freitas, L. J. Dixon, and H. L. Wong, “Supersymmetric regularization, two loop QCD amplitudes and coupling shifts,” *Phys. Rev.* **D66** (2002) 085002, [arXiv:hep-ph/0202271 \[hep-ph\]](#).
- [385] G. 't Hooft and M. J. G. Veltman, “Regularization and Renormalization of Gauge Fields,” *Nucl. Phys.* **B44** (1972) 189–213.
- [386] T. Dennen, Y.-t. Huang, and W. Siegel, “Supertwistor space for 6D maximal super Yang-Mills,” *JHEP* **04** (2010) 127, [arXiv:0910.2688 \[hep-th\]](#).
- [387] S. Dawson, I. M. Lewis, and M. Zeng, “Usefulness of effective field theory for boosted Higgs production,” *Phys. Rev.* **D91** (2015) 074012, [arXiv:1501.04103 \[hep-ph\]](#).
- [388] D. Neill, “Analytic Virtual Corrections for Higgs Transverse Momentum Spectrum at $O(\alpha(s)**2/m(t)**3)$ via Unitarity Methods,” [arXiv:0911.2707 \[hep-ph\]](#).

- [389] L. J. Dixon and Y. Shadmi, “Testing gluon selfinteractions in three jet events at hadron colliders,” *Nucl. Phys.* **B423** (1994) 3–32, [arXiv:hep-ph/9312363 \[hep-ph\]](#). [Erratum: *Nucl. Phys.*B452,724(1995)].
- [390] A. Yu. Morozov, “MATRIX OF MIXING OF SCALAR AND VECTOR MESONS OF DIMENSION $D \leq 8$ IN QCD. (IN RUSSIAN),” *Sov. J. Nucl. Phys.* **40** (1984) 505. [*Yad. Fiz.*40,788(1984)].
- [391] J. A. Gracey, “Classification and one loop renormalization of dimension-six and dimension-eight operators in quantum gluodynamics,” *Nucl. Phys.* **B634** (2002) 192–208, [arXiv:hep-ph/0204266 \[hep-ph\]](#). [Erratum: *Nucl. Phys.*B696,295(2004)].
- [392] M. B. Green and J. H. Schwarz, “Supersymmetrical Dual String Theory. 2. Vertices and Trees,” *Nucl. Phys.* **B198** (1982) 252–268.
- [393] J. H. Schwarz, “Superstring Theory,” *Phys. Rept.* **89** (1982) 223–322.
- [394] A. A. Tseytlin, “Vector Field Effective Action in the Open Superstring Theory,” *Nucl. Phys.* **B276** (1986) 391. [Erratum: *Nucl. Phys.*B291,876(1987)].
- [395] C. R. Schmidt, “ $H \rightarrow g g g$ ($g q$ anti- q) at two loops in the large $M(t)$ limit,” *Phys. Lett.* **B413** (1997) 391–395, [arXiv:hep-ph/9707448 \[hep-ph\]](#).
- [396] R. Mertig, M. Bohm, and A. Denner, “FEYN CALC: Computer algebraic calculation of Feynman amplitudes,” *Comput. Phys. Commun.* **64** (1991) 345–359.
- [397] V. Shtabovenko, R. Mertig, and F. Orellana, “New Developments in FeynCalc 9.0,” *Comput. Phys. Commun.* **207** (2016) 432–444, [arXiv:1601.01167 \[hep-ph\]](#).
- [398] E. D’Hoker and D. Z. Freedman, “Supersymmetric gauge theories and the AdS / CFT correspondence,” in *Strings, Branes and Extra Dimensions: TASI 2001: Proceedings*, pp. 3–158. 2002. [arXiv:hep-th/0201253 \[hep-th\]](#).